

## From waste to products

### Valorizing food side streams to recover natural products

Moreno Gonzalez, M.

#### DOI

[10.4233/uuid:c2d667d7-09a2-435f-9142-4368b06a0631](https://doi.org/10.4233/uuid:c2d667d7-09a2-435f-9142-4368b06a0631)

#### Publication date

2021

#### Document Version

Final published version

#### Citation (APA)

Moreno Gonzalez, M. (2021). *From waste to products: Valorizing food side streams to recover natural products*. [Dissertation (TU Delft), Delft University of Technology]. <https://doi.org/10.4233/uuid:c2d667d7-09a2-435f-9142-4368b06a0631>

#### Important note

To cite this publication, please use the final published version (if applicable). Please check the document version above.

#### Copyright

Other than for strictly personal use, it is not permitted to download, forward or distribute the text or part of it, without the consent of the author(s) and/or copyright holder(s), unless the work is under an open content license such as Creative Commons.

#### Takedown policy

Please contact us and provide details if you believe this document breaches copyrights. We will remove access to the work immediately and investigate your claim.

# From waste to products: Valorizing food side streams to recover natural products

## Dissertation

for the purpose of obtaining the degree of doctor  
at Delft University of Technology  
by the authority of the Rector Magnificus Prof.dr.ir. T.H.J.J. van der Hagen  
chair of the Board for Doctorates  
to be defended publicly on  
Friday 4, June 2021 at 12:30 o'clock

by

**Monica MORENO GONZALEZ**

Master of Science in Life Science and Technology, Delft University of  
Technology, the Netherlands  
born in Mexico City, Mexico

This dissertation has been approved by the promotor.

Composition of the doctoral committee:

Rector Magnificus	chairperson
Dr.ir. M. Ottens	Delft University of Technology, promotor
Prof.dr.ir. L.A.M. van der Wielen	Delft University of Technology, promotor

Independent members:

Prof.dr. F. Hollmann	Delft University of Technology
Prof.dr.ir. A.J. van der Goot	University of Wageningen
Prof.dr. M.H.M Eppink	University of Wageningen / Byondis
Prof.dr.ir. H.J. Noorman	Delft University of Technology / DSM
Prof.dr.ir. M.C.M van Loosdrecht	Delft University of Technology

The research described in this thesis was performed at the Department of Biotechnology, Faculty of Applied Sciences, Delft University of Technology, the Netherlands.

This project was co-funded by TKI-E&I with the supplementary grant 'TKI- Toeslag' for Topconsortia for Knowledge and Innovation (TKI's) of the Ministry of Economic Affairs and Climate Policy.

Copyright© 2021 Monica Moreno Gonzalez

# Table of Contents

---

<b>Summary</b>	<b>iii</b>
<b>Samenvatting</b>	<b>v</b>
<b>Chapter 1</b>	<b>1</b>
General Introduction & Thesis Outline	
<b>Chapter 2</b>	<b>9</b>
A structured approach to recover valuable compounds from agri-food side streams	
<b>Chapter 3</b>	<b>39</b>
Recovery of sinapic acid from canola/rapeseed meal extracts by adsorption	
<b>Chapter 4</b>	<b>63</b>
High Throughput Process Development for the purification of rapeseed proteins napin and cruciferin by ion exchange chromatography	
<b>Chapter 5</b>	<b>99</b>
Continuous adsorption in food industry: The recovery of sinapic acid from rapeseed meal extract	
<b>Chapter 6</b>	<b>129</b>
Upgrading food industry side streams: A techno-economic analysis to remove off-flavors	
<b>Chapter 7</b>	<b>167</b>
Conclusions and Outlook	
<b>Appendix</b>	<b>171</b>
Acknowledgments, List of publications & Curriculum Vitae	



# Summary

---

This thesis presents novel ways of recovering of valuable compounds from food industry side streams. It does so via evaluating two case studies for the valorization of such streams. These types of streams are often referred to as waste and discarded. However, they are rich sources of nutraceuticals (e.g polyphenols), proteins and dietary fiber. Recently the use of these side streams has gained significant interest in the scientific community and different alternatives to recover high value products are being investigated that may contribute to the transition from the current linear economy to a more circular economy (**Chapter 1**).

Some of the technological challenges related to the utilization of these side streams include the low concentration of valuable compounds and the presence of other unwanted low value components (e.g off-flavors and colorants). The use of adsorption as separation and purification technology can contribute to an efficient recovery of the target compounds.

This thesis focuses exclusively on the utilization of plant-based food side streams. It begins with a literature overview (**Chapter 2**) discussing different side streams commonly present and their respective valuable products. The study identifies that multiple valuable products can be recovered from a single source. It additionally provides a processing strategy and a few examples of side stream processing. A side stream processing approach is defined including the following processing steps: pretreatment, volume reduction, phase change, purification/conversion and formulation. It is clear that depending on the source material some of these steps might not be needed. A special attention is given to adsorption as a purification technology, as it has the ability to achieve high selectivity and product purity.

As first example, rapeseed meal extract is studied to recover sinapic acid, by means of adsorption (**Chapter 3**). Different food grade hydrophobic resins are compared under different adsorption/desorption conditions to selectively capture sinapic acid. Resin screening is done using robotic high throughput experimentation (HTE) and reliable single and multicomponent data is obtained. Resin selection is done considering capacity, selectivity and ease of desorption. Adsorption isotherms are used to describe the generated set of adsorption data and to understand the specifics of the interaction between sinapic acid and the evaluated resins. This chapter demonstrates that Sinapic acid is selectively adsorbed by the chosen optimal resin Amberlite FPX66 and that desorption is very effective using ethanol mixtures. This significantly decreases the isotherm slope (affinity towards the resin) of Sinapic acid as compared the extract conditions. The high selectivity is a result of the hydrophobic character of this compound as the other components (sugar, glucosinolates and phytic acid) are more hydrophilic.

As part of the valorization of rapeseed meal extract, protein from this source can be additionally recovered. Two main storage proteins are presented in this meal, i.e. cruciferin and napin. These proteins have shown similar characteristics like soybean proteins and can be used for human consumption. **Chapter 4** presents a technically feasible industrial process for the recovery of sinapic acid and proteins from rapeseed meal. The recovery of the proteins makes use of an ion exchange resin (POROS 50HS) for the selective capture of napin. Equilibrium information at various different conditions is presented.

A mathematical column adsorption model is described in **Chapter 3** and **Chapter 4** which is validated with experimental results. The model uses as input the generated adsorption/desorption equilibrium data and is applied for the design of an industrial scale column and the definition of the chromatographic cycle. This characteristic batch model (1 column) is used further for optimization (**Chapter 5**) of the adsorption of sinapic acid to maximize productivity.

As the food sector is characterized by continuous operation, the processing of side streams using continuous technologies might be more efficient. This could also facilitate the re-integration/circulation of the recovered products to other processes. Adsorption is typically a batch operation, however, systems such as simulated moving bed (SMB) technology provide continuous operation. **Chapter 5** compares the performance of batch operation with the semi-continuous system CaptureSMB to recover sinapic acid. It uses the pre-defined adsorption model to optimize both operating modes with the objective of maximizing productivity for a given yield (98%) and a minimum resin utilization of 70% for efficient operation. This study demonstrates that CaptureSMB performs better than batch operation, and that efficient adsorption can be applied in the food sector not only by the more traditional simulated moving bed (SMB) technology.

The approach presented in **Chapter 3** to **Chapter 5**, is applied in a different case study, where instead of capturing valuable compounds the *impurities* are captured. **Chapter 6** presents the upgrading of a food industry side stream via a conceptual process design. This study demonstrates that generation of high value products from food waste streams is possible and profitable. This study indicates how treatment of side streams is significant in the transition to a circular economy.

# Samenvatting

---

Dit proefschrift presenteert innovatieve manieren om waardevolle producten terug te winnen uit zij-/rest- of nevenstromen in de voedingsindustrie. Deze stromen worden vaak betiteld als afval en als zodanig behandeld. Het blijken echter rijke bronnen van gezondheid bevorderende componenten, de zgn. “*nutraceuticals*” (bijvoorbeeld polyfenolen), eiwitten en voedingsvezels te zijn. Onlangs heeft het nuttig gebruik van deze zij/reststromen zich in een aanzienlijke belangstelling mogen verheugen in de wetenschappelijke gemeenschap en industrie. Verschillende alternatieven worden nu onderzocht om hoogwaardige producten terug te winnen om zo bij te dragen aan de overgang van de huidige lineaire economie naar een meer circulaire economie (**hoofdstuk 1**).

Enkele van de technologische uitdagingen die verband houden met het nuttig gebruik van deze nevenstromen, zijn onder meer de zeer lage concentratie van de beschikbare waardevolle verbindingen en de aanwezigheid van andere ongewenste laagwaardige componenten (bijv. onaangename smaken en ongewenste kleurstoffen).

Dit proefschrift richt zich uitsluitend op het gebruik van voedingsreststromen van plantaardige aard. Het begint met een literatuuroverzicht (**hoofdstuk 2**) waarin de verschillende gangbare zijstromen en hun respectievelijke waardevolle producten worden besproken. Dit hoofdstuk toont aan dat meerdere waardevolle producten kunnen worden teruggewonnen uit slechts een enkele bron. Een benadering voor het verwerken van zijstromen wordt gepresenteerd met volgende verwerkingsstappen: voorbehandeling, volumevermindering, faseverandering, zuivering/conversie en formulering. Het is duidelijk dat afhankelijk van het bronmateriaal sommige van deze stappen wellicht niet nodig zijn. Speciale aandacht wordt besteed aan adsorptie als zuiveringstechnologie, omdat dit een zeer hoge selectiviteit en productzuiverheid kan realiseren.

Als eerste voorbeeld wordt koolzaadmeel bestudeerd om sinapinezuur terug te winnen door middel van adsorptie (**hoofdstuk 3**). Verschillende hydrofobe adsorbens (harsen of “*resins*”) worden vergeleken onder verschillende adsorptie/desorptie-omstandigheden om selectief sinapinezuur te binden. De “*resin screening*” wordt uitgevoerd met behulp van gerobotiseerde “*high-throughput*”-experimenten (HTE) om betrouwbare bindingsdata voor enkel- en meervoudige component systemen te verkrijgen. De harsselectie wordt gedaan op basis van bindingscapaciteit, selectiviteit en gemak van desorptie. Adsorptie-isothermen worden gebruikt om de gegenereerde set adsorptiedata te beschrijven en om de specifieke kenmerken van de interactie tussen sinapinezuur en de geëvalueerde harsen te begrijpen. Dit hoofdstuk laat zien dat sinapinezuur selectief wordt geadsorbeerd door de uiteindelijk gekozen optimale hars Amberlite FPX66 en dat desorptie zeer effectief is met ethanol-water mengsels. Ethanol verlaagt significant de helling van de bindingsisotherm (bindingsaffiniteit voor de hars) van sinapinezuur ten opzichte van de adsorptieomstandigheden. De hoge selectiviteit is het

resultaat van het hydrofobe karakter van deze binding, daar de andere componenten (suiker, glucosinolaten en fytinezuur) meer hydrofiel van karakter zijn.

In het kader van valorisatie van koolzaadmeel extract kan ook eiwit uit deze bron worden teruggewonnen. Twee belangrijke opslagproteïnen worden onderzocht, namelijk cruciferine en napine. Deze eiwitten hebben vergelijkbare eigenschappen als soja-eiwitten en kunnen worden gebruikt voor menselijke consumptie. **Hoofdstuk 4** presenteert een technisch haalbaar industrieel proces voor het terugwinnen van sinapinezuur en eiwitten uit koolzaadmeel. De winning van de eiwitten maakt gebruik van een ion-wisseling adsorbens (POROS 50HS) voor het selectief binden van napine. Relevante bindingsevenwicht data onder verschillende omstandigheden wordt gepresenteerd.

Een wiskundig adsorptiemodel wordt beschreven in **hoofdstuk 3** en **hoofdstuk 4**, en gevalideerd met experimentele resultaten. Het model gebruikt als input de gegenereerde adsorptie/desorptie-bindingsevenwicht gegevens en wordt toegepast voor het ontwerp van een industriële schaal adsorptie kolom tezamen met het ontwerp van de chromatografische cyclus. Dit karakteristieke “*batch*” model (1 kolom) wordt verder gebruikt voor optimalisatie (**hoofdstuk 5**) van de adsorptie van sinapinezuur om de productiviteit te maximaliseren.

Aangezien de voedingssector wordt gekenmerkt door continue procesvoering, is de verwerking van nevenstromen met behulp van eveneens continue technologieën efficiënter. Dit zou ook de toevoeging/circulatie van de teruggewonnen producten naar andere processen kunnen vergemakkelijken. Adsorptie is typisch een “*batch*” bewerking, maar systemen zoals “*Simulated Moving Bed*” (SMB) -technologie zorgen voor een continue werking. **Hoofdstuk 5** vergelijkt de prestaties van “*batch*”-operatie met het semi-continue systeem “*CaptureSMB*” om sinapinezuur terug te winnen. Het gebruikt het eerder ontwikkelde wiskundige adsorptiemodel om beide bedrijfsmodi te optimaliseren met als doel de productiviteit te maximaliseren voor een gegeven opbrengst (98%) en een minimaal “*resin*” gebruik van 70% om een efficiënte werking te garanderen. Deze studie toont duidelijk aan dat “*CaptureSMB*” beter presteert dan “*batch*” verwerking, en dat efficiënte continue adsorptie in de voedingssector niet alleen kan worden toegepast door de meer traditionele “*Simulated Moving Bed*” (SMB) -technologie.

De benadering ontwikkeld en gepresenteerd in **Hoofdstuk 3** tot **Hoofdstuk 5** wordt toegepast in een casestudie waar, in plaats van waardevolle producten te adsorberen, de onzuiverheden worden geadsorbeerd. **Hoofdstuk 6** presenteert als zodanig de opwaardering van een nevenstroom in de voedingsindustrie via een conceptueel procesontwerp. Deze studie toont aan dat het genereren van hoogwaardige producten uit voedselreststromen mogelijk en winstgevend is. Dit onderzoek toont aan hoe het gebruik van zijstromen belangrijk is in de benodigde transitie naar een circulaire economie.

# Chapter 1

## General Introduction & Thesis Outline

---

### Contents

1.1.	General Introduction .....	2
1.1.1.	The role of food side streams in a circular economy .....	2
1.2.	ISPT project CM-20-07 .....	4
1.3.	Thesis outline.....	4
1.4.	References.....	5

## 1.1. General Introduction

Society is facing several global challenges such as climate change, depletion of fossil resources, waste generation and proper (and fair) distribution of resources and food. To tackle the issue of wasting resources, concepts such as biorefinery are being established and applied. However, there are still many opportunities, regarding tackling the issue of waste generation.

Particularly, waste generated by the food sector (including production and consumers) contributes significantly to greenhouse global emissions, accounting around 7%.<sup>1, 2</sup> Food waste can be subdivided in a) production losses and b) consumers' waste (unavoidable and avoidable).<sup>3</sup> Regarding the waste generated by the consumers, it is important to encourage them to reduce this waste. Addressing the issue through direct communication, with marketing campaigns, has proven to be effective in the UK<sup>4</sup> (case study 2 Household food waste prevention (UK)).

In this work, production losses are defined as side streams generated specifically during the manufacturing of plant-based food products, e.g. fruit pomace (from juice production), olive mill wastewater, cereal bran, oilseed meal, amongst others. These side streams are sources of valuable components such as dietary fibers, natural antioxidants and proteins<sup>5</sup> just to mention a few. Currently, these side streams are discarded as waste (incineration) or are used for animal feed. This underestimates their potential applications in food, pharma and (bio)chemical sectors, opening the opportunity to investigate on how to recover these valuable compounds. Lately, it has been proved<sup>6</sup> that processing of these side streams into bulk or fine (bio)chemicals is more profitable than its conversion into energy, animal feed or biofuels.<sup>6</sup>

The use of these side streams fits in two important strategies suggested by the European Commission that aim to take action against the global challenges. The strategies are: the Circular Economy package<sup>7</sup> and the Bioeconomy strategy.<sup>8</sup>

The following paragraphs will give a brief overview of how the use of these food side streams contributes to the above mentioned initiatives and forms the motivation of this PhD dissertation.

### 1.1.1. The role of food side streams in a circular economy

Voluminous side streams are generated during animal and plant-based food processing. These particular side streams are sources of valuable products such as complex carbohydrates, proteins, polyphenols, lipids, amongst others. The presence of these valuable products opens the possibility to recover them and (re)used as raw materials in other processes (Figure 1).

In the circular economy concept, the main driver is to use waste as a resource and generate products out of it<sup>9</sup>. In addition, it aims to re-introduce/circulate these products which is considered sustainable.<sup>10</sup> The use of the recovered products significantly contributes in the transition to a circular economy as waste is minimized. However, this does not necessarily close the material loop (another objective of the circular economy initiative) as still some waste might be generated.

Currently, side streams generated by the food sector are mostly used for animal feed or generation of energy such as biogas, which is within the circular economy concept. As mention before, recovery of added-value products can also be done using these side streams. This fits in the bioeconomy strategy which aims to enhance the use of these biomaterials. Re-using/circulate the obtained new products from side streams can be done not only in the food sector (e.g proteins for human consumption<sup>11</sup>) but also in cosmetics (e.g. polyphenols as UV filters in sunscreen<sup>12</sup>) or (bio)chemical sectors (as building blocks for other chemicals).

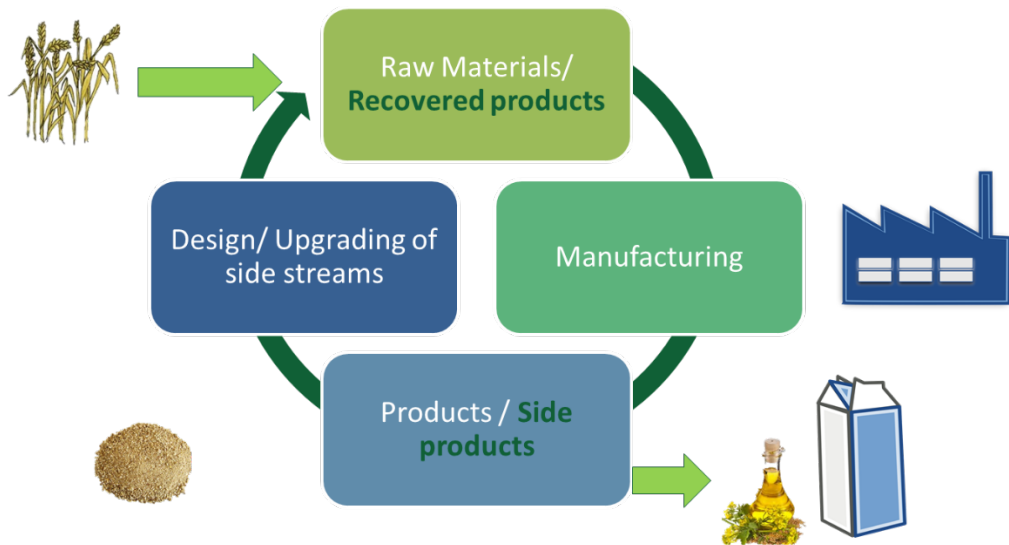


**Figure 1.** Food side streams in circular processing

As the bioeconomy strategy goal is to investigate innovative ways to use renewable resources for industrial applications, research on current or new technologies should be done to ensure the effective application (enhancement) of food side streams.

Research on producing/recovering valuable products from food side streams has recently increased all over the globe.<sup>5</sup> However, the use of these streams is still limited due to public acceptance and legislative pressure, which often increase the requirements of finding new methods to treat these streams. These requirements are in no doubt dependent to which sector the products will be applied and the necessary purity.

Strategies for product design<sup>13</sup> and recovery<sup>14</sup> could be adapted for the processing of these side streams, considering the type of side streams (liquid or solid) and the valuable compounds to be recovered. The processing train might include different stages – pretreatment, volume reduction, phase change, purification & conversion and formulation – that can be defined with conventional or emerging technologies<sup>15</sup>.

This thesis focusses on adsorption as purification (separation) technology. It is a powerful technique that allows separation of complex mixtures and can be operated at mild conditions. Mild conditions are

often desired within the food sector as thermal processes might generate undesirable components (off-flavors) and product degradation (loss of nutritional value and functionality<sup>16</sup>). Many efforts have been put in developing the application of adsorption in the food sector. It has been successfully implemented in large scale for the separation of fructose and glucose,<sup>17-19</sup> and desugarization of molasses.<sup>19</sup> Other studies have shown promising results for debittering of citrus juices.<sup>20</sup> However, the application of adsorption in other food processes is still limited due to it is considered an expensive technology. This opens the possibility to investigate and better understand the interaction between components and the adsorbents for proper application at industrial scale.

## 1.2. ISPT project CM-20-07

The project CM-20-07 *Adsorption of non-volatiles from food products* was defined under the umbrella of the Institute for Sustainable Process Technology (ISPT). This project is co-funded by TKI-E&I with the supplementary grant 'TKI- Toeslag' for Topconsortia for Knowledge and Innovation (TKI's) of the Ministry of Economic Affairs and Climate Policy. The project is performed at Delft University of Technology (TU Delft) in close collaboration with the industry through the ISPT cluster "Mild Fractionation for Food".

The main objective of this project is to evaluate different possibilities to selectively recover/remove different components (valuable or non-valuable) from a plant-based food side stream. Adsorption is selected as separation/recovery technique as it has been proven to be promising for capture of polyphenols,<sup>21-24</sup> proteins,<sup>25, 26</sup> sugars<sup>27</sup> and flavor components.<sup>28-30</sup> In this project, existing adsorption technologies are implemented or new ones are adapted to recover/remove the target components keeping in mind the importance of economic feasibility.

To evaluate the project different activities are defined namely: 1) adsorbent screening (using high throughput experimentation and robotics) for fast and appropriate selection of an adsorbent that selectively captures the target components. 2) determination of equilibrium information. This with the goal of understanding the interaction between the components and the adsorbents and applying different isotherms models. In addition, isotherms are used in mathematical mechanistic column models for 3) optimization and comparison on different operating modes (fixed packed bed and continuous adsorption. 4) Finally, a conceptual process design for upgrading a food side stream is generated. The use of adsorption in food industry is evaluated in this project using two case studies provided by industry, one with the goal of capturing via adsorption valuable products and the other with the goal of capturing the impurities.

## 1.3. Thesis outline

The work developed in this thesis aimed to valorize different plant-based food side streams for the recovery of valuable products by applying adsorption as a separation/recovery technology. In addition, it meant to evaluate a feasible process for the upgrading of a food side streams.

In **Chapter 2**, the different valuable compounds present in the plant-based side streams were identified and discussed. The different process steps that are required for the recovery of the valuable products were also presented with a holistic strategy. From this review it is recognized that adsorption is a

promising technology for recovering/removing target components (valuable or non-valuable) with high purity.

Two case studies were selected for valorization of valuable compounds and their recovery. The first case study uses rapeseed meal to recover proteins (albumins and globulins) and antioxidants (sinapic acid). Adsorption was selected as a capturing technique for all products. Rapeseed proteins and polyphenols can be separated from each other using membrane techniques due to their difference in size. Sinapic acid has proven to have antioxidative and antimicrobial activities and can be used in food, cosmetic and pharmaceutical sectors. A set of different food-grade hydrophobic resins are evaluated in **Chapter 3**, for their ability to selectively capture this compound over sugars, glucosinolates and phytic acid. Moreover, adsorption and desorption isotherms are measured.

Proteins from rapeseed meal have shown similar characteristics than proteins from eggs or soybeans, therefore they are potential candidates to satisfy protein demand for humans. **Chapter 4** discusses a high throughput process development (HTPD) approach for the separation and purification of these proteins. Different cation exchangers and mixed mode resins are compared with the objective of capturing napin (albumin protein fraction) and flow through cruciferin (globulin protein fraction). High throughput experimentation (HTS) is successfully applied to identify adsorption/desorption equilibrium.

The equilibrium data of both set of products (proteins and polyphenols) is used as an input in a column (adsorption) mechanistic model (**Chapter 3** and **Chapter 4**), which is experimentally validated for both cases and the validated adsorption model is used for industrial scale design.

As voluminous food side streams are usually generated, it is important to adapt typical batch adsorption operation into continuous mode. **Chapter 5** clearly demonstrates the benefits of semi-continuous adsorption, comparing fixed bed batch adsorption with the semi-continuous system CaptureSMB. The previously defined column model is adapted to CaptureSMB operation mode and validated. In -silico adsorption optimization at industrial scale is presented in this chapter for both operating modes.

Finally, following the same approach from previous chapters, the techno-economic feasibility of using a food wastewater stream to produce a valuable product was assessed (**Chapter 6**). In this process the critical step is the *removal of unwanted* components (off-flavors) which was done using a food grade hydrophobic resin. The simulation program SuperPro Designer is used to solve mass and energy balances of the designed process and the economic potential is determined. This chapter is a clear example of how the recovery of a high value product (instead of conversion into energy) from a food side stream can be profitable.

## 1.4. References

- 1 Food and Agriculture Organization of the United Nations (FAO), 2014, Food wastage footprint - full-cost accounting - final report (accessed 25 August 2020). <http://www.fao.org/3/a-i3991e.pdf>:
- 2 Slorach P.C., Jeswani H.K., Cuéllar-Franca R., Azapagic A., Environmental and economic implications of recovering resources from food waste in a circular economy, Science of The Total Environment, 693 (2019) 133516.

- 3** Maina S., Kachrimanidou V., Koutinas A., A roadmap towards a circular and sustainable bioeconomy through waste valorization, *Current Opinion in Green and Sustainable Chemistry*, 8 (2017) 18-23.
- 4** Food and Agriculture Organization of the United Nations (FAO), 2014, Mitigation of Food Waste. Societal costs and benefits (accessed 25 August 2020). <http://www.fao.org/3/a-i3989e.pdf>
- 5** Virtanen S., Chowreddy R.R., Irmak S., Honkapää K., Isom L., Food Industry Co-streams: Potential Raw Materials for Biodegradable Mulch Film Applications, *Journal of Polymers and the Environment*, (2016) 1-21.
- 6** Tuck C.O., Pérez E., Horváth I.T., Sheldon R.A., Poliakoff M., Valorization of Biomass: Deriving More Value from Waste, *Science*, 337 (2012) 695-699.
- 7** European Commission, 2017, Circular Economy - European Commission (accessed 11 August 2017). [https://ec.europa.eu/growth/industry/sustainability/circular-economy\\_en](https://ec.europa.eu/growth/industry/sustainability/circular-economy_en)
- 8** European Commission, 2018, A sustainable Bioeconomy for Europe: strengthening the connection between economy, society and the environment (accessed 25 August 2020). [https://ec.europa.eu/research/bioeconomy/pdf/ec\\_bioeconomy\\_strategy\\_2018.pdf](https://ec.europa.eu/research/bioeconomy/pdf/ec_bioeconomy_strategy_2018.pdf)
- 9** Ghosh S.K., Introduction to Circular Economy and Summary Analysis of Chapters, in: S.K. Ghosh (Ed.) *Circular Economy: Global Perspective*, Springer Singapore, Singapore, 2020, pp. 1-23.
- 10** Teigiserova D.A., Hamelin L., Thomsen M., Towards transparent valorization of food surplus, waste and loss: Clarifying definitions, food waste hierarchy, and role in the circular economy, *Science of The Total Environment*, 706 (2020) 136033.
- 11** Wanasundara J.P.D., McIntosh T.C., Perera S.P., Withana-Gamage T.S., Mitra P., Canola/rapeseed protein-functionality and nutrition, *OCL*, 23 (2016) D407.
- 12** Galanakis C.M., Tsatalas P., Galanakis I.M., Implementation of phenols recovered from olive mill wastewater as UV booster in cosmetics, *Industrial Crops and Products*, 111 (2018) 30-37.
- 13** Almeida-Rivera C., Bongers P., Zondervan E., Chapter 15 - A Structured Approach for Product-Driven Process Synthesis in Foods Manufacturea, in: M. Martín, M.R. Eden, N.G. Chemmangattuvalappil (Eds.) *Computer Aided Chemical Engineering*, Elsevier, 2016, pp. 417-441.
- 14** Galanakis C.M., *Food Waste Recovery - Processing Technologies and Industrial Techniques*, Elsevier, USA, 2015.
- 15** Galanakis C.M., Recovery of high added-value components from food wastes: Conventional, emerging technologies and commercialized applications, *Trends in Food Science & Technology*, 26 (2012) 68-87.
- 16** Moure A., Sineiro J., Domínguez H., Parajó J.C., Functionality of oilseed protein products: A review, *Food Research International*, 39 (2006) 945-963.
- 17** Azevedo D.C.S., Rodrigues A.E., Fructose-glucose separation in a SMB pilot unit: Modeling, simulation, design, and operation, *AIChE Journal*, 47 (2001) 2042-2051.
- 18** Hashimoto K., Continuous separation of glucose-salts mixture with nonlinear and linear adsorption isotherms by using a simulated moving-bed adsorber, *Journal of Chemical Engineering of Japan*, 20 (1987) 405.

- 19 Ganetsos G., Barker P., Developments in large-scale batch chromatography, in: G. Ganetsos, P. Barker (Eds.) Preparative and production scale chromatography, 1992, pp. 3-10.
- 20 Kranz P., Adler P., Kunz B., Sorption of citrus flavour compounds on XAD-7HP resin during the debittering of grapefruit juice, *International Journal of Food Science & Technology*, 46 (2011) 30-36.
- 21 Soto M.L., Moure A., Domínguez H., Parajó J.C., Recovery, concentration and purification of phenolic compounds by adsorption: a review, *Journal of Food Engineering*, 105 (2011) 1-27.
- 22 Weisz G.M., Schneider L., Schweiggert U., Kammerer D.R., Carle R., Sustainable sunflower processing — I. Development of a process for the adsorptive decolorization of sunflower [*Helianthus annuus* L.] protein extracts, *Innovative Food Science and Emerging Technologies*, 11 (2010) 733-741.
- 23 Silva M., Castellanos L., Ottens M., Capture and Purification of Polyphenols Using Functionalized Hydrophobic Resins, *Industrial & Engineering Chemistry Research*, 57 (2018) 5359-5369.
- 24 Sevillano D.M., van der Wielen L.A.M., Hooshyar N., Ottens M., Resin selection for the separation of caffeine from green tea catechins, *Food and Bioproducts Processing*, 92 (2014) 192-198.
- 25 Bérot S., Compoin J., Larré C., Malabat C., Guéguen J., Large scale purification of rapeseed proteins (*Brassica napus* L.), *Journal of Chromatography B*, 818 (2005) 35-42.
- 26 Sewekow E., Kessler L.C., Seidel-Morgenstern A., Rothkötter H.-J., Isolation of soybean protein P34 from oil bodies using hydrophobic interaction chromatography, *BMC biotechnology*, 8 (2008) 27.
- 27 Chilamkurthi S., Willemsen J.-H., van der Wielen L.A.M., Poiesz E., Ottens M., High-throughput determination of adsorption equilibria for chromatographic oligosaccharide separations, *Journal of Chromatography A*, 1239 (2012) 22-34.
- 28 Gernat D.C., Penning M.M., Swinkels F.M., Brouwer E.R., Ottens M., Selective off-flavor reduction by adsorption: A case study in alcohol-free beer, *Food and Bioproducts Processing*, 121 (2020) 91-104.
- 29 Kaneda H., Takashio M., Shinotsuka K., Okahata Y., Adsorption to or desorption of beer components from a lipid membrane related to sensory evaluation, *Journal of Bioscience and Bioengineering*, 92 (2001) 221-226.
- 30 Saffarionpour S., Ottens M., Recent Advances in Techniques for Flavor Recovery in Liquid Food Processing, *Food Engineering Reviews*, 10 (2018) 81-94.



# Chapter 2

## A structured approach to recover valuable compounds from agri-food side streams

---

### Abstract

Food side streams contain useful compounds such as proteins, sugars, polyphenols and amino acids that might get discarded during processing. Research to recover valuable components from different food side streams has increased in the past years. The concentration of these components may be low and therefore effective separation techniques should be evaluated.

The aim of this review is to identify the different process steps required to recover high-value products from agri-food residues. Therefore, this work reviews different plant-based byproducts as sources (cereal bran, fruit pomace, oilseed meals, fruit wastewater) of valuable compounds and the high value products such as proteins and nutraceuticals that can be purified from these sources. Furthermore, it discusses the different processing steps and relevant applied technologies required for processing to purify diverse valuable compounds. Multiple high-value products can be recovered from a single agri-food side stream depending on the processing steps and the origin source.

**Keywords:** Valorization of food side streams, protein, polyphenols, separation technologies

---

*Submitted for publication*

## Table of Contents

Abstract.....	9
2.1. Introduction.....	11
2.2. Food side streams valuable products .....	12
2.3. Plant-based byproducts processing: recovery and purification techniques .....	18
2.3.1. Milling and pretreatment of agri-food byproducts.....	19
2.3.2. Valuable compounds extraction from agri-food byproducts .....	19
2.3.3. Purification of valuable compounds from plant-based extracts .....	21
2.3.3.1. Protein purification .....	21
2.3.3.2. Polyphenol purification .....	22
2.3.3.3. Polysaccharides purification.....	23
2.3.3.4. Flavor ingredients recovery /purification.....	23
2.3.4. Final product formation .....	24
2.3.4.1. Food powders/ solid extracts .....	24
2.4. Food byproducts processing examples.....	25
2.5. Concluding remarks .....	28
2.6. References.....	29

## 2.1. Introduction

The increasing waste generation and the limited availability of natural resources has motivated the scientific community to investigate possibilities to recover valuable products from different waste streams such as wastewater and agri-food residues.

Food industry is recognized as one of the most important industries in the world but generates a significant amount of waste<sup>1</sup>. On December 2015, the European commission established a package to motivate EU members to move in the direction of a more circular economy<sup>2</sup> and has taken the issue of food waste generation with seriousness. According to the European Commission (2014)<sup>3</sup>, most of the waste is produced by the food manufacturing sector, and by 2020 is expected to rise to 126 million tons compared to 96 million tons generated in 2007<sup>4</sup>. In order to contribute to this initiative, side streams of food industry can become inputs of other processes as they are sources of proteins, lipids, complex carbohydrates and nutraceuticals. Therefore, valorization and recovery of high-value products from food byproducts is an attractive area that has been investigated lately around the globe <sup>1</sup>. Recently, it has been proven that the conversion of biomass waste to bulk chemicals might be more profitable than its conversion to animal feed or transportation fuel<sup>5</sup>. In addition, increasing protein demand due to population growth could be satisfied by using plant-based residues as proteins from canola meal resulted to be competitive and suitable for human consumption.<sup>6</sup>

Among the generated food byproducts, plant-based byproducts include: fruit pomace, oilseed meals, cereal brans, wastewaters, etc. These residues are rich sources of dietary fiber (cellulose, hemicellulose and lignin) and could be used within the biorefinery concept to produce biofuels or biochemicals from their respective hydrolysates. However, proteins and other nutraceuticals, mainly phenolic compounds (presented in the outer layers of most plant-based products<sup>7</sup>) could be recovered. Extraction of proteins and nutraceuticals might be a fundamental step in order to recover more valuable compounds from food byproducts.

This review describes and discusses the different valuable products presented exclusively in plant-based byproducts, such as oilseed meals, pea pods, cereal brans, fruit pomace amongst others. This is followed by the discussion of the different process techniques needed to recover these valuable compounds. Commonly, in these agri-food side streams, valuable compounds concentration is low (diluted systems, e.g. wastewater) and additionally the presence of other low values impurities such as off-flavors and insoluble solids represents a technological challenge. Recovery and purification of the valuable compounds presented will additionally depend on the composition and volume of the side streams. Therefore, it is important to define different process stages. Combining the information available in literature for processing <sup>8,9</sup> with some modifications, a generalized process flow scheme as the one defined in Figure 2.1, could be applied as an starting point for the process synthesis of agri-food side streams.

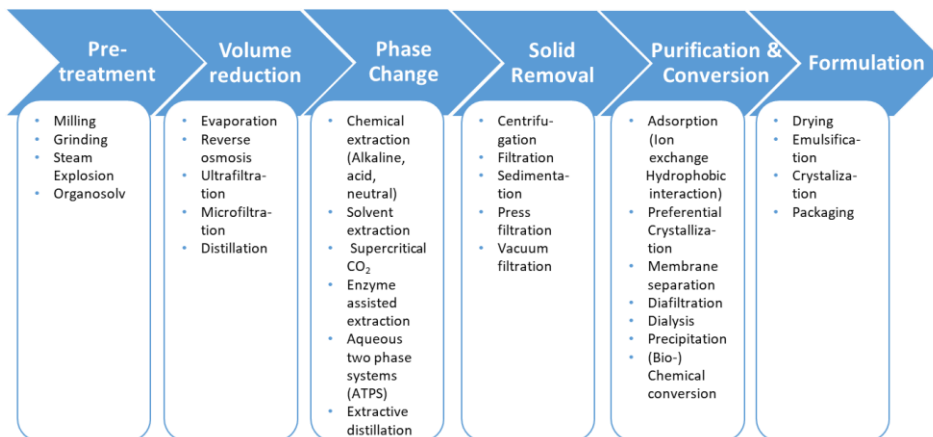


**Figure 2.1.** Process flow scheme for processing of agri-food side streams

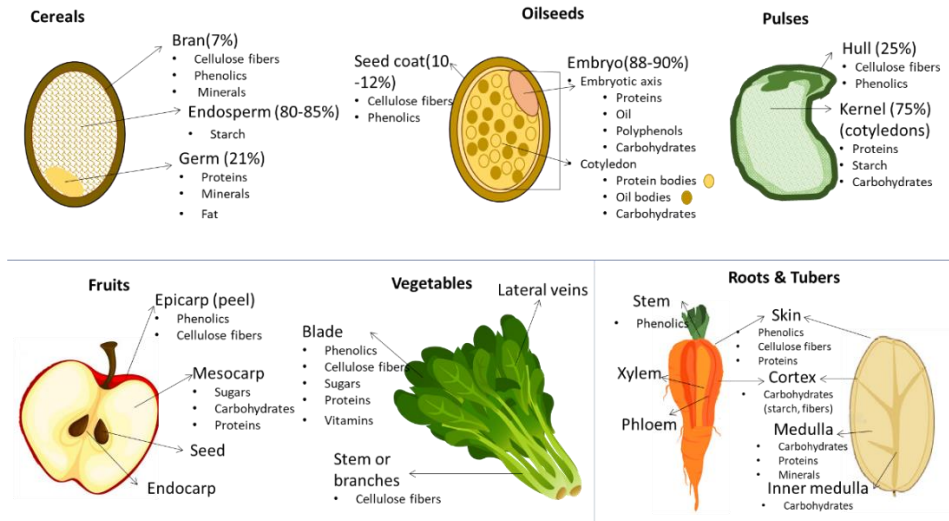
The objective of the pretreatment step is to break the strong-linked structure of (solid) agri-food residues, such as cereal bran, in order to facilitate following processing steps, this might lead to recovery and purification of dietary fibers, or to conversions on sugars into biofuels. It is important to keep in mind that not all agri-food residues possess this strong matrix, therefore this step is dependent of the source and the products to be recovered. For voluminous fruit and vegetable wastewaters, a volume reduction step is suggested at the beginning of the purification train, with the objective to concentrate and decrease volumetric load in the following steps. The third step, phase change, aims to extract the valuable components to a (different) liquid phase. The remained solids are removed (solid removal) and could be additionally treated for recovery of other products such as dietary fiber. The obtained liquid stream undergoes to a purification steps, where the different compounds are separated or converted into other (bio) chemicals (e.g. sugars into bioethanol) and finally the last stage corresponds to formulation. This last stage has as a main objective to get the product to its final form, e.g. powders and emulsions. The different unit tasks that can be applied in each stage of the processing of agri-food products are additionally indicated in Figure 2.1.

This work discusses the different technologies for processing agri-food side streams to recovery valuable compounds as described in Figure 2.1. Moreover, it provides an overview of possible purification processes of proteins, polyphenols and dietary fibers from different plant-based starting materials

## 2.2. Food side streams valuable products

The co-streams from food can be originated from several branches mainly divided in two main groups, plant based and animal based. This study will only focus on plant-based byproducts and their valuable compounds. Plant-based byproducts can be additionally subdivided in four groups namely: (1) cereals, (2) roots & tubers, (3) oil crop and pulses and (4) fruits & vegetables<sup>10</sup>. The average composition and the distribution of the different nutrients from plant-based sources are presented in Figure 2.2 while Table 2.1 summarizes different plant-based byproduct sources and the valuable products that could be recovered.

a)



b)

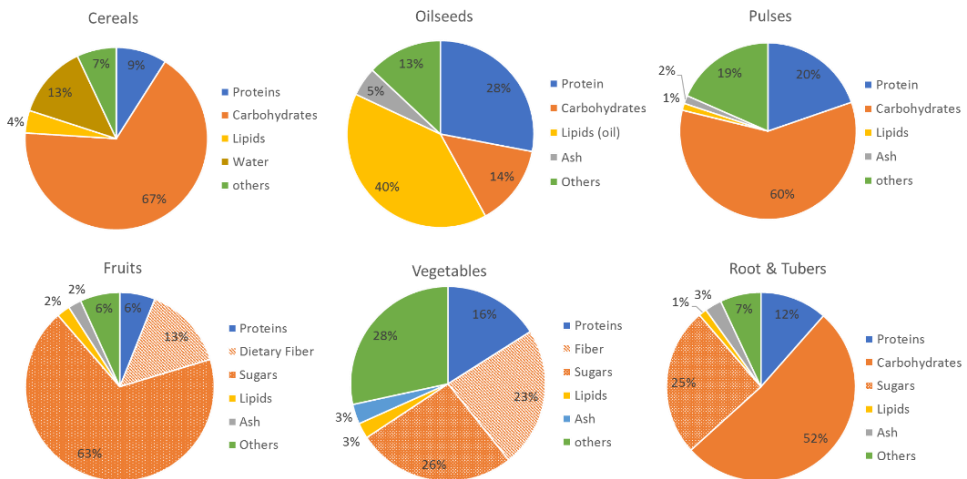


**Figure 2.2.** Plant-based sources composition. a) Nutrient distribution, b) Proximate composition. Adapted from Naczek, et al.<sup>7</sup> Butnariu, et al.<sup>11</sup> Carrillo-López, et al.<sup>12</sup> González-Pérez, et al.<sup>13</sup> Islam, et al.<sup>14</sup> List<sup>15</sup> Rosell, et al.<sup>16</sup> Shukla, et al.<sup>17</sup>

Cereal grains possess three botanical parts, endosperm germ and bran. The bran is usually separated from the cereal grain, during milling operations, as it might have negative effects with the final product<sup>18</sup> such as darker colors. However, cereal brans are sources of nutritional compounds such as

polyphenols, dietary fibers and minerals<sup>19</sup>. Different studies have shown the potential of using wheat bran as a source of valuable compounds. Rosa-Sibakov, et al.<sup>18</sup> compared the application of wheat bran in different baking products to increase their nutritional value. The study of Ahmad, et al.<sup>20</sup> demonstrated the different polyphenols available in wheat, barley, millet and sorghum brans, assessing the antioxidant profiles, showing that millet and sorghum brans contain higher antioxidant activities than wheat and barley. Other byproducts obtained from the cereal sources are, husks and straw which are rich on dietary fibers, glucoarabinobinoxylans<sup>21</sup> and proteins.<sup>22</sup> Wheat, oat, barley and rice straw are rich lignocellulosic biomasses around the world<sup>23</sup> and can be used in biorefineries to obtain second generation bioethanol or building blocks for other chemicals.

Fruit and vegetable byproducts involve peels, leaves, pomace and kernels, which are generated depending of the processing technology (juices, jams canning, jellies etc.). The side streams generated are mostly composed of water and hydrocarbons (80%-90%) with a low percentage of fat and proteins<sup>24, 25</sup>. Orange peel is a rich source of essential oils (limonene), carotenoids, phenolic antioxidants and pectin<sup>26-29</sup>. A broad range of food products can be derived from this fruit namely sweet orange oil, orange blossom, honey or marmalade<sup>30</sup>. Residues from pigmented orange pulp were valorized by Scordino, et al.<sup>31</sup> and successfully treated to recover sugars, citric acid and pectin. Moreover, citrus fruits are rich on flavonoids, D-limonene, pulp and molasses (sugars) and essences<sup>1</sup>. Around twenty five percent of the processed apple is represented by apple pomace<sup>32</sup> and it is a natural source for commercial pectin around the world. In addition, it is also characterized by a high content of carbohydrates (cellulose, hemicellulose) and important polyphenols such as catechins, flavanols, hydroxycinnamates and anthocyanins<sup>33</sup>. Grape pomace, the byproduct of wine production, are rich sources of dietary fiber, oil and phenolic compounds (anthocyanins and flavanols)<sup>34</sup>. While tomato pomace is rich source of lycopene (principal carotenoid) proteins, dietary fiber and oil<sup>35</sup>. In addition, olive byproducts, olive mill wastewater, pomace, leaves and seed are important sources of phenolic compounds, pectin, polysaccharides and lignocellulosic fibers.<sup>36</sup>

According to Food and Agriculture Organization of the United Nations (FAO)<sup>37</sup>, cassava, potatoes, sweet potatoes, yams and carrots are the main root and tubers produced worldwide. Many bioactive compounds can be found in the byproducts of these food products, such as dietary fiber, proteins, antioxidants and starch<sup>24, 38-44</sup>. For instance, potato peel composition consists mainly of dietary fiber (around 50%)<sup>38</sup> and phenolic compounds<sup>45</sup>. Polyphenol antioxidative activity, from potato peel extracts, has been evaluated by Rodriguez de Soltillo, et al.<sup>40</sup> showing a similar performance that butylated hydroxyanisole (BHA) which is a food additive commonly used in food products to prevent rancidity<sup>46</sup>. Carrot pomace, accounts around 50% of the raw material during carrot juice production. This pomace still contains a significant amount of  $\alpha$ - and  $\beta$ -carotene, which can be recovered and used as functional ingredient<sup>47</sup>. Similarly, sweet potato peels contain important antioxidants with chlorogenic acid the highest phenolic in the root tissues<sup>48</sup>.

At last, oilseed (flaxseed, canola/rapeseed, sunflower and cotton) meals are rich sources of proteins, mainly storage proteins of two types, globulins and albumins<sup>49, 50</sup>. Fleddermann, et al.<sup>51</sup> evaluated the amino acids composition of canola meal proteins and compared with the one from soy protein for human nutrition. The authors demonstrated that the bioavailability of the proteins from canola protein isolate and soy protein isolate is similar, proving that are canola proteins are relevant for nutrition.<sup>51</sup> In addition, oilseed meal are sources of polyphenols, such as sinapic acid (mayor phenolic acid in rapeseed)<sup>52</sup> which possesses antioxidant, antimicrobial and anti-inflammatory properties<sup>53</sup>.

Beans, chick peas, lentils lupins and peas are the most cultivated and consume pulses<sup>37</sup>. The byproducts generated after processing pulses include: broken grains, husks, powder, unprocessed seeds and shriveled pulses.<sup>24</sup> Mateos-Aparicio, et al.<sup>54</sup> evaluated byproducts of pea, broad bean and okara (soybean byproduct) as rich sources of dietary fiber and polyphenols<sup>55</sup>. Moreover, the authors identified high quantity of vegetable proteins (around 30% dry matter) and fat (8.5% composed by linoleic and oleic acid) in okara which could be potentially recovered.

Using the process scheme presented in Figure 2.1 and applying well-established methodologies such as the 5-stage universal recovery strategy proposed by Galanakis<sup>10</sup> or the product-driven process synthesis<sup>56</sup> the processing of these agri-food side streams could be defined.

**Table 2.1.** Sources of plant-based byproducts and the potential valuable compounds

Source	Byproducts	Valuable compounds	Reference
<b>Cereals</b>			
<b>Barley</b>	Bran Malt Straw	Polyphenols (hydroxycinnamic acids) Protein Dietary fiber	Ahmad, et al. <sup>20</sup> , Szwajgier, et al. <sup>57</sup>
<b>Corn</b>	Cods  Husk Silks	Dietary fiber (cellulose and xylans) Minerals (P, K, Mg) Proteins Polyphenols Starch	Pfaltzgraff, et al. <sup>23</sup> , Lau, et al. <sup>58</sup>
<b>Oat</b>	Bran Straw	$\beta$ -glucan Polyphenols	Patsioura, et al. <sup>59</sup>
<b>Rice</b>	Bran  Straw	Proteins Dietary fiber Polyphenols Lipids Xylans	Ahmad, et al. <sup>20</sup> , Prakash, et al. <sup>22</sup> , Sohail, et al. <sup>60</sup> , Liu, et al. <sup>61</sup> , Orthoefer <sup>62</sup>
<b>Wheat</b>	Bran	Proteins Arabinoxylan $\beta$ -glucan	Ahmad, et al. <sup>20</sup> , Baladrán-Quintana, et al. <sup>63</sup>

<i>Source</i>	<i>Byproducts</i>	<i>Valuable compounds</i>	<i>Reference</i>
<b>Cereals</b>			
	Straw	Polyphenols (ferulic, sinapic and p-coumaric, flavonoids) Cellulose Xylans	
<b>Root &amp; Tubers</b>			
Asparagus	Roots	Carbohydrates Phenolics (flavonoids and hydroxycinnamic acids) Protein Saponins Oil	Zhang, et al. <sup>64</sup>
Carrots	Pomace	Dietary fiber $\alpha$ - and $\beta$ -carotene Sugars Uronic acids	Sharma, et al. <sup>43</sup> , Nawirska, et al. <sup>44</sup>
	Peel	Carotenoids	
Cassava	Peels	Starch Dietary fiber Protein	Mullen, et al. <sup>24</sup> , Versino, et al. <sup>41</sup> , Ubalua <sup>42</sup>
	Pomace Bagasse	Lipids Starch	
Potato	Peel	Dietary fiber Proteins Polyphenols (chlorogenic and hydroxycinnamic acid) Sugars Vitamins (B)	Mullen, et al. <sup>24</sup> , Camire, et al. <sup>38</sup> , Arapoglou, et al. <sup>39</sup> , Rodriguez de Soltillo, et al. <sup>40</sup>
	Stillage (distillery water)	Amino acids	
	Pulp	Pectin	

Source	Byproducts	Valuable compounds	Reference
<b>Oil Crops &amp; pulses</b>			
Hazelnut/ Almond/ Peanut	Hard shells Skin Leaf Hull	Phenolics compounds (catechin, hydroxycinnamic acids, phenyl benzoic acid)	Siriwardhana, et al. <sup>65, 66</sup>
Oilseed	Oilseed meals (rapeseed, sunflowers, flaxseed, cotton)	Proteins Polyphenols Dietary fiber	49, 50
Pea	Pod Husk Broken grains Powder Cotyledon	Dietary fiber Proteins Phenolics (Hydroxycinnamic acids)	Mateos-Aparicio, et al. <sup>54</sup> . Mateos-Aparicio, et al. <sup>55</sup>
<b>Fruits &amp; vegetables</b>			
Apple	Peel Pomace Seeds	Dietary fiber Pectin Polyphenols (catechins and proanthocyanidins)	Mourtzinou, et al. <sup>33</sup> , Sudha <sup>67</sup>
Pineapple	Peel Core Stem Shells	Dietary fiber Proteins (bromelain) Starch Polyphenols (myricetin, salicylic acid and tannic acid)	Roda, et al. <sup>68</sup> , Larrauri, et al. <sup>69</sup> , Seguí Gil, et al. <sup>70</sup>
Orange	Peel Pomace	Dietary fiber Essential oils (limonene) Pectin Phenolics (Flavonoids) Carotenoids	Espina, et al. <sup>26</sup> , May <sup>27</sup> , Chedea, et al. <sup>28</sup> , Aravantinos-Zafiris, et al. <sup>29</sup> , Scordino, et al. <sup>31</sup>
Tomato	Pomace  Peels Seeds	Lycopene Dietary fiber Pectin Polysaccharides Proteins Oil	Lu, et al. <sup>35</sup>
Broccoli	Pomace Stems Leaves	Proteins Dietary fiber Polyphenols (chlorogenic, neochlorogenic and quinic acids)	Shi, et al. <sup>71</sup>

### 2.3. Plant-based byproducts processing: recovery and purification techniques

After the identification of the valuable components, processing of food side streams will undergo several steps (Figure 2.1) and actual process synthesis will require different unit tasks. Depending on the source origin, some of the steps presented in Figure 2.1 could be removed. In this work, source origin is divided in three groups: 1) lignocellulosic biomass which are characterized by plant fibers with a strong structure (e.g. cereal brans, oilseed meals), 2) fruit and vegetable pomaces (softer structures) and 3) fruits and vegetable wastewater (e.g. olive mill wastewater).

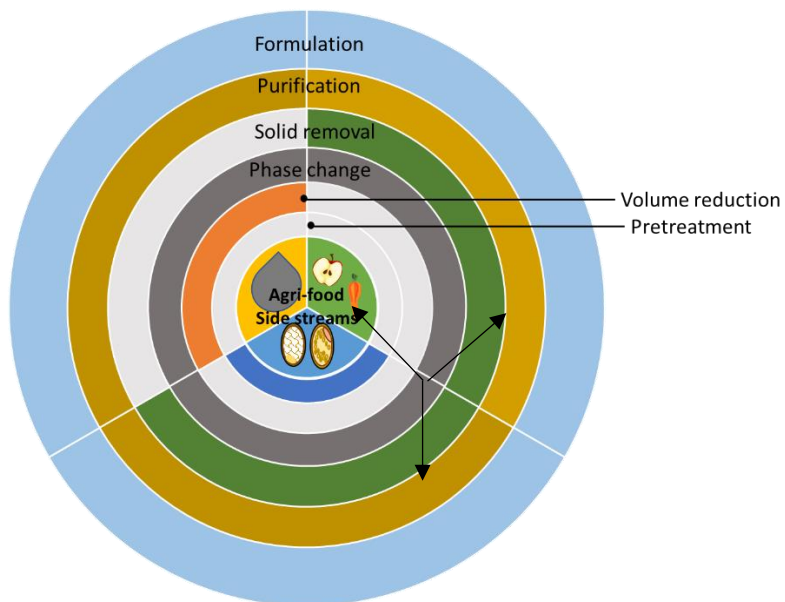


**Figure 2.3.** Process flow scheme depending on source origin. Different process steps are indicated in each concentric circle. Three sources: strong plant-matrix (blue, center circle lower), soft plant-based matrix (green, center circle upper right) and wastewater (yellow, center circle upper left). Processing steps start from the center of the figure to outside. Uncolored part of concentric circle indicates the process step that is not required for that source type

Considering strong structure side streams, such as bran from cereals, it has been proved that mechanical and thermal treatments<sup>72</sup> of these solids improve the subsequent steps of the processing (pretreatment). The next step would correspond to the extraction of the components from the plant-based matrix to a liquid state (phase change). Depending on the conditions and medium to be used during the extraction, other components (valuable and non-valuable) might be co-extracted, therefore separation and purification of the target components is required (solid removal and purification). Lastly, the final product will be formulated with a drying phase to remove water and generate the product form (e.g. powder).

For soft matrixes, such as fruit pomaces, pretreatment might not be needed and extraction of valuable products could be directly applied followed by purification and formulation. While for food wastewater

streams a volume reduction step is important in order to concentrate the streams and reduce the large volume generated. This will additionally benefit the overall process as smaller equipment would be needed for processing.

The following paragraphs of this section describe and discuss the different technologies that have been applied for processing plant-based residues (milling and pretreatment, extraction, purification and formulation). It gives especially attention to adsorption as it proves to be the most promising purification technique for recovery of valuable products. Note that the downstream processing of the plant-based byproduct will be dictated by the components to be recovered and the nature of the source.

### 2.3.1. Milling and pretreatment of agri-food byproducts

Milling is a common operation in cereal, legumes and oilseed processing as this operation generating several byproducts such as hulls, husk, seed coat, bran, among others. As previously mentioned, these byproducts are rich in bioactive compounds such as polyphenols, proteins or dietary fibers (cellulose, hemicellulose). If the aim is to recover proteins and polyphenols these byproducts can be sent to the extraction phase after grinding in order to homogenize particle size.

A by-product from cereals is lignocellulosic biomass that can be implemented in a biorefinery concept for the production of sugars and further conversion into biofuels or other chemicals. When this is intended, a pretreatment step is required in order to make the enzymes or enzyme producing microorganisms accessible to the plant matrix. Many lignocellulosic biomass pretreatment techniques have been developed since early 2000 which involved mechanical pretreatments, such as physical pretreatment (milling), physicochemical pretreatments and chemical and biochemical pretreatments. For further information about lignocellulosic pretreatment the reader is referred to the work of Agbor, et al.<sup>72</sup>, Sun, et al.<sup>73</sup>, and Zhang, et al.<sup>74</sup>.

The goal of pretreatment is to increase the accessibility of enzymes, to hydrolyze cellulose and hemicellulose into reducing sugars, available in the solid biomass. Chemical and biochemical pretreatments are often the extraction methods for other compounds such as proteins and polyphenols which are discussed in the following section.

### 2.3.2. Valuable compounds extraction from agri-food byproducts

Proteins, polyphenols and soluble dietary fiber (oligosaccharides) can be co-extracted from different plant-based byproducts. Extraction techniques can be classified into chemical, physical-chemical and biochemical extraction.<sup>75</sup>

Among chemical extraction, solvent extraction and aqueous extraction have been widely applied. Capellini, et al.<sup>76</sup> developed a new method to extract oil from rice bran using safe solvents (ethanol and isopropanol) and mixtures of these solvents with water. The authors obtained around 80% yield of oil with pure ethanol and isopropanol. Additionally, the authors identified that the yield of co-extracted proteins varied up to 20% depending on the solvent, water content and extraction temperature. The remained protein fraction stays in the defatted rice bran meal however, the type of solvent and extraction conditions might affect the solubility and functional properties of the proteins.

Traditionally, pectin is extracted mainly from orange peel and apple pomace, in which pectin content ranges from 20 to 40 g/100 g on dry weight basis<sup>77</sup>, through a process called conventional acid extraction. It makes use of hot water acidified with a mineral or organic acid (e.g. H<sub>2</sub>SO<sub>4</sub>), however the use of strong acid leads to the generation of toxic waste, which should be neutralized before disposal. Additionally, the high temperature and long extraction time can lead to degradation of the pectin structure and decrease in functionality.<sup>78, 79</sup> Other innovative extractive techniques have been studied to recover pectin, such as ultrasound-assisted heating extraction<sup>80</sup>, ohmic heating<sup>79</sup>, ultra-high pressure<sup>81</sup>, microwave-assisted extraction<sup>82</sup> or the use of electric fields<sup>83</sup>.

Lycopene, which is an important carotenoid with antioxidant properties has been extracted from tomato pomace and tomato peel using solvent extraction with hexane, ethyl acetate, and ethanol with yields ranging between 5mg/100g (using ethanol) and 120 mg/100g (using ethyl acetate).<sup>84</sup> However, due to all the environmental implications of using organic solvents other technologies have been suggested and successfully applied for the extraction of lycopene. Among these technologies supercritical CO<sub>2</sub> extraction is suggested as a sustainable alternative, which leads to comparable extraction yields than the ones obtained with conventional solvent extraction. Topal, et al.<sup>85</sup> and Kehili, et al.<sup>86</sup> evaluated different operating conditions, temperature and pressure, using supercritical CO<sub>2</sub> extraction on tomato peel. The authors obtained 94% and 57% yield of total carotenoids respectively, using this emerging technique.

Essential oils from citrus fruits have been extracted from the citrus peel by several physical-chemical, mechanical and thermal techniques, such as cold pressing, solvent extraction, steam distillation and microwave assisted extraction.<sup>87</sup> Ferhat, et al.<sup>88</sup> extracted essential oils from lemon peels using cold pressing, hydrodistillation and microwave-accelerated distillation. In hydrodistillation, the plant material is packed and water is added (sufficient amount) and brought to boil, steam is then introduced and contacted with the plant material and the water producing the release of the components by hydrodiffusion and hydrolysis. Microwave-accelerated distillation consists on placing the plant material in a microwave reactor and heated. The internal water in the plant material is then released carrying the essential oils which are then condensed in a condenser outside the reactor.<sup>88</sup> The findings from Ferhat, et al.<sup>88</sup> indicate that the microwave-accelerated distillation (MAD) shows comparable yields with hydrodistillation, with a much shorter extraction time (6 times lower). In addition, better antimicrobial activities for oils extracted by MAD were assessed against yeast and gram-negative bacteria, and it is considered an environmentally friendly technique.

Another extraction technique involves the degradation of the cell wall using enzymes. Stoll, et al.<sup>47</sup> developed a process using enzymatic hydrolysis of carrot pomace to recover carotene-rich hydrolysate that can be used as a functional ingredient in e.g. model beverages (based on apple juice). The process consisted of the application of an enzyme mixture of cellulase and pectinase (cellulolytic and pectolytic activities) to degrade the cell wall of the carrot pomace after milling of this residue. Optimization of the hydrolysis step was the main aspect of the study by Stoll, et al.<sup>47</sup>, which was successfully implemented at pilot scale (10 liters). The conditions applied in the pilot run are pH 4.0, 50 °C, enzyme combination corresponding to 750 ppm of Pectinex Ultra SP-L (Novo Nordisk Ferment) and 750 ppm of Cytolase CL (DSM Food Specialties). The obtained hydrolysate corresponds to 64 mg total carotene per kilogram of hydrolysate. Another well-known application of enzymes is for the hydrolysis of lignocellulosic residues (e.g. sugarcane bagasse) into sugars and later conversion into second generation ethanol. For this

enzymatic reaction a pretreatment step is required to facilitate the enzyme accessibility to cellulose and hemicellulose presented in the lignocellulosic residues.<sup>89</sup>

Many studies have evaluated protein extraction from agri-food residues. Contreras, et al.<sup>75</sup> provides an excellent review on protein extraction from different agri-food residues, reviewing solvent and aqueous extraction (at alkaline, neutral and acid conditions), biochemical extraction using enzymes, physical and physical-chemical methods under dry and non-dry conditions. Regarding protein extraction, it seems that alkaline extraction provides higher yields (up to 95%), however this method is not selective, so other components such as polyphenols, hemicellulose and lignin can be co-extracted. Sari, et al.<sup>90</sup> evaluate the protein extraction yield, at alkaline conditions, of different agri-food residues (rapeseed meal, sunflower meal, soybean meal, soybean hull, malt by-products among others). The authors identified that biomass composition affect the extraction yield, finding that cellulose and oil can significantly affect the extraction performance. When chemical extraction is low, the use of enzyme assisted processes might improve protein extraction. For instance, the use of carbohydrate degrading enzymes (cellulase, hemicellulase, xylase, arabanase and glucanase), might benefit from the release of protein from the plant based matrix, as they can degrade the cellulose and hemicellulose from the cell wall.<sup>75</sup> The use of enzymes can be combined with neutral conditions, preventing the formation of protein-polyphenols complexes and also maintain the functional properties of the proteins.<sup>91</sup>

As previously mentioned, many valuable compounds are co-extracted and depending on the application, can be further purified. The following section will outline purification technologies for further separation of valuable compounds mainly in aqueous plant-based extracts.

### 2.3.3. Purification of valuable compounds from plant-based extracts

Separation and purification of the valuable components from a plant-based extract can be done using different (conventional and emerging) purification techniques such as: adsorption, precipitation or crystallization, membrane separation, aqueous two-phase system separation (ATPS)<sup>10</sup> or combinations of these technologies. Adsorption is a promising technology able to purify complex mixtures (plant-based extracts) and also can be operated at mild conditions. Mild operation is often desired in food processing as thermal technologies can generate undesired flavors and change the organoleptic properties of the final products. In addition, adsorption can be a selective process when appropriate adsorbents (polymeric resins, zeolites, activated carbon) are used for capturing the target molecules (products or impurities).

#### 2.3.3.1. Protein purification

Protein from vegetable sources are composed of storage proteins (globulin and albumins), structural proteins (ribosomal, membrane proteins) and biological active proteins (lectins).<sup>13</sup> Pulses, oilseeds and vegetables sources are rich in proteins (Figure 2.2). Particularly, oilseed meals are rich protein source accounting to up to 40% dry matter.

Oilseed proteins have been successfully purified by different techniques such as isoelectric precipitation<sup>92-96</sup> and adsorption<sup>97-101</sup>, being the former one the most applied.<sup>13</sup> Both techniques are often combined with membrane separation to increase purity in the products. Isoelectric precipitation has been additionally applied in the manufacturing of pulse proteins, after milling of the sources to produce protein rich flour.<sup>102</sup> Ultrafiltration can be used to separate proteins (large molecules) from

nutraceutical (small molecules, i. e. polyphenols, sugars, lipids) and antinutritional compounds (phytic acid).

Akbari, et al.<sup>96</sup> purified napin and cruciferin (storage proteins) from rapeseed meal extract by isoelectric precipitation of cruciferin, and subsequent napin purification by removing phytic acid, glucosinolates and phenolic acids using ultrafiltration (10kDa) and diafiltration. The obtained total yield of 52% while successfully removing higher than 80% of phytic and phenolic acids. Similarly, Xu, et al.<sup>94</sup> and Ghodsvali, et al.<sup>95</sup> successfully purified canola proteins using ultrafiltration and diafiltration before and after isoelectric precipitation of cruciferin fraction. Even though, precipitation is widely applied it has some disadvantages as it can affect the functional properties of the proteins such as solubility and additionally promotes aggregation<sup>13</sup>. Therefore, the use of mild conditions and technologies such as adsorption, could benefit the functionality of the proteins.

Oilseed proteins have been successfully purified by adsorption, decreasing denaturalization and obtaining higher purities. Chung, et al.<sup>99</sup> purified the globulin fraction from flaxseed meal using the weak anion exchanger DEAE Sephacel, at basic pH (pH 8.6) and mid salt conditions recovering 63% of the total protein content in the meal with high purity. Interestingly the authors only focused on the recovery of the globulin fraction while an additional minor peak is observed in the chromatogram. This flow through peak corresponded to around 30% of the protein content, which could represent the albumin fraction. Bérot, et al.<sup>100</sup> proposed to purify both protein fractions (albumins and globulins) from rapeseed meal extract using a combination of adsorptive steps. The author used the cation exchange resin, Source 30S, to capture napin and lipid proteins while cruciferin flow through. Cruciferin is subsequently polished by size exclusion (Sephacryl S-300) and napin is polished by HIC (Phenyl sepharose 6 fast flow). After polishing both proteins, polyphenols and other antinutritional compounds were removed by dialysis. Purities greater >99% were obtained for both proteins.

#### 2.3.3.2. Polyphenol purification

Polyphenol has been purified from the plant based extract or fermentation broth by means of membrane separation, liquid-liquid extraction,<sup>103</sup> preferential crystallization,<sup>104</sup> adsorption.<sup>105-108</sup>

Silva, et al.<sup>103</sup> evaluated the use of liquid-liquid extraction to purify polyphenols from fermentation broth. As one of the critical factors to design a liquid-liquid extraction process is solvent selection the authors suggested the use of the NTRL-SAC thermodynamic model to predict partitioning into different solvents and suggested different process configurations to purify polyphenols with similar characteristics. In another study, Silva, et al.<sup>104</sup> used preferential crystallization (commonly used for enantiomer purification) to separate naringenin and *trans*-resveratrol (chemically related polyphenols). This study showed an alternative technique besides adsorption for recovering similar compounds, however, the solution needs to be concentrated and cooled to induce supersaturation and later crystallization.

Adsorption has been widely applied for recovery of phenolic compounds from liquid food streams, often applied before or after a protein precipitation step. The studies performed by Pickardt, et al.<sup>109</sup> and Weisz, et al.<sup>110</sup> evaluated the adsorption of phenolics onto a polymeric resin and an ion exchange resin (XAD16 and Lewatit S 6328) using sunflower meal extract. Both studies aimed to recover proteins, however they suggested the co-recovery of polyphenols compounds as a possibility to improve economic potential of the process. Thiel, et al.<sup>93</sup> evaluated the recovery of proteins, sinapic acid and

phytic acid from rapeseed meal extract. After extraction, purification was assessed with two processes using a  $\beta$ -zeolite in the  $H^+$  form ( $SiO_2/Al_2O_3$  ratio of 150:1) and the anion exchanger Purolite A200. Both purification processes accomplished the separation of the three components of interest. Ferri, et al.<sup>111</sup> studied the recovery of hydroxycinnamic acids from olive mill wastewater, using a synthetic mixture of ten polyphenols, which are the most representative ones of this side stream. The authors of this work also used macroporous food grade resins and a weak anion exchanger (XAD4, XAD7, XAD16, IRA96 and ENV+). An overall of 90% polyphenol recovery was found when desorbing with ethanol. Similarly, Moreno-González, et al.<sup>105</sup> evaluated the recovery of sinapic acid from rapeseed meal extract using a model feed system. Adsorption of sinapic acid on the polymeric resin FPX66 resulted to be selective. They demonstrated that other components such as sugars, glucosinolates and phytic acid (often presented in food matrixes) poorly interact with the resin which benefits sinapic acid capture. At last, Schieber, et al.<sup>112</sup> developed a process using apple pomace extract to recover polyphenols and pectin. Phenolics are purified by adsorption on XAD16 and subsequently eluted using methanol. Solvent was evaporated and polyphenols were freeze dried.

#### 2.3.3.3. Polysaccharides purification

Pectin purification from citrus and fruit extracts (peels and pomace) can be purified by solvent precipitation, ion exchange chromatography, dialysis,<sup>113</sup> among others technologies. In addition to bioactive phenolics from apple pomace, Schieber, et al.<sup>112</sup> purified pectin by alcohol precipitation of the pectin-containing effluent from the adsorption column where phenolics were captured.

Solvent precipitation with ethanol was applied by Galanakis, et al.<sup>114</sup> to purify dietary fibers from olive mill waste water. After concentration of the wastewater (3.5-fold) and subsequent liquid-liquid extraction using ethanol/acids and ethanol/water mixtures, dietary fibers were precipitated by an increase of ethanol concentration up to 85 mL/100 mL. Precipitated fibers were deflated with acetone and dried. As mentioned earlier olive mill wastewater also contains significant amount of polyphenols. The suggested purification process by the authors allows the co-recovery of dietary fibers and polyphenols as fibers precipitate in ethanol while the phenolics are soluble in this solvent. The recovered dietary fiber was further characterized, finding that the soluble fraction is rich on pectin polysaccharides while the insoluble fraction is rich of glucose, xylose, galacturonic acid and rhamnose.

Ion exchange chromatography has been successfully implemented for sucrose purification from beet molasses<sup>115</sup> and separation of fructose and glucose.<sup>116-118</sup> Chilamkurthi, et al.<sup>119</sup> assessed different cation exchangers in the form of  $Na^+$ ,  $H^+$ ,  $K^+$  and  $Ca^{2+}$ , to evaluate the separation of arabinose and sugars. The model components used in this study were: galactose, glucose, arabinose, lactose and sugar acid. Their findings indicate that appropriate separation of the different components is accomplished using the cation exchangers in the form of  $Ca^{2+}$  and  $K^+$ .

Another purification method for polysaccharides like sugars, glucose is crystallization. As crystallization occurs when the solution is supersaturated, therefore, a pre-concentration is required. The shape and size of crystal will determine the subsequent steps to separate them from their mother liquids. These steps will involve filtration and drying.<sup>120</sup>

#### 2.3.3.4. Flavor ingredients recovery /purification

Natural flavors, which are generally obtained from plant or animal sources, are widely used in the food sector mainly in beverages. Saffarionpour, et al.<sup>121</sup> provide an excellent review on the different

technologies applied for purifying these types of products, including distillation, pervaporation and adsorption.

Additionally adsorption has been applied for capturing of impurities (e. g. off-flavors) instead of the valuable products. Gernat, et al.<sup>122</sup> successfully decreased the concentration of wort off-flavors (2-methylbutanal, 3-methylbutanal, methional, 2 methylpropanal and furfural) in alcohol free beer using zeolites at pilot scale (150 L). The authors evaluated other adsorbents such as polymeric resins, however, it was proved that resins are able to adsorb other flavor component, affecting the quality of the final product, as the aim was only to removed wort flavors. Off-flavor components are additionally composed of hydrophobic organic molecules (aldehydes, ketones, carboxylic acids). The results from Gernat, et al.<sup>122</sup> introduced the possibility of removing these components from food liquid streams by using zeolites to increase selectivity to aldehydes or by using hydrophobic resins for overall off-flavors removal.

#### 2.3.4. Final product formation

The last step toward the manufacturing of a product from a side stream of a food process corresponds to the formulation, defined here as the ultimate product form (emulsions, powders, pieces, liquid, among others).

##### 2.3.4.1. Food powders/ solid extracts

Drying technology is mostly used for food preservation, as minimization of moisture content in food products inhibit microbial growth. However, drying can also be used to improve the physical properties of a product<sup>123</sup>, for instance, spray drying is used to dry liquid food and form a powder product. Among the different types for dryers utilize by food industry, pneumatic drying, spray drying, drum drying, tray drying and freeze drying are applied in formulation.

Spray drying has been applied to concentrate food liquids such as coffee, milk and juices. This technique is also used for encapsulation of food ingredient, such as flavors and whole food substances (e.g. chocolate). Where materials can be encapsulated as single particle structure (ingredient surrounded by a matrix wall) or in an aggregate structure (ingredient particles fixed in a matrix)<sup>124</sup>. One of the main advantages of spray drying is that it produces a stable particulate solid product from a liquid in a one-continuous step. However, wall matrix materials are limited, being the most applied maltodextrins, hydrophobically modified starch, gum acacia,<sup>124</sup> whey, gelatin and sucrose.<sup>125</sup> Spray drying seems to be a suitable technique in the final formulation of a product prevent from a byproduct of food (plant extract, wastewater) as these streams are mainly liquid streams. In addition, spray drying is relatively economical and suitability for heat sensitive materials.<sup>125</sup>

Freeze drying is mostly applied in the pharmaceutical field but also in the production of expensive biological products when product quality is the most important attribute of the product. Its application in the food sector for the recovery of products might be limited to high value products such as proteins, enzymes and heat sensitive products as flavors. The principle consists on freezing the feed on a chamber where vacuum is applied. Dehydration occurs by sublimation, mostly of water which is recovered by mechanical vacuum pumps.<sup>126</sup> Note that freeze drying is usually operated in batch mode, as it requires of a drying chamber where the product is frozen and longer drying times than other techniques such as

spray and drum drying, which limits its application to small throughputs. The product form obtained from freeze drying is pieces, which are usually grounded after processing.<sup>126</sup>

Desobry, et al.<sup>127</sup> evaluated the drying process of  $\beta$ -carotene encapsulation using freeze drying, spray drying and drum drying. The authors demonstrated that the characteristics of the dried  $\beta$ -carotene obtained from drum drying possesses similar characteristics than the one obtained with the other two methods. In addition, during storage, the authors identified that drum drying gave higher product retention comparing to the other two methods. The solid obtained in the shape of sheets can be grounded to different particle size.

Other types of dryers that can be used for product formulations are tray dryers, bin dryers, rotatory dryers, pneumatic dryers. Particularly these dryers are used (but not limited) when the feeds stream is composed of solids (particulate, grains, granulated materials, precipitates or crystals). Bin and tray dryers are operated in batch mode while rotatory and pneumatic dryers can be operated in continuous mode.<sup>128</sup>

Selection of drying technique will highly depend on the desired product characteristics and the processing volume.

## 2.4. Food byproducts processing examples.

As previously mentioned, the recovery and purification of valuable compounds from food byproducts (bran, wastewater, oilseed meal, fruit pomace, among others) is dictated by the products to be recovered and the nature of the source material. In the following paragraphs, examples of purification processes are described based the previously discussed techniques and literature.

Galanakis, et al.<sup>114</sup> co-recovered dietary fiber from olive mill wastewater (Figure 2.4a). The suggested process consisted in a pre-concentration step of the wastewater, which might help to increase the extraction yield. Valuable compounds were extracted from the wastewater using ethanol by adding 5 mL of ethanol and 1g of citric acid and completed 100 mL of mixture with the concentrated wastewater. Extraction was done at 80 °C for 10 minutes. Dietary fiber was precipitated by contacting the extraction mixture in 95% (v/v) ethanol up to a concentration of 85% (v/v) and boiled for 10 minutes. Precipitated dietary fiber was filtrated and washed with acetone and chloroform to remove remained oil and dried for further analysis. The discarded liquid from the precipitation is rich in polyphenols. The authors found a concentration of 1.25g/L which is similar to the concentration of phenolics found in extra virgin oil. The phenolic rich fraction might contain different types of phenolics compounds, mainly hydroxycinnamic acids. These phenolic compounds could be further separated from the liquid by crystallization and dried as suggested by Silva, et al.<sup>103</sup> Recovery of solvents could be accomplished by distillation and can be recycled to the extraction system which might additionally benefit process economics.

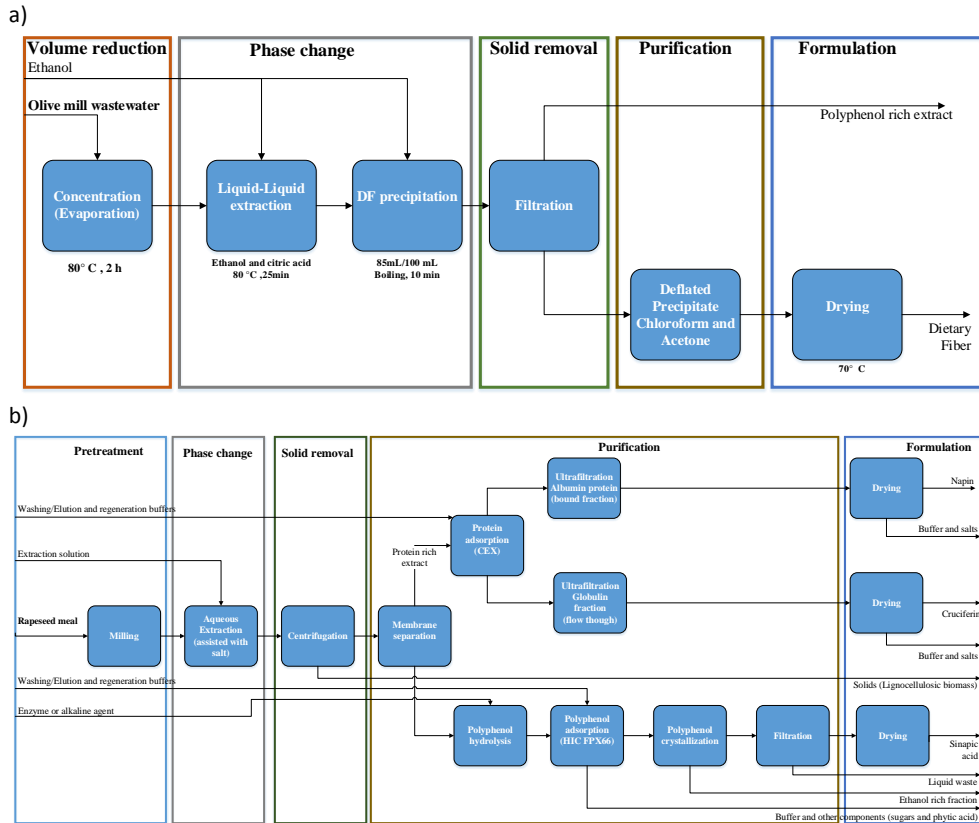


**Figure 2.4** Process purification of different valuable compound from food stream byproducts a) olive mill wastewater, b) rapeseed meal

When using oilseed meals as a byproducts, proteins, dietary fibers and polyphenols, could be purified. Aqueous extraction assisted with salt could be applied as an alternative method, instead of solvent extraction or alkaline extraction. Separation of small molecules (sugars and polyphenols) from the large molecules (proteins) can be accomplished using membranes.<sup>94, 95</sup> Isolate of both proteins could be further processed by further membrane concentration and freeze drying, however each protein has specific applications. Napin is a basic protein stable at a wide pH range and holds foaming properties while cruciferin possesses emulsifying, gelling and binding properties.<sup>6, 129</sup> Purification of both proteins by ion exchange chromatography as suggested by Moreno-González et al. (submitted manuscript), where napin is bound to the resin while cruciferin flow through. The purified protein fractions after chromatography can be sent to another membrane unit to remove buffer salts and dried. The permeate, from the small molecules separation contains the remained co-extracted components, polyphenols, sugars, phytic acids and glucosinolates.

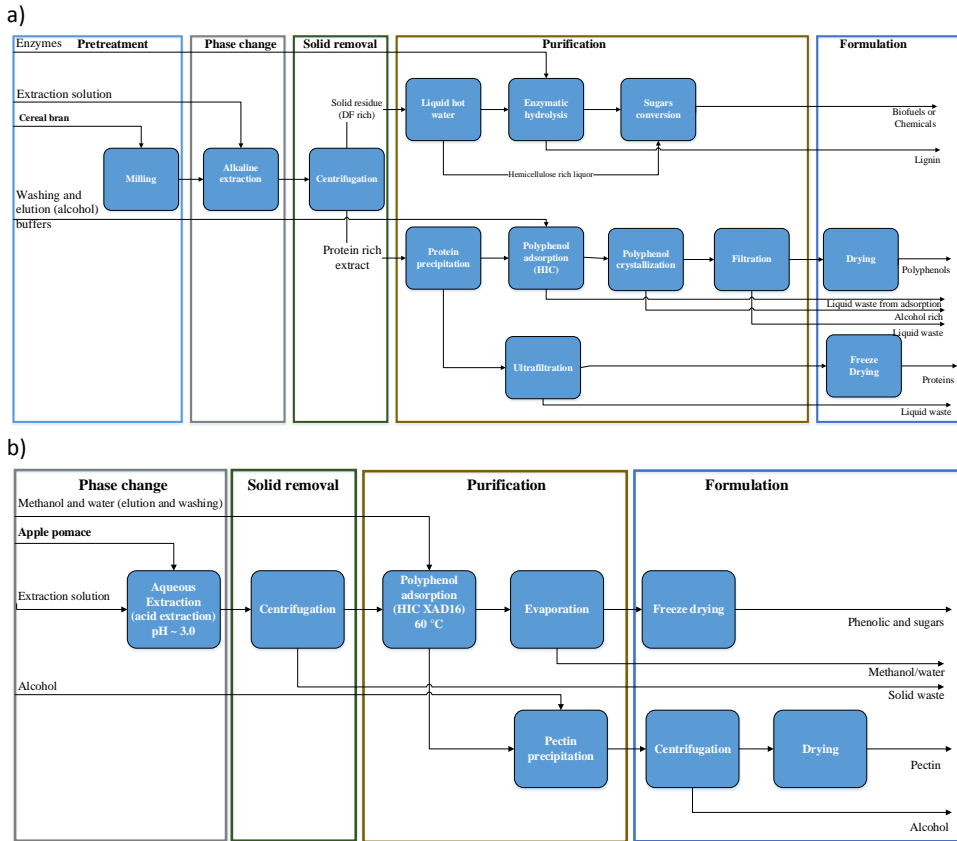


**Figure 2.5** Process purification of different valuable compound from food stream byproducts a) cereal bran b) apple pomace

Moreno-González, et al.<sup>105</sup> suggested capturing the polyphenols compounds using a food grade macroporous resin (FPX66). The authors demonstrated that the other components, sugar, phytic acid and glucosinolates poorly interact with the resin. The obtained sinapic acid (mayor phenolic in rapeseed meal) fraction, recovered using ethanol/water mixture<sup>105, 107, 111</sup> could be crystallized,<sup>103</sup> washed and dried (Figure 2.4b). As with the previous example, solvent could be additionally recovered by distillation. the flow through fraction from the adsorption column contains sugars, phytic acid and glucosinolates. Phytic acid is well known as an antinutrient compound due to its ability to bind to mineral ions such as magnesium and calcium, therefore is often removed from food products. However, sugars are valuable compounds and further purification of sugars could be accomplished by chemical precipitation of phytic acid. The remained solid fraction from the aqueous extraction is rich in dietary fibers hemicellulose, cellulose and lignin, which could additionally be processed to obtain reducing sugars for biofuels (Figure 2.5a).

Following some of the strategies suggested previously, processing of fruit/tuber pomace (Figure 2.5b) could start with the acid extraction of the polyphenols and soluble carbohydrates, which was applied for apple pomace by Schieber, et al.<sup>112</sup> and could be extended to other type of pomace such as carrot

or tomato. The extract contains polyphenol components and soluble sugars which could be purified by adsorption using food grade hydrophobic polymeric resins such as XAD16 and FPX66 as soluble sugars might poorly interact with the hydrophobic matrixes.<sup>105, 111, 112</sup> After polyphenol elution, Schieber, et al.<sup>112</sup> recommended to evaporate the solvent, which could be recovered by distillation and remove the remained water by freeze drying. Among the polyphenols that could be potentially recovered there is lycopene from tomato pomace,<sup>35</sup> carotene from carrot pomace,<sup>47</sup> and phloridzin & chlorogenic acid from apple pomace.<sup>112</sup> The flow through obtained liquid from the adsorption is rich in pectin, which can be purified by alcohol precipitation, filtrate or centrifuge to removed liquid and finally dry.

Lignocellulosic biomasses from food byproducts such as cereal bran could be processes to recover antioxidants (polyphenols), proteins and fermentable sugars (Figure 2.5a). As previously mention cereal brans are rich on phenolics and dietary fibers. Aqueous extraction (alkaline or acid) of proteins and polyphenols. Keeping in mind that alkaline conditions could oxidize the phenolic compounds or form protein-polyphenols complexes, milder conditions, like neutral extraction are preferred. Solid liquid separation between the extract and the insoluble fiber can be done by centrifugation or filtration. Purification of the plant-based extract can be done by isoelectric protein precipitation as recommended by Celiktas, et al.<sup>130</sup>, and polyphenols could be further purified by adsorption (hydrophobic polymeric resins).<sup>105, 107, 111, 112</sup> The protein precipitate could be filtrated and dried while phenolics could be crystallized and dried. The solid fraction from the aqueous extraction could be further treated by liquid hot water pretreatment for auto-hydrolysis of hemicellulose followed by the hydrolysis of the plant fibers using enzymes to produce fermentable sugars that can be later converted into biofuels or other biochemicals.

## 2.5. Concluding remarks

As can be seen in the afore mentioned schemes, a multitude of valuable compounds can be recovered from a single side stream including in most of the cases polyphenols, carbohydrates (dietary fibers) and proteins. They are the byproducts obtained from oilseed meals, cereals and pulses. The byproducts from these sources are often solids, therefore the selection of a suitable extraction technique is crucial in order to recover several products. Different extraction techniques can affect the properties of the products to be recovered. Even though, alkaline extraction is the most reported method, it also could promote protein denaturation and phenolic acid oxidation, which consequently reduce product yield and quality. Milder conditions such as neutral extraction or alternative technique such as supercritical CO<sub>2</sub> should be further studied and optimized for this step.

In the reviewed literature, the disposal of the solid fraction obtained after the extraction is often not mentioned. This fraction might be rich in dietary fiber (cellulose, hemicellulose and lignin) and can be further processed for the generation of fermentable sugars for biofuels or other biochemicals in the well-known biorefinery concept.

Fruits and vegetables residues are low in protein content but rich in polyphenols and carbohydrates such as pectin. As with the residues from cereal, oilseed and pulses, extraction methods will greatly influence the following purification steps. Alcohol extraction is a very effective technique for polyphenols as it utilizes the higher solubility of these type of components in alcohols. Even though solvents could be recovered by distillation, the environmental implications that they represent encourage the need of utilize alternative extraction techniques. Great progress has been accomplished

with supercritical fluid extraction, which additionally provides selectivity toward the extracted compounds.<sup>121</sup> However, large scale implementation has not been fully established and more effort is needed in order to guaranty safety during operation.

It is clear that to fully isolate the extracted compounds, several separation technologies will be combined and a detailed Life Cycle Assessment (LCA) and Techno- economic evaluation (TEE) should be performed to evaluate feasibility and profitability.

Among other separation techniques, adsorption is an attractive alternative for capturing of valuable products such as proteins and polyphenols due to its simplicity, high efficiency, ease to scale up and selectivity when appropriate adsorbents are available. Particularly for polyphenols adsorption, it has been demonstrated that food grade polymeric resins (e.g. XAD16, FPX66 from the Amberlite series) are highly effective. Often elution of the bound compounds, concentrate them which facilitates their further processing by crystallization/precipitation and drying. Adsorption could also be used for removal of unwanted compounds in a liquid streams such as off-flavors<sup>122</sup> and colorants, as already applied for de-bittering of fruit juices. Better understanding of the interactions between the adsorbent and the bound components, might accelerate the implementation of more adsorptive processes in the food sector. This opens an additional challenge for future research, their integration in continuous mode not only with SMB systems (simulated moving bed systems) but with emerging systems such as periodic countercurrent chromatography (PCC).

Finally, the last stage of the processing will be related to the ultimate product form, which commonly is a solid form. Therefore, water of other solvents should be additionally removed by drying. Spray drying, drum drying and freeze drying are the few drying technologies able to dry liquid streams, which could be obtained from the purification of water-soluble molecules such as sugars or flavor components such as nucleotides.

This work describes the recovery of multiple value-added compounds from agri-food streams by separating the from the mix, and therefore, with high purity. High purity of the compounds is often desired when their application involves pharmaceutical or cosmetic products. However, if their application is in a food product, where functionality (emulsification, gelling formation, thickening, viscosity) is given by combining several ingredients, high degree of purity might not be needed. Limited studies are available<sup>131-133</sup> exploring this new way of thinking and they have shown that the properties of the final products are not significantly changed.

As previously mentioned, the application of the different technologies will depend on their suitability to continuous operation. Moreover, the processing of plant-based byproducts should be cost-effective, and keeping the functionality of the products, e.g. nutritional value of proteins and antioxidant activity in polyphenols, in order to be successfully applied in pharmaceutical, cosmetic and food products.

## 2.6. References

1 Virtanen S., Chowreddy R.R., Irmak S., Honkapää K., Isom L., Food Industry Co-streams: Potential Raw Materials for Biodegradable Mulch Film Applications, Journal of Polymers and the Environment, (2016) 1-21.

- 2** European Commission, 2017, Circular Economy - European Commission (accessed 11 August 2017). [https://ec.europa.eu/growth/industry/sustainability/circular-economy\\_en](https://ec.europa.eu/growth/industry/sustainability/circular-economy_en)
- 3** European Commission, 2014, Impact assessment on measures addressing food waste to complete swd (2014) 207 regarding the review of eu waste management targets (accessed 1 September 2019). <http://ec.europa.eu/environment/euswd/pdf/IA.PDF>
- 4** European Commission, 2011, Evolution Of (Bio-) Waste Generation/Prevention And (Bio-) Waste Prevention Indicators (accessed 1 September 2017). [http://ec.europa.eu/environment/waste/prevention/pdf/SR1008\\_FinalReport.pdf](http://ec.europa.eu/environment/waste/prevention/pdf/SR1008_FinalReport.pdf)
- 5** Tuck C.O., Pérez E., Horváth I.T., Sheldon R.A., Poliakoff M., Valorization of Biomass: Deriving More Value from Waste, *Science*, 337 (2012) 695-699.
- 6** Wanasundara J.P.D., McIntosh T.C., Perera S.P., Withana-Gamage T.S., Mitra P., Canola/rapeseed protein-functionality and nutrition, *OCL*, 23 (2016) D407.
- 7** Naczki M., Shahidi F., Phenolics in cereals, fruits and vegetables: Occurrence, extraction and analysis, *Journal of Pharmaceutical and Biomedical Analysis*, 41 (2006) 1523-1542.
- 8** Bongers P.M.M., Almeida-Rivera C., Product Driven Process Synthesis Methodology, in: J. Jeżowski, J. Thullie (Eds.) *Computer Aided Chemical Engineering*, Elsevier, 2009, pp. 231-236.
- 9** Galanakis C.M., 3. The Universal Recovery Strategy, in: *Food Waste Recovery - Processing Technologies and Industrial Techniques*, Elsevier.
- 10** Galanakis C.M., Recovery of high added-value components from food wastes: Conventional, emerging technologies and commercialized applications, *Trends in Food Science & Technology*, 26 (2012) 68-87.
- 11** Butnariu M., Butu A., Chemical Composition of Vegetables and Their Products, in: P.C.K. Cheung, B.M. Mehta (Eds.) *Handbook of Food Chemistry*, Springer Berlin Heidelberg, Berlin, Heidelberg, 2015, pp. 627-692.
- 12** Carrillo-López A., Yahia E.M., Chapter 6 - Morphology and Anatomy, in: E.M. Yahia (Ed.) *Postharvest Physiology and Biochemistry of Fruits and Vegetables*, Woodhead Publishing, 2019, pp. 113-130.
- 13** González-Pérez S., Arellano J.B., 15 - Vegetable protein isolates, in: G.O. Phillips, P.A. Williams (Eds.) *Handbook of Hydrocolloids (Second Edition)*, Woodhead Publishing, 2009, pp. 383-419.
- 14** Islam S., Ma W., Lupine, in: B. Caballero, P.M. Finglas, F. Toldrá (Eds.) *Encyclopedia of Food and Health*, Academic Press, Oxford, 2016, pp. 579-585.
- 15** List G.R., 2 - Oilseed Composition and Modification for Health and Nutrition, in: T.A.B. Sanders (Ed.) *Functional Dietary Lipids*, Woodhead Publishing, 2016, pp. 23-46.
- 16** Rosell C.M., Garzon R., Chemical Composition of Bakery Products, in: P.C.K. Cheung, B.M. Mehta (Eds.) *Handbook of Food Chemistry*, Springer Berlin Heidelberg, Berlin, Heidelberg, 2015, pp. 191-224.

- 17** Shukla B.D., Srivastava P.K., Gupta R.K., *Oilseeds Processing Technology*, Central Institute of Agricultural Engineering, India 1992.
- 18** Rosa-Sibakov N., Poutanen K., Micard V., How does wheat grain, bran and aleurone structure impact their nutritional and technological properties?, *Trends in Food Science & Technology*, 41 (2015) 118-134.
- 19** Heiniö R.L., Noort M.W.J., Katina K., Alam S.A., Sozer N., de Kock H.L., Hersleth M., Poutanen K., Sensory characteristics of wholegrain and bran-rich cereal foods – A review, *Trends in Food Science & Technology*, 47 (2016) 25-38.
- 20** Ahmad F., Pasha I., Saeed M., Asgher M., Antioxidant profiling of native and modified cereal brans, 54 (2019) 1206-1214.
- 21** Hollmann J., Lindhauer M.G., Pilot-scale isolation of glucuronoarabinoxylans from wheat bran, *Carbohydrate Polymers*, 59 (2005) 225-230.
- 22** Prakash J., Ramaswamy H.S., Rice bran proteins: Properties and food uses, *Critical Reviews in Food Science and Nutrition*, 36 (1996) 537-552.
- 23** Pfaltzgraff L.A., De bruyn M., Cooper E.C., Budarin V., Clark J.H., Food waste biomass: a resource for high-value chemicals, *Green Chemistry*, 15 (2013) 307-314.
- 24** Mullen A.M., Álvarez C., Pojić M., Hadnadev T.D., Papageorgiou M., Chapter 2 - Classification and target compounds, in: C.M. Galanakis (Ed.) *Food Waste Recovery*, Academic Press, San Diego, 2015, pp. 25-57.
- 25** Mirabella N., Castellani V., Sala S., Current options for the valorization of food manufacturing waste: a review, *Journal of Cleaner Production*, 65 (2014) 28-41.
- 26** Espina L., Somolinos M., Lorán S., Conchello P., García D., Pagán R., Chemical composition of commercial citrus fruit essential oils and evaluation of their antimicrobial activity acting alone or in combined processes, *Food Control*, 22 (2011) 896-902.
- 27** May C.D., Industrial pectins: Sources, production and applications, *Carbohydrate Polymers*, 12 (1990) 79-99.
- 28** Chedea V.S., Kefalas P., Socaciu C., Patterns of carotenoid pigments extracted from two orange peel wastes (Valencia and Navel var.), *Journal of Food Biochemistry*, 34 (2010) 101-110.
- 29** Aravantinos-Zafiridis G., Oreopoulou V., Tzia C., Thomopoulos C.D., Utilisation of orange by-products—orange peel carotenoids, 59 (1992) 77-79.
- 30** Ángel Siles López J., Li Q., Thompson I.P., Biorefinery of waste orange peel, *Critical reviews in biotechnology*, 30 (2010) 63-69.
- 31** Scordino M., Di Mauro A., Passerini A., Maccarone E., Highly purified sugar concentrate from a residue of citrus pigments recovery process, *LWT - Food Science and Technology*, 40 (2007) 713-721.

- 32** Rodríguez Madrera R., Pando Bedriñana R., García Hevia A., Arce M.B., Suárez Valles B., Production of spirits from dry apple pomace and selected yeasts, *Food and Bioproducts Processing*, 91 (2013) 623-631.
- 33** Mourtzinos I., Goula A., Chapter 2 - Polyphenols in Agricultural Byproducts and Food Waste, in: R.R. Watson (Ed.) *Polyphenols in Plants (Second Edition)*, Academic Press, 2019, pp. 23-44.
- 34** Bordiga M., Travaglia F., Locatelli M., Valorisation of grape pomace: an approach that is increasingly reaching its maturity – a review, 54 (2019) 933-942.
- 35** Lu Z., Wang J., Gao R., Ye F., Zhao G., Sustainable valorisation of tomato pomace: A comprehensive review, *Trends in Food Science & Technology*, 86 (2019) 172-187.
- 36** Nunes M.A., Pimentel F.B., Costa A.S.G., Alves R.C., Oliveira M.B.P.P., Olive by-products for functional and food applications: Challenging opportunities to face environmental constraints, *Innovative Food Science & Emerging Technologies*, 35 (2016) 139-148.
- 37** Food and Agriculture Organization of the United Nations (FAO), 2020, FAOSTAT Production Quantity (accessed 29 April 2020). <http://www.fao.org/faostat/en/#data/QC>
- 38** Camire M.E., Violette D., Dougherty M.P., McLaughlin M.A., Potato Peel Dietary Fiber Composition: Effects of Peeling and Extrusion Cooking Processes, *Journal of Agricultural and Food Chemistry*, 45 (1997) 1404-1408.
- 39** Arapoglou D., Varzakas T., Vlyssides A., Israilides C., Ethanol production from potato peel waste (PPW), *Waste Management*, 30 (2010) 1898-1902.
- 40** Rodriguez de Soltillo D., Hadley M., Holm E.T., Potato Peel Waste: Stability and Antioxidant Activity of a Freeze-Dried Extract, 59 (1994) 1031-1033.
- 41** Versino F., López O.V., García M.A., Sustainable use of cassava (*Manihot esculenta*) roots as raw material for biocomposites development, *Industrial Crops and Products*, 65 (2015) 79-89.
- 42** Ubalua A.O., Cassava wastes: treatment options and value addition alternatives, *African Journal of Biotechnology*, 6 (2007) 2065-2073.
- 43** Sharma K.D., Karki S., Thakur N.S., Attri S., Chemical composition, functional properties and processing of carrot—a review, *Journal of Food Science and Technology*, 49 (2012) 22-32.
- 44** Nawirska A., Kwaśniewska M., Dietary fibre fractions from fruit and vegetable processing waste, *Food Chemistry*, 91 (2005) 221-225.
- 45** Schieber A., Saldaña M.D., Potato peels: a source of nutritionally and pharmacologically interesting compounds—a review, *Food*, 3 (2009) 23-29.
- 46** Prival M.J., CANCER | Carcinogens in the Food Chain, in: B. Caballero (Ed.) *Encyclopedia of Food Sciences and Nutrition (Second Edition)*, Academic Press, Oxford, 2003, pp. 799-804.

- 47** Stoll T., Schweiggert U., Schieber A., Carle R., Process for the recovery of a carotene-rich functional food ingredient from carrot pomace by enzymatic liquefaction, *Innovative Food Science & Emerging Technologies*, 4 (2003) 415-423.
- 48** Truong V.-D., McFeeters R.F., Thompson R.T., Dean L.L., Shofran B., Phenolic Acid Content and Composition in Leaves and Roots of Common Commercial Sweetpotato (*Ipomea batatas* L.) Cultivars in the United States, 72 (2007) C343-C349.
- 49** Lomascolo A., Uzan-Boukhris E., Sigoillot J.-C., Fine F., Rapeseed and sunflower meal: a review on biotechnology status and challenges, *Appl Microbiol Biotechnol*, 95 (2012) 1105-1114.
- 50** Wanasundara J.P., Proteins of Brassicaceae oilseeds and their potential as a plant protein source, *Critical reviews in food science and nutrition*, 51 (2011) 635-677.
- 51** Fleddermann M., Fechner A., Rößler A., Bähr M., Pastor A., Liebert F., Jahreis G., Nutritional evaluation of rapeseed protein compared to soy protein for quality, plasma amino acids, and nitrogen balance – A randomized cross-over intervention study in humans, *Clinical Nutrition*, 32 (2013) 519-526.
- 52** Vuorela S., Meyer A.S., Heinonen M., Impact of isolation method on the antioxidant activity of rapeseed meal phenolics, *Journal of agricultural and food chemistry*, 52 (2004) 8202-8207.
- 53** Nićiforović N., Abramović H., Sinapic Acid and Its Derivatives: Natural Sources and Bioactivity, *Comprehensive Reviews in Food Science and Food Safety*, 13 (2014) 34-51.
- 54** Mateos-Aparicio I., Redondo-Cuenca A., Villanueva-Suárez M.-J., Zapata-Revilla M.-A., Tenorio-Sanz M.-D., Pea pod, broad bean pod and okara, potential sources of functional compounds, *LWT - Food Science and Technology*, 43 (2010) 1467-1470.
- 55** Mateos-Aparicio I., Redondo-Cuenca A., Villanueva-Suárez M.-J., Broad bean and pea by-products as sources of fibre-rich ingredients: potential antioxidant activity measured in vitro, 92 (2012) 697-703.
- 56** Almeida-Rivera C., Bongers P., Zondervan E., Chapter 15 - A Structured Approach for Product-Driven Process Synthesis in Foods Manufacturea, in: M. Martín, M.R. Eden, N.G. Chemmangattuvalappil (Eds.) *Computer Aided Chemical Engineering*, Elsevier, 2016, pp. 417-441.
- 57** Szwajgier D., Borowiec K., Phenolic acids from malt are efficient acetylcholinesterase and butyrylcholinesterase inhibitors, 118 (2012) 40-48.
- 58** Lau T., Harbourne N., Oruña-Concha M.J., Valorisation of sweet corn (*Zea mays*) cob by extraction of valuable compounds, 54 (2019) 1240-1246.
- 59** Patsioura A., Galanakis C.M., Gekas V., Ultrafiltration optimization for the recovery of  $\beta$ -glucan from oat mill waste, *Journal of Membrane Science*, 373 (2011) 53-63.
- 60** Sohail M., Rakha A., Butt M.S., Iqbal M.J., Rashid S., Rice bran nutraceuticals: A comprehensive review, *Critical Reviews in Food Science and Nutrition*, 57 (2017) 3771-3780.
- 61** Liu Y.Q., Strappe P., Shang W.T., Zhou Z.K., Functional peptides derived from rice bran proteins, *Critical Reviews in Food Science and Nutrition*, 59 (2019) 349-356.

- 62** Orthoefer F.T., Rice bran oil, in: *Bailey's industrial oil & fat products*, John Wiley and Sons, New Jersey 2005, pp. 465-489.
- 63** Balandrán-Quintana R.R., Mercado-Ruiz J.N., Mendoza-Wilson A.M., Wheat Bran Proteins: A Review of Their Uses and Potential, *Food Reviews International*, 31 (2015) 279-293.
- 64** Zhang H., Birch J., Pei J., Ma Z.F., Bekhit A.E.-D., Phytochemical compounds and biological activity in *Asparagus* roots: a review, 54 (2019) 966-977.
- 65** Siriwardhana S.S.K.W., Shahidi F., Antiradical activity of extracts of almond and its by-products, *Journal of the American Oil Chemists' Society*, 79 (2002) 903-908.
- 66** Shahidi F., Alasalvar C., Liyana-Pathirana C.M., Antioxidant Phytochemicals in Hazelnut Kernel (*Corylus avellana* L.) and Hazelnut Byproducts, *Journal of Agricultural and Food Chemistry*, 55 (2007) 1212-1220.
- 67** Sudha M.L., Chapter 36 - Apple Pomace (By-Product of Fruit Juice Industry) as a Flour Fortification Strategy, in: V.R. Preedy, R.R. Watson, V.B. Patel (Eds.) *Flour and Breads and their Fortification in Health and Disease Prevention*, Academic Press, San Diego, 2011, pp. 395-405.
- 68** Roda A., Lambri M., Food uses of pineapple waste and by-products: a review, 54 (2019) 1009-1017.
- 69** Larrauri J.A., Rupérez P., Calixto F.S., Pineapple Shell as a Source of Dietary Fiber with Associated Polyphenols, *Journal of Agricultural and Food Chemistry*, 45 (1997) 4028-4031.
- 70** Seguí Gil L., Fito Maupoey P., An integrated approach for pineapple waste valorisation. Bioethanol production and bromelain extraction from pineapple residues, *Journal of Cleaner Production*, 172 (2018) 1224-1231.
- 71** Shi M., Hlaing M.M., Ying D., Ye J., Sanguansri L., Augustin M.A., New food ingredients from broccoli by-products: physical, chemical and technological properties, 54 (2019) 1423-1432.
- 72** Agbor V.B., Cicek N., Sparling R., Berlin A., Levin D.B., Biomass pretreatment: Fundamentals toward application, *Biotechnology Advances*, 29 (2011) 675-685.
- 73** Sun S., Sun S., Cao X., Sun R., The role of pretreatment in improving the enzymatic hydrolysis of lignocellulosic materials, *Bioresource Technology*, 199 (2016) 49-58.
- 74** Zhang K., Pei Z., Wang D., Organic solvent pretreatment of lignocellulosic biomass for biofuels and biochemicals: A review, *Bioresource Technology*, 199 (2016) 21-33.
- 75** Contreras M.d.M., Lama-Muñoz A., Manuel Gutiérrez-Pérez J., Espínola F., Moya M., Castro E., Protein extraction from agri-food residues for integration in biorefinery: Potential techniques and current status, *Bioresource Technology*, 280 (2019) 459-477.
- 76** Capellini M.C., Giacomini V., Cuevas M.S., Rodrigues C.E.C., Rice bran oil extraction using alcoholic solvents: Physicochemical characterization of oil and protein fraction functionality, *Industrial Crops and Products*, 104 (2017) 133-143.

- 77** Kulkarni S., Vijayanand P., Effect of extraction conditions on the quality characteristics of pectin from passion fruit peel (*Passiflora edulis f. flavicarpa* L.), *LWT-Food Science and Technology*, 43 (2010) 1026-1031.
- 78** Rezzadori K., Benedetti S., Amante E., Proposals for the residues recovery: Orange waste as raw material for new products, *Food and bioproducts processing*, 90 (2012) 606-614.
- 79** Saberian H., Hamidi-Esfahani Z., Gavlighi H.A., Barzegar M., Optimization of pectin extraction from orange juice waste assisted by ohmic heating, *Chemical Engineering and Processing: Process Intensification*, 117 (2017) 154-161.
- 80** Wang W., Ma X., Xu Y., Cao Y., Jiang Z., Ding T., Ye X., Liu D., Ultrasound-assisted heating extraction of pectin from grapefruit peel: Optimization and comparison with the conventional method, *Food chemistry*, 178 (2015) 106-114.
- 81** Guo X., Han D., Xi H., Rao L., Liao X., Hu X., Wu J., Extraction of pectin from navel orange peel assisted by ultra-high pressure, microwave or traditional heating: A comparison, *Carbohydrate Polymers*, 88 (2012) 441-448.
- 82** Bagherian H., Ashtiani F.Z., Fouladitajar A., Mohtashamy M., Comparisons between conventional, microwave-and ultrasound-assisted methods for extraction of pectin from grapefruit, *Chemical Engineering and Processing: Process Intensification*, 50 (2011) 1237-1243.
- 83** de Oliveira C.F., Giordani D., Gurak P.D., Cladera-Olivera F., Marczak L.D.F., Extraction of pectin from passion fruit peel using moderate electric field and conventional heating extraction methods, *Innovative Food Science & Emerging Technologies*, 29 (2015) 201-208.
- 84** Calvo M.M., Dado D., Santa-María G., Influence of extraction with ethanol or ethyl acetate on the yield of lycopene,  $\beta$ -carotene, phytoene and phytofluene from tomato peel powder, *European Food Research and Technology*, 224 (2007) 567-571.
- 85** Topal U., Sasaki M., Goto M., Hayakawa K., Extraction of Lycopene from Tomato Skin with Supercritical Carbon Dioxide: Effect of Operating Conditions and Solubility Analysis, *Journal of Agricultural and Food Chemistry*, 54 (2006) 5604-5610.
- 86** Kehili M., Kammlott M., Choura S., Zammel A., Zetzl C., Smirnova I., Allouche N., Sayadi S., Supercritical CO<sub>2</sub> extraction and antioxidant activity of lycopene and  $\beta$ -carotene-enriched oleoresin from tomato (*Lycopersicon esculentum* L.) peels by-product of a Tunisian industry, *Food and Bioproducts Processing*, 102 (2017) 340-349.
- 87** Mahato N., Sharma K., Koteswararao R., Sinha M., Baral E., Cho M.H., Citrus essential oils: Extraction, authentication and application in food preservation, *Critical Reviews in Food Science and Nutrition*, 59 (2019) 611-625.
- 88** Ferhat M.A., Meklati B.Y., Chemat F., Comparison of different isolation methods of essential oil from Citrus fruits: cold pressing, hydrodistillation and microwave 'dry' distillation, 22 (2007) 494-504.
- 89** Mussatto S.I., Dragone G., Guimarães P.M.R., Silva J.P.A., Carneiro L.M., Roberto I.C., Vicente A., Domingues L., Teixeira J.A., Technological trends, global market, and challenges of bio-ethanol production, *Biotechnology Advances*, 28 (2010) 817-830.

- 90** Sari Y.W., Syafitri U., Sanders J.P.M., Bruins M.E., How biomass composition determines protein extractability, *Industrial Crops and Products*, 70 (2015) 125-133.
- 91** Fetzter A., Herfellner T., Stähler A., Menner M., Eisner P., Influence of process conditions during aqueous protein extraction upon yield from pre-pressed and cold-pressed rapeseed press cake, *Industrial Crops and Products*, 112 (2018) 236-246.
- 92** Karaca A.C., Low N., Nickerson M., Emulsifying properties of canola and flaxseed protein isolates produced by isoelectric precipitation and salt extraction, *Food Research International*, 44 (2011) 2991-2998.
- 93** Thiel A., Muffler K., Tippkötter N., Suck K., Sohling U., Hruschka S.M., Ulber R., A novel integrated downstream processing approach to recover sinapic acid, phytic acid and proteins from rapeseed meal, *Journal of Chemical Technology and Biotechnology*, 90 (2015) 1999-2006.
- 94** Xu L., Diosady L.L., Removal of phenolic compounds in the production of high-quality canola protein isolates, *Food Research International*, 35 (2002) 23-30.
- 95** Ghodsvali A., Khodaparast M.H.H., Vosoughi M., Diosady L.L., Preparation of canola protein materials using membrane technology and evaluation of meals functional properties, *Food Research International*, 38 (2005) 223-231.
- 96** Akbari A., Wu J., An integrated method of isolating napin and cruciferin from defatted canola meal, *LWT - Food Science and Technology*, 64 (2015) 308-315.
- 97** Marshall Jr H.F., Isolation and purification of cottonseed 7S storage protein and its subunits, *Journal of agricultural and food chemistry*, 38 (1990) 1454-1457.
- 98** Sewekow E., Kessler L.C., Seidel-Morgenstern A., Rothkötter H.-J., Isolation of soybean protein P34 from oil bodies using hydrophobic interaction chromatography, *BMC biotechnology*, 8 (2008) 27.
- 99** Chung M.W.Y., Lei B., Li-Chan E.C.Y., Isolation and structural characterization of the major protein fraction from NorMan flaxseed (*Linum usitatissimum* L.), *Food Chemistry*, 90 (2005) 271-279.
- 100** Bérot S., Compoint J.P., Larré C., Malabat C., Guéguen J., Large scale purification of rapeseed proteins (*Brassica napus* L.), *Journal of Chromatography B*, 818 (2005) 35-42.
- 101** Zhang C., Glatz C.E., Process engineering strategy for recombinant protein recovery from canola by cation exchange chromatography, *Biotechnology progress*, 15 (1999) 12-18.
- 102** Boye J., Zare F., Pletch A., Pulse proteins: Processing, characterization, functional properties and applications in food and feed, *Food Research International*, 43 (2010) 414-431.
- 103** Silva M., García J.C., Ottens M., Polyphenol Liquid-Liquid Extraction Process Development Using NRTL-SAC, *Industrial & engineering chemistry research*, 57 (2018) 9210-9221.
- 104** Silva M., Vieira B., Ottens M., Preferential crystallization for the purification of similar hydrophobic polyphenols, *Journal of Chemical Technology & Biotechnology*, 93 (2018) 1997-2010.

- 105** Moreno-González M., Girish V., Keulen D., Wijngaard H., Lanteslager X., Ferreira G., Ottens M., Recovery of sinapic acid from canola/rapeseed meal extracts by adsorption, *Food and Bioproducts Processing*, 120 (2020) 69-79.
- 106** Sevillano D.M., van der Wielen L.A.M., Hooshyar N., Ottens M., Resin selection for the separation of caffeine from green tea catechins, *Food and Bioproducts Processing*, 92 (2014) 192-198.
- 107** Silva M., Castellanos L., Ottens M., Capture and Purification of Polyphenols Using Functionalized Hydrophobic Resins, *Industrial & Engineering Chemistry Research*, 57 (2018) 5359-5369.
- 108** Soto M.L., Moure A., Domínguez H., Parajó J.C., Recovery, concentration and purification of phenolic compounds by adsorption: a review, *Journal of Food Engineering*, 105 (2011) 1-27.
- 109** Pickardt C., Eisner P., Kammerer D.R., Carle R., Pilot plant preparation of light-coloured protein isolates from de-oiled sunflower (*Helianthus annuus* L.) press cake by mild-acidic protein extraction and polyphenol adsorption, *Food Hydrocolloids*, 44 (2015) 208-219.
- 110** Weisz G.M., Schneider L., Schweiggert U., Kammerer D.R., Carle R., Sustainable sunflower processing — I. Development of a process for the adsorptive decolorization of sunflower [*Helianthus annuus* L.] protein extracts, *Innovative Food Science and Emerging Technologies*, 11 (2010) 733-741.
- 111** Ferri F., Bertin L., Scoma A., Marchetti L., Fava F., Recovery of low molecular weight phenols through solid-phase extraction, *Chemical engineering journal*, 166 (2011) 994-1001.
- 112** Schieber A., Hilt P., Streker P., Endreß H.-U., Rentschler C., Carle R., A new process for the combined recovery of pectin and phenolic compounds from apple pomace, *Innovative Food Science & Emerging Technologies*, 4 (2003) 99-107.
- 113** Lampitt L.H., Money R.W., Judge B.E., Urie A., Pectin studies. Part I. Method of purification, *Journal of the Society of Chemical Industry*, 66 (1947) 121-124.
- 114** Galanakis C.M., Tornberg E., Gekas V., A study of the recovery of the dietary fibres from olive mill wastewater and the gelling ability of the soluble fibre fraction, *LWT - Food Science and Technology*, 43 (2010) 1009-1017.
- 115** Ganetsos G., Barker P., Developments in large-scale batch chromatography, in: G. Ganetsos, P. Barker (Eds.) *Preparative and production scale chromatography*, 1992, pp. 3-10.
- 116** Azevedo D.C.S., Rodrigues A.E., Fructose–glucose separation in a SMB pilot unit: Modeling, simulation, design, and operation, *AIChE Journal*, 47 (2001) 2042-2051.
- 117** Hashimoto K., Continuous separation of glucose-salts mixture with nonlinear and linear adsorption isotherms by using a simulated moving-bed adsorber, *Journal of Chemical Engineering of Japan*, 20 (1987) 405.
- 118** Hashimoto K., Models for the separation of glucose/fructose mixture using a simulated moving-bed adsorber, *Journal of Chemical Engineering of Japan*, 16 (1983) 400.

- 119** Chilamkurthi S., Willemsen J.-H., van der Wielen L.A.M., Poiesz E., Ottens M., High-throughput determination of adsorption equilibria for chromatographic oligosaccharide separations, *Journal of Chromatography A*, 1239 (2012) 22-34.
- 120** Berk Z., Crystallization and Dissolution, in: Z. Berk (Ed.) *Food Process Engineering and Technology*, Elsevier Science & Technology, San Diego, USA, 2013, pp. 353-371.
- 121** Saffarionpour S., Ottens M., Recent Advances in Techniques for Flavor Recovery in Liquid Food Processing, *Food Engineering Reviews*, 10 (2018) 81-94.
- 122** Gernat D.C., Penning M.M., Swinkels F.M., Brouwer E.R., Ottens M., Selective off-flavor reduction by adsorption: A case study in alcohol-free beer, *Food and Bioproducts Processing*, 121 (2020) 91-104.
- 123** Smith P.G., Evaporation and Drying, in: *Introduction to Food Process Engineering*, Springer US, Boston, MA, 2011, pp. 299-334.
- 124** Desai K.G.H., Jin Park H., Recent Developments in Microencapsulation of Food Ingredients, *Drying Technology*, 23 (2005) 1361-1394.
- 125** Anandharamakrishnan C., Ishwarya S P., Introduction to encapsulation of food ingredients, in: C. Anandharamakrishnan, P. Ishwarya S (Eds.) *Spray Drying Techniques for Food Ingredient Encapsulation*, John Wiley & Sons, Incorporated, Newark, USA, 2015, pp. 37-64.
- 126** Barbosa-Cánovas G.V., Ortega-Rivas E., Juliano P., Yan H., Drying, in: *Food Powders: Physical Properties, Processing, and Functionality*, Springer US, Boston, MA, 2005, pp. 271-304.
- 127** Desobry S.A., Netto F.M., Labuza T.P., Comparison of Spray-drying, Drum-drying and Freeze-drying for  $\beta$ -Carotene Encapsulation and Preservation, *Journal of Food Science*, 62 (1997) 1158-1162.
- 128** Berk Z., Dehydration, in: *Food Process Engineering and Technology*, Elsevier Science & Technology, San Diego, USA, 2013.
- 129** Aider M., Barbana C., Canola proteins: composition, extraction, functional properties, bioactivity, applications as a food ingredient and allergenicity – A practical and critical review, *Trends in Food Science & Technology*, 22 (2011) 21-39.
- 130** Celiktas M.S., Kirsch C., Smirnova I., Cascade processing of wheat bran through a biorefinery approach, *Energy Conversion and Management*, 84 (2014) 633-639.
- 131** Geerts M.E.J., Mienis E., Nikiforidis C.V., van der Padt A., van der Goot A.J., Mildly refined fractions of yellow peas show rich behaviour in thickened oil-in-water emulsions, *Innovative Food Science & Emerging Technologies*, 41 (2017) 251-258.
- 132** Karefyllakis D., van der Goot A.J., Nikiforidis C.V., Multicomponent emulsifiers from sunflower seeds, *Current Opinion in Food Science*, 29 (2019) 35-41.
- 133** Kornet C., Venema P., Nijse J., van der Linden E., van der Goot A.J., Meinders M., Yellow pea aqueous fractionation increases the specific volume fraction and viscosity of its dispersions, *Food Hydrocoll.*, 99 (2020) 105332.

# Chapter 3

## Recovery of sinapic acid from canola/rapeseed meal extracts by adsorption

---

### Abstract

Sinapic acid is a potential valuable compound to be recovered from rapeseed meal extracts as it processes antioxidant and antimicrobial properties. However, the concentration of this compound might be low and the presence of other low value compounds could complicate its downstream processing. Adsorption is an alternative technique that might allow selective recovery of this compound. This work was focused on establishing the foundation of an industrial process design to recover sinapic acid by adsorption. The obtained results from multicomponent experiments indicate that, resin Amberlite™ FPX66 is the best performing one showing a maximum adsorption capacity of  $102.6 + 11.7$  mg/gresin, easy sinapic acid recovery by desorbing it with 70% ethanol and high selectivity to sinapic acid over glucose, phytic acid and glucosinolates. The obtained equilibrium information was applied as input in a dynamic column model and compared with experimental results, showing a good agreement ( $r^2 = 0.98$ ). The model can be further applied for a large-scale chromatography process design to recover sinapic acid from rapeseed/canola meal extracts.

**Keywords:** Food Valorization, Adsorption, Chromatography, Polyphenols, Hydrophobic interaction

---

**Published as:** Moreno-González M., Girish V., Keulen D., Wijngaard H., Lauteslager X., Ferreira G., Ottens M. Recovery of sinapic acid from canola/rapeseed meal extracts by adsorption, *Food Bioprod. Process.* 120 (2020) 69-79. <https://doi.org/10.1016/j.fbp.2019.12.002>

### 3.1. Introduction

On December 2015, the European Commission established a research and innovation initiative (Document 52015DC0614) to motivate EU members to move towards a circular economy<sup>1</sup> and has taken the issue of food waste generation with seriousness. According to European Commission<sup>2</sup> most of the food waste is produced by the food manufacturing sector, and by 2020 is expected to rise to 126 million tons compared to 96 million tons generated in 2007<sup>3</sup>. In order to contribute to this initiative, byproducts of side streams of food industry can become seed of other processes. These types of streams are sources of proteins, lipids, complex carbohydrates and nutraceuticals that can be used as feedstock for metabolites. Furthermore, extraction of value-added products such as biopolymers, antioxidants and dietary fiber is also possible.

Research on producing/recovering valuable products from these streams is being done around the world<sup>4</sup> and has been reported elsewhere.<sup>4,5</sup> Well-established methodologies like the 5-stages universal recovery strategy (macroscopic pretreatment, macro-and micro molecule separation, extraction, purification and product formation<sup>6</sup> are used. These stages can be populated with either conventional process technologies (i.e. wet milling, solvent extraction, precipitation, adsorption) or with emerging technologies such as e.g. electro-osmotic dewatering, high-hydrostatic pressure for sterilization, enzyme deactivation or extraction of nutraceuticals, pulse electric field fragmentation<sup>7</sup>.

For instance, the byproduct generated from vegetable oil crops are oilseed meals (canola, rapeseed, cottonseed, soybeans, and sunflower seed). Particularly rapeseed meal is an interesting byproduct as it contains > 30% protein content, ~16% carbohydrates, 3% of phenolic compounds, among others<sup>8</sup>. One of the disadvantages of using these meals is the presence of phenolic compounds that can interact with the proteins by different mechanisms (hydrophobic interactions, hydrogen bonding, covalent bonding and ionic bonding in aqueous media<sup>9</sup> and reduce their nutritional value. However, phenolic compounds and phytic acid are also valuable products to be recovered. Nićiforović, et al.<sup>10</sup> provides an excellent review of sinapic acid and its beneficial properties as antioxidant, antimicrobial and anti-inflammatory actions. This makes it an interesting compound to be considered as preservative in cosmetic, pharmaceutical and food industry<sup>10</sup>. Phytic acid has chelating properties and might be used as natural antioxidant or as phosphorus source.<sup>11</sup>

Recovery of valuable product from rapeseed meal has been mainly focused on the purification of the proteins and the removal of polyphenols. Only the work evaluated by Thiel, et al.<sup>11</sup> includes the additional recovery of sinapic acid and phytic acid. Selective recovery of polyphenol compounds from oilseed meal might improve protein purification and add an additional product to be applied in food, cosmetic or pharmaceutical products

After oil production, most of the phenolic components adsorbed to the meal and can be extracted with methanol, aqueous methanol, acetone and by alkaline, acid or neutral extraction<sup>12</sup>. Pickardt, et al.<sup>13</sup> and Weisz, et al.<sup>14</sup> extracted valuable compounds from the meals by aqueous extraction assisted with salt, under mid-acidic conditions, which prevents protein-polyphenols interactions and autoxidation. Since rapeseed meal phenolics contain other derivatives of sinapic acid such as sinapine, hydrolysis using enzymes or NaOH at an alkaline pH is performed to convert them into their sinapic acid form, previous to their purification.

Even though, the previously mentioned emerging technologies have been investigated for the purification of food side streams, industrial application of these technologies is still limited, as some of them are energy intensive, difficult to scale up and require high capital cost<sup>7</sup>. Adsorption, however, is a well-described and established technology that can be operated at mild conditions, often desired in food industry as e.g. thermal processes often cause the generation of unwanted Maillard by-products<sup>15</sup>. Moreover, resin adsorption might be more selective than other techniques which might lead to improvement in product quality. Weisz et al. (2010) studied the recovery of polyphenols from sunflower meal using macroporous hydrophobic food grade resins (Amberlite XAD16 and FPX66) and an anion exchange resin. The authors found that polyphenols are favorably adsorbed in these types of adsorbents. pH has a significant impact on the adsorption of polyphenols compounds as identified in the work of Dávila-Guzman, et al.<sup>16</sup> and Ferri, et al.<sup>17</sup> since lower pH than the pKa of the phenolic acid, increases polyphenol adsorption on hydrophobic resins and zeolites.

Recovered phenolic compounds find application in different industries. In cosmetics, natural polyphenols are used as UV filters for instance in sunscreen products; in food, polyphenols are used as additives and as preservative in meat products and as antimicrobial agents for bakery and meat products<sup>18-21</sup>.

This study focuses on the evaluations of different food grade adsorbents to selectively adsorb sinapic acid from rapeseed meal extract using a model system. Single component and multicomponent adsorption equilibrium experiments were evaluated and compared in order to select the most suitable resin for capturing sinapic acid in terms of capacity, selectivity and desorption. The best performing resin data was used to model column chromatography using the transport-dispersive model combined with the linear force approximation. Selective adsorption was tested in a column experiments and compared with simulation results. This work lays the foundation of process design for recovering sinapic acid from canola/rapeseed meal extracts at industrial scale.

## 3.2. Materials and Methods

### 3.2.1. Chemicals

Sinigrin hydrate ( $\geq 99\%$ ), thioglucosidase from *Sinapis alba* (white mustard) seed ( $\geq 100$  U/g), 40 wt% phytic acid solution in H<sub>2</sub>O, trichloroacetic acid 6.1 N, ammonium molybdate tetrahydrate ( $\geq 99\%$ ), ascorbic acid: L-ascorbic acid ( $\geq 99.0\%$ ), sulphuric acid (95-97%), Ethanol: Emsure absolute for analysis, Sinapic acid ( $\geq 99\%$ ), BIS-TRIS ( $\geq 98\%$ ), Iron (III) chloride hexahydrate ( $\geq 99\%$ ), 5-sulfosalicylic acid dehydrate ( $\geq 99\%$ ), glucose anhydrous for biochemistry, citric acid ( $>99\%$ ), sodium phosphate ( $\geq 99\%$ ), sodium phosphate dibasic ( $\geq 99\%$ ), acetonitrile (HPLC grade) and formic acid were purchased from Sigma-Aldrich, The Netherlands.

### 3.2.2. Resins

Seven food grade macroporous resins were selected to evaluate polyphenol adsorption. From the Amberlite™ series, resins XAD16, XAD7, XAD4, XAD1180N, XAD761 and FPX66 were used. From Diaion™, resin HP20 was evaluated. Only resin FPX66 was obtained from Dow Chemicals while the rest were purchased by Sigma-Aldrich, The Netherlands. Resins characteristics are found in Table 3.1

**Table 3.1.** Hydrophobic resin characteristics

Resins	Matrix	Dry density (wet density) (g/mL)	Particle size (mm)	Surface area (m <sup>2</sup> /g)
<b>Amberlite XAD 16</b>	Styrene-DVB	1.08 (1.02)	0.560 - 0.710	≥ 800
<b>Amberlite XAD 4</b>	Styrene-DVB	1.08 (1.02)	0.490 - 0.690	≥ 750
<b>Amberlite FPX66</b>	Styrene-DVB	N/A (1.02)	0.600- 0.750	≥ 700
<b>Diaion HP20</b>	Styrene-DVB	N/A (1.01)	0.250 - 0.850	600
<b>Amberlite XAD 1180N</b>	Styrene-DVB	1.04 (1.02)	0.350 - 0.600	≥ 450
<b>Amberlite XAD 7HP</b>	Acrylic ester	1.24 (1.08)	0.560 - 0.710	≥ 380
<b>Amberlite XAD 761</b>	Phenol-formaldehyde	1.24 (1.11)	0.560 - 0.760	150-250

### 3.2.3. Buffer solutions and preparation

Citric acid, disodium phosphate and bis-tris solutions were prepared by dissolving the corresponding amount of each chemical in MilliQ water. Citrate-phosphate buffer was prepared following the method proposed by McIlvaine<sup>22</sup>, combining the corresponding weak acid solution (0.1M citric acid) with the conjugated base (0.2M disodium phosphate) at a given ratio depending on the desired pH.

A stock solution of sinapic acid (2 g/L) was prepared in Citrate-phosphate buffer pH 6.0 and pH 8.0. To simulate the behavior of the complex polyphenol rich extract from rapeseed meal, a multicomponent model solution was prepared by dissolving the equivalent amount of sinapic acid, glucose, sinigrin hydrate and phytic acid in buffer at pH 6.

### 3.2.4. Analytical methods

Sinapic acid concentration was analyzed by Ultra High-Performance Liquid Chromatography (UHPLC, Ultimate 3000, Thermo Scientific, USA) equipped with a C18 column (Acquity UPCL HSS column 1.8µm, 2,1mmx1000mm Waters, Milford, USA). The column was maintained at 30°C with a flow of 0.3 mL/min (isocratic elution 66.7% solvent A). Solvent A is MilliQ Q water (acidified with 10% ferulic acid) and solvent B is acetonitrile (acidified with 10% ferulic acid). Data acquisition was obtained at 325 nm wavelength.

Glucose and phytic acid concentration were determined spectrophotometrically using Glucose HK Assay kit (Sigma-Aldrich) and Phytic Acid (Total Phosphorus Assay Kit) (Megazyme) respectively.

Since there are no direct kits available for sinigrin hydrate (glucosinolates) detection, the method of Miranda Rossetto, et al.<sup>23</sup> was followed. The glucosinolates were hydrolyzed by thioglucosidase (myrosinase) first, after which the resulting glucose was measured using the glucose assay kit. A myrosinase solution with a concentration of 0.009375 U/mL was prepared based on the concentration used by Li, et al.<sup>24</sup>.

### 3.2.5. Batch adsorption experiments

Batch adsorption experiments consisted in single components and multicomponent experiments to determined adsorption equilibrium information and selectivity of sinapic acid over the other components on the tested hydrophobic resins.

#### 3.2.5.1. Single component experiments

##### 3.2.5.1.1. Adsorption equilibrium isotherms

Adsorption equilibrium isotherms were obtained using Tecan EVO Freedom 200 robotic liquid handling system and Multiscreen Filter plates (catalog number: MDRPN0410) from Millipore, USA. The procedure involved adding a known amount of resin (0.02 g) in each well of the filter plate. Resins were added using Titan 96 well resin loader (Radleys, UK). Resins were washed two times with ethanol and three times with MilliQ water. After washing, equilibration with the corresponding buffer was done. Sinapic acid isotherms were obtained by contacting different concentrations of a stock solution (from 2.0 to 0.1 g/L) with the resins under agitation (1200 rpm) until equilibrium was reached. The plate was centrifuged, and the liquid was collected on a 96 deep well collector plate. Liquid concentration was measured by UHPLC analysis. The adsorbed amount was calculated using the mass balance equation (3.1)

$$q_e = \frac{(C_0 - C_e)V}{m} \quad (3.1)$$

Where  $C_0$  is the initial concentration (g/L),  $C_e$  is the equilibrium concentration (g/L),  $V$  is the volume of the liquid phase (L) and  $m$  is the amount of resin (g).

Isotherm adsorption experiments were conducted at pH 6 and at pH 8. An additional set of experiments was done using different ethanol concentrations, 20%, 30% 40% 70% and 96% (w/w) in order to identify the effect of ethanol in the adsorption of sinapic acid. The experiments with ethanol were used to determine the isotherm dependence on ethanol concentration.

#### 3.2.5.2. Multicomponent experiments

Effect of glucose, sinigrin hydrate and phytic acid on sinapic acid adsorption was evaluated with multicomponent experiments. The experiments were performed following the same procedure as in 3.2.5.1.1 Adsorption equilibrium isotherms

### 3.2.6. Resin Selection

The desired scenario in this work is to selectively capture sinapic acid over sugars, sinigrin hydrate and phytic acid using a hydrophobic resin. To evaluate the different resins, the methodology suggested by Sevillano, et al.<sup>25</sup> was used with some modifications. Three criteria were determined based on capacity, selectivity and easy of desorption. A weight between 0 and 1 was given to each criterion.

The first criterion is the capacity of the sinapic acid ( $q_{SA}$ ) from the isotherm at feed condition (weight of 0.5). The second criterion is the selectivity of the resin for the sinapic acid ( $S_{imp,SA}$ ) over the impurities and is defined as follows:

$$S_{imp,SA} = \frac{Slope_{sA}}{\pi_{imp}^n \sqrt[n]{Slope_{imp}}} \quad (3.2)$$

On the numerator is the slope of sinapic acid isotherm at pH 6 ( $Slope_{sA}$ ), and the denominator is the product of the  $n^{\text{th}}$  roots of the slopes of the isotherm of the other compounds ( $Slope_{imp}$ ). Here,  $n$  refers to the number of impurities being considered. This criterion was given a lower weight of 0.2 as the effect of the impurities on polyphenol adsorption resulted very low.

The third criterion is the inverse slope at desorption condition, which was based on the lowest obtained capacity in the experiments at different ethanol concentration. The selected desorption condition was 70% ethanol, as it was found to have the lowest capacity and slope of sinapic acid.

$$1/Slope_{70\% EtOH} \quad (3.3)$$

This criterion was given a weight of 0.3.

Each criterion was normalized and resin score was calculated using equation (3.4)

$$Resin\ score = \sum weight * \frac{criterion}{maximum\ value\ of\ criterion} \quad (3.4)$$

### 3.2.7. Column experiments

The highest-scoring resin (FPX66) was chosen to perform column experiments. Breakthrough curves of sinapic acid and a mixture of sinapic acid and glucose were done at room temperature (25 °C) using an AKTA™ Avant systems (GE Healthcare Bio-Sciences AB, Uppsala, Sweden). Unicorn 7.0 operating software was used and conductivity, pH and UV at 325 nm were monitored online. The prepared solutions were pumped through the column using a flow rate of 1 mL/min. Fractions were taken during the experiments and analyzed for sinapic acid by UHPLC as explained in section 3.2.4 Analytical methods. The collected fractions were kept at a constant temperature of 6°C

Around 5 grams of pre-wetted resin was placed in an adjustable height Omnifit glass column (1cm internal diameter and 15 cm height). Packing of the resin was done using a slow upfront water flow and applying vibration. Total volume of the column was 7.4 mL. An extraparticle porosity of 0.3 was determined with a pulse injection of NaCl and the intraparticle porosity was calculated using the difference between dry and wet weight of the resin. The pressure limit of the Omnifit glass column was used (4.1MPa). The mobile phase characteristics were assumed to be the same as water. The dead volume of the system was also determined by means of tracer injection.

### 3.2.8. Theory: Chromatography model

#### 3.2.8.1. Isotherm model

The Langmuir isotherm has been widely applied to describe adsorption equilibrium. This model assumes chemisorption as reaction and it is restricted to a monomolecular layer. The model can be expressed as:

$$q_i = \frac{q_{max,i}K_iC_i}{1 + K_iC_i} \quad (3.5)$$

where  $q_i$  is the adsorption capacity (g/L<sub>R</sub>),  $q_{max}$  is the maximum adsorption capacity (g/L<sub>R</sub>),  $K_i$  is the equilibrium constant (mL/g) and  $C_i$  is the concentration (g/L) of the species being adsorbed<sup>26</sup>.

The standard equation for the Langmuir isotherm can be rewritten as follows in equation (3.6) in order to incorporate a modifier (in this case ethanol) concentration term.

$$q_i = \frac{H_iC_i}{1 + \frac{H_iC_i}{q_{max,i}}} \quad \text{where } H = K_iq_{max,i} \quad (3.6)$$

The  $H$  represents slope term of the isotherm. The dependency of the slope of the isotherm as a function of the ethanol concentration was modelled using a power function as described in equation (3.7):

$$H = \alpha \cdot (c_{mod} + 1)^{-\beta} \quad (3.7)$$

where  $c_{mod}$  is the modifier concentration (in this work ethanol), and  $\alpha$  and  $\beta$  are the power function parameters. The parameter  $\alpha$  was set to be the isotherm slope at 0% ethanol, and only parameter  $\beta$  was regressed.

Langmuir parameter  $q_{max}$  and  $K$  were obtained by fitting the Langmuir isotherm equation (3.5) with the experimental data using MATLAB R2017b and the function *Isqcurvefit*. Similarly, empirical parameter  $\beta$  from equation (3.7) was obtained.

#### 3.2.8.2. Dynamic column model

Several dynamic models have been introduced to describe adsorption behavior. The most complex model is the general rate model, followed by the lumped pore model and the lumped kinetic model. The latter two models are simplifications of the general rate model. The general rate model and its simplifications are presented in the work of Felinger, et al.<sup>27</sup>. For column simulation the lumped kinetic model was used. The simplification made here is that there are no intraparticle pores, and  $\epsilon_p = 0$ . Therefore there is no longer a separate mass balance for the pores, and instead one overall balance as shown in equation (3.8):

$$\frac{\partial C_i}{\partial t} + F \frac{\partial q_i}{\partial t} + v \frac{\partial C_i}{\partial z} = D_L \frac{\partial^2 C_i}{\partial z^2} \quad (3.8)$$

The solid stationary phase concentration term  $\frac{\partial q}{\partial t}$  is defined as follows in equation (3.9):

$$\frac{\partial q_i}{\partial t} = k_{ov,i}(C_i - C_{eq,i}) \quad (3.9)$$

Where  $C$  represents the bulk liquid phase concentration (g/L)  $C_{eq}^*$  is the liquid phase concentration in equilibrium with the solid phase (g/L), which is obtained using equation (3.6),  $F$  is the phase ratio, defined as  $F = (1 - \varepsilon_b) / \varepsilon_b$ , where  $\varepsilon_b$  is the bed porosity,  $q$  is the concentration in the adsorbent,  $v$  is the interstitial velocity of the mobile phase,  $D_L$  is the axial dispersion coefficient (m<sup>2</sup>/s) and  $k_{ov}$  is the overall mass transfer coefficient (1/s).

The overall mass transfer coefficient  $k_{ov}$  is defined according to equation (3.10):

$$\frac{1}{k_{ov,i}} = \frac{d_p}{6} \left( \frac{1}{k_f} + \frac{1}{k_{pore}} \right) \quad (3.10)$$

where  $d_p$  is the particle diameter (m),  $k_{pore}$  is the pore diffusion coefficient (m/s), defined as in equation (3.11) and  $k_f$  is the film mass transfer coefficient (m/s).

$$k_{pore} = \frac{10\varepsilon_p D_p}{d_p} \quad (3.11)$$

Where  $D_p$  is the pore diffusivity (m<sup>2</sup>/s). Table 3.2 summarizes other mass transfer correlations used in the column modelling.

It is assumed that initially there is none of the components to be loaded present in the column. Therefore, the initial conditions in the liquid and solid phases are as follow in equation (3.12) and equation (3.13).

$$C(t = 0) = 0 \quad (3.12)$$

$$q(t = 0) = 0 \quad (3.13)$$

And the following boundary conditions:

$$C(t, x = 0) = C_{inlet} - \frac{D_L}{u_h} \cdot \frac{\partial C(t, x = 0)}{\partial x} \quad (3.14)$$

$$\frac{\partial C(t, x = L)}{\partial x} = 0 \quad (3.15)$$

**Table 3.2.** Mass transfer correlations

Mass transfer parameter	Correlation	Reference
Free diffusivity	Wilke-Chang	Wilke, et al. <sup>28</sup>
Film mass transfer coefficient	Wilson & Geankoplis	Wilson, et al. <sup>29</sup>
Pore tortuosity	Wakao & Smith	Wakao, et al. <sup>30</sup>
Pore diffusivity	Brenner & Gaydos	Brenner, et al. <sup>31</sup>
Axial dispersion coefficient	Chung & Wen	Chung, et al. <sup>32</sup>

The set of partial differential equations (PDEs) was solved using MATLAB R2017b by discretizing the PDEs in space using the method of lines following the approach developed by Nfor, et al.<sup>33</sup>. The discretized set of PDEs was solved numerically using MATLAB ODE solver, *ode15s*.

### 3.3. Results and Discussion

#### 3.3.1. Single component adsorption equilibrium isotherms

Adsorption equilibrium isotherms indicate the concentration of the absorbed compound at equilibrium with the liquid (mobile) phase. Since proteins and polyphenols are usually extracted from the oilseed meal at mild-acidic conditions using sodium chloride,<sup>13</sup> batch adsorption experiments of sinapic acid in Citrate-phosphate buffer were performed at pH 6.0 by equilibrating the resins with sinapic acid solutions for three hours which was sufficient to reach equilibrium as determines in kinetic studies (data not shown, see supplementary material). The results at pH 6 are presented in Figure 3.1a and the regressed parameters can be found in Table 3.3.

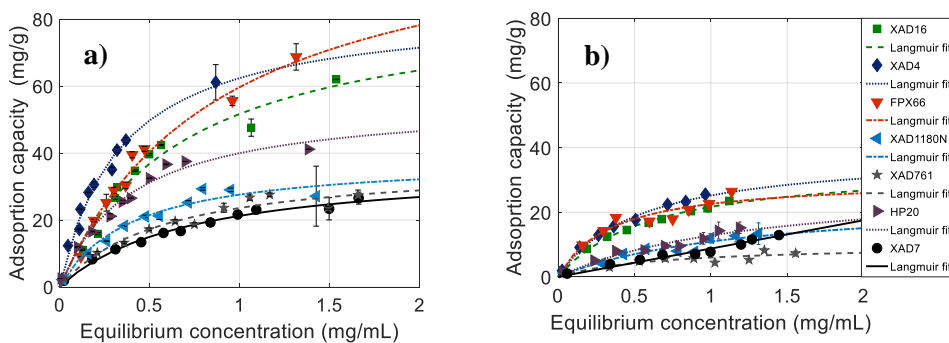


**Figure 3.1.** Sinapic acid adsorption equilibrium isotherms on macroporous hydrophobic resins a) at pH 6.0 and b) at pH 8.0. Lines represent Langmuir isotherm fitting using parameters of Table 3.3. Markers are experimental data: (■) XAD16, (◆) XAD4, (▼) FPX66, (◀) XAD1180N, (★) XAD761, (▶) HP20 (●), XAD7. Error bars resulted from duplicate experiments

The tested adsorbents differ from each other in surface area and matrix. Regarding the surface area, resins XAD16, FPX66 and XAD4 showed the higher maximum capacity, which was expected as these resins have the higher surface area (>700 m<sup>2</sup>/g). Resin FPX66 gives the higher maximum adsorption

capacity followed by XAD16. The initial slope of the isotherm is an indication of the affinity of sinapic acid to the resins. It can be observed from the graph that sinapic acid has a higher affinity for resin XAD4 followed by FPX66 and XAD16. The initial slope of the isotherm can be obtained from the regressed parameter of the Langmuir isotherm,  $q_{\max}$  and  $K$ . The product of these two parameters corresponds to the initial slope.

Thiel, et al.<sup>34</sup> evaluated the adsorption of sinapic acid, ferulic acid and p-coumaric acid into zeolites and hydrophobic resins, including XAD16 and XAD7, the same resins presented in this work. The values are in the same order of magnitude, being the one here presented higher than the ones presented by Thiel, et al.<sup>34</sup>, however these authors evaluated the experiments at different pH conditions which might explain the difference in the values.

Regularly, oilseed valuable products are extracted from the meal using an aqueous extraction at mid or alkaline conditions as suggested by other authors.<sup>35-37</sup> Since at higher pH, derivatives of sinapic acid can be hydrolyzed,<sup>11</sup> evaluation of the adsorption of sinapic acid at different pH values was done and is described in the following section.

### 3.3.2. Effect of pH on adsorption behavior of sinapic acid

pH 8.0 was selected to evaluate the adsorption at alkaline condition. The results are presented in Figure 3.1b. Langmuir isotherm parameters were regressed from the data and are shown in Table 3.3. The initial slope of the isotherm and the maximum capacity followed the same behavior as with the isotherm at pH 6, being the highest the one of XAD4. From Figure 3.1, one can notice that the adsorption capacity decreases when the pH increases. A similar trend was observed by Dávila-Guzman, et al.<sup>16</sup> and Simon, et al.<sup>38</sup> for ferulic acid and for p-coumaric acid respectively. The pKa values of the carboxylic group and the phenolic group of sinapic acid are 4.47 and 9.21 respectively.<sup>39</sup> The decrease in adsorption might be due to this ionization which reduces the affinity of the polyphenol to the hydrophobic bed.

**Table 3.3** Estimated Langmuir parameters of sinapic acid on the tested adsorbents at pH 6.0 and pH 8

pH 6.0				
Resin	$q_{\max}$ (mg/g <sub>resin</sub> )	K (mL/mg)	$q_{\max} * K$ (mL/g <sub>resin</sub> )	R <sup>2</sup>
FPX66	102.6 ± 11.7	1.3 ± 0.3	133.4 ± 34.3	0.93
XAD16	86.6 ± 6.0	1.5 ± 0.2	128.2 ± 19.5	0.96
XAD4	83.7 ± 5.2	2.9 ± 0.4	245.3 ± 33.8	0.97
HP20	55.7 ± 2.7	2.6 ± 0.3	142.0 ± 17.6	0.97
XAD761	37.2 ± 2.6	1.7 ± 0.3	64.7 ± 12.7	0.94
XAD7	36.6 ± 2.3	1.4 ± 0.2	48.4 ± 7.6	0.97
XAD1180N	35.5 ± 3.8	2.5 ± 0.7	89.3 ± 25.1	0.90

pH 8.0				
Resin	$q_{\max}$ (mg/g <sub>resin</sub> )	K (mL/mg)	$q_{\max} * K$ (mL/g <sub>resin</sub> )	R <sup>2</sup>
FPX66	30.4 ± 2.7	2.9 ± 0.7	87.6 ± 23.4	0.81
XAD16	34.9 ± 1.7	1.6 ± 0.2	57.1 ± 6.7	0.99
XAD4	38.6 ± 2.1	1.9 ± 0.2	72.4 ± 9.4	0.91
HP20	29.4 ± 8.6	0.8 ± 0.4	22.7 ± 12.7	0.87
XAD761	9.9 ± 2.0	1.5 ± 0.8	15.0 ± 8.0	0.70
XAD7	-	-	8.7 ± 0.2*	0.95*
XAD1180N	24.4 ± 7.7	0.8 ± 0.4	19.8 ± 8.6	0.79

\*Linear isotherm was fitted to the data

Sinapic acid can dissociates in three species, sinapic acid (protonated) ion sinapinate and ion sinapinate-phenolate. At pH 6 and pH 8 two sinapic acid species are presented, 98% the ion sinapinate 2% sinapic acid while at pH 8, 94% of sinapic acid is in sinapinate form and 6% in the sinapinate-phenolate form. Even though, similar percentage of ion sinapinate was presented at both tested pH, the adsorption capacity at pH 8.0 is around half of the one obtained at pH 6.0. This behavior suggests that the hydrophobicity of the acid decreases with pH and therefore also its interaction with the resins. At pH 8.0, a darker solution than the one obtained at pH 6.0 was observed, which is attributed to ion sinapinate-phenolate<sup>40</sup> only presented at pH 8. Color changing (darker) in the stock solution at pH 8 was observed over time, after ten days, the solution turned from yellow to dark brown. This color changing is attributed to the autoxidation of sinapic acid into the intermediate thomasidioic acid, which is further converted into 2,6-dimethoxy-p-benzoquinone and 6-hydroxy 5,7-dimethoxy-2-naphthoic acid which was also observed in the research of Cai, et al.<sup>40</sup> During the adsorption experiment, no color changing was observed (3 h or agitation) which indicates that oxidation did not occur during the time selected for the experiments.

Even though desorption of sinapic acid could be performed using alkaline conditions, this might lead to oxidation of sinapic acid and product loss, therefore other desorbing agents should be evaluated. Desorption of polyphenols from macroporous resins has been studied using ethanol/water mixtures.<sup>17, 34, 38</sup> The following section describes the experimental results of sinapic acid adsorption on hydrophobic resins using ethanol.

### 3.3.3. Effect of ethanol on sinapic acid adsorption

Batch adsorption experiments were evaluated at different ethanol concentration to determine sinapic acid adsorption equilibrium as a function of the ethanol concentration. Results are shown in Figure 3.2 for all the evaluated resins.

Here it can clearly be seen that there is a significant difference between the isotherm slopes for 0% ethanol and the ones where ethanol is presented. The trend seems to follow a parabolic shape: 20% ethanol seems to be the least effective among the other ethanol concentration tested, however there is a significant decrease on the value of the slope if it is compared to the 0%. At 30% and 40% ethanol

solutions exhibit similar sinapic acid isotherm slopes, and at 70%, the slopes are at their lowest, followed by a slight increase in slope for 96% ethanol.

This behavior can possibly be explained by the effect of the activity coefficient: the solubility of sinapic acid increases with increasing ethanol concentration, reaching a peak at 70% ethanol, and decreases at concentrations higher than 70%. This was observed for similar molecules in the research of Sevillano, et al.<sup>41</sup> for which the solubility of green tea catechins was modelled using the NRTL-SAC model. A similar trend was found in the experimental as well as the modelled solubility data: the solubility of the catechins increased with increasing mol fraction of ethanol, peaked at a mol fraction of ethanol of 0.7 and decreased for higher mol fractions.

As mentioned before, the isotherm slope is an indication of the affinity of sinapic acid to the resins. Therefore, the above results can be used to model the dependency of the isotherm slope with ethanol. This was done by fitting the power function as expressed in equation (3.7). As mentioned previously the parameter alpha was set to be the isotherm slope at 0% ethanol (Table 3.3) and parameter beta was regressed. Values for beta of 8.6, 13.6, 7.0, 8.3, 7.1, 3.9 and 5.4 were found for resins FPX66, XAD4, XAD16, HP20, XAD1180N, XAD7 and XAD761 respectively.

The results of these experiments were used to evaluate the desorption criterion for resin selection. The dependency of the slope of the isotherm on ethanol concentration was implemented in the column dynamic model to evaluate the adsorption/desorption of sinapic acid on the best performing resin (FPX66) see 3.3.6 Column adsorption and elution

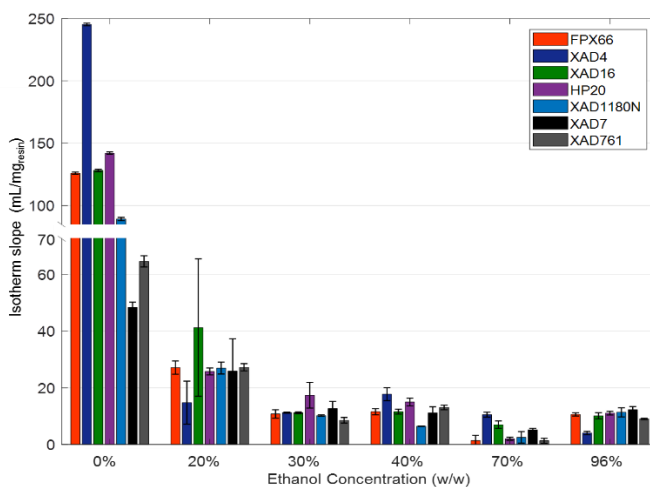


**Figure 3.2.** Effect of ethanol concentration on isotherm slope of sinapic acid. From left to right in each ethanol concentration FPX66, XAD4, XAD16, HP20, XAD1180N, XAD7 and XAD761. Error bar resulted of duplicate experiments

### 3.3.4. Multicomponent adsorption

The effect of sugars, glucosinolates and phytic acid on the adsorption of sinapic acid on the food grade macroporous resins, was evaluated by comparing the adsorption capacity of sinapic acid in the multicomponent system with the single component system. Figure 3.3 shows the results of this

comparison. The capacity ( $q$  Expected) in the single component system (blue bars) was calculated using the pre-determined isotherm parameters, while the capacity of the multicomponent system ( $q$  Experimental) is obtained experimentally (green bars).

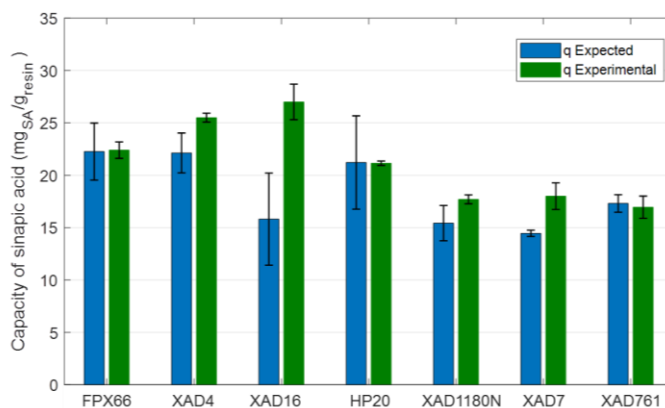


**Figure 3.3.** Comparison between expected sinapic acid capacity based on Langmuir isotherm and obtained sinapic acid capacity from multicomponent experiments at pH 6.0. Bar order per resin: left expected capacity, right experimentally obtained capacity

It can be seen that there is very little to none significant difference on the sinapic acid adsorption with the presence of impurities, specially FPX66, HP20, and XAD761. The capacity of sinapic acid seems to have improved with the presence of the other compounds for resins XAD4, XAD7, XAD16 and XAD1180N. A comparison of the isotherm slopes of all components was made. The results are shown in Figure 3.4 and where used to calculate the selectivity of sinapic acid over the other components in the extract.

Figure 3.4 clearly shows that the slope of the isotherm of phytic acid, sugars and glucosinolates is significantly lower compared to the slope of sinapic acid for all hydrophobic resins. The isotherm slope of phytic acid (average of all resins) is around 40 times lower than the one of sinapic acid, while the slopes of sugars and glucosinolates are 165 and 48 times smaller than sinapic acid slope respectively. It is widely known that sugars are hydrophilic and dissolve in water easily, which might explain the lowest slope value. Phytic acid is negatively charged around neutral pH<sup>42</sup> and dissociated molecules have higher solubility in water. As the tested resins are neutral and hydrophobic, and the stream solution was neutral, phytic acid has a low interaction with the resins. Similarly, glucosinolates are typically in an ionic form, and are therefore hydrophilic. The pKa of glucosinolates is very low, at around 2<sup>43</sup> therefore, at the tested pH value these components will always be in the anionic form and their affinity with the resins is smaller than the one of sinapic acid.

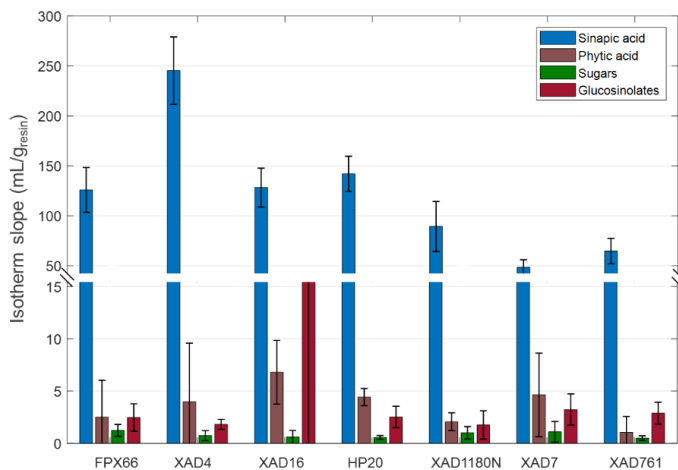


**Figure 3.4.** Isotherm slope comparison between sinapic acid, phytic acid, sugars and glucosinolates at pH 6. From left to right per resin Sinapic acid, phytic acid, sugars and glucosinolates. Value of isotherm slope of glucosinolates for XAD16 is  $17.6 + 18.1$  mL/g<sub>resin</sub>. Error bars resulted of duplicate experiments

The affinity (isotherm slope) of sinapic acid is much higher than the affinity of the other compounds (sugars, glucosinolates and phytic acid) in all resins, which indicates that these resins selectively capture sinapic acid.

### 3.3.5. Resin Selection

Following the strategy proposed by Sevillano, et al.<sup>25</sup> with modification and using the data obtained from the previous experimental stages (isotherm determination and multicomponent experiments), three criteria were determined in order to select the best-performing resin. Each criterion was given a weight between 0 and 1 (with the total weight assigned equal to 1), with a final score out of 100. The numerical values determined for each criterion are shown in Table 3.4.

**Table 3.4.** Values of each criterion for resin selection

	Capacity (mg/g <sub>resin</sub> )	Selectivity $S_{SA, others}$	Desorption (inverse of slope 70% ethanol)
<b>FPX66</b>	66.99	63.88	0.73
<b>XAD4</b>	66.30	140.49	0.09
<b>XAD16</b>	56.99	30.59	0.14
<b>HP20</b>	42.78	76.61	0.50
<b>XAD1180N</b>	27.23	57.86	0.40
<b>XAD7</b>	23.15	19.00	0.19
<b>XAD761</b>	25.77	55.98	0.77

The normalized criteria values and the total resin scores, calculated using equation (3.4) are shown in Figure 3.5.

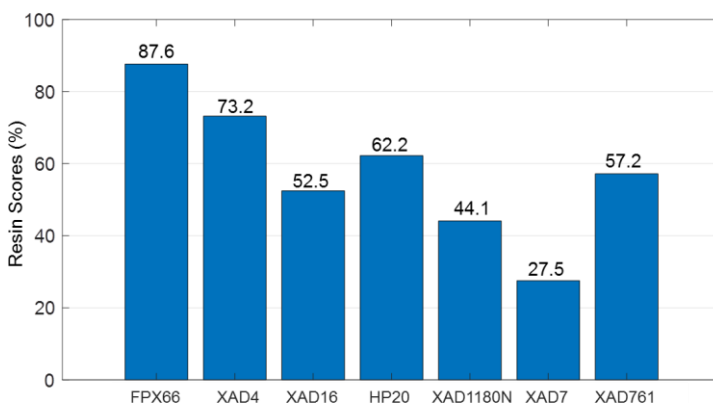


**Figure 3.5.** Weighted resin score of evaluated food macroporous resins

From the above figure (Figure 3.5), resin FPX66 shows the highest resin score as it has the highest adsorption capacity, is the third highest in selectivity and second highest in desorption. Resin XAD4 also shows good performance in terms of capacity and selectivity as it has the highest adsorption slope isotherms, which also indicates strong binding. Nevertheless, the isotherm slope at desorption conditions (70% ethanol) was higher than all other resins, indicating more difficulties for desorption, which also reduces its resin score.

### 3.3.6. Column adsorption and elution

The selected resin, FPX66, was then used to perform column experiments where the mechanistic model previously described in 3.2.8.2 Dynamic column model section was applied to verify whether it is possible to predict chromatographic behavior.

The results are shown in Figure 3.6. Adsorption experiments were performed using a solution of sinapic acid and sinapic acid (SA) combined with glucose, as the concentration of glucose in the stream is significantly higher (8 g/L) than glucosinolates and phytic acid concentration.

The results showed that at the selected flow rate, the breakthrough of sinapic acid is at about 3 column volumes, showing a slightly spread front. It can be seen that the presence of glucose does not affect the adsorption of sinapic acid, as suggested by the multicomponent experiments. The total amount adsorbed in both experiments and the model is shown in Table 3.5 together with the corresponding capacity ( $q$ ). Not enough fractions were collected towards the end of the runs, which explain why the concentration of the fractions does not reach the concentration in the inlet.

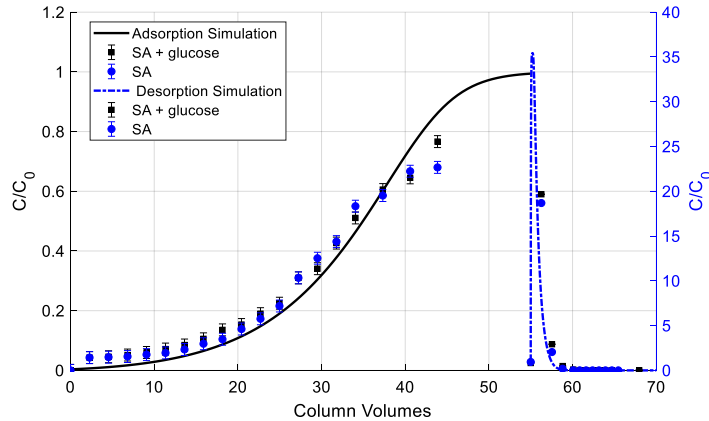


**Figure 3.6.** Breakthrough comparison between modelled and experimental data for adsorption/desorption of sinapic acid on 7.4 mL column filled with FPX66 at 1 mL/min and room temperature. Adsorption was performed at pH 6 and desorption using 70% ethanol

It can be seen that the model and the experimental results show a very good agreement. The shape of modeled curve seems to correspond to the experimental points except at the end of the breakthrough curve, where the model slightly deviates from the experimental values. This difference might be attributed to dispersion, as the axial dispersion coefficient is calculated using the empirical correlation of Chung, et al.<sup>32</sup> which might be underestimated, as higher axial dispersion is suggested by the experimental results.

**Table 3.5** Experimental and modelling comparison of the adsorbed amount of sinapic acid and capacity obtained from column experiment on resin FPX66 at 1 mL/min

Experiment	Adsorbed amount (g)	Capacity (mg/g <sub>resin</sub> )
<b>Sinapic acid</b>	0.32	63.53
<b>Sinapic acid + sugars</b>	0.32	64.34
<b>Modelling</b>	0.35	67.48

Desorption was performed using 70% ethanol, which was also modelled. The amount of sinapic acid obtained was calculated by numerical integration and corresponds to 0.26 grams which is slightly less than the expected amount to be recovered. The second collected fraction was obtained at 1.3 column volumes (56.3 CV of the total run), which, based on the simulation, might not be the highest concentration point. The limited number of experimental values, at the initial stage of the desorption, might explain the difference between the adsorbed and desorbed amount of sinapic acid. Nevertheless, the values are in the same order or magnitude, which also indicates that the simulation is in good agreement with the experimental points as they lay very close to the simulation curve having a correlation factor ( $r^2$ ) of 0.98.

Using the selected resin, FPX66, and the chromatography model, a large-scale process for the selective capture of sinapic acid from oilseed meal can be designed.

As the food sector usually deals with voluminous side streams, continuous chromatography might therefore be a suitable mode of operation. The dynamic column model, presented here, can very well be used to evaluate different continuous chromatography systems such as CaptureSMB<sup>44</sup> and Simulated Moving Bed (SMB).<sup>45</sup>

### 3.4. Conclusions

Selective capture of sinapic acid on resin FPX66 was observed in this study. Adsorption equilibrium was evaluated at different pH values and using ethanol/water mixtures. Higher pH leads to lower adsorption capacity and also oxidation of sinapic acid, meaning loss of product, therefore, ethanol was chosen as desorbing agent. From multicomponent experiments it was found that the adsorption of sinapic acid on hydrophobic resins is not significantly affected by the presence of sugars, glucosinolates or phytic acid. The screening of different desorption conditions leads to select ethanol as an effective desorbing agent. All the tested ethanol percentages showed a far lower sinapic acid isotherm slope.

Isotherm parameters were accurately regressed and used as input for a dynamic column chromatography model that shows a very good agreement with the experimental results which confirms that sinapic acid is selectively adsorbed on resin FPX66.

E- Supplementary data of this work can be found in online version of the paper

### 3.5. Acknowledgements

This work was supported by the ISPT (Institute for Sustainable Process Technology) under the project CM-20-07 in Adsorption of non-volatiles from food products. Thank you to the industrial partners DSM, Unilever, Friesland Campina and Royal Cosun for their valuable comments.

### 3.6. References

- 1 European Commission, 2017, Circular Economy - European Commission (accessed 11 August 2017). [https://ec.europa.eu/growth/industry/sustainability/circular-economy\\_en](https://ec.europa.eu/growth/industry/sustainability/circular-economy_en)
- 2 European Commission, 2014, Impact assessment on measures addressing food waste to complete swd (2014) 207 regarding the review of eu waste management targets (accessed 1 September 2019). <http://ec.europa.eu/environment/eussd/pdf/IA.PDF>
- 3 European Commission, 2011, Evolution Of (Bio-) Waste Generation/Prevention And (Bio-) Waste Prevention Indicators (accessed 1 September 2017). [http://ec.europa.eu/environment/waste/prevention/pdf/SR1008\\_FinalReport.pdf](http://ec.europa.eu/environment/waste/prevention/pdf/SR1008_FinalReport.pdf)
- 4 Virtanen S., Chowreddy R.R., Irmak S., Honkapää K., Isom L., Food Industry Co-streams: Potential Raw Materials for Biodegradable Mulch Film Applications, Journal of Polymers and the Environment, (2016) 1-21.

- 5** Ottens M., Chilamkurthi S., Rizvi S., Advances in process chromatography and applications in the food, beverage and nutraceutical industries, Separation, Extraction and Concentration Processes in the Food, Beverage and Nutraceutical Industries, Woodhead Pub., Oxford, (2010) 109-147.
- 6** Galanakis C.M., Recovery of high added-value components from food wastes: Conventional, emerging technologies and commercialized applications, Trends in Food Science & Technology, 26 (2012) 68-87.
- 7** Galanakis C.M., Emerging technologies for the production of nutraceuticals from agricultural by-products: A viewpoint of opportunities and challenges, Food and Bioproducts Processing, 91 (2013) 575-579.
- 8** Wanasundara J.P.D., Tan S., Alashi A.M., Pudel F., Blanchard C., Chapter 18 - Proteins From Canola/Rapeseed: Current Status, in: Sustainable Protein Sources, Academic Press, San Diego, 2017, pp. 285-304.
- 9** Xu L., Diosady L.L., Interactions between canola proteins and phenolic compounds in aqueous media, Food Research International, 33 (2000) 725-731.
- 10** Nićiforović N., Abramovič H., Sinapic Acid and Its Derivatives: Natural Sources and Bioactivity, Comprehensive Reviews in Food Science and Food Safety, 13 (2014) 34-51.
- 11** Thiel A., Muffler K., Tippkötter N., Suck K., Sohling U., Hruschka S.M., Ulber R., A novel integrated downstream processing approach to recover sinapic acid, phytic acid and proteins from rapeseed meal, Journal of Chemical Technology and Biotechnology, 90 (2015) 1999-2006.
- 12** Vuorela S., Meyer A.S., Heinonen M., Impact of isolation method on the antioxidant activity of rapeseed meal phenolics, Journal of agricultural and food chemistry, 52 (2004) 8202-8207.
- 13** Pickardt C., Neidhart S., Griesbach C., Dube M., Knauf U., Kammerer D.R., Carle R., Optimisation of mild-acidic protein extraction from defatted sunflower (*Helianthus annuus* L.) meal, Food Hydrocolloids, 23 (2009) 1966-1973.
- 14** Weisz G.M., Schneider L., Schweiggert U., Kammerer D.R., Carle R., Sustainable sunflower processing — I. Development of a process for the adsorptive decolorization of sunflower [*Helianthus annuus* L.] protein extracts, Innovative Food Science and Emerging Technologies, 11 (2010) 733-741.
- 15** Galanakis C.M., Tornberg E., Gekas V., The effect of heat processing on the functional properties of pectin contained in olive mill wastewater, LWT - Food Science and Technology, 43 (2010) 1001-1008.
- 16** Dávila-Guzman N.E., Cerino-Córdova F.J., Diaz-Flores P.E., Rangel-Mendez J.R., Sánchez-González M.N., Soto-Regalado E., Equilibrium and kinetic studies of ferulic acid adsorption by Amberlite XAD-16, Chemical Engineering Journal, 183 (2012) 112-116.
- 17** Ferri F., Bertin L., Scoma A., Marchetti L., Fava F., Recovery of low molecular weight phenols through solid-phase extraction, Chemical engineering journal, 166 (2011) 994-1001.
- 18** Fang Z., Bhandari B., Encapsulation of polyphenols – a review, Trends in Food Science & Technology, 21 (2010) 510-523.
- 19** Galanakis C.M., Tsatalas P., Charalambous Z., Galanakis I.M., Control of microbial growth in bakery products fortified with polyphenols recovered from olive mill wastewater, Environmental Technology & Innovation, 10 (2018) 1-15.

- 20** Galanakis C.M., Tsatalas P., Galanakis I.M., Implementation of phenols recovered from olive mill wastewater as UV booster in cosmetics, *Industrial Crops and Products*, 111 (2018) 30-37.
- 21** Galanakis C.M., Phenols recovered from olive mill wastewater as additives in meat products, *Trends in Food Science & Technology*, 79 (2018) 98-105.
- 22** McIlvaine T., A buffer solution for colorimetric comparison, *Journal of Biological Chemistry*, 49 (1921) 183-186.
- 23** Miranda Rossetto M.R., Shiga T.M., Vianello F., Pereira Lima G.P., Analysis of total glucosinolates and chromatographically purified benzylglucosinolate in organic and conventional vegetables, *LWT - Food Science and Technology*, 50 (2013) 247-252.
- 24** Li X., Kushad M.M., Correlation of Glucosinolate Content to Myrosinase Activity in Horseradish (*Armoracia rusticana*), *Journal of Agricultural and Food Chemistry*, 52 (2004) 6950-6955.
- 25** Sevillano D.M., van der Wielen L.A.M., Hooshyar N., Ottens M., Resin selection for the separation of caffeine from green tea catechins, *Food and Bioprocesses Processing*, 92 (2014) 192-198.
- 26** Carta G., Jungbauer A., *Protein chromatography: process development and scale-up*, John Wiley & Sons, 2010.
- 27** Felinger A., Guiochon G., Comparison of the Kinetic Models of Linear Chromatography, *Chromatographia*, 60 (2004) S175-S180.
- 28** Wilke C.R., Chang P., Correlation of diffusion coefficients in dilute solutions, *AIChE Journal*, 1 (1955) 264-270.
- 29** Wilson E.J., Geankoplis C.J., Liquid Mass Transfer at Very Low Reynolds Numbers in Packed Beds, *Industrial and Engineering Chemistry Fundamentals*, 5 (1966) 9-14.
- 30** Wakao N., Smith J.M., Diffusion in catalyst pellets, *Chemical Engineering Science*, 17 (1962) 825-834.
- 31** Brenner H., Gaydos L.J., The constrained brownian movement of spherical particles in cylindrical pores of comparable radius: Models of the diffusive and convective transport of solute molecules in membranes and porous media, *Journal of Colloid and Interface Science*, 58 (1977) 312-356.
- 32** Chung S.F., Wen C.Y., Longitudinal dispersion of liquid flowing through fixed and fluidized beds, *AIChE Journal*, 14 (1968) 857-866.
- 33** Nfor B.K., Zuluaga D.S., Verheijen P.J.T., Verhaert P.D.E.M., van der Wielen L.A.M., Ottens, Marcel, Model-based rational strategy for chromatographic resin selection, *Biotechnology Progress*, 27 (2011) 1629-1643.
- 34** Thiel A., Tippkötter N., Suck K., Sohling U., Ruf F., Ulber R., New zeolite adsorbents for downstream processing of polyphenols from renewable resources, *Engineering in Life Sciences*, 13 (2013) 239-246.
- 35** Bérot S., Compoint J., Larré C., Malabat C., Guéguen J., Large scale purification of rapeseed proteins (*Brassica napus* L.), *Journal of Chromatography B*, 818 (2005) 35-42.
- 36** Moure A., Sineiro J., Domínguez H., Parajó J.C., Functionality of oilseed protein products: A review, *Food Research International*, 39 (2006) 945-963.

- 37** Tan S.H., Mailer R.J., Blanchard C.L., Agboola S.O., Canola proteins for human consumption: extraction, profile, and functional properties, *Journal of Food Science*, 76 (2011) R16-R28.
- 38** Simon V., Thuret A., Candy L., Bassil S., Duthen S., Raynaud C., Masseron A., Recovery of hydroxycinnamic acids from renewable resources by adsorption on zeolites, *Chemical Engineering Journal*, 280 (2015) 748-754.
- 39** Smyk B., Drabent R., Spectroscopic investigation of the equilibria of the ionic forms of sinapic acid, *Analyst*, 114 (1989) 723-726.
- 40** Cai R., Arntfield S.D., Charlton J.L., Structural changes of sinapic acid during alkali-induced air oxidation and the development of colored substances, *Journal of the American Oil Chemists' Society*, 76 (1999) 757-764.
- 41** Sevillano D.M., van der Wielen L.A., Trifunovic O., Ottens M., Model comparison for the prediction of the solubility of green tea catechins in ethanol/water mixtures, *Industrial & Engineering Chemistry Research*, 52 (2013) 6039-6048.
- 42** Emanuelli T., Milbradt B.G., Kolinski Callegaro M.d.G., Augusti P.R., Chapter 19 - Wheat Bran and Cadmium in Human Health, in: R.R. Watson, V.R. Preedy, S. Zibadi (Eds.) *Wheat and Rice in Disease Prevention and Health*, Academic Press, San Diego, 2014, pp. 241-260.
- 43** Chen S., Halkier B.A., Characterization of glucosinolate uptake by leaf protoplasts of *Brassica napus*, *Journal of Biological Chemistry*, 275 (2000) 22955-22960.
- 44** Baur D., Angarita M., Müller-Späth T., Steinebach F., Morbidelli M., Comparison of batch and continuous multi-column protein A capture processes by optimal design, *Biotechnology Journal*, 11 (2016) 920-931.
- 45** Aniceto J.P.S., Silva C.M., Simulated Moving Bed Strategies and Designs: From Established Systems to the Latest Developments, *Separation & Purification Reviews*, 44 (2015) 41-73.

## Appendix 3A. Adsorption kinetics

Kinetic experiments were performed in order to determine the time required to reach equilibrium and a suitable agitation speed that allows proper mixing between the resins and the liquid phase. Sinapic acid experiments were done using XAD16 resin.

Experiments were done using one single deep well filter plate with the aid of an EVO Freedom 200 robotic station. They consisted of adding an aliquot of the component solution in reverse order with respect to the liquid and resin contact time. The first sample is therefore the longest incubated one and the last sample is the shortest. Once incubation time is over, liquid was recovered by centrifugation (3 mins at 4000 rpm) and the samples were analyzed to determine sinapic acid concentration.

Table 3.6 shows the conditions used for sinapic acid kinetic experiments.

**Table 3.6** Adsorption kinetic experiments

Component	Initial concentration (mg/mL)	Tested phase ratios (mL/g* or mL/mL**)	Tested agitation speeds (rpm)	Incubation time (min)
Sinapic acid	2	25* and 30*	1200	180 min

\* mL of liquid per gram of wet resin

A control well(s) (well without resin) was evaluated in all experiments. All the experiments were performed at pH 6. Sinapic acid kinetic experiments were evaluated using resin XAD16. The other proposed resins have similar characteristics; therefore, it is expected that the time required to reach equilibrium will be similar. Transient adsorption experiments results are presented in Figure 3.7

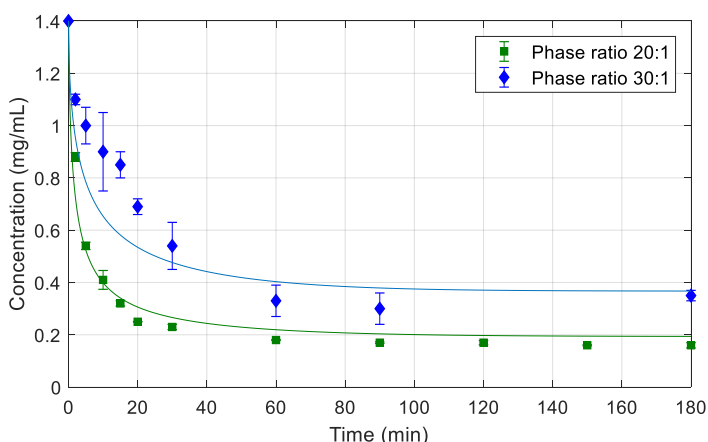


**Figure 3.7.** Sinapic acid adsorption kinetics on resin XAD16 with two phase ratios (mL/g<sub>resin</sub>) 20:1 green squares and 30:1 blue diamonds. Agitation performed at 1200 rpm. Error bar resulted of duplicate experiments. Lines are used to guide the eye

## Appendix 3B. Error analysis

Two types of errors were taken into account in this research, namely, the errors associated with measurements and the errors related to regressed parameters. The first one is calculated according to error propagation using:

$$\sigma_U = \sqrt{\left(\sigma_{x_1} \frac{\partial U}{\partial x_1}\right)^2 + \left(\sigma_{x_2} \frac{\partial U}{\partial x_2}\right)^2 + \dots + \left(\sigma_{x_n} \frac{\partial U}{\partial x_n}\right)^2}$$

Where  $\sigma$  is the standard deviation,  $U$  is the property that the error is being calculated and  $x$  are the parameters experimentally measured that the property is calculated from.

To calculate the standard error in the parameters, the covariance matrix was used, which was calculated using:

$$Cov = (J^T J)^{-1} \frac{1}{n-k} \sum (y - f(x, \beta))^2$$

Where  $J$  is the Jacobian matrix that is calculated by the *lsqcurvefit* optimizer and  $\frac{1}{n-k} \sum (y - f(x, \beta))^2$  is the mean squared error, for which  $n$  is the number of data points,  $k$  is number of times a data point was measured,  $y$  is the measured adsorption and  $f(x, \beta)$  is the adsorption predicted by the model. From the covariance matrix the standard errors of the parameters were calculated by:

$$e_p = \sqrt{\text{diag}(cov)}$$

Appendix 3C. Sinapic acid dissociation

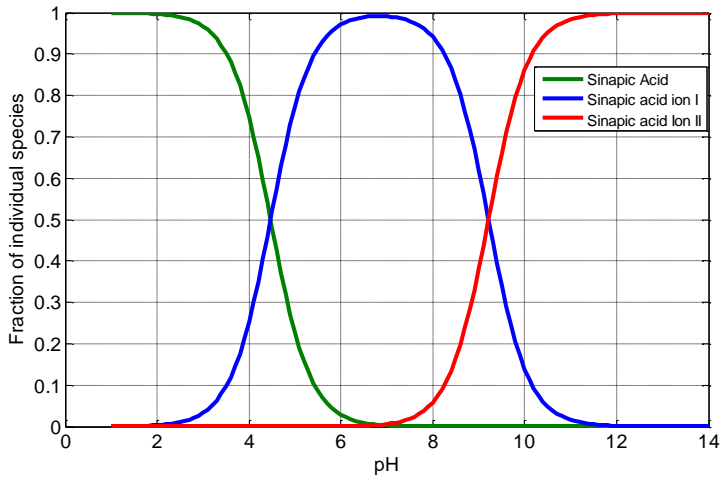


Figure 3.8. Sinapic acid dissociation as a function of pH



# Chapter 4

## High Throughput Process Development for the purification of rapeseed proteins napin and cruciferin by ion exchange chromatography

---

### Abstract

Proteins derived from plant resources such as oilseed meals, canola and sunflower, are considered a viable alternative to animal proteins for food consumption. This work presents a rational methodology, using high throughput experimentation (HTE), for the separation of cruciferin and napin, the two major proteins of canola meal, by chromatography. Eight different mixed mode and ion exchange resins were evaluated at different conditions with the aim of capturing napin and identifying adsorption/desorption behavior, ease of desorption and selectivity. POROS 50 HS resulted as the most promising resin. The obtained equilibrium adsorption data for napin and cruciferin was used in a mechanistic chromatography model and compared with experimental results showing a very good agreement. The model was used to identify column operating parameters that lead to >98% yield and purity for both proteins. Subsequently a conceptual downstream processing was proposed.

**Keywords:** Canola meal proteins, High Throughput Experimentation, Chromatography, Ion Exchange, Column simulation

---

**Published as:** *Moreno-González M., Chuekitkumchorn P., Silva M., Groenewoud G., Ottens M., High throughput process development for the purification of rapeseed proteins napin and cruciferin by ion exchange chromatography, Food Bioprod. Process, 125 (2021), 228-241 DOI: <https://doi.org/10.1016/j.fbp.2020.11.011>*

## 4.1. Introduction

Global protein demand has risen as a result of growing population and in order to satisfy this demand protein with appropriate quality needs to be generated from animal and plant sources.<sup>1</sup> Valorization of agri-food byproducts, such as oilseed meal, could help to satisfy the demand of the future food supply across the world. Canola meal is a competitive plant-based protein source, it contains ~40% protein content; ~12 % of crude fiber, 3% phenolic compounds and 3% of phytic acid among others.<sup>2-4</sup> Proteins from this meal have potential applications in bakery products as emulsifiers, in dairy and dressing products as egg white protein replacement,<sup>5</sup> in beverages as protein supplement, meat binders, mayonnaise and in cheese-like products.<sup>1</sup> Moreover, canola proteins are reported to have antiemetic, anti-oxidative, antihypertensive, anorectic and antithrombotic properties.<sup>1, 3</sup>

Napin and cruciferin are the two major proteins in canola meal, these are storage proteins with different characteristics. Napin (2S albumin) is a basic protein with an isoelectric point around 11 and a molecular weight between 12-14 kDa. Highly soluble in water at a wide pH range, stable at high temperatures (75°C)<sup>6, 7</sup> and holds foaming properties.<sup>1, 8, 9</sup> Napin protein constitutes around 20% of the protein content of canola meal, while cruciferin represents<sup>3</sup> 60%. Cruciferin (11S globulin) has an isoelectric point of around 7.2 and a molecular weight between 230-300 kDa, much higher than napin protein. This protein resembles structural features of other seed storage proteins<sup>10</sup> and has well organized structural levels.<sup>4</sup> In contrast with napin, cruciferin possesses gelling, binding and emulsifying properties which makes it an interesting product for food applications.<sup>3, 8</sup>

Several methods have been described to successfully extract proteins from defatted oilseed meals including solvent extraction, aqueous and alkaline extraction assisted with salt and enzymes, reporting protein yields between 50% and 80%.<sup>11-14</sup> Despite the high protein level in canola meal extracts, the presence of glucosinolates, phytic acid and phenolics, which are also co-extracted, could limit application of the proteins in food products. Therefore, effective separation techniques such as membrane processes<sup>15-17</sup> are required for the separation of such antinutritional components.<sup>4</sup> Even though phenolics are considered antinutritional components, their recovery might present some economic potential. Given their antioxidative properties, they have potential application in the field of cosmetics, pharmaceuticals and food products.<sup>18</sup>

Purification of the extracted proteins can be accomplished by several methods such as isoelectric precipitation followed by membrane separation<sup>16, 17</sup> and protein micellar formation,<sup>19</sup> being isoelectric precipitation (after alkaline extraction) the most applied. However, extreme alkaline conditions can have a negative effect in the functionality of the proteins due to denaturalization, loss of essential amino acids and lysinoalanine formation.<sup>12, 20-22</sup> In addition, high pH might create protein-polyphenols complexes, which make protein products dark and have bitter flavor. Similarly, protein precipitation might reduce the solubility of products and promotes protein denaturation caused by globulin aggregates.<sup>23, 24</sup> Moreover, co-precipitation of both proteins might occur leading to protein mixtures rather than individual protein isolates. Application of more selective and milder conditions, such as aqueous extraction and chromatography could be applied to keep protein functionality and improve purity of each protein product. Studies in purification of canola proteins by chromatography have been evaluated<sup>23, 25, 26</sup> using cation exchange resins (CEX), hydrophobic interaction (HIC) and size exclusion (SEC), showing the promising potential of applying this technology.

This study presents a rational strategy for the separation of cruciferin and napin proteins from canola meal extract by preparative protein chromatography. Protein extraction is assumed to be done at pH6 and at 0.3M NaCl. The strategy involves the evaluation of different cation exchange resins (CaptoS, POROS 50HS, CM Shearose and MacroPrep 50) and mixed mode resins (CaptoMMC, Nuvia cPrime, PPA HyperCel and Toyopearl MX-Trp-650M) at different pH values and salt concentrations to identify adsorption/desorption conditions with the goal of capturing napin. Resin screening was done by means of high throughput experimentation (HTE) Additionally, resin selection was done by establishing a resin selection criteria based on napin capacity, selectivity, ease of desorption and resin price. The obtained equilibrium information was used in a column adsorption/desorption model which is then used to suggest a conceptual downstream process for the separation of the two major proteins (cruciferin and napin) from canola meal extract.

## 4.2. Materials and Methods

### 4.2.1. Chemicals

For preparation of the buffers and solutions analytical grade chemicals were used. Bis-tris (>98%), tris-HCl (>98%), acetonitrile (HPLC grade), hydrochloric acid analytical reagent (37%), trifluoroacetic acid (>99%) were obtained from Sigma-Aldrich, the Netherlands. Sodium chloride (>99%) was purchased from J.T. Baker, Denmark, sodium hydroxide from Mallinckrodt Baker, The Netherlands, and Ethanol: Emsure absolute for analysis was obtained from Merck, The Netherlands.

The used proteins are: napin isolate (>98%, ABIN1995012), cruciferin isolate (>98%, ABIN1995013) and rapeseed protein mixture (57% napin and 43% cruciferin, ABIN1995014). The products were acquired from antibodies-online, GmbH, Germany. As cruciferin isolate presented very limited solubility properties in water, it was decided to use the rapeseed protein mixture to perform binary adsorption experiments.

Napin isolate, cruciferin isolate and rapeseed protein mixture were characterized by SDS-PAGE under non-reducing conditions and reducing conditions (reducing agent TCEP solution). SDS-PAGE was performed on a 4-12%Bis-Tris Gel (NuPAGE™ Novex) at constant voltage (200 V). The non-reduced sample was prepared with NuPAGE™ LDS sample buffer. The reduced sample was incubated with LDS sample buffer before loading on gel. NuPAGE Mark12™ was used as a molecular marker. The electrophoresis was carried out using MES SDS Running buffer. After running, the gel was stained in GelCode™ Blue Safe Protein Stain and detained with Milli-Q water. All SDS-PAGE reagents were obtained from ThermoScientific, The Netherlands.

### 4.2.2. Resins

Three mixed mode cation resins: Capto MMC (GE Healthcare, Sweden), Nuvia cPrime (Bio Rad, USA) and Toyopearl MX-Trp-650M (Tosoh, Japan); one mixed mode anion resin, PPA HyperCel (Pall Life Sciences, France), two strong cation resins, Capto S (GE Healthcare, Sweden) and POROS 50HS (ThermoFisher Scientific, The Netherlands) and two weak cation resins, CM Sepharose Fastflow (GE Healthcare, Sweden) and MacroPrep50 CM (Bio Rad, USA), were used to evaluate napin and cruciferin adsorption. The characteristics of all resins are shown in Table 4.1

**Table 4.1.** Mixed mode resin and Ion exchange resins

Name/Type	pKa	Matrix composition <sup>a</sup>	Ligand density <sup>a</sup> (mmol/L) <sup>a</sup>
<b>Capto MMC</b> Mixed mode weak cation exchanger	~4.6 <sup>b</sup>	Highly cross-linked agarose	80
<b>Nuvia cPrime</b> Mixed mode weak cation exchanger	~4.5 <sup>b</sup>	Macroporous highly cross-linked hydrophilic polymer	65
<b>Toyopearl MX-Trp-650M</b> Mixed mode weak cation exchanger	2.9 and 9.4 <sup>c</sup>	Methacrylic polymer matrix	110
<b>PPA HyperCel</b> Weak anion exchanger	8	High porosity cross-linked cellulose	65
<b>Capto S</b> Strong cation exchanger	1.2	Highly cross-linked agarose with dextran surface extender	125
<b>POROS 50 HS</b> Strong cation exchanger	1.2	Cross-linked polystyrene- divinylbenzene	104
<b>CM Sepharose Fastflow</b> Weak cation exchanger	4.7	Cross-linked agarose with 6% spherical	80
<b>MacroPrep50 CM</b> Weak cation exchanger	4.7	Methacrylate polymer based	210

<sup>a</sup> Provided by resin suppliers. <sup>b</sup> Based on Zhu, et al.<sup>27</sup>. <sup>c</sup> Based on the pKa of the tryptophan ligand (Pubchem.ncbi.nlm.nih.gov, 2020)

#### 4.2.3. Buffer solution and preparations

For buffers at pH 4, pH 5, pH 6 and pH 8, lactic acid, acetic acid, bis-tris and tris-HCl were used respectively. All buffers were prepared by dissolving the amount of salt corresponding to 50 mM in Milli-Q water, adjusting the pH using 2 M HCl or 2 M NaOH. The salt concentration was adjusted to 0.1M, 0.3M, 0.7M and 1.0M by adding the corresponding amount of NaCl before completing buffer final volume. All buffers were filtered previous to use using filters with 0.45 µm pore size.

Napin stock solution was prepared by dissolving napin protein (8g/L) in the appropriate buffer and filtered with a disposable 0.22 µm PVDF filter. This Napin stock solution was diluted to different napin concentrations (from 1 to 8g/L) using Milli-Q water.

In binary component experiments, protein mixture (napin/cruciferin) was dissolved in the corresponding buffer. Then the solution was sonicated at room temperature for 30 minutes in order to increase the solubility of cruciferin. After that, insolubilized protein was removed by filtering with a

disposable 0.22 µm PVDF filter, this stock solution was diluted to evaluate cruciferin effect on napin adsorption.

#### 4.2.4. Analytical methods

In single component napin experiments, the concentration of the protein was measured spectrophotometrically, measuring the absorbance at 280 nm using the spectrophotometer InfiniTe Pro 200 plate reader (Tecan, Switzerland). The measurement was performed with 100 µL of liquid solution in a 96-well half-area microplate (UV-STAR®, Greiner bio-one, Germany)

To measure the concentration of both proteins, in the protein mixture experiments, reverse phase liquid chromatography (RPC) was applied. The analysis was done using an Ultra High Performance Liquid Chromatography system (UHPLC Ultimate 3000) (Thermo Scientific, USA) equipped with a Zorbax 300 SB-C8 Rapid Resolution HD column (2.1x100 mm, 1.8 micron) (Agilent, USA). The column was equilibrated with 20% acetonitrile supplemented with 0.1% Trifluoroacetic acid (TFA) at 0.3 mL/min keeping column temperature at 30 °C. The sample was injected and a gradient of acetonitrile started from 20% to 75% in 7 min, detection was done at 280 nm. Then column was washed with 75% Acetonitrile supplemented with 0.1% TFA for 5 min before the next injection. Napin calibration lines were evaluated using napin protein isolate. Since cruciferin isolate did not show the expected characteristics, as the polypeptide profile did not show the corresponding bands (Appendix 4B. Protein characteristics), a standard curve could not be obtained. The relative change of concentration was used to evaluate cruciferin, assuming that the ratio between equilibrium concentration and initial concentration is proportional to peak area ratio  $\left(\frac{C_e}{C_{feed}} = \frac{\text{Area peak after adsorption}}{\text{Area peak of feed}}\right)$  determined by UHPLC.

#### 4.2.5. Batch adsorption experiments

Batch experiments were performed in order to determine adsorption equilibrium isotherms of napin and cruciferin at different adsorption/desorption conditions on different mixed mode and ion exchange resins, in order to separate both proteins.

##### 4.2.5.1. Adsorption equilibrium isotherms

Napin adsorption equilibrium isotherms were evaluated using a Tecan EVO Freedom 200 robotic station (Tecan, Switzerland) equipped with an orbital mixer (Te-shake), an automated vacuum system (Te-VacS), a plate reader (InfiniTe Pro 200), a robotic manipulator (RoMa) arm (to move microplates to the different positions of the robotic station) and two liquid handling arms (LiHa and MCA96). The procedure involves the different steps of the chromatography run until adsorption (washing, equilibration and adsorption). A known amount of each resin (15.6µL or 23.4µL) was added to the wells of a 96 deep-well filter plate (catalog number: MDRLN0410) from Millipore, USA. Resins were added using MediaScout® ResiQuot resin loader (Atoll, Germany). Resin were washed two times with Milli-Q water using the vacuum system (Te-VacS) and equilibrated with the corresponding buffer for 20 mins under agitation (1200rpm). Equilibration buffer was removed by centrifugation with an Eppendorf centrifuge 5810 R (rotation speed 4000 rpm for 3 minutes). After centrifugation, resins were contacted with 312µL of napin solutions under agitation until equilibrium was reached (2 hours at 1200 rpm). Once equilibrium

was reached, the filter plate was centrifuged to collect the supernatant and equilibrium concentration was measured spectrophotometrically (see 4.2.4 Analytical methods). Napin experiments were performed in duplicate.

Effect of pH and ionic strength were evaluated for Napin adsorption by performing experiments at 4 different pH (pH 4, 5, 6, 8) keeping NaCl concentration (0.3M) constant and at pH 6 varying salt concentration from 0.1M to 1M NaCl. This allows to identify desorption conditions.

Napin adsorption capacity was calculated according to the mass balance equation (4.1)

$$q_{p,eq} = \frac{C_{p,load} * V_{load} - C_{p,eq}(V_H + V_{load})}{V_{resin}} \quad (4.1)$$

Where  $q_{p,eq}$  is the adsorption capacity (mg/mL<sub>resin</sub>),  $C_{p,load}$  is the protein initial concentration (mg/mL),  $V_{load}$  is volume of the liquid phase (mL)  $C_{p,eq}$  is the protein equilibrium concentration (mg/mL),  $V_H$  is the holdup volume (mL) and  $V_{resin}$  is the volume of resin (mL).

After centrifugation, some liquid could remain in the resin. This liquid holdup was determined using the method suggested by Nfor et al. (2010). The resins were placed in the deep-well filter plate and equilibrated with 350  $\mu$ L of 1 M NaCl. After 45 minutes the filter plate was centrifuged with 5810 R centrifuge (Eppendorf, Germany) for 3 min at 4000 rpm and the flow through was collected to measure conductivity. This cycle was repeated until the conductivity of flow through was equal to the conductivity of 1 M NaCl solution. Consequently, the equilibrated resins were contacted with 312  $\mu$ L of Milli-Q water and incubated overnight without agitation. After contacting, the filter plate was centrifuged and the conductivity of the flow-through was measured. All the conditions were done in triplicate. The conductivity was measured with a multi-parameter analyzer C832 (Consort NV, Belgium).

The holdup volume was measured using the salt mass balance equation (4.2)

$$C_{S,initial} * V_H = C_{S,final} * (V_H + V_W) \quad (4.2)$$

Initial salt concentration in all resins was 1 M NaCl ( $C_{S,initial}$ ),  $V_H$  is holdup volume (mL),  $C_{S,final}$  is the final salt concentration after contacting with Milli-Q water and  $V_W$  is the added volume of Milli-Q water.

Since cruciferin has low solubility in water, cruciferin adsorption isotherms were evaluated using the protein mixture. A similar procedure to the one applied for napin adsorption isotherms was used with the protein mixture in the liquid handling robotic station. The evaluated conditions were: pH 6 and 0.3M NaCl since they are the same conditions in the protein extract (adsorption condition). Cruciferin experiments were performed in duplicate.

As the absolute cruciferin liquid concentration values could not be determined experimentally, cruciferin adsorption capacity was determined by dividing equation (4.1) by the reference concentration ( $C_0$ ) (equation (4.3)), assuming that  $\frac{C_{p,eq}}{C_0} = \frac{Area\ at\ equilibrium}{Area\ of\ reference}$

$$\bar{q}_{p,eq} = \frac{q_{p,eq}}{C_0} = \frac{C_{p,load} * V_{load} - C_{p,eq}(V_H + V_{load})}{V_{resin} C_0} \quad (4.3)$$

The reference cruciferin area peaks were the ones corresponding to the conditions of 0.3M NaCl and Napin concentration of around 6g/L for experiments at pH6 (feed condition).

#### 4.2.5.2. Parameter estimation

Adsorption isotherm experimental results of napin were fitted to a linear isotherm or to a Langmuir type isotherm (equation (4.4)) to identify the initial isotherm slope, which is an indication of the affinity of napin to the resin.

$$q_{p,eq} = \frac{K_{p,i} q_{p,i}^{max} C_{p,i}}{1 + b_{p,i} C_{p,i}} \quad (4.4)$$

where  $q_{p,i}^{max}$  is the maximum adsorption capacity (mg/mL<sub>resin</sub>) and  $K_{p,i}$  is the Langmuir constant also known as equilibrium constant.<sup>28</sup> The initial isotherm slope, at the evaluated conditions, was later used to evaluate resin selection (see 4.2.6 Resin selection).

The most suitable resin equilibrium data (POROS 50 HS) was fitted to the mixed mode isotherm, developed by Nfor et al. (2010). This isotherm is based on the thermodynamic framework of Mollerup, et al.<sup>29</sup> A more detail explanation of this isotherm is found in 4.2.8.1 Mixed mode isotherm model section of this paper.

The fitted parameters of this isotherm model were: 1) the thermodynamic equilibrium constant ( $K_{eq}$ ); 2) the stoichiometric coefficient of salt counter ion ( $\nu$ ); 3) the parameter that describes the difference between water-protein and protein-protein interactions ( $K_p$ ) and 4) the parameter that describes the difference between water – protein and salt – protein interaction ( $K_s$ ). As previously mentioned, binary component experiments (napin + cruciferin) were performed using a protein mixture powder. Binary component adsorption experiments showed a higher napin adsorption capacity than napin single component experiments. For isotherm modelling this was adjusted by considering the value obtained from binary mixture experimental results, which corresponds to 44 mg/mL.

Data regressions were done using MATLAB R2017b and the function *lsqcurvefit*. In the mixed mode model,  $q_p$  appears in both sides of the equation (equation (4.7)). The numerical solution of this equation was found using the *fsolve* function of MATLAB and it was combined with the regression using *lsqcurvefit* optimizer. Thus, the procedure of the parameter regression is applying *lsqcurvefit* optimizer to minimize the sum of squared residuals between the experimental data and the numerically solved adsorption data using *fsolve* function.

In addition, as binary mixture experiment presented a very low change in cruciferin concentration. A linear isotherm model was considered for this protein by estimating isotherm slope by fitting a linear curve to the experimental data.

#### 4.2.6. Resin selection

The generated equilibrium data was used to select the most suitable resin for the separation of both proteins and for the capture of napin. The desired scenario is the adsorption of napin while cruciferin flows through. The selection criteria were defined as suggested by Sevillano, et al.<sup>30</sup> considering napin

adsorption capacity at feed conditions (pH 6 and 0.3M NaCl) and napin desorption, which was evaluated using the inverse of the lowest isotherm slope determined at the evaluated conditions. The third criterion, selectivity, was evaluated using the ratio between the napin and cruciferin isotherm slopes at adsorption conditions. The fourth criterion was the price of the resin obtained from suppliers. A weight between 0 and 1 was given to each criterion, being 0.5 for napin capacity, 0.3 for napin desorption, 0.1 for selectivity and 0.1 for price. The reason for giving a low weight to the selectivity criterion had to do with the observed poor binding of cruciferin onto most of the evaluated resins.

Each criterion was normalized and resin score was calculated using equation (4.5).

$$\text{Resin score} = \sum \text{weight} * \frac{\text{criterion}}{\text{maximum value of criterion}} \quad (4.5)$$

#### 4.2.7. Column adsorption/desorption experiments

The highest scoring resin, POROS 50 HS, was used to perform pulse column experiments using napin and the protein mixture (napin/cruciferin). The experiments were performed in an AKTA™ Avant system (GE Healthcare Bio-Sciences AB, Uppsala, Sweden) at room temperature (25 °C) operated with Unicorn 7.0 software. Conductivity, pH and UV at 280 nm signals were monitored during the experiments.

A ValiChrom 11.3-100 POROS® 50 HS (Repligen, Sweden) column was used. The column internal diameter was 1.12 cm and the total bed height was 10 cm, providing a total column volume of 9.8 mL. Extraparticle and total porosities were determined by pulse injections of blue dextran and 1M NaCl respectively. The obtained values were 0.83 total porosity ( $\epsilon_T$ ) and 0.3 extraparticle porosity ( $\epsilon_b$ ).

For napin and protein mixture experiments, the column was equilibrated with 50 mM bis-tris pH6 with 0.3 M NaCl buffer for 5 column volumes (CV) at 2.5 mL/min. Then 1mL of napin solution at 6 g/L was injected in the column (10.1 % CV), column was washed with the equilibration buffer for 5 CV in order to remove non-binding substrates out of the column. Step elution was done by applying 5 CV of elution buffer, Tris-HCl pH 8 with 0.7 M NaCl. After each experiment, the column was regenerated with 1 M NaCl solution for 5 CV as recommended by supplier.

For rapeseed protein mixture, 12 g/L of protein was dissolved) in 50 mM Bis-Tris pH 6 with 0.3 M NaCl buffer. This corresponds to 6.84 g/L of napin and 5.16 g/L of cruciferin. The protein mixture solution was then sonicated for 30 min in order to increase protein solubility. The solution was filtered with 0.22  $\mu$ m PVDF filter before injection in column. After use, the column was stored in 20 % (v/v) ethanol as suggested by supplier.

#### 4.2.8. Chromatography modeling

##### 4.2.8.1. Mixed mode isotherm model

The mixed mode adsorption isotherm model from Nfor, et al.<sup>31</sup> was applied in this work. The model is a combination of HIC and IEX models from Mollerup<sup>32</sup> This mixed mode isotherm is based on the assumption that a protein ( $P$ ) binds to  $n$  amount of ligand ( $L$ ) by hydrophobic interaction and concurrently exchanges with  $v$  amount of salt counter-ion ( $S$ ) generating a protein-ligand complex ( $L_{n+}$ ) in a fixed stoichiometry as shown in equation (4.6). The stoichiometric coefficient of salt counter ion is

defined as the ratio between the protein binding charge divided by the charge of the salt counter ion ( $v = \frac{z_p}{z_s}$ ). In this work, sodium chloride was used as a salt counter ion. The single component adsorption isotherm, based on reaction in equation (4.6), results in the isotherm model described in equation (4.7).



$$\frac{q_p}{c_p} = A * \left(1 - \frac{q_p}{q_p^{max}}\right)^{v+n} * \tilde{\gamma}_p \quad (4.7)$$

$$\text{where } A = \tilde{K}_{eq}(\Lambda)^{v+n} \left(\frac{1}{z_s c_s}\right)^v \left(\frac{1}{c}\right)^n \text{ and } \tilde{\gamma}_p = \exp(K_p c_p + K_s c_s) \quad (4.8)$$

In equation (4.7),  $q_p$  is the adsorbed protein concentration (mg/mL<sub>resin</sub>),  $c_p$  is the protein concentration in solution (mg/mL),  $K_{eq}$  is thermodynamic equilibrium constant of reaction (mL/mg),  $c_s$  is the concentration of salt in liquid phase.  $c$  is molarity of the solution (assumed to be water concentration<sup>32</sup> and  $q_p^{max}$  is maximum adsorption capacity of protein (mg/mL<sub>resin</sub>),  $\Lambda$  is ligand density of the mixed mode resins which are assumed to be equal for HIC and IEX ligands (mmol/L) and was obtained based on supplier specifications. The activity coefficient of the protein ( $\tilde{\gamma}_p$ ) was determined using the Van der Waals equation of state shown in equation (4.8) as suggested by Mollerup<sup>33</sup>.  $K_p$  parameter describes the difference between water-protein and protein-protein interactions while  $K_s$  parameter describes the difference between water – protein and salt – protein interactions.<sup>31</sup> In the model,  $\left(1 - \frac{q_p}{q_p^{max}}\right)$  describes the fraction of free ligands, which is 1 if no protein is bound and decreases asymptotically to zero. This isotherm incorporates the effect of salt concentration in the term  $C_s$ .

The mixed mode isotherm described in equation (4.7) reduces to the HIC and IEX isotherm models derived by Mollerup<sup>33</sup> when  $v = 0$  (electrostatic interactions not present) and  $n = 0$  (no hydrophobic interactions), respectively.

#### 4.2.8.2. Column chromatography model

Column chromatography was simulated based on the transport-dispersive column model which can be described per component as shown in equation (4.9)

$$\frac{\partial c_{p,i}}{\partial t} + \left(\frac{1 - \varepsilon_b}{\varepsilon_b}\right) \frac{\partial q_{p,i}}{\partial t} = -v \frac{\partial c_{p,i}}{\partial x} + D_{L,i} \frac{\partial^2 c_{p,i}}{\partial x^2} \quad (4.9)$$

where,  $\varepsilon_b$  is the bed porosity,  $v$  is the interstitial velocity of the mobile phase (m/s), and  $D_L$  is the axial dispersion coefficient (m<sup>2</sup>/s)

Mass transfer can be quantified by the liquid-film linear driving force approximation. The solid stationary phase concentration term  $\frac{\partial q_{p,i}}{\partial t}$  is defined as follows in equation (4.10):

$$\frac{\partial q_{p,i}}{\partial t} = k_{ov,i}(C_{p,i} - C_{p,eq,i}^*) \quad (4.10)$$

$k_{ov,i}$  is the overall mass transfer coefficient (1/s) and  $C_{p,eq,i}^*$  is the bulk equilibrium concentration which is obtained using the mixed mode isotherm (equation (4.7)). Mixed mode isotherm parameters were used to model napin chromatography while a linear isotherm was considered to model cruciferin chromatography.

The film mass transfer coefficient is defined in equation (4.11).<sup>34</sup>

$$\frac{1}{k_{ov,i}} = \frac{d_p}{6 * k_f} + \frac{d_p^2}{60 * \varepsilon_p * D_p} \quad (4.11)$$

where  $d_p$  is the particle diameter (m),  $k_f$  is the film mass transfer coefficient (m/s),  $\varepsilon_p$  is the intraparticle porosity and  $D_p$  is the pore diffusivity (m<sup>2</sup>/s). To determine additional relevant model parameters, mass transfer correlations shown in Table 4.2 were used.

Column boundary conditions are described by Danckwerts for dispersive systems and it is assumed that the column is not preloaded with the proteins  $C_p(t=0)=0$  and  $q_p(t=0)=0$ .

$$C(t, x = 0) = C_{inlet} - \frac{D_L}{u_h} \cdot \frac{\partial C(t, x = 0)}{\partial x} \quad (4.12)$$

$$\frac{\partial C(t, x = L)}{\partial x} = 0 \quad (4.13)$$

where  $x$  is the axial position. Equation (4.12) represents the boundary at the inlet of the column and equation (4.13) the boundary conditions at the column outlet. As pulse experiments were performed, the injection profile is modelled as a rectangular pulse with a constant feed concentration for a given time, where  $t_{pulse} = V_{inj}/\Phi_v$ , where  $\Phi_v$  is the volumetric flow rate (m<sup>3</sup>/s) and  $V_{inj}$  is the injection volume.

Pulse

$$C_{inlet}(t) = C_{feed}, i \text{ at } 0 < t < t_{pulse} \quad (4.14)$$

Elution

$$C_{inlet}(t) = 0 \text{ at } t > t_{pulse} \quad (4.15)$$

Equation (4.9) is partial differential equation, dependent on time and column position, that can be approximated to an ordinary differential equation by spatial discretization. The method of lines was used to discretize equation (4.9) in space. The set of ordinary differential equations was solved in MATLAB R2017b using the ODE solver *ode15s*.

**Table 4.2.** Engineering correlations for column modelling

Mass transfer parameter	Correlation	Reference
<b>Hydrodynamic radius</b>	Stokes Einstein	LeVan, et al. <sup>35</sup>
<b>Free diffusivity</b>	Young	Young, et al. <sup>36</sup>
<b>Film mass transfer coefficient</b>	Wilson & Geankoplis	Wilson, et al. <sup>37</sup>
<b>Pore tortuosity</b>	Wakao & Smith	Wakao, et al. <sup>38</sup>
<b>Pore diffusivity</b>	Brenner & Gaydos	Brenner, et al. <sup>39</sup>
<b>Axial dispersion coefficient</b>	Gunn	Gunn <sup>40</sup>
<b>Pressure drop</b>	Karman-Cozeny	Carta, et al. <sup>28</sup>

### 4.3. Results and Discussion

#### 4.3.1. Resin and proteins characteristics

The used protein isolates, cruciferin, napin and protein mixture were analyzed by SDS-PAGE (Appendix 4B. Protein characteristics). Napin and the protein mixture showed expected band profiles that were comparable to the ones reported elsewhere.<sup>7</sup> Cruciferin did not show the expected profile and the solubility of this protein isolate in any of the tested conditions was very limited, therefore the protein mixture was used to evaluate cruciferin isotherms.

To avoid an overestimation of the adsorbed phase protein concentration, the resin liquid hold-up was evaluated. The obtained values were 9.3  $\mu\text{L}$ , 8.7  $\mu\text{L}$ , 7.0  $\mu\text{L}$ , 9.2  $\mu\text{L}$ , 10.0  $\mu\text{L}$ , 9.8  $\mu\text{L}$ , 12.4  $\mu\text{L}$  and 8.5  $\mu\text{L}$  for CptoMMC, Nuvia cPrime, Toyopearl MX, PPA HyperCel, CptoS, POROS 50 HS, CM Sepharose and MacroPrep50 CM respectively. These hold up volumes correspond to  $\sim$ 3-4% of the total volume applied in the adsorption experiments (350  $\mu\text{L}$ ).

#### 4.3.2. Napin adsorption equilibrium isotherms

Napin adsorption equilibrium isotherms were determined for all resins at feed conditions, (0.3M NaCl at pH6). Results are shown in Figure 4.1 where the experimental napin adsorption capacity is plotted against the equilibrium bulk concentration for all the evaluated resins. From the figure, one can observe that at feed conditions, the highest adsorption capacity is obtained using resin Cpto MMC, followed by Nuvia cPrime, POROS HS, PPA HyperCel, Toyopearl, Cpto S, MacroPrep and CM Sepharose. Most of the resins showed a maximum limit in the amount adsorbed, which can be described with a Langmuir isotherm model (equation (4.4)). Resins CptoS and CM Sepharose presented a linear behavior. The experimental data was fitted with two isotherm models - Langmuir or linear type.

In addition to the resin isotherm shape presented in Figure 4.1, the affinity of napin to the resins was also obtained by determining the initial isotherm slopes. The initial isotherm slope is an indication of the interaction strength between the protein and the resin. The larger the isotherm slope, the stronger the interaction. At feed conditions, the isotherms' initial slopes, for each different resin, can be ranked from largest to smallest: CptoMMC, Nuvia cPrime, POROS HS, PPA HyperCel, Toyopearl, Macro Prep, Cpto S and CM Sepharose. The absolute values (obtained from fitting) can be found in Table 4.3.

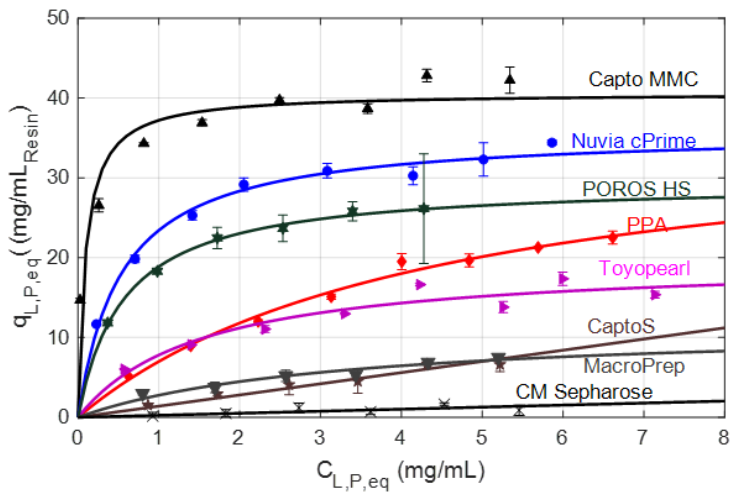


**Figure 4.1.** Napin adsorption isotherms on mixed mode and ion exchange resins at pH6 and 0.3M NaCl. Symbols represent experimental results. Error bars resulted from duplicate experiments. Lines represent Langmuir isotherm for CaptoMMC, Nuvia cPrime, POROS HS, Toyopearl, PPA Hypercel and MacroPrep and linear isotherm for Capto S and CM Sepharose

The difference between the napin binding strength onto the different resins can be explained based on the pKa of the resin (Table 4.1), the isoelectric point of napin protein - in this case around 11 -, and the protein net charge at the evaluated conditions. At pH 6, all resins are negatively charged and napin has a positive net charge. Therefore, attractive electrostatic interactions are possible. However, there is also salt presented in the medium (NaCl) which could promote hydrophobic interactions between napin and the mixed mode resins. A salt concentration of 0.3M NaCl – which can be considered medium -, proved to be already too high for the weak ion exchangers here evaluated (CM Sepharose and MacroPrep) and even for the strong cation exchanger Capto S. As the preferable scenario is the adsorption of napin at pH 6 and 0.3 M NaCl, CM Sepharose, Macro-Prep and CaptoS resins were discarded as suitable candidates due to the poor binding of napin under such conditions.

The effect of ionic strength and pH was evaluated for all resins in order to determine suitable desorption conditions.

#### 4.3.2.1. Effect of pH on napin adsorption

Ionic strength and pH might have a significant impact on the adsorption of napin on mixed mode cationic resins, cation exchange resins and the anion mixed mode resins here evaluated. Experiments were performed at different pH values keeping the salt concentration constant at 0.3M NaCl, which correspond to the same ionic strength as in the protein extract. Napin isotherm results are shown in Figure 4.2 and Figure 4.3.

From Figure 4.2, one can notice that for Capto MMC, Nuvia cPrime and Toyopearl, there is a decrease on napin adsorption capacity with increasing pH. This can be explained by the protein's net charge and

the resin ligand's pKa. The weak cation exchangers are negatively charged at pH higher than the pKa, while the opposite occurs for weak anion exchangers, which are positively charged at pH lower than the pKa. Strong cation exchangers are practically always charged at any pH.<sup>28</sup> The interaction between mixed mode resins and proteins, have been explained by different authors.<sup>31</sup> The interaction is strongest close to the pKa of the ligand and decreases if the pH is close to the pI of the protein, which is clearly observed here for Toyopearl, Capto MMC, Nuvia cPrime and POROS HS. At pH 4, the net charge of napin is around 12 while at pH 8, the net charge decreases significantly to around 4. The net charge of napin at different pH values was estimated using the amino acid sequence (obtained from the RCSB Protein Data Bank (PDB) and equation (4.16) (Appendix 4B. Protein characteristics).

$$z_{net} = \sum_i \frac{N_{basic,i}}{1 + 10^{pH-pKa_i}} - \frac{N_{acidic,i}}{1 + 10^{pH-pKa_i}} \quad (4.16)$$

Where  $z_{net}$  is the net charge  $N_{basic,i}$  is the number of basic amino acids and N terminal, and  $N_{acidic,i}$  is the number of acidic amino acids and C terminal.

The opposite behavior is observed with the weak anion mixed mode resin PPA HyperCel: an increase in adsorption capacity with an increase of pH. Since the pKa of the PPA HyperCel resin ligand is around 8, the resin is positively charged. Because napin is also positively charged at all the evaluated pH values, there is an electrostatic repulsion between the resin and the protein. The adsorption is consequently a result of the hydrophobic interactions between napin and the resin and the electrostatic repulsion. pH has a big influence on the adsorption of napin in PPA resin, as the isotherm slope and isotherm shape change with pH: there is a higher napin affinity to the resin at a higher pH. However, the adsorption capacity is still lower than the maximum obtained at feed condition pH 6 and 0.3M NaCl with other resins (e.g. 40 mg/mL by Capto MMC), which decreases PPA resin score.

Even though, there is a notorious change on napin adsorption at different pH values, the Capto MMC resin is the least influenced, showing a favorable isotherm even at pH 8. On the other hand, the napin adsorption strength on Nuvia cPrime, POROS 50 HS and Toyopearl is significantly reduced. The isotherm slopes of all the resins at different conditions are indicated in Table 4.3.

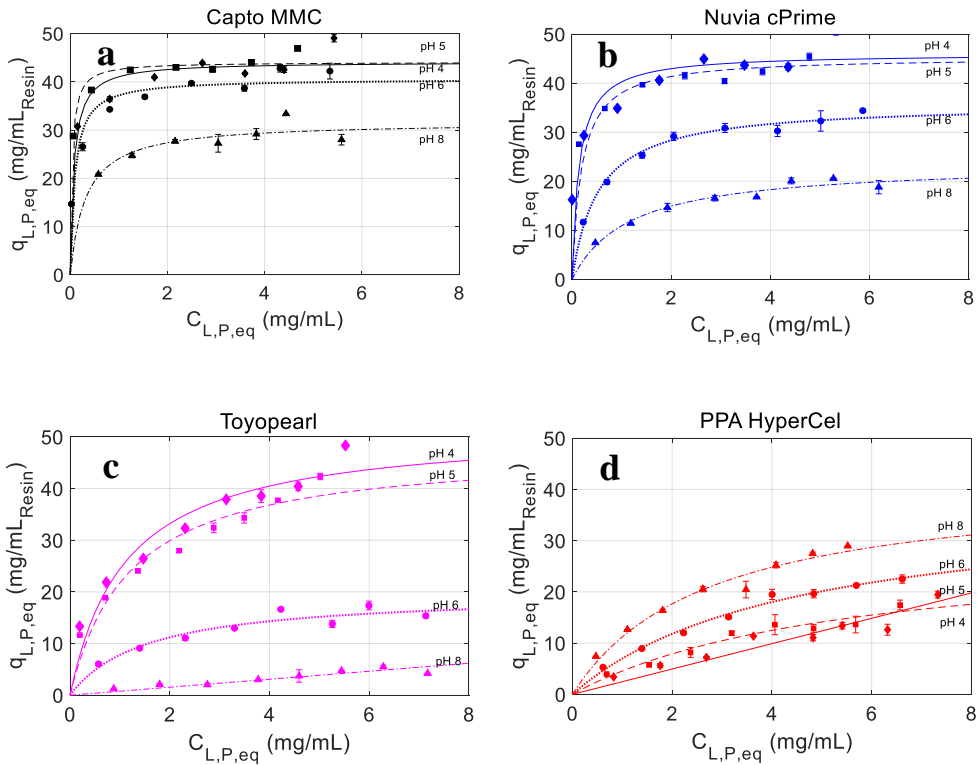


**Figure 4.2** Napin adsorption isotherms at different pH keeping salt concentration at 0.3 M NaCl a) Capto MMC resin, b) Nuvia cPrime resin, c) Toyopearl resin and d) PPA HyperCel resin. Symbols represent experimental results. Error bars resulted from duplicate experiments. Lines represent the Langmuir isotherm

The isotherm slope represents the affinity of the protein to the resin (the binding strength) which is clearly much higher for Capto MMC at almost any pH value. However, this is not necessary an advantage, as a higher pH might be needed to desorb napin with this resin, possibly interfering with its native structure, stable between pH 3 – 12<sup>3</sup> thus with its physico-chemical properties.

These results can be used to identify desorption conditions of the best performing resin.

#### 4.3.2.2. Effect of ionic strength on napin adsorption

Higher ionic strength is known to promote hydrophobic interactions due to the so-called “salting-out” effect. Three different salt concentrations (ionic strengths) were tested at two different pH conditions. Most of the tested resins showed similar trends: a decrease of napin adsorption strength with an increase of ionic strength. This can be observed by the lower isotherm slope values and experimental capacities obtained at higher salt concentrations (See Figure 4.3 and

Table 4.3. This suggests that napin adsorption on mixed mode resins is mainly controlled by ionic interactions.

The exception was PPA resin, which presented an increase in napin adsorption with increasing salt concentration. As previously mentioned, since for this resin electrostatic interactions are repulsive, an increase in the binding capacity of napin should be mainly due to an increase in the strength of hydrophobic interactions. No significant improvement in the adsorption of napin was observed between pH 6 and pH 8, at different salt concentrations. This might support the fact that napin adsorption on PPA HyperCel is characterized only by hydrophobic interactions in that range.

Based on the isotherm slope, one can notice that Capto MMC has the largest affinity for napin. However, this might complicate the desorption and recovery of the protein after the capture step, as even at high pH and salt concentrations the isotherm is favorable. As a consequence, especially harsh conditions (e.g. pH higher than the pI of the napin) might need to be applied. The determined napin isotherm slopes at all tested conditions are shown in Table 4.3.

From the obtained results it is clear that the effect of ionic strength is more significant than the effect of pH, especially for the PPA HyperCel resin. When comparing the results for that resin (Figure 4.3e and 4.3f), the isotherms seem to overlap. This was expected, as the adsorption of napin occurs mainly through hydrophobic interactions. This effect can be evaluated by comparing the ratio between the isotherm slope at two different salt concentration (at a specific pH) and the ratio between the isotherm slopes at two different pH conditions (at a specific salt concentration).

Similar isotherm trends to the ones determined in this work were observed in the research of Nfor, et al.<sup>31</sup> The authors evaluated lysozyme (similar pI and molecular weight as napin) adsorption on Capto MMC and PPA HyperCel. The adsorption capacity of lysozyme was in the same order of magnitude as the one obtained for napin in this work. In addition, similar isotherm curves were observed when comparing two pH values and one salt concentration.

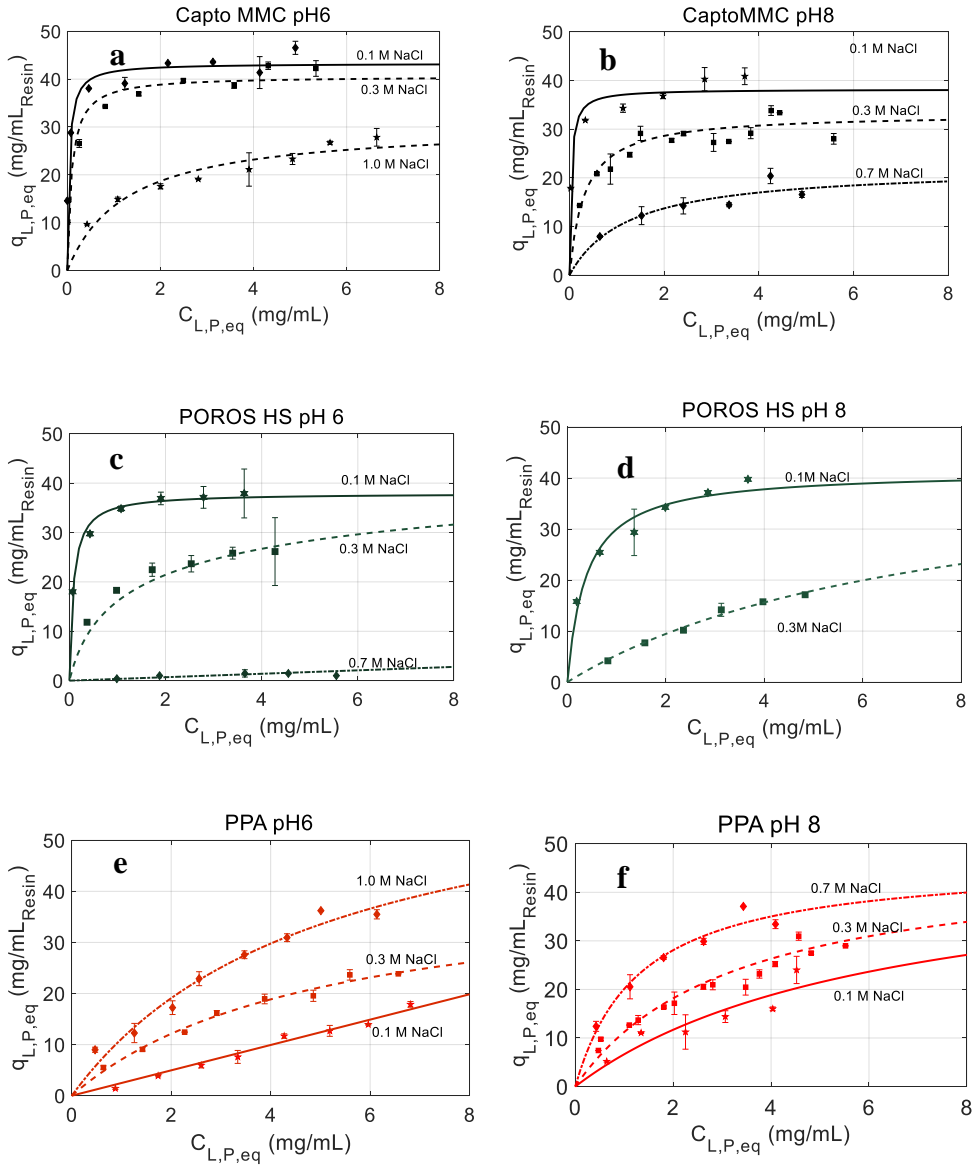


**Figure 4.3.** Effect of ionic strength on napin adsorption on Capto MMC, POROS HS and PPA HyperCel at pH6 and pH8. Symbols represent experimental results. Error bars resulted from duplicate experiments. Lines represent the mixed mode isotherm that the data has been fitted to.

**Table 4.3.** Napin isotherm slope on mixed mode resin and ion exchange resin at pH6 and pH8 and different NaCl ( $C_s$ ) concentration

Resin	pH	$C_s$ (M)	Isotherm slope (mL/mL <sub>resin</sub> )	Resin	pH	$C_s$ (M)	Isotherm slope (mL/mL <sub>resin</sub> )
<b>Capto MMC</b>	6	0.1	1185.4 ± 245.2	<b>Capto S</b>	6	0.1	146.1 ± 12
		<b>0.3</b>	<b>437.6 ± 266.1</b>			<b>0.3</b>	<b>1.4 ± 0.1</b>
		1.0	23.1 ± 7.9			0.7	Not adsorbed
	8	0.1	1114.4 ± 248.8		8	0.1	25.2 ± 3.8
		0.3	99.3 ± 25.6			0.3	0.2 ± 0.0
		0.7	17.8 ± 6.8			0.7	Not adsorbed
<b>Nuvia cPrime</b>	6	0.1	620.9 ± 78.3	<b>POROS 50 HS</b>	6	0.1	453.8 ± 76.2
		<b>0.3</b>	<b>67.5 ± 17.23</b>			<b>0.3</b>	<b>52.5 ± 14.9</b>
		1.0	1.3 ± 0.01			0.7	0.7 ± 0.9
	8	0.1	276.6 ± 57.5		8	0.1	108.9 ± 22.5
		0.3	20.2 ± 3.5			0.3	6.0 ± 1.8
		0.7	2.1 ± 0.2			0.7	Not adsorbed
<b>Toyopearl</b>	6	0.1	97.4 ± 13.6	<b>CM Sepharose</b>	6	0.1	8.5 ± 3.0
		<b>0.3</b>	<b>5.9 ± 5.02</b>			<b>0.3</b>	<b>0.3 ± 0.0</b>
		1.0	0.4 ± 0.2			0.7	Not adsorbed
	8	0.1	52.4 ± 9.1		8	0.1	13.5 ± 1.9
		0.3	1.8 ± 0.3			0.3	0.2 ± 0.0
		0.7	0.5 ± 0.1			0.7	Not adsorbed
<b>PPA HyperCel</b>	6	0.1	1.9 ± 0.1	<b>Macro Prep</b>	6	0.1	67.4 ± 14.8
		<b>0.3</b>	<b>8.5 ± 3.4</b>			<b>0.3</b>	<b>3.6 ± 1.3</b>
		1.0	13.0 ± 3.7			0.7	Not adsorbed
	8	0.1	7.7 ± 7.5		8	0.1	19.8 ± 2.6
		0.3	15.4 ± 2.8			0.3	0.8 ± 0.1
		0.7	35.4 ± 7.9			0.7	Not adsorbed

All this information was used to select the most suitable resin for napin capture.

#### 4.3.3. Protein mixture adsorption experiments

Batch adsorption experiments were performed using solutions of a protein mixture (napin/cruciferin), to evaluate both, the effect of cruciferin on napin's adsorption and to determine cruciferin's adsorption isotherms. At feed conditions, it is expected that cruciferin poorly binds to the resins, as the pH is close to the pI of this protein (~7). A comparison between the expected napin adsorption capacity and the adsorption capacity obtained from the experiments using the protein mixture was done and the results can be found in Figure 4.4.

The presence of cruciferin seems to enhance napin adsorption at pH6 and 0.3 M NaCl for POROS HS and CaptoS where higher adsorption capacities than expected were obtained. This behavior might be

explained by the charge of the proteins. At pH 6, both cruciferin and napin possess a positive net charge, allowing cruciferin to bind to the resins as well. However, cruciferin is considered a large protein, and in solution with napin, the positive charge on cruciferin's surface might have resulted in a strong electrostatic repulsion of napin molecules. By creating a less favorable chemical environment in the liquid solution, the presence of cruciferin might then be improving the adsorption of napin molecules onto the tested resins.

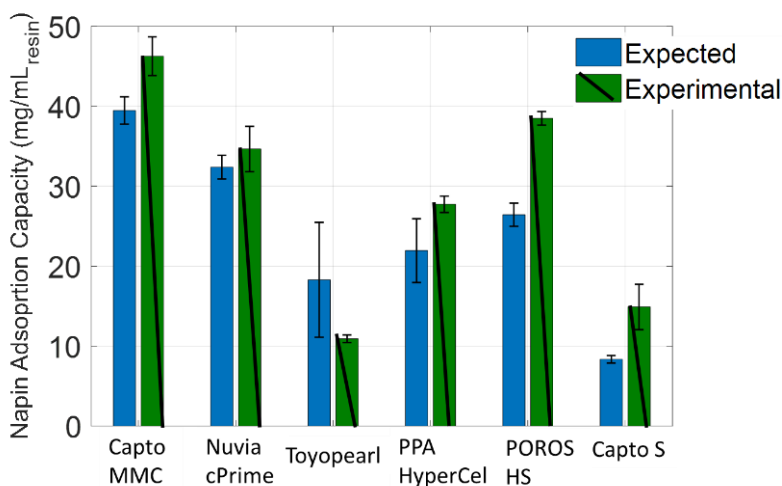


**Figure 4.4.** Napin adsorption capacity comparison between expected capacity and experimentally obtained from protein mixture experiments at pH6 and 0.3M NaCl. Expected capacity was calculated from single component isotherm.

In all experiments (Appendix 4D. Cruciferin adsorption experiments), cruciferin showed a very small change in concentration after equilibration with the resins, which indicated a low binding strength. Only resin PPA HyperCel showed a relatively high cruciferin concentration change. The cruciferin's isotherm slope values were obtained by fitting a linear curve to the experimentally obtained capacities (as function of the equilibrium liquid concentrations). The obtained values were  $2.0 \pm 1.3$ ,  $0.8 \pm 0.1$ ,  $2.3 \pm 1$ ,  $22.1 \pm 8.2$ ,  $1.6 \pm 0.5$  and  $0.9 \pm 0.7$  mL/mL<sub>resin</sub> for Capto MMC, Nuvia cPrime, Toyopearl, PPA HyperCel, POROS HS and Capto S respectively. Cruciferin's isotherm slope is significantly lower than the one of napin for resin Capto MMC, Nuvia cPrime and POROS HS, suggesting a preferential binding of napin to these resins. The napin isotherm slope values were slightly higher for resins CaptoS and Toyopearl and cruciferin's isotherm slope was higher than napin's isotherm slope for resin PPA HyperCel. As discussed before, for the PPA HyperCel resin, binding is mainly characterized by hydrophobic interactions. Because, cruciferin is a more hydrophobic molecule than napin, this might explain the higher affinity towards this resin. All the obtained results were used to identify the most suitable resin for the capture of napin.

#### 4.3.4. Resin selection

The most suitable resin for the separation of napin and cruciferin was selected using the previously defined selection criteria (4.2.6 Resin selection) 1) napin adsorption capacity at feed conditions (pH6

with 0.3M NaCl), 2) best desorption conditions (based on the lowest isotherm slope obtained for each resin), 3) selectivity of napin over cruciferin and 4) resin price. Adsorption (napin capacity) and desorption were the two criteria with higher importance in the selection process. As previously mentioned, resins CaptoS, CM Shearose and MacroPrep were discarded, as they showed significantly lower napin capacity compared to the other resins at feed conditions. The results are shown in Table 4.4.

**Table 4.4.** Values of each criterion (napin capacity, selectivity, resin price and desorption) used for resin selection and resin scores.

	Napin capacity <sup>1</sup> (mg/mL)	Selectivity <sup>2</sup> (-)	1/slope desorption <sup>3</sup> (mL <sub>resin</sub> /mL)	Price/highest price (-)	Resin score
<b>Capto MMC</b>	<b>40.0</b>	<b>219.9</b>	0.1 <sup>4</sup>	0.8	66%
<b>Nuvia cPrime</b>	34.3	81.3	0.8 <sup>5</sup>	0.8	57%
<b>Toyopearl</b>	14.1	2.5	2.6 <sup>6</sup>	1.0	37%
<b>PPA HyperCel</b>	26.6	0.4	0.5 <sup>7</sup>	1.0	41%
<b>POROS HS50</b>	30.0	33.0	<b>5.6<sup>8</sup></b>	<b>0.5</b>	<b>75%</b>

<sup>1</sup>Napin capacity at 0.3M NaCl and pH 6

<sup>2</sup>Ratio between napin and cruciferin isotherm slopes at 0.3M NaCl and pH 6

<sup>3</sup>Inverse of isotherm slope: <sup>4</sup>at 0.7M NaCl and pH 8; <sup>5</sup>at 1.0M NaCl and pH 6; <sup>6</sup>at 1.0M NaCl and pH 6; <sup>7</sup>at 0.1M NaCl and pH 6;

<sup>8</sup>at 0.7M NaCl and pH 8

Even though resin Capto MMC possesses the highest napin capacity (in all conditions tested) and selectivity, this resin was not selected as the most promising. The reason has to do mainly with desorption, possibly requiring a pH higher than napin's pI, which, as previously mentioned, can lead to problems with the structural stability of napin. Therefore, desorbing at a pH above the pI is not recommended. The best performing resin in terms of desorption performance was POROS HS, since its results indicate that desorption can be performed at high salt concentration without increasing the pH to a higher value than napin's pI. Despite being second best on desorption criteria, the Toyopearl resin also showed a much lower adsorption capacity for napin when compared to Capto MMC and Nuvia cPrime at feed conditions. Therefore, the Toyopearl resin scored the lowest in the adsorption capacity criterion.

PPA HyperCel and POROS HS showed comparable adsorption capacities at feed condition. Nevertheless, from the experiments performed with the protein mixture it was clear that cruciferin also interacts with resin PPA HyperCel having an even larger isotherm slope than napin. This was observed with the obtained selectivity value which was lower than unity, indicating that at pH6 and 0.3 M NaCl, cruciferin interacts more favorably with PPA HyperCel resin than napin.

The last evaluated selection criterion was resin cost, with resin POROS HS being the cheapest one, as the price range is around half the price obtained for the mixed mode resin. Even though this criterion was evaluated with a lower weight, it was taken into account, as process economics is a significant factor in process development.

## 4.3.5. Mixed mode isotherm parameter estimation

Napin adsorption data obtained for POROS HS resin was used in order to fit the isotherm model described in Mixed mode isotherm model. Since POROS HS is a strong cation resin, there are no hydrophobic interactions presented and the parameter  $n$  from equation (4.7) was set to zero. In order to reduce the complexity of solving the non-linear system, the model was linearized by applying the natural logarithm in both sides of the equation and the regression was performed as explained in 4.2.5.2 Parameter estimation. The experimental data from the three evaluated salt concentrations were fitted to determine the set of parameters  $K_{eq}$ ,  $\nu$ ,  $K_p$  and  $K_s$ , for each pH value. The maximum adsorption capacity ( $q_p^{max}$ ) was obtained from adsorption equilibrium isotherm experiments from protein mixture and the obtained value was 44 mg/mL<sub>resin</sub>. The regressed parameters are shown in Table 4.5.

**Table 4.5.** Ion exchange isotherm parameters of napin protein in POROS HS resin at pH6 and pH8

	$\ln K_{eq}$	$\nu$	$K_p$ (mM <sup>-1</sup> )	$K_s$ (mM <sup>-1</sup> )	$R^2$	SD
<b>POROS HS pH6</b>	$6.6 \pm 0.3$	$1.9 \pm 0.4$	$2.3 \pm 2.7$	$-5 \times 10^{-3} \pm 1 \times 10^{-3}$	0.97	0.2
<b>POROS HS pH8</b>	$5.8 \pm 0.2$	$1.2 \pm 0.2$	$0.8 \pm 1.0$	$-9 \times 10^{-3} \pm 8 \times 10^{-3}$	0.98	0.1

The stoichiometric coefficient ( $\nu$ ) of the salt counter ion at pH6 was higher than at pH8, which was expected. For this system,  $\nu$  is equal to protein binding charge. At pH values approaching the pI of the protein (napin pI  $\sim 11$ ), the net charge of the protein approaches zero (lower  $\nu$ ) and the electrostatic binding strength becomes weaker, resulting in a lower binding capacity.  $K_p$  is the parameter that describes the difference between water-protein and protein-protein interactions (Mollerup, 2006). The regressed  $K_p$  for both pH values (6 and 8) had a positive value, suggesting that interactions between protein-water were stronger than protein-protein interactions. This also matches the observations obtained in this work and the data from literature, indicating a high solubility of napin in water. Similar to  $K_p$ , the parameter  $K_s$  describes the difference between water-protein and salt-protein interactions.<sup>33</sup> The obtained  $K_s$  values at both evaluated pH conditions were around zero, implying that the strength of protein-salt interactions is not significantly different than protein-water interactions. By analyzing the two different interaction parameters -  $K_p$  and  $K_s$  -, the strength of water-protein, protein-salt and protein-protein interactions could be inferred. In this system, given that  $K_p > 0$  and  $K_s \approx 0$ , protein-water interactions were dominant.

The pH value of mobile phase has an influence on the binding charge of the protein which consequently changes the  $\nu$  value and it is expected to be lower when the pH is closer to the pI of the protein. In order to include the influence of pH on the stoichiometric coefficient  $\nu$ , approaches like the one applied by Pirrung, et al.<sup>41</sup> could be used. The  $\nu$  for POROS decreases with increasing of pH which corresponds to the influence of pH on electrostatic interactions.

A linear isotherm model was considered for cruciferin protein due to the low binding observed with resin POROS HS.

## 4.3.6. Column chromatography

Two pulse experiments were performed at small scale (~10 mL column volume) using either a solution of napin or a solution of protein mixture (napin + cruciferin). The experimental results were compared with the model output and can be found in Figure 4.5. The data obtained from the chromatography station was normalized for easier comparison with the modeling results.

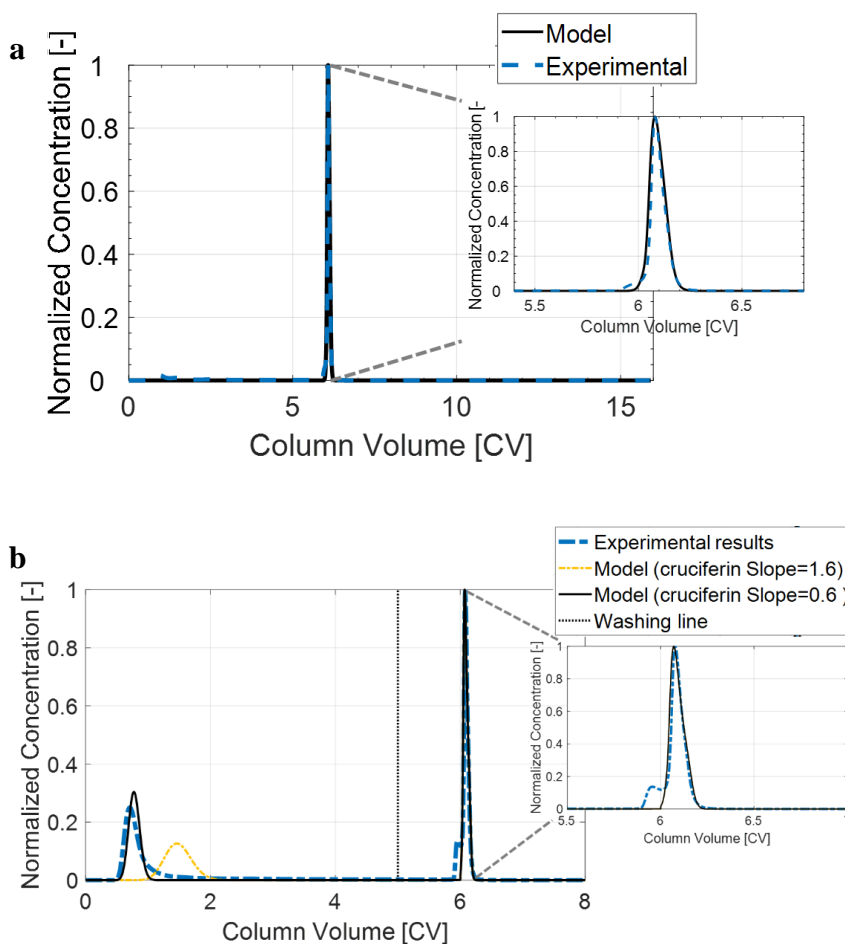


**Figure 4.5.** Model prediction vs Experimental data of Napin (a) and Protein mixture (b) on POROS 50HS column. Loading condition pH 6 and 0.3M NaCl, step elution at pH 8 and 0.7M NaCl

As can be seen in Figure 4.5, the model is in excellent agreement with the experimental results for both napin as single component and also when it is in the presence of the second protein, cruciferin. Analyzing napin results (Figure 4.5a), one can notice that no desorption of napin occurs after 5 CV of washing step, which suggests a strong binding at these conditions (as shown by the determined isotherm). Elution with high salt concentration (0.7M NaCl) and pH8 shows a very sharp peak. This is expected as at these conditions, napin capacity in POROS HS is close to zero. High salt and pH conditions

were chosen in order to have high recovery, which correspond to 100% based on mass balance (evaluated by numerical integration). However, one might notice that high pH might not be needed to fully desorb this protein. After desorption phase, the column was washed with a concentrated salt solution (1M NaCl) until no absorbance at 280 nm was detected. The maximum protein concentration detected was  $6.8 \pm 0.1$  g/L.

Protein mixture chromatogram is presented in Figure 4.5b. Napin elution profile using this binary mixture corresponds to the one obtained using single component napin. After applying the elution buffer, again a sharp peak is observed with a peak maximum at around 6.0 CV (approximately one column volume after the switch in conditions). In this experiment, an extra peak is observed during the washing step, which might correspond to cruciferin protein. Using a linear isotherm model for cruciferin protein (slope 1.6 mL/mL) and performing the simulation, one can observe a peak at around 1.8CV (washing step). Comparing cruciferin simulation results with experimental results, it is clear that cruciferin isotherm slope was overestimated. This because the experimental peak is eluted earlier ( $\sim 1$ CV) and it is sharper but also presented tailing. This tailing might be caused by the size of cruciferin, which is around 300 kDa. The difference between the experimental and simulated results might be attributed to cruciferin equilibrium parameter. As previously mentioned, during binary mixture experiments cruciferin data presented very small changes which were difficult to quantify. Besides these difficulties, the model shows excellent agreement in respect to napin protein. The maximum napin concentration obtained in the chromatogram of the protein mixture pulse experiment was  $7.8 \pm 0.1$  g/L. This value is higher than the one obtained in the experiment with pure napin experiment due to the slightly higher napin concentration applied.

Using the experimental results from the protein mixture, the slope of cruciferin was calculated to be 0.6 ml/mLresin, which consequently increased the selectivity of napin to POROS HS resin to 87.0.

The validated model can be then used for industrial column design to identify column sizing and operating parameters. Scale up of chromatography processes from laboratory results is usually done by keeping bed height and velocity constant and changing column diameter. However, this makes scalability inflexible, often resulting in column volumes that cannot satisfy the desired capacity or that do not match the capacities found at pilot and industrial scale, where companies often possess already existing equipment and, therefore, pre-determined volumes<sup>42</sup> with fixed column diameter and adjustable headers. The use of the previous model could reduce the number of experiments or investment required to satisfy production.

The following section describe the use of the previous model to design an ion exchange column for the separation of these proteins, applied in a hypothesized case study considering the production of rapeseed meal in the Netherlands. This case study can be used as base for large scale purification of oilseed meals.

#### 4.3.7. Adsorptive process design for the purification of napin, cruciferin and sinapic acid from rapeseed meal

Rapeseed production has significantly increased in the last years, having a global production of 75 million Mt in 2018 where 25 million Mt were produced in Europe.<sup>43</sup> As mentioned before the main product obtained from rapeseed is oil for human consumption, usually extracted from the seed by

mechanical and solvent extraction.<sup>4,12</sup> As byproduct, rapeseed meal with a high protein content (~40% dry basis), mainly consisting of cruciferin and napin,<sup>2,4,11</sup> is generated. In the Netherlands, around 3500 MT of rapeseed meal were generated in 2018, corresponding to around 1400 MT of total protein. A conceptual downstream process (DSP) of rapeseed meal for the purification of proteins and polyphenols is shown in Figure 4.6. The DSP includes: an aqueous extraction assisted with salts<sup>23</sup> to solubilize the different components in the meal, followed by a small molecule separation (phytic acid, polyphenols compounds, carbohydrates) using ultrafiltration with a cut-off membrane of 3 kDa. The protein rich retentate is sent to an ion exchange (IEX) column where napin is captured and cruciferin flows through. The permeate can be further processed to recover sinapic acid (major polyphenol in rapeseed meal) using adsorption (hydrophobic resins), as recommended by Moreno-González, et al.<sup>18</sup> and Silva, et al.<sup>44</sup> or liquid-liquid extraction (with organic solvents or ionic liquids) as suggested by Silva, et al.<sup>45</sup> The purified fractions of napin and cruciferin, obtained after the chromatography column, are then sent to another membrane unit to remove the salts before being sent to the final drying stage. Following the adsorption method for sinapic acid recovery from Moreno-González, et al.<sup>18</sup> elution and regeneration of the adsorption column can be done with ethanol/water mixtures which can be recovered by distillation and recycled to the column. To obtain sinapic acid crystals, a multiple effect evaporation can be used to crystalize the polyphenol.<sup>46</sup> The evaporated solvent is directed to the distillation column and sinapic acid crystals are then filtered, washed and dried.

Considering that the annual production of rapeseed in the Netherlands is 5836 tons<sup>43</sup> and assuming that the first stages of the process (aqueous extraction, centrifugation, small molecules separation) account an overall protein yield of 90% the initial protein extract flow rate can be estimated.

The ion exchange column for protein purification can be sized using the previous model. The selected resin POROS 50 HS has a polymeric matrix (rigid particles) and a particle size of 50 $\mu$ m and based on supplier specification, this resin possesses high mechanical resistance (100 bars). For a stainless-steel column, a maximum of 50 bar pressure drop was set for a column diameter of 1 meter.<sup>47</sup> Maximum column height using this resin can be estimated using Karman-Cozeny equation, and it corresponds to 1 meter.

The column model is then used to determine the operation of the ion exchange column, in specific to identify the loading volume, which in this case is two column volumes. The loading volume is low because the concentration of each protein in the protein rich extract is relatively high (higher than 8g/L) and the resin gets to equilibrium saturation with relatively low volume. For this simulation, an isotherm slope of 0.6 mL/mresin was considered for cruciferin equilibrium. Resin utilization of 82% was obtained from the model with a napin yield of 98% and >99% purity. In the flow through, cruciferin is recovered (>99% yield and >98% purity). The productivity calculated with this column size (1m diameter and 1 m height) is 26.3 gNapin/L<sub>R</sub>/h, which consequently produces 52.1 MT/a. This accounts to 12% of the total amount of napin than can be recovered from the rapeseed meal generated in the Netherlands using one ion exchange column.

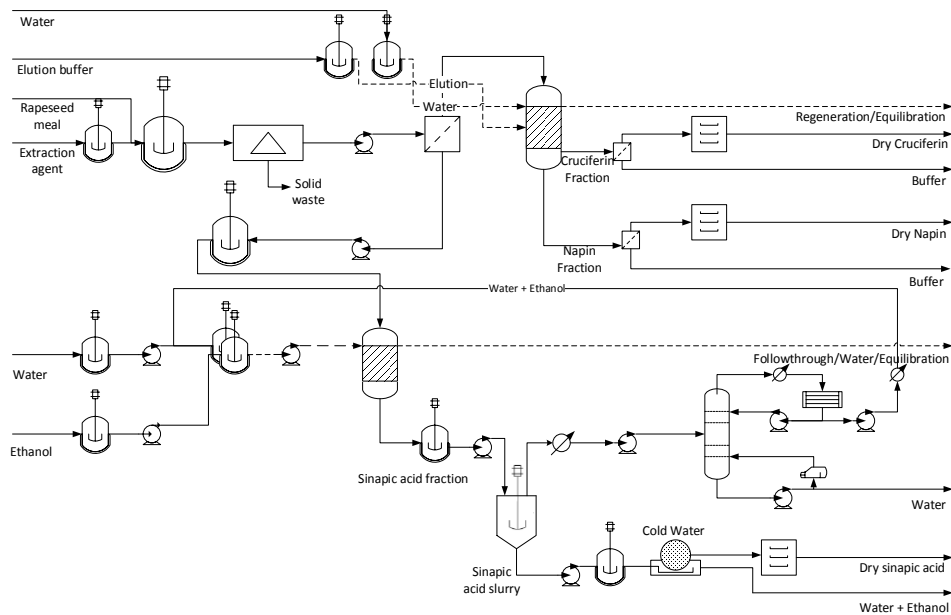


**Figure 4.6.** Conceptual process design for purification of napin, cruciferin and sinapic acid from rapeseed meal

It is possible to purify the annual production of rapeseed meal by calculating the number of columns needed to operate in parallel and the number of cycles that each column can be run. It is important to keep in mind that this is a preliminary evaluation and that breakthrough curve experiments for napin will be still needed to corroborate the selected loading. In addition, for this estimation a similar column operation in terms of desorption was selected (5CV) which could be reduced, as based on the column experiments, full napin might be achieved with less volume. Operation of the ion exchange column can also be adapted to continuous (Simulated moving bed) or semi-continuous (CaptureSMB and Periodic Countercurrent Chromatography, PCC) with multiple columns connected in series or operating in parallel. In addition, economic feasibility should be assessed with a detail economic evaluation to identify overall capital expenditure (CAPEX) and the overall operational cost (OPEX) and performing for instance a cash flow analysis.

#### 4.4. Conclusions

High throughput process development (HTPD) generates reliable and significant information in a short time period. In the case of adsorptive processes, HTPD, different resins and conditions could be assessed in parallel which allows proper resin choice. The generated information can be used in combination with mechanistic models to evaluate technical feasibility of a process design which involves process understanding and contributes to fast process development.

#### 4.5. Acknowledgments

This work was supported by the ISPT (Institute of Sustainable Process Technology) under the project CM-20-07 in Adsorption of non-volatiles from food products. Thank you to the industrial partners DSM,

Unilever, Friesland Campina and Royal Cosun for their valuable input through the project. The authors are also thankful to Yi Song from Delft University for all the provided lab support.

#### 4.6. References

- 1 Wanasundara J.P.D., McIntosh T.C., Perera S.P., Withana-Gamage T.S., Mitra P., Canola/rapeseed protein-functionality and nutrition, *OCL*, 23 (2016) D407.
- 2 Lomascolo A., Uzan-Boukhris E., Sigoillot J.-C., Fine F., Rapeseed and sunflower meal: a review on biotechnology status and challenges, *Appl Microbiol Biotechnol*, 95 (2012) 1105-1114.
- 3 Wanasundara J.P., Proteins of Brassicaceae oilseeds and their potential as a plant protein source, *Critical reviews in food science and nutrition*, 51 (2011) 635-677.
- 4 Wanasundara J.P.D., Tan S., Alashi A.M., Pudiel F., Blanchard C., Chapter 18 - Proteins From Canola/Rapeseed: Current Status, in: *Sustainable Protein Sources*, Academic Press, San Diego, 2017, pp. 285-304.
- 5 Kodagoda L.P., Nakai S., Powrie W.D., Some Functional Properties of Rapeseed Protein Isolates and Concentrates, *Canadian Institute of Food Science and Technology Journal*, 6 (1973) 266-269.
- 6 Jyothi T.C., Sinha S., Singh S.A., Surolia A., Appu Rao A.G., Napin from Brassica juncea: Thermodynamic and structural analysis of stability, *Biochimica et Biophysica Acta (BBA) - Proteins and Proteomics*, 1774 (2007) 907-919.
- 7 Perera S.P., McIntosh T.C., Wanasundara J.P., Structural Properties of Cruciferin and Napin of Brassica napus (Canola) Show Distinct Responses to Changes in pH and Temperature, *Plants*, 5 (2016) 36.
- 8 Aider M., Barbana C., Canola proteins: composition, extraction, functional properties, bioactivity, applications as a food ingredient and allergenicity – A practical and critical review, *Trends in Food Science & Technology*, 22 (2011) 21-39.
- 9 Schmidt I., Renard D., Rondeau D., Richomme P., Popineau Y., Axelos M.A.-V., Detailed Physicochemical Characterization of the 2S Storage Protein from Rape (Brassica napus L.), *Journal of Agricultural and Food Chemistry*, 52 (2004) 5995-6001.
- 10 Adachi M., Kanamori J., Masuda T., Yagasaki K., Kitamura K., Mikami B., Utsumi S., Crystal structure of soybean 11S globulin: glycinin A3B4 homohexamer, *Proceedings of the National Academy of Sciences of the United States of America*, 100 (2003) 7395-7400.
- 11 Contreras M.d.M., Lama-Muñoz A., Manuel Gutiérrez-Pérez J., Espínola F., Moya M., Castro E., Protein extraction from agri-food residues for integration in biorefinery: Potential techniques and current status, *Bioresource Technology*, 280 (2019) 459-477.
- 12 Fetzer A., Herfellner T., Stäbler A., Menner M., Eisner P., Influence of process conditions during aqueous protein extraction upon yield from pre-pressed and cold-pressed rapeseed press cake, *Industrial Crops and Products*, 112 (2018) 236-246.
- 13 Pickardt C., Neidhart S., Griesbach C., Dube M., Knauf U., Kammerer D.R., Carle R., Optimisation of mild-acidic protein extraction from defatted sunflower (*Helianthus annuus* L.) meal, *Food Hydrocolloids*, 23 (2009) 1966-1973.

- 14** Vuorela S., Meyer A.S., Heinonen M., Impact of isolation method on the antioxidant activity of rapeseed meal phenolics, *Journal of agricultural and food chemistry*, 52 (2004) 8202-8207.
- 15** Akbari A., Wu J., An integrated method of isolating napin and cruciferin from defatted canola meal, *LWT-Food Science and Technology*, 64 (2015) 308-315.
- 16** Ghodsvali A., Khodaparast M.H.H., Vosoughi M., Diosady L.L., Preparation of canola protein materials using membrane technology and evaluation of meals functional properties, *Food Research International*, 38 (2005) 223-231.
- 17** Xu L., Diosady L.L., Removal of phenolic compounds in the production of high-quality canola protein isolates, *Food Research International*, 35 (2002) 23-30.
- 18** Moreno-González M., Girish V., Keulen D., Wijngaard H., Lanteslager X., Ferreira G., Ottens M., Recovery of sinapic acid from canola/rapeseed meal extracts by adsorption, *Food and Bioproducts Processing*, 120 (2020) 69-79.
- 19** Murray D.E., Terrence M.J., Barker L.D., Myers C.D., Process for isolation of proteins using food grade salt solutions at specified pH and ionic strength, in, USA, 1980.
- 20** Gerzhova A., Mondor M., Benali M., Aider M., A comparative study between the electro-activation technique and conventional extraction method on the extractability, composition and physicochemical properties of canola protein concentrates and isolates, *Food Bioscience*, 11 (2015) 56-71.
- 21** Hou F., Ding W., Qu W., Oladejo A.O., Xiong F., Zhang W., He R., Ma H., Alkali solution extraction of rice residue protein isolates: Influence of alkali concentration on protein functional, structural properties and lysinoalanine formation, *Food Chemistry*, 218 (2017) 207-215.
- 22** Rommi K., Ercili-Cura D., Hakala T.K., Nordlund E., Poutanen K., Lantto R., Impact of Total Solid Content and Extraction pH on Enzyme-Aided Recovery of Protein from Defatted Rapeseed (*Brassica rapa* L.) Press Cake and Physicochemical Properties of the Protein Fractions, *Journal of Agricultural and Food Chemistry*, 63 (2015) 2997-3003.
- 23** Bérot S., Compoin J.P., Larré C., Malabat C., Guéguen J., Large scale purification of rapeseed proteins (*Brassica napus* L.), *Journal of Chromatography B*, 818 (2005) 35-42.
- 24** Raab B., Schwenke K.D., Simplified isolation procedure for the 12 S globulin and the albumin fraction from rapeseed (*Brassica napus* L.), *Food / Nahrung*, 28 (1984) 863-866.
- 25** Pudiel F., Tressel R.P., Düring K., Production and properties of rapeseed albumin, *Lipid Technology*, 27 (2015) 112-114.
- 26** Zhang S.B., Wang Z., Xu S.Y., Downstream Processes for Aqueous Enzymatic Extraction of Rapeseed Oil and Protein Hydrolysates, *Journal of the American Oil Chemists' Society*, 84 (2007) 693.
- 27** Zhu M., Carta G., Protein adsorption equilibrium and kinetics in multimodal cation exchange resins, *Adsorption*, 22 (2016) 165-179.
- 28** Carta G., Jungbauer A., *Protein chromatography: process development and scale-up*, John Wiley & Sons, 2010.
- 29** Mollerup J.M., Hansen T.B., Kidal S., Staby A., Quality by design—Thermodynamic modelling of chromatographic separation of proteins, *Journal of Chromatography A*, 1177 (2008) 200-206.

- 30** Sevillano D.M., van der Wielen L.A.M., Hooshyar N., Ottens M., Resin selection for the separation of caffeine from green tea catechins, *Food and Bioproducts Processing*, 92 (2014) 192-198.
- 31** Nfor B.K., Noverraz M., Chilamkurthi S., Verhaert P.D.E.M., van der Wielen L.A.M., Ottens M., High-throughput isotherm determination and thermodynamic modeling of protein adsorption on mixed mode adsorbents, *Journal of Chromatography A*, 1217 (2010) 6829-6850.
- 32** Mollerup J.M., The thermodynamic principles of ligand binding in chromatography and biology, *Journal of biotechnology*, 132 (2007) 187-195.
- 33** Mollerup J.M., Applied thermodynamics: A new frontier for biotechnology, *Fluid Phase Equilibria*, 241 (2006) 205-215.
- 34** Felinger A., Guiochon G., Comparison of the Kinetic Models of Linear Chromatography, *Chromatographia*, 60 (2004) S175-S180.
- 35** LeVan D.M., Carta G., Yon C.M., Adsorption and Ion Exchange, in: R.H. Perry, D.W. Green (Eds.) *Perry's Chemical Engineers' Handbook*, McGraw-Hill, New York, 1999, pp. 16-19.
- 36** Young M.E., Carroad P.A., Bell R.L., Estimation of diffusion coefficients of proteins, *Biotechnology and Bioengineering*, 22 (1980) 947-955.
- 37** Wilson E.J., Geankoplis C.J., Liquid Mass Transfer at Very Low Reynolds Numbers in Packed Beds, *Industrial and Engineering Chemistry Fundamentals*, 5 (1966) 9-14.
- 38** Wakao N., Smith J.M., Diffusion in catalyst pellets, *Chemical Engineering Science*, 17 (1962) 825-834.
- 39** Brenner H., Gaydos L.J., The constrained brownian movement of spherical particles in cylindrical pores of comparable radius: Models of the diffusive and convective transport of solute molecules in membranes and porous media, *Journal of Colloid and Interface Science*, 58 (1977) 312-356.
- 40** Gunn D.J., Axial and radial dispersion in fixed beds, *Chemical Engineering Science*, 42 (1987) 363-373.
- 41** Pirrung S.M., Parruca da Cruz D., Hanke A.T., Berends C., Van Beckhoven R.F.W.C., Eppink M.H.M., Ottens M., Chromatographic parameter determination for complex biological feedstocks, 34 (2018) 1006-1018.
- 42** Staby A., Rathore A.S., Ahuja S., *Preparative Chromatography for Separation of Proteins*, John Wiley & Sons, Incorporated, New York, UNITED STATES, 2017.
- 43** Food and Agriculture Organization of the United Nations (FAO), 2019, FAOSTAT Production Quantity (accessed 24 March 2019 2019). <http://www.fao.org/faostat/en/#data/QC>
- 44** Silva M., Castellanos L., Ottens M., Capture and Purification of Polyphenols Using Functionalized Hydrophobic Resins, *Industrial & Engineering Chemistry Research*, 57 (2018) 5359-5369.
- 45** Silva M., García J.C., Ottens M., Polyphenol Liquid-Liquid Extraction Process Development Using NRTL-SAC, *Industrial & engineering chemistry research*, 57 (2018) 9210-9221.
- 46** Silva M., Vieira B., Ottens M., Preferential crystallization for the purification of similar hydrophobic polyphenols, *Journal of Chemical Technology & Biotechnology*, 93 (2018) 1997-2010.

**47** Schmidt-Traub H., Schulte M., Seidel-Morgenstern A., Schmidt-Traub H., Seidel-Morgenstern A., Preparative Chromatography, John Wiley & Sons, Incorporated, Weinheim, GERMANY, 2013.

Appendix 4A. Napin resin uptake kinetics in deep well plates

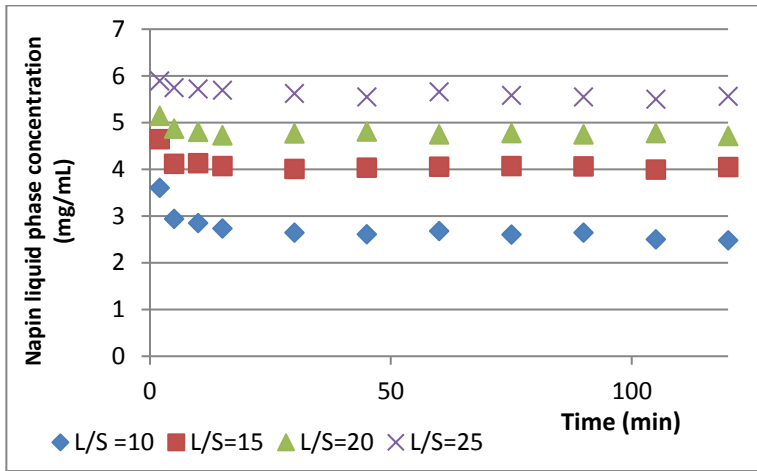


Figure 4.7. Batch uptake experiments of napin at different phase ratios

## Appendix 4B. Protein characteristics

Three different protein isolate products were used in this work. Napin isolate (ABIN1995012), cruciferin isolate (ABIN1995013), and protein mixture, cruciferin + napin (ABIN1995014). All products were obtained from antibodies online. The source origin (based on supplier specification is rapeseed). Napin isolate was used to evaluate single component adsorption isotherms, this because it is hypothesized that cruciferin will poorly interact with the selected resins. Napin standards were prepared for reverse phase chromatography (RPC) analytical method and also for spectrophotometric measurement.

Cruciferin isolate (ABIN1995013) presented very low solubility, consequently standards for analytical method were not generated. Instead of using cruciferin isolate, a protein mixture powder (cruciferin + napin ABIN1995014), suggested by the supplier, was characterized. Protein mixture composition corresponds to 57% napin and 43% cruciferin (based on supplier data), this product has a significantly higher solubility and was properly dissolved in all used buffers.

The chromatograms obtained from the analytical RPC of napin isolate and protein mixture are shown in Figure 1. It can be seen that napin isolate results present two unresolved peaks at 4.4 and 4.8 minutes which correspond to napin protein. The same peaks and peak shape are observed in the protein mixture sample. The protein mixture, additionally presents two extra peaks at 6.4 and 6.9 minutes. These later peaks are hypothesized to be cruciferin. To corroborate this hypothesis, the injected sample was fractionated and characterized by SDS-PAGE. Results of the last two peaks (four samples) are shown in Figure B2. Analyzing total peak areas, napin peak area corresponds to 55% of the total area while cruciferin to 45%, which is in agreement with the composition indicated by the supplier.

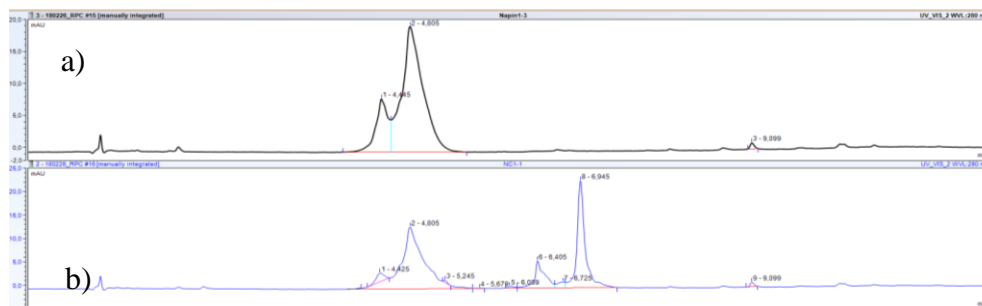


**Figure 4.8.** Analytical reverse phase chromatography (RPC) chromatograms a) Napin isolate and b) Protein mixture.

SDS-PAGE results from the fractionated sample indicates that the protein is cruciferin. The polypeptide bands appeared between 36.5 and 55.4 kDa under non-reducing condition corresponded with size of cruciferin subunit (~50 kDa) reported in literature.<sup>7</sup> Bands around 31 kDa and 21 kDa were expected to be free alpha- and beta- chains of cruciferin subunit. The result was confirmed from samples under reducing conditions. Under reducing conditions, disulfide bonds were broken resulting in small chains of the subunit. Disappearance of the band of cruciferin subunit (~50 kDa) and detection of only bands of small chains indicated that the harvested fraction was cruciferin since small chains of cruciferin formed a subunit by disulfide bonds.

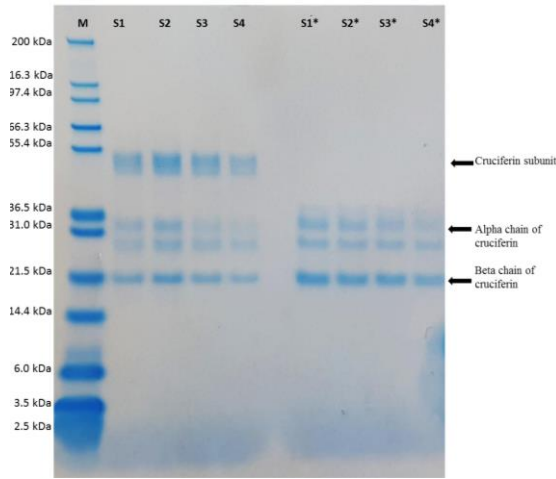


**Figure 4.9.** SDS-PAGE of last two peaks from RPC column of rapeseed protein mixture. S1-S4 under non-reducing condition and S1\*-S4\* under reducing condition, M protein ladder.

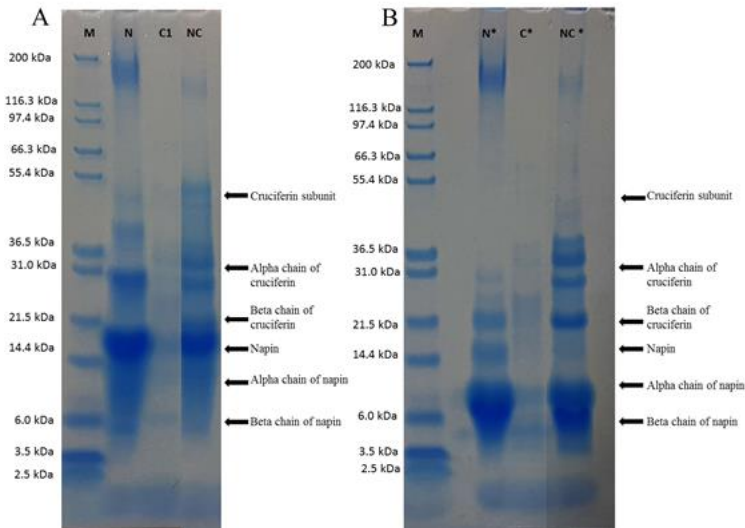


**Figure 4.10.** Polypeptide profile of napin isolate (N), cruciferin (C) and protein mixture (NC) under non-reduced (A) and reduced conditions(B)

Napin protein and protein mixture were analyzed by SDS-PAGE under reduced and non-reduced conditions. Polypeptide profiles are shown in Figure 4.10. Napin profile under non-reducing condition showed the most intense band at 14 kDa which is the size of napin corresponding to the result under reducing condition that the highest intensity appeared around 10 kDa, the size of napin alpha-chain. However, the bands around 30 kDa or higher are expected to be the complex of protein since napin contains several cysteines, leading to form the structure by disulfide bonds. The rapeseed protein

mixture under both conditions provided the expected profile of cruciferin and napin as reported in Perera, et al.<sup>7</sup>. The polypeptide profile of cruciferin isolate did not show the expected bands, therefore, it was decided to use the protein mixture for adsorption experiments to identify the effect of cruciferin on napin adsorption and for cruciferin adsorption isotherm determination.

Napin and cruciferin protein net charge

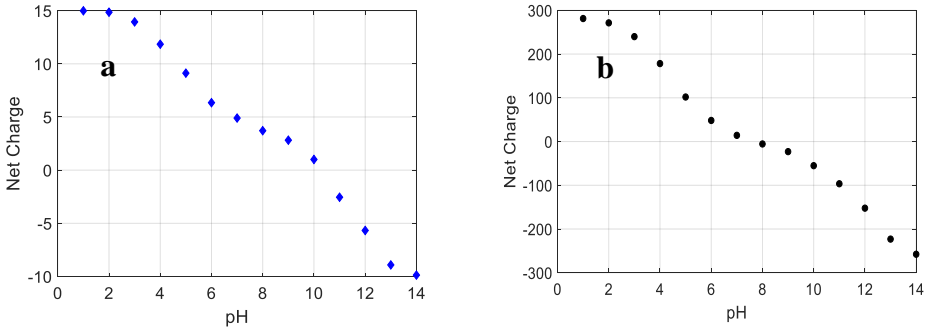


Figure 4.11. Napin and cruciferin estimated titration curves a) Napin b) Cruciferin

Appendix 4C. Mixed mode resins isotherm slope comparison

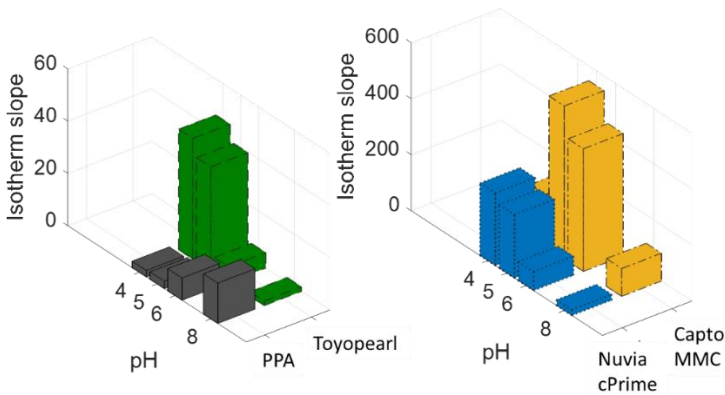


Figure 4.12. Napin isotherm slope ( $m_{L_i}/m_{L_R}$ ) on mixed mode resins at different pH values with 0.3M NaCl

## Appendix 4D. Cruciferin adsorption experiments

**Table 4.6.** Cruciferin relative concentration  $C_e/C_{reference}$  in multicomponent adsorption experiments at different conditions

Reference	Capto MMC			Nuvia cPrime			Toyopearl		
Conditions	pH 6, 0.1 M	pH 6, 0.3 M	pH6, 1.0 M	pH 6, 0.1 M	pH 6, 0.3 M	pH6, 1.0 M	pH 6, 0.1 M	pH 6, 0.3 M	pH6, 1.0 M
<b>1.0</b>	1.0	1.0	1.0	0.9	1.0	1.0	0.9	1.0	1.0
<b>0.5</b>	0.4	0.4	0.5	0.4	0.5	0.5	0.4	0.4	0.5
	PPA HyperCel			Capto S			POROS 50HS		
Conditions	pH 6, 0.1 M	pH 6, 0.3 M	pH6, 1.0 M	pH 6, 0.1 M	pH 6, 0.3 M	pH6, 1.0 M	pH 6, 0.1 M	pH 6, 0.3 M	pH6, 1.0 M
<b>1.0</b>	0.5	0.5	0.7	0.9	0.9	0.9	0.9	0.9	0.9
<b>0.3</b>	0.1	0.1	0.3	0.3	0.3	0.3	0.3	0.3	0.3

**Table 4.6** shows the relative concentration of cruciferin after adsorption experiments at different conditions. One can notice that the change in concentration is minimum, when comparing to the reference concentration (first column) except with resin PPA HyperCel where the hydrophobicity of cruciferin protein seems to benefit the adsorption of cruciferin to the resin.

## Appendix 4E. Simulation parameters industry column

**Table 4.7.** Simulation Parameters

Bed characteristics	Unit	Value
Diameter	m	1.0
Height	m	1.0
Volume	L	201.1
Total porosity	-	0.83
Extraparticle porosity	-	0.3
Intraparticle porosity	-	0.75
Pressure limit	MPa	5
<b>Resin Characteristics (POROS 50 HS)</b>		
Particle diameter	m	5E-5
Pore size	m	470e-9*
Ionic capacity	mM	104
<b>Mobile phase characteristics</b>		
Density	kg/m <sup>3</sup>	1000
Viscosity	Pas	8.9E-4
Temperature	K	294
Linear velocity	cm/h	1760

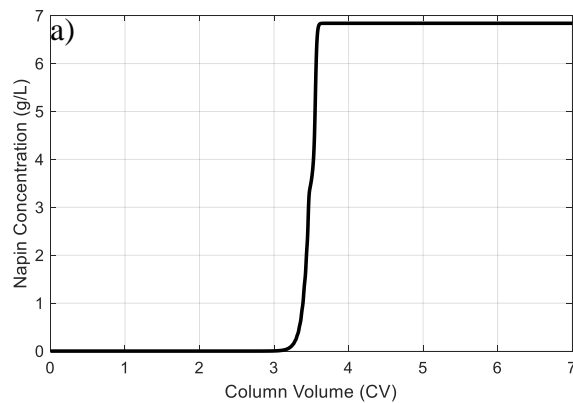


**Figure 4.13.** a) Simulated napin breakthrough curve in POROS HS at 0.3M NaCl and pH 6. Conditions 1760cm/h. Column characteristics specified in Table 4.7.

## Appendix 4F. Rapeseed meal production in The Netherlands

5836 tons of rapeseed were produced in 2018 in the Netherlands (Food and Agriculture Organization of the United Nations).<sup>43</sup> Around 30% of the composition of the seed accounts for oil and ~20% to proteins. After oil is extracted ~3500 tons of rapeseed meal are generated (rich in proteins).

Aqueous extraction of the proteins can be done using a solid: liquid ratio of 1:15,<sup>23</sup> producing around 50,000 MT/a of extract (assuming water density). Large and small molecules are separated with a membrane unit.

**Table 4.8.** Rapeseed meal composition and mass flow rates

Component	%	kg/year
<b>Proteins</b>	40	1,400,640
<b>Carbohydrates</b>	18	630,288
<b>Others</b>	39	1,365,624
<b>Phytic</b>	3	105,048
<b>Total</b>	100	3,501,600

**Table 4.9.** Rapeseed meal extract mass flow rates

Component	Value	Units
<b>Proteins</b>	1330.6	MT/year
<b>Carbohydrates</b>	598.8	MT/year
<b>Others</b>	1297.3	MT/year
<b>Phytic</b>	99.8	MT/year

**Table 4.10.** Protein rich fraction after small molecules separation

Component	Value	Units
<b>Proteins</b>	1,264.08	MT/year
<b>Cruciferin</b>	632.04	MT/year
<b>Napin</b>	379.22	MT/year
<b>Others</b>	252.82	MT/year

**Table 4.11.** Chromatography process parameters

Chromatography cycle	Parameter	Unit
<b>Equilibration</b>	5	CV
<b>Loading</b>	2	CV
<b>Washing</b>	3	CV
<b>Elution</b>	5	CV
<b>CIP</b>	3	CV
<b>Total CV</b>	18.2	CV
<b>Vol liquid in cycle</b>	14.3	m <sup>3</sup>
<b>Volume resin</b>	551.2	L <sub>R</sub>
<b>Ac (cross sectional area)</b>	0.8	m <sup>2</sup>
<b>Qv (Volumetric flow rate)</b>	13.8	m <sup>3</sup> /h
<b>Cycle time</b>	62.2	min
<b>Production</b>		
<b>Product per year</b>	1	Column
<b>Napin</b>	52.1	ton/year
<b>Year</b>	3600	h
<b>Percentage of total napin in the Netherlands</b>	12.3%	

# Chapter 5

## Continuous adsorption in food industry: The recovery of sinapic acid from rapeseed meal extract

---

### Abstract

Efficient recovery and utilization of valuable components from industrial food side streams is a main driver towards a circular economy. Among different available purification techniques, adsorption can effectively recover these components. However, the conventional batch mode of operation can limit its applicability in food processes due to limited efficiency. This work compares conventional batch packed bed adsorption with semi-continuous adsorption (so-called CaptureSMB) for the recovery of sinapic acid at industrial scale, using a food grade resin Amberlite™ FPX66. A mathematical mechanistic model able to describe semi-continuous operation is successfully validated and used to identify optimum operating parameters to maximize productivity and resin capacity utilization in batch and semi-continuous operating modes. The results indicate that CaptureSMB outperforms batch operation, increasing productivity from 5.18 g/L/h to 10.3 g/L/h for a given yield (>97%). A resin capacity utilization (RU) of around 70% is observed in both operating modes when productivity is maximized. A 92% RU can be accomplished for a given yield using the CaptureSMB process at a productivity of 7.0 g/L/h, higher than for conventional batch operation. The use of semi-continuous adsorption operation in food industry contributes to more efficient processes at reduced purification costs.

**Keywords:** Adsorption, Batch, Semi-continuous, CaptureSMB, Model-based optimization, Polyphenols, Industrial side stream valorization

---

**Published as:** Moreno-González M., Keulen D., Gomis-Fons J., Lopez Gomez G., Nilsson B., Ottens M. *Continuous adsorption in food industry: The recovery of sinapic acid from rapeseed meal*, *Sep. Purif. Technol.* 254 (2020) 117403. <https://doi.org/10.1016/j.seppur.2020.117403>

## 5.1. Introduction

Voluminous side streams are generated during the supply chain of food products. These side streams are complex mixtures that often contain valuable products that can be valorized, via recovery and reuse in the food chain.<sup>1</sup> For instance, proteins can be recovered from agricultural residues such as oilseed meals,<sup>2-4</sup> cereals are sources of complex carbohydrates such as hemicellulose, arabinoxylans and glucans while fruits and vegetables are sources of polyphenols.<sup>1</sup> Valorization and recovery of these compounds have been conducted using well established methodologies, like the universal 5 step methodology suggested by Galanakis<sup>1</sup> with the application of conventional techniques such as precipitation, filtration, adsorption and extraction, amongst others<sup>1</sup>. Recovering these valuable products can contribute to a more circular economy by reducing waste generation and maximizing resource potential. In addition, the improved efficiency could lead to cost reduction.

Among different separation techniques, adsorption is a powerful technology able to separate complex mixtures at mild operating conditions, often desired in food processes. Large scale batch adsorption processes have been implemented for sugar and isomers separation, fractionation of amino acids and proteins, purification of penicillin and enzyme production<sup>5</sup>. However, some disadvantages of batch adsorption are: high buffer consumption, low productivity and high stationary phase cost, as not all the adsorbent in the column is efficiently used.

The application of continuous or semi-continuous adsorption can overcome the limitations of batch operation. Improved capacity utilization, which subsequently results in reduced buffer consumption, shorter processing times and cost savings.<sup>6</sup> The usage of connecting columns (smaller packed beds) in series and a flexible valve system to switch the inlets (feed, wash and eluting buffers) at the right time (simulating countercurrent movement) allows a more efficient operation.

Continuous chromatography has been successfully implemented in the (petro)chemical field mainly with variants of simulated moving bed (SMB)<sup>7-10</sup> technology. The Hypersorption process,<sup>11</sup> purification of L-Lysine from Calgon Carbon, Vitamin C production from Sep Tor Technologies and the different applications of the UOP Sorbex process (Parex, Molex, Olex)<sup>12</sup> are some examples. The applied flow rates could go up to 150 m<sup>3</sup>/h and these SMB systems are typically operated with more than four columns having product capacities from 30 – 400 kton/a<sup>13</sup>. The pharmaceutical sector has found SMB applications in chiral separation<sup>14</sup> at a significant lower production scale, up to 10 ton/a. The biopharmaceutical sector has increased its interests in continuous operation and new developments in semi-continuous systems have been introduced such as periodic countercurrent chromatography (PCC),<sup>15, 16</sup> the sequential multicolumn chromatography (Varicol) from Novasep,<sup>17, 18</sup> the multicolumn countercurrent solvent gradient purification (MCSGP),<sup>19, 20</sup> mainly used for monoclonal antibody purification. While in the food sector, SMB technology has been investigated in different areas such as desugarization and fractionation of molasses, oligosaccharides and organic acid separations, dairy streams protein purification, peptides isolation from hydrolysates<sup>21-26</sup> and separation of fructose-glucose<sup>27-29</sup> and the Sarex process.<sup>13</sup> These applications show the potential of using continuous chromatography for purification of more complex streams such as food by-products for the recovery of nutraceuticals (polyphenols) or natural food ingredients, which can also be aligned with the continuous operation of food processes.

In terms of equipment complexity, systems with few columns are preferred, as control and number of devices needed for operation (valves, pumps, pipes and detectors) increase with the number of columns.<sup>30</sup> The recently developed twin column system, CaptureSMB (2-PCC system), proposed by Angarita, et al.<sup>31</sup> has been successfully implemented for the capture step of monoclonal antibodies, showing comparable or better performance than systems with higher number of columns,<sup>31, 32</sup> which makes it an interesting system with potential application in food industry.

This work compares the performance of the semi-continuous system CaptureSMB with conventional batch operation (packed bed) for the recovery of sinapic acid (a nutraceutical) from rapeseed meal extract (food by-product). The study begins with the adaptation of a previously developed one-column adsorption model<sup>33</sup> to a two-column system, CaptureSMB, followed by its experimental validation at lab scale. Both models (batch and semi-continuous) were later used to find optimum operating parameters to maximize productivity and resin capacity utilization at industrial scale (up to 118 m<sup>3</sup>/h). The use of modelling allows the fair comparison of both processes, as the same constraints could be established. Additionally, it minimizes the number of pilot trials. The methodology used in this work can be used as a guide for other food products that involves an adsorption step, where pilot or industrial scale experimentation are not possible.

## 5.2. Case study

Rapeseed meal contains mainly crude proteins (40%), crude fibers (12%) and nitrogen-free extract fractions (34%).<sup>34</sup> When processing the rapeseed meal to acquire the proteins, it is important to remove phytic acid and phenolic content to prevent nutritional value lost. However, phenolic compounds are valuable compounds that can be recovered. Particularly, sinapic acid, mayor phenolic compound in rapeseed meal, presents antioxidant, antimicrobial, anti-inflammatory activities.<sup>35</sup> Therefore, sinapic acid has potential application in food, cosmetic and pharmaceutical products. Previous studies have demonstrated that sinapic acid is selectively captured using the polymeric resins Amberlite™ FPX66, while phytic acid, glucose and glucosinolates (impurities) poorly interact with the adsorbent.<sup>33</sup>

For industrial applications, a column of 1 m internal diameter and column height between 3 and 12 m was assumed to evaluate the optimization of two adsorptive operating modes. The two adsorption configurations evaluated in this study were: 1) batch operation with packed bed and 2) semi-continuous operation with CaptureSMB.

In both configurations, elution and regeneration phases were assumed to be the same and consisted of washing with 2 column volumes (CV) of water, elution and regeneration with 8 CV of 70% w/w ethanol/water and re-equilibration with 5 CV of citrate-phosphate buffer at pH 6.

## 5.3. Materials and methods

### 5.3.1. Theory: Adsorption column model

The equilibrium-transport-dispersive chromatography model in combination with the liquid-film linear driving force approximation is used to describe the dynamic adsorption of one column, as described in equation (5.1)

$$\frac{\partial C_i}{\partial t} + F \frac{\partial q_i}{\partial t} + v \frac{\partial C_i}{\partial z} = D_L \frac{\partial^2 C_i}{\partial z^2} \quad (5.1)$$

Where  $C_i$  represents the bulk liquid concentration (g/L) of component  $i$ ,  $v$  is the interstitial velocity of the mobile phase (m/s) defined as superficial velocity divided by the bed porosity ( $u/\varepsilon_b$ ),  $q_i$  is the stationary phase concentration of component  $i$  (g/L<sub>R</sub>),  $F$  is the phase ratio defined as  $F = (1 - \varepsilon_b)/\varepsilon_b$ , where  $\varepsilon_b$  is the bed porosity, and  $D_L$  is the axial dispersion coefficient (m<sup>2</sup>/s). The solid stationary phase concentration term  $\frac{\partial q}{\partial t}$  is defined according to equation (5.2). The lumped kinetic model (LKM) was used for column modelling. This model assumes that the mobile phase concentration in the pores and between the particles is the same,<sup>36</sup> therefore a separate mass balance for the pore is not required.

$$\frac{\partial q_i}{\partial t} = k_{ov,i}(C_i - C_{eq,i}^*) \quad (5.2)$$

The LKM lumps the internal and external mass transfer resistances into an overall mass transfer coefficient  $k_{ov,i}$  (1/s) as defined in equation (5.3).

$$\frac{1}{k_{ov,i}} = \frac{d_p}{6 * k_f} + \frac{d_p^2}{60 * \varepsilon_p * D_p} \quad (5.3)$$

where  $d_p$  is the particle diameter (m),  $k_f$  is the film mass transfer coefficient (m/s),  $\varepsilon_p$  is the intraparticle porosity and  $D_p$  is the pore diffusivity (m<sup>2</sup>/s).  $D_L$  and other relevant model parameters were calculated using different mass transfer correlations as described in Moreno-González, et al.<sup>33</sup> The equilibrium concentration  $C_{eq,i}^*$ , is calculated using the Langmuir isotherm (equation (5.4))

$$q_i = \frac{H_i C_{eq,i}^*}{1 + \frac{H_i}{q_{max,i}} C_{eq,i}^*} \quad (5.4)$$

where  $q_i$  is the adsorption capacity (g/L<sub>R</sub>),  $H_i$  is the isotherm slope ( $H_i = q_{max,i} K_i$ ),  $q_{max,i}$  is the maximum adsorption capacity (g/L<sub>R</sub>),  $K_i$  is the equilibrium constant (L/g) of the species being adsorbed.<sup>37</sup> In order to include the isotherm slope dependency on the modifier concentration a power function was used as described elsewhere.<sup>33, 38</sup>

In the adsorption model an initial condition (at  $t = 0$ ) and two boundary conditions are required. The assumption for the initial condition is that the column is not preloaded (free of components  $C_i(t = 0) = 0$ ;  $q_i(t = 0) = 0$ ). The in- and outlet conditions are described by Danckwerts boundary conditions for dispersive systems (equations (5.5) and (5.6)):

$$\text{Inlet:} \quad C_i(t, x = 0) = C_{inlet,i} - \frac{D_{L,i}}{v} \frac{\partial C_i(t, x = 0)}{\partial x} \quad (5.5)$$

$$\text{Outlet:} \quad \frac{\partial C_i(t, x = L)}{\partial x} = 0 \quad (5.6)$$

### 5.3.1.1. CaptureSMB process

The concept of periodic countercurrent chromatography (PCC) is to switch the connection between columns during the different steps (e.g. loading, washing, elution and regeneration) of the chromatography process. In this study the 2-PCC, patented by ChromaCon as CaptureSMB, is studied.<sup>39</sup> The operation mode depends on the breakthrough moments for the applied flow rates during the interconnected and disconnected phase. An overview of the process is shown in Figure 5.1, separated in four steps

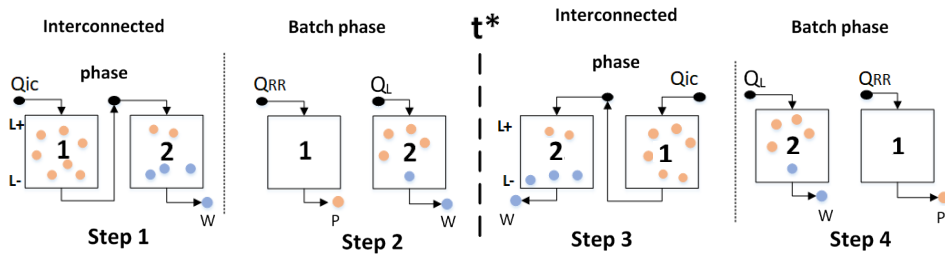


Figure 5.1 Schematic presentation of a CaptureSMB system.

There are two different phases in one-time switch ( $t^*$ ), indicated in Figure 5.1 as interconnected and batch phase. First the columns are connected in series (i.e. interconnected time), the first column is loaded up to a certain percentage of dynamic binding capacity (DBC), step 1 and the breakthrough is captured by the second column. Subsequently (step 2) the first column is washed, eluted and regenerated to obtain the product while the second column is loaded with the feed. Once the first column is regenerated, the columns are connected again (time switch,  $t^*=t_b+t_{ic}$ ), and switch positions (column 2 becomes column 1). Step 3 is performed; the columns are connected in series and subsequently disconnected. In Step 4, the product is recovered from column 1 while column 2 is loaded with the feed. A cycle is completed when two-times switches are completed and the columns return to their starting positions (steps 1 to 4). In this work column 1 is referred as the first column in the column interconnection.

The interconnected phase has a certain duration (interconnected time,  $t_{ic}$ ) and it is performed at an interconnected flow rate  $Q_{ic}$  ( $m^3/h$ ). The time needed in the batch phase is defined by the elution/regeneration protocol. While the first column performs the task of recovering the bound product and regenerating the column at a flow rate  $Q_{rr}$ , the second column is loaded with the feed at a flow rate  $Q_L$ . The parameters to be optimized in the CaptureSMB process are the interconnected and loading flow rates ( $Q_{ic}$  and  $Q_L$ ) and the interconnected time ( $t_{ic}$ ).<sup>32</sup> In this work, superficial velocities were used instead of flow rates, as the flow rate is a function of this velocity and the cross-sectional area of the columns.

Even though there is a continuous input of feed using the CaptureSMB process, the operation is semi-continuous due to discontinuous collection of the product.

### 5.3.1.2. Capture SMB model

Adapting the adsorption model of one column to a CaptureSMB configuration results in the simulation of the transport-dispersive model<sup>36</sup> for two columns connected, where the output of one column is the input of the next one. The main changes and/or additions compared to batch chromatography are:

different boundary conditions for each column, multiple flow rates, time switches, timespan and operating variables.

In the CaptureSMB model the balance of each solute ( $i$ ) transported through each column ( $j$ ) is solved<sup>9</sup> (equation (5.1)).

The connecting nodes between the columns (black nodes in Figure 5.1) are set-up according to the specific process configuration, and they determine the boundary conditions for each column. Column switching was implemented by a periodic movement of the concentration vector. The concentration vector is moved at the end of the switching interval by a step size of one column length against the direction of fluid flow. The duration of one cycle is equal to the amount of columns times the time-span of one time-switch ( $t_{\text{cycle}}=2t^*$ ). Moreover, the total time depends on the amount of cycles set and after multiple time switches a cyclic steady state is reached, which means that the same elution profile is repeated every cycle. The initial conditions at ( $t = 0$ ) assume that the columns are not preloaded with the product (start-up phase) and this is subsequently altered after every switch. The new initial conditions are equal to the conditions at the time switch (equations (5.7) and (5.8))

$$C_{0,i} = C_i(t = n \cdot t^*) \quad (5.7)$$

$$q_{0,i} = q_i(t = n \cdot t^*) \quad (5.8)$$

Where  $t^*$  denotes the time switch and  $n$  the number of switches set. The main assumptions made for the continuous model are that the columns are identical and the dead volume between the columns is neglected.

The boundary conditions are different for each column and changes from interconnected to batch phase in one-time switch. The beginning and end of the column in Figure 5.1 is denoted by  $L^+$  and  $L^-$ . The boundary conditions for the interconnected phase are expressed in equations (5.9) and (5.10).

$$C_i(t, L^+(\text{column I})) = C_{feed,i} \quad (5.9)$$

$$C_i(t, L^+(\text{column II})) = C_i(t, L^-(\text{column I})) \quad (5.10)$$

Since the two columns are connected in series, the inlet of the second column is equal to the outlet of the first column.

The boundary conditions for the batch phase are shown in equation (5.11) and equation (5.12).

$$C_i(t, L^+(\text{columnI})) = 0 \quad (5.11)$$

$$C_i(t, L^+(\text{columnII})) = C_{feed,i} \quad (5.12)$$

The first column in the batch phase undergoes elution and regeneration, therefore, the inlet feed concentration is zero, while the second column is loaded with the feed at a flow rate ( $Q_L$ ).

The dynamic model is a function of time and space (equation (5.1)) and can be described by a partial differential equation (PDE), while ordinary differential equations (ODEs) only include one variable. The Method of Lines was applied for the spatial discretization in order to transfer the PDE into a set of ordinary differential equations (ODEs) with respect to time. The system of ODEs was numerically solved using an implicit solver (*ode15s*) for stiff differential equations in MATLAB R2017b software.

### 5.3.1.3. Batch and continuous process optimization

Batch and continuous operations were optimized for large-scale implementation in food industry, where column dimensions are significantly bigger than the ones used by pharmaceutical companies. Maximum productivity is important for food industry as voluminous streams are usually generated. The following optimization problems were defined:

#### Batch optimization

$$\text{Optimization function} \quad \max \text{Prod}(u_{batch}) \quad (5.13)$$

$$\text{Subject to} \quad C_i(t = t_{ads}, z = L_c) \leq 0.04C_{feed,i} \quad (5.14)$$

$$\text{Yield} \geq 97\%$$

$$L_c = 3m, 6m \text{ and } 12m$$

$$0 < t_{ads}; \quad 2.45 < u_{batch} \leq 205 \text{ m/h}$$

Where  $u_{batch}$  is the superficial velocity and  $t_{ads}$  is the adsorption time. Velocity was varied based on the maximum allowed pressure drop, indicated by the resin supplier (Dow Chemicals).

*CaptureSMB optimization*

$$\text{Optimization function} \quad \max \text{Prod}(u_{ic}, u_b, t_{ic}) \quad (5.15)$$

$$\text{Subject to} \quad \text{Yield} \geq 97\% \quad (5.16)$$

$$L_c = 3m, 6m \text{ and } 12m$$

$$0 < t_{ic}; 0 < u_b \leq u_{ic}$$

$$2.45 < u_{ic} \leq 60 \text{ m/h at } L_c = 3m;$$

$$2.45 < u_{ic} \leq 110 \text{ m/h at } L_c = 6m$$

$$2.45 < u_{ic} \leq 205 \text{ m/h at } L_c = 12m$$

Column length was varied, as experiments showed that lowering the bed height increases the productivity performance of the CaptureSMB process when comparing to batch.

### 5.3.2. CaptureSMB adsorption experiments

#### 5.3.2.1. Resin preparation and column characteristics.

Following resin supplier recommendations, resin FPX66 was washed with water prior to use, to remove chlorine and sodium carbonate salts. Water excess was removed using a glass filter under vacuum and the resin was contacted with ethanol for 30 min. A second washing step was performed to remove ethanol and re-suspend the resin in water prior column packing.

CaptureSMB process requires two identical columns for operation. A known amount of pre-treated resin FPX66 (2.5 g per column) was placed in two adjustable height Omnifit glass columns (1 cm inner diameter and 15 cm height). The volume of each column was 3.5 mL (4.5 cm column height). Trace pulse experiments with NaCl were done to determine bed porosity corresponding to 0.32 and intraparticle porosity was obtained using the difference between wet and dry weight of the resin which corresponds to a value of 0.56. Resin characteristics can be found in section 5.3.3..

#### 5.3.2.2. Equipment set up

Experiments were performed using an Äkta Avant coupled with the operating system Unicorn 7, provided by GE Healthcare Life Sciences (Uppsala, Sweden). The system configuration is shown in Figure 5.2. The implementation of three versatile valves (VV1, VV2 and VV3 in Figure 5.2) made it possible to switch between phases. In particular, versatile valve 1 is used to choose between batch and interconnected step, and versatile valves 2 and 3 are used to choose the column to be loaded first, that is, to determine the specific process step. The outlet valve is used to fractionate the breakthrough of the column being loaded during the batch step and the breakthrough of the second column during the interconnected step. The collection of the product pool was carried out with a sample valve used as a second outlet valve, with seven different outlets.

The process was monitored using two UV detectors, a U9-M monitor able to measure up to three wavelengths, equipped with a U9-D UV detector (GE Healthcare Life Sciences, Uppsala, Sweden), the second detector is a U9-L able to measure only one wavelength (280 nm). pH and conductivity were monitored using a V9-pH and a C9 conductivity monitor respectively (GE Healthcare Life Sciences, Uppsala, Sweden). In addition, fractions were collected during the whole process run.

In order to adapt the Äkta Avant system to run a complex process like the CaptureSMB, the research software **Orbit**, developed at Lund University (Sweden), was used. Orbit controller is a program developed in Python that enables the execution of chromatography processes through scripting. Orbit executes its commands through Unicorn via OPC (Object Linking and Embedding for Process Control), i.e., it sends instructions sequentially at different times, and Unicorn executes them. Orbit has been successfully adapted to work in Äkta Pure (with Unicorn 7)<sup>40, 41</sup> with column sequences for the purification of biopharmaceuticals. Additionally, it has been adapted to run a 3-column periodic countercurrent chromatography (PCC) process in Äkta Pure.<sup>42</sup> In this case, the scheduling of the CaptureSMB process determines the times at which Orbit sends every instruction to Unicorn.

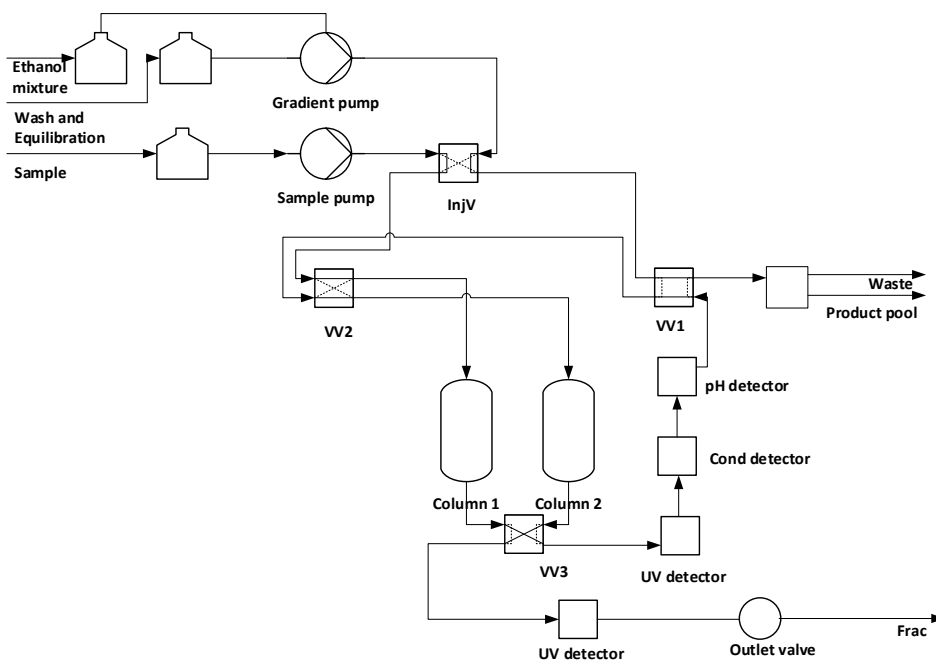


**Figure 5.2.** CaptureSMB process configuration in chromatography system (Step 1). Continuous line represents active flow path.

### 5.3.2.3. CaptureSMB run

Initial determination of CaptureSMB operating parameters were done following the methodology described by Angarita, et al. (2015) and using the simulation of sinapic acid breakthrough curves on FPX66, as previous study showed that the dynamic column model is in good agreement with experimental results.<sup>33</sup>

Batch time ( $t_b$ ) is a function of the elution protocol, which was defined based on the dynamic column model and experiments presented by Moreno-González, et al.<sup>33</sup> The process was run for four cycles. CaptureSMB operating parameters are shown in Table 5.1. As suggested by Angarita, et al.<sup>31</sup> a start-up phase was implemented in order to achieve steady state operation since the second switch. Elution and regeneration protocols are described in Section 5.2 Case study of this work.

**Table 5.1.** Lab scale CaptureSMB operating parameters

Parameter	Value
Start-up time	125 min
Interconnected time	83 min
Batch time	42 min
Interconnected superficial velocity	61 cm/h
Batch velocity	30 cm/h
Elution velocity	100 cm/h
Washing and Equilibration velocity	115 cm/h
Resin	FPX66
Column Volume	3.5 mL (1cm x 4.5 cm; id x h)

The above parameters were used in the lab scale CaptureSMB process and were later optimized for industrial scale application as described in 5.3.1.3 Batch and continuous process optimization.

UV, pH and conductivity detectors were used to monitor breakthrough of column 1 while breakthrough of column 2 was fractionated (2 mL per fraction) and analyzed for sinapic acid concentration by UHPLC (5.3.5 Analytical methods). In addition, during step 4 of the last cycle (in the process shut-down), it was decided to continue loading the column up to interconnected time was accomplished. The outlet was fractionated to verify the product breakthrough in column 1.

### 5.3.3. Chemicals

All chemicals were analytical grade: Sodium phosphate, dibasic, 12-hydrate ( $\geq 99\%$ ) and citric acid ( $\geq 99\%$ ) were purchased from J.T. Baker, Denmark. Glucose anhydrous for biochemistry and Ethanol: Emsure absolute for analysis were purchased from Merck. Sinapic acid ( $\geq 99\%$ ), acetonitrile (HPLC grade) formic acid ( $\geq 99\%$ ) and food grade macroporous resin Amberlite™ FPX66 were purchased from Sigma-Aldrich, The Netherlands. Resin characteristics can be found in Table 5.2.

**Table 5.2.** FPX66 resin characteristics

Resin	Matrix	Particle size (mm)	Surface area (m <sup>2</sup> /g)/capacity	Pore diameter (nm)	Density (g/mL)
FPX66	Macroeticular aromatic polymer	0.600 – 0.750	$\geq 700$	25	1.025

#### 5.3.4. Buffer solutions

Disodium phosphate.  $\text{Na}_2\text{HPO}_4$ , (0.2M) and citric acid (0.1M) solutions were prepared using MilliQ water and dissolving the corresponding amount of each chemical. Citrate-phosphate buffer at pH 6 was prepared following the method from McIlvaine<sup>43</sup>, the used ratio corresponds to 64.8:35.2 ( $\text{Na}_2\text{HPO}_4$  mL/Citric acid mL).

Mimicked plant-based extract was prepared by dissolving sinapic acid and glucose in citrate-phosphate buffer at pH 6. The corresponding concentrations were 1.2 g/L sinapic acid and 8 g/L glucose. The selected concentrations are similar to the concentrations of the aqueous extract from rapeseed meal.

All buffer and solutions were filtered previous to use with disposable filters of 0.45 $\mu\text{m}$  pore size.

#### 5.3.5. Analytical methods

Sinapic acid concentration was analyzed by Ultra High-Performance Liquid Chromatography (UHPLC, Ultimate 3000, Thermo Scientific, USA) equipped with a C18 column (Acquity UPCL HSS column 1.8 $\mu\text{m}$ , 2.1mmx1000mm Waters, Milford, USA). The column was maintained at 30°C with a flow of 0.3 mL/min (isocratic elution 66.7% solvent A). Solvent A is MilliQ water (acidified with 10% ferulic acid) and solvent B is acetonitrile (acidified with 10% ferulic acid). Data acquisition was obtained at 325 nm wavelength.

### 5.4. Results and Discussion

#### 5.4.1. CaptureSMB experiments

CaptureSMB experiments were performed in an Äkta Avant system for the capture of sinapic acid. The process was monitored by UV and by fractionation as sinapic acid detection by UV easily exceeded the linearity of the detector at concentration higher than 0.2g/L. Eight product pools were obtained from the four cycles. Sinapic acid breakthrough in column 1, was measured at the end of the run (Figure 5.3a), where a breakthrough of around 50% was achieved. The average concentration of sinapic acid in the pools was  $3.58 \pm 0.22$  g/L, and the product was concentrated 3.2 times.

Breakthrough of sinapic acid at the exit of the second column (Figure 5.3b) during the interconnected phase, is observed and not desirable as product is consequently lost. Product breakthrough continues during the batch phase, when column 1 is being eluted and regenerated and column two is loaded with a lower flowrate. The observed breakthrough is minimum and does not exceed 1% in each cycle, and therefore did not significantly affect sinapic acid recovery yield.

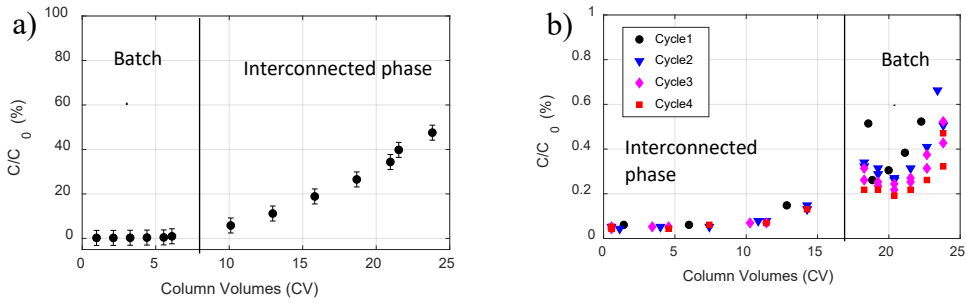


**Figure 5.3** a) Sinaptic acid breakthrough in column 1, b) Sinaptic acid concentration at the exit of column 2 during interconnected and batch phase in four cycles

Process mass balance was evaluated (mass balance error of 6%) and the performance indicators, such as, yield, productivity, buffer consumption and resin capacity utilization were calculated (Table 5.3) and compared with semi-continuous CaptureSMB modelling results. In addition, these results were compared with batch operation at lab scale.

**Table 5.3.** Performance comparison between CaptureSMB (experimental and simulation) & batch simulation results

	CaptureSMB		Batch	Units
	Exp	Simulation	Simulation	
<b>Flow rate</b>	Qic 0.8 mL/min Qb 0.4 mL/min		0.8 mL/min	
<b>Yield</b>	95	96	98	%
<b>Productivity</b>	8.8	9.0	6.7	g/L <sub>R</sub> /h
<b>Buffer consumption</b>	0.7	0.7	1.5	L/g
<b>Capacity utilization</b>	60	62	30	%
<b>Product concentration</b>	3.6	3.7	1.7	g/L

It can be seen in Table 5.3 that the yield predicted by the simulation of the CaptureSMB process is slightly higher than the one obtained experimentally, however this difference could be attributed to experimental error. The missing sinaptic acid might have been lost during the washing step, as observed with the model, where the loss is around 4%.

Comparison between batch and CaptureSMB process was done using the same resin volume. This means that in the CaptureSMB process, the two columns connected have the same total volume as one batch column, and the superficial velocity of the batch process corresponds to the interconnected phase velocity of the CaptureSMB. The results of one single column (batch operation) showed much lower resin capacity utilization due to the limited feed loading. This because the column is loaded just before 4% product breakthrough while in the CaptureSMB the loading reached almost 50% breakthrough. Consequently, higher buffer consumption and lower productivity are observed compared to the semi-continuous process.

It is important to note that the velocities and parameters used in the experiments were pre-estimations and were not optimized. Optimization of both processes is shown in Section 5.4.2 Batch and CaptureSMB industrial scale optimization.

The previous results validated the CaptureSMB model previously described, and the batch and semi-continuous model were used to perform an industrial-scale process optimization, with the objective of maximizing productivity. The following sections explain the optimization results.

#### 5.4.2. Batch and CaptureSMB industrial scale optimization

##### 5.4.2.1. Batch optimization

For batch adsorption analysis, a column of 1m internal diameter and three different column lengths, 3m, 6m, and 12m, were simulated. Mechanical resistance of resin FPX66 goes up to 224 kPa/m with a maximum service superficial velocity of 223.0 m/h at 27 °C. The lower velocity limit was set to 2.4 m/h and the upper limit to 205 m/h. Batch optimization was performed to identify the optimum velocity that maximizes productivity without compromising yield (> 97%) and without exceeding maximum pressure drop, having as an additional constraint at least 70% of resin utilization. The superficial velocity for elution/regeneration was set to 80 m/h as the elution is done with 70% ethanol, the column was also regenerated.

A Pareto chart of resin utilization versus productivity for the batch process is shown in Figure 5.4a, for different column lengths. In all data points, the yield condition was accomplished. Figure 5.4a shows that higher resin utilization can be reached at any column length but this might decrease productivity, because the points that are closer to 100% resin utilization are the ones that correspond to lower velocities and consequently higher residence time.<sup>42</sup> From Figure 5.4a, one can notice that the resin utilization constraint can be accomplished with any column height, and that similar productivity values are also obtained as the curves are almost overlapped at higher than 70% resin utilization.

The highest productivity achieved for a 97% yield (at 4% breakthrough) was found with the shortest column, 10.4 g/L/h, corresponding to resin utilization of 35.5%, which is lower than the desired value of 70%.

It is known that there is a residence time that maximizes productivity in a batch process, independently of column length,<sup>37</sup> which in this case is around 10 minutes. The peak height in Figure 5.4b, changes with column length because the superficial velocity for wash, elution and re-equilibration was set to 80 m/h, which makes the duration of these steps be different with column length as they are based on column volumes. As the column height increases, higher volumes and more time is required in order to complete this task. This consequently reduces the maximum productivity values for longer columns. It is clear that a batch process can achieve high productivity but inevitably at expense of resin capacity utilization and vice versa, higher resin utilization with lower productivity.

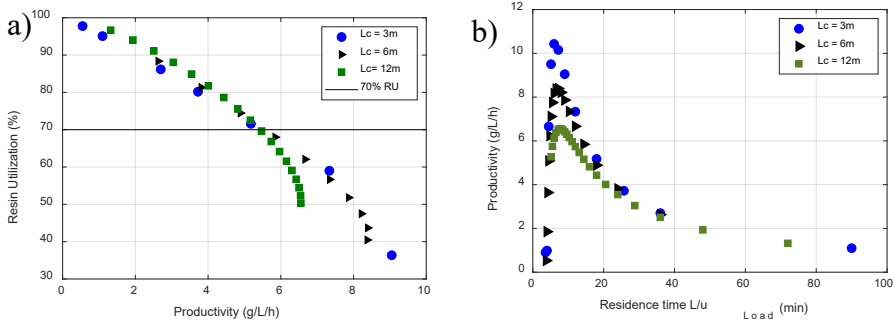


**Figure 5.4.** a) Productivity vs Resin Utilization in batch process. b) Productivity vs Residence time

Operating the 12m column at 50 m/h, the 6m column at 22 m/h and the 3m column at 10 m/h results in a process productivity of  $5.1 \pm 0.2$  g/L<sub>R</sub>/h, while satisfying both constraints of at least 70% resin utilization and >97% yield. The dimension of the columns will be therefore determined by the feed stream volume.

The use of a semi-continuous operation might increase the resin capacity utilization and productivity as observed in the CaptureSMB experiments. The following section presents the optimization of the CaptureSMB process.

#### 5.4.2.2. CaptureSMB optimization

An initial estimate of the loading velocity can be done by using the overall mass balance of sinapic acid (at  $t^*$ ) assuming 100% resin utilization and 100 % yield in column 1.

$$Q_{ic} \cdot C_f \cdot t_{ic} + Q_b \cdot C_f \cdot t_b = Q_{rr} \cdot C \cdot t_b \quad (5.17)$$

Where  $Q_{ic}$ ,  $Q_b$ ,  $Q_{rr}$  are the interconnected, batch and regeneration flow rates (m<sup>3</sup>/h),  $C_f$  is the product feed concentration (g/L).  $C$  is the product concentration at the exit of column 1, and  $t_b$  and  $t_{ic}$  are, respectively, the batch time and interconnected time (s).

With the assumption of 100% resin utilization, the right-hand side of equation (5.17) can be calculated with the isotherm, equation (5.4) and the resin volume. Assuming that the interconnected time is zero, equation (5.17) becomes:

$$Q_b \cdot C_f \cdot t_b = q_{SA,C_f} \cdot V_c \cdot (1 - \varepsilon_b) \quad (5.18)$$

$$A \cdot u_b \cdot C_f \cdot t_b = q_{SA,C_f} \cdot A \cdot L \cdot (1 - \varepsilon_b) \quad (5.19)$$

Where A is the cross-sectional area (m<sup>2</sup>) and L the column length (m),  $q_{SA,C_f}$  is the resin adsorption capacity at feed concentration, (g/L<sub>R</sub>). The batch time( $t_b$ ) is then equal to the regeneration time, which is defined with the elution protocol and flow rate.

$$t_b = t_{wash} + t_{elution} + t_{cip} + t_{equilibration} \quad (5.20)$$

$$t_b = \frac{CV_{rr} \cdot V_c}{Q_{rr}} = \frac{CV_{rr} \cdot A \cdot L}{A \cdot u_{rr}} \quad (5.21)$$

Combining equation (5.21) with (5.19), a maximum superficial velocity for the batch time can be estimated:

$$u_b^{max} = \frac{q_{SA,C_f} \cdot (1 - \varepsilon_b) \cdot u_{rr}}{C_f \cdot CV_{rr}} \quad (5.22)$$

Where  $CV_{rr}$  are the number of column volumes needed for washing, elution and regeneration. Note that equation (5.22) is a function of the feed concentration and the elution/regeneration velocity ( $u_{rr}$ ). The elution velocity ( $u_{rr}$ ) is independent of the column size and it was set to 80m/h. As  $t_b$  scales with column length, the maximum batch velocity is 205 m/h. The pressure drop calculated at this velocity is still lower than the mechanical resistance of resin FPX66, for the longest column.

Equation (5.17) indicates that the amount of sinapic acid captured in the system (both columns in batch and interconnected phase) should be lower or equal to the maximum capacity assuming that sinapic acid is not lost at the exit of column 2 during the interconnected and batch phase. This amount is equal to the product between the feed concentration, batch time and maximum flow rate, as expressed in equation (5.23).

$$A \cdot u_{ic} \cdot C_f \cdot t_{ic} + A \cdot u_b \cdot C_f \cdot t_b = A \cdot u_b^{max} \cdot C_f \cdot t_b \quad (5.23)$$

$$u_{ic} \cdot t_{ic} + u_b \cdot t_b = u_b^{max} \cdot t_b \quad (5.24)$$

Assuming that  $t_{ic}$  is equal to  $t_b$  and that the batch and interconnected velocities are similar, the resulting velocity would be half of the maximum loading velocity ( $u_b^{max}$ ). If  $u_{ic}$  and  $u_b$  are lower than  $u_b^{max}$ , it is clear that the interconnected time would always be higher than the batch time. With this analysis it is not possible to identify the upper limit of the interconnected superficial velocity or interconnected time. This is because it was assumed 100% resin capacity utilization, which might not be true. Nevertheless, an indication could be made if the length of the mass transfer zone is known. Using the model, the liquid concentration inside the column can be estimated at different superficial velocities up to 4% breakthrough. The results for a system with 6m columns (12m both columns connected) are shown in Figure 5.5.

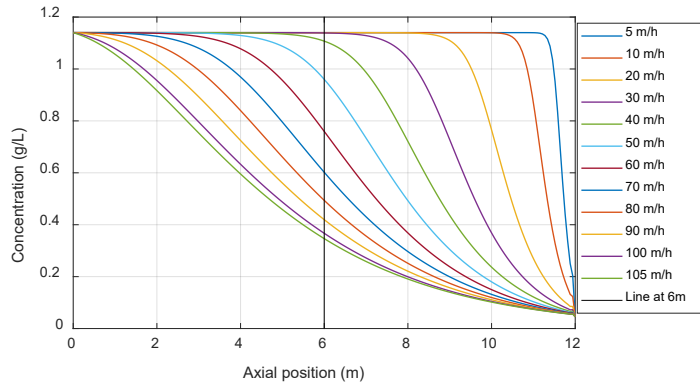


**Figure 5.5.** Product concentration profile inside the column at 4% breakthrough at different superficial velocities.

As can be seen (Figure 5.5), higher velocities shallow the concentration profiles up to a point where the velocity is so high that will achieve the 4% breakthrough in a very short time, resulting in an unrealistic interconnected phase. Using a 6m column system, interconnected velocities higher than 100 m/h would lead to lower resin utilization, and depending on the selected interconnected time, it might also affect yield.

Even though, the aforementioned analysis can help to identify the velocity boundaries in the CaptureSMB process, there is still one more variable to be optimized, the interconnected time.

Optimizing the interconnected time is not an easy task, as relatively short interconnected time might lead to lower resin utilization, while long interconnected time can compromise yield. Because of the breakthrough in the second column, thus causing product loss.

Figure 5.6 shows the relationship between productivity, yield and resin utilization (y axis) versus the interconnected time. Longer interconnected time benefits resin utilization but decreases the yield. It can also be seen that productivity increases with longer interconnected times due to the increase of resin utilization, however it starts decreasing when the yield is reduced due to product loss. Longer interconnected time will allow the product to reach the end of the second column and breakthrough. Product loss continues during the disconnected phase as the second column is continuously loaded with the feed at a lower flow rate. Therefore, in order not to compromise yield and still improve resin utilization, a trade-off between interconnected velocity and time should be found. In the case of the CaptureSMB system using 6m columns, the maximum productivity obtained is around 8.5 g/L<sub>R</sub>/h by operating the system at 80 m/h during the interconnected phase for 105 min. Even though the CaptureSMB system could be operated at lower interconnected velocities (Figure 5.5) to increase resin utilization, it will also require that the columns are connected for a longer period, and this might reduce productivity.

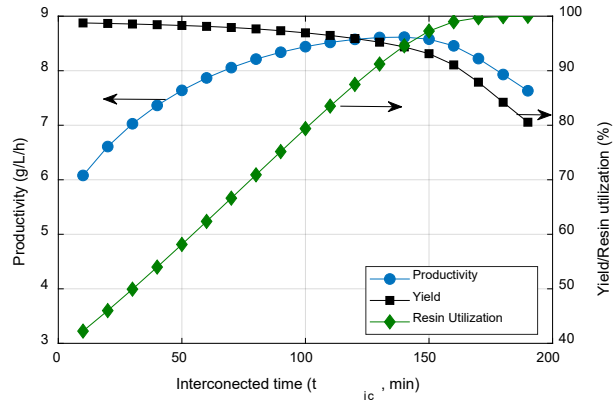


Figure 5.6. Productivity, Yield and Resin utilization vs interconnected time. CaptureSMB  $L_c=6m$ ,  $u_{ic} = 80$  m/h  $u_b=40$  m/h

Similarly to the 1-column process (batch process), the maximum achievable productivity decreases if the column length is higher, due to the much longer time needed to complete the elution and regeneration of the columns. The productivity values can be found in Table 5.4, where the highest is obtained with the CaptureSMB system with shortest columns. The opposite happens with resin utilization, which improves with higher column lengths. This might be attributed to mass transfer limitation, as the breakthrough curve of sinapic acid is relatively shallow which also allows the product to reach the exit of the second column relatively fast, which becomes more evident if the CaptureSMB system is short.

Table 5.4. Optimized parameters for batch (packed bed) and semi-continuous (CaptureSMB) processes to recover sinapic acid

	Batch process	Capture SMB 1	Capture SMB 2	Capture SMB3
Column length (m)	3 / 6 / 12	3	6	12
Interconnected time / Time switch (min)	533 *	85 / 119	105 / 173	120 / 255
Interconnected velocity, $u_{ic}$ (m/h)	10**/ 22** / 50	80	80	150
Batch velocity, $u_b$ (m/h)	N/A	10	40	68
Yield (%)	98	97	97	97
Productivity (g/L/h)	5.18	10.3	8.7	7.2
Resin utilization (%)	71	72	82	92
Product concentration (g/L)	3.8	3.8	4.2	5.1
Buffer consumption (L/g)	0.5	0.5	0.4	0.4

\* Batch cycle time \*\* Adsorption velocity

The optimized parameters for the batch (packed bed) and semi-continuous (CaptureSMB) process are shown in Table 5.4. In all evaluated column lengths, the productivity and resin utilization values are higher than the ones obtained for batch operation. The highest productivity value, accomplishing the yield condition of 97%, was found in the shortest column system ( $L_c = 3$  m) with a resin utilization of 72%. Increasing column size in the CaptureSMB process improves resin utilization, but as with the batch process, the productivity is reduced due to the increasing time of elution and regeneration steps at the same superficial velocity of 80 m/h.

## 5.5. Conclusions

This work demonstrates that the semi-continuous CaptureSMB process outperforms batch packed-bed operation for the recovery of sinapic acid, showing higher productivity, resin capacity utilization and lower buffer consumption without compromising yield. The obtained equilibrium information in combination with mechanistic models is a powerful tool to optimize process parameters, both in batch and semi-continuous mode. In addition, the validated model can be used as a predictive tool to evaluate performances at different column sizes. This methodology could be extended to recover similar molecules from voluminous food side streams using similar adsorbents, as it allows operating the purification process continuously, which is desired in the food sector as most of its operation is performed in continuous mode.

## 5.6. Acknowledgments

This work was supported by the ISPT (Institute of Sustainable Process Technology) under the project CM-20-07 in Adsorption of non-volatiles from food products. Thank you to the industrial partners DSM, Unilever, Friesland Campina and Royal Cosun for their valuable input through the project.

## 5.7. References

- 1 Galanakis C.M., Recovery of high added-value components from food wastes: Conventional, emerging technologies and commercialized applications, *Trends in Food Science & Technology*, 26 (2012) 68-87.
- 2 Bérot S., Compoin J., Larré C., Malabat C., Guéguen J., Large scale purification of rapeseed proteins (*Brassica napus* L.), *Journal of Chromatography B*, 818 (2005) 35-42.
- 3 Wanasundara J.P., Proteins of Brassicaceae oilseeds and their potential as a plant protein source, *Critical reviews in food science and nutrition*, 51 (2011) 635-677.
- 4 Fetzer A., Herfellner T., Stäbler A., Menner M., Eisner P., Influence of process conditions during aqueous protein extraction upon yield from pre-pressed and cold-pressed rapeseed press cake, *Industrial Crops and Products*, 112 (2018) 236-246.
- 5 Ganetsos G., Barker P., Developments in large-scale batch chromatography, in: G. Ganetsos, P. Barker (Eds.) *Preparative and production scale chromatography*, 1992, pp. 3-10.
- 6 Steinebach F., Muller-Spath T., Morbidelli M., Continuous counter-current chromatography for capture and polishing steps in biopharmaceutical production, *Biotechnology Journal*, 11 (2016) 1126-1141.

- 7** Aniceto J.P.S., Silva C.M., Simulated Moving Bed Strategies and Designs: From Established Systems to the Latest Developments, *Separation & Purification Reviews*, 44 (2015) 41-73.
- 8** Mazzotti M., Storti G., Morbidelli M., Optimal operation of simulated moving bed units for nonlinear chromatographic separations, *Journal of Chromatography A*, 769 (1997) 3-24.
- 9** Rajendran A., Paredes G., Mazzotti M., Simulated moving bed chromatography for the separation of enantiomers, *Journal of Chromatography A*, 1216 (2009) 709-738.
- 10** Rodrigues A.E., Pereira C., Minceva M., Pais L.S., Ribeiro A.M., Ribeiro A., Silva M., Graça N., Santos J.C., *Simulated Moving Bed Technology*, 1st Edition ed., Butterworth-Heinemann, Oxford, 2015.
- 11** Berg C., Hypersorption design - Modern Advancements, *Chemical Engineering Progress*, 47 (1951) 585-590.
- 12** Ganetsos G., Barker P.E., Semicontinuous countercurrent chromatography refineries, in: G. Ganetsos, P.E. Barker (Eds.) *Preparative and production scale chromatography* Marcel Dekker, Inc, New York 1993, pp. 233-255.
- 13** Johnson J.A., Kabza R.G., Sorbex: Industrial scale adsorptive separation, in: G. Ganetsos, P.E. Barker (Eds.) *Preparative and production scale chromatography*, Marcel Dekker, Inc, New York 1993, pp. 257-271.
- 14** Juza M., Mazzotti M., Morbidelli M., Simulated moving-bed chromatography and its application to chirotechnology, *Trends in Biotechnology*, 18 (2000) 108-118.
- 15** Godawat R., Brower K., Jain S., Konstantinov K., Riske F., Warikoo V., Periodic counter-current chromatography – design and operational considerations for integrated and continuous purification of proteins, *Biotechnology Journal*, 7 (2012) 1496-1508.
- 16** Warikoo V., Godawat R., Brower K., Jain S., Cummings D., Simons E., Johnson T., Walther J., Yu M., Wright B., McLarty J., Karey K.P., Hwang C., Zhou W., Riske F., Konstantinov K., Integrated continuous production of recombinant therapeutic proteins, *Biotechnology and Bioengineering*, 109 (2012) 3018-3029.
- 17** Ng C.K.S., Rousset F., Valery E., Bracewell D.G., Sorensen E., Design of high productivity sequential multi-column chromatography for antibody capture, *Food and Bioproducts Processing*, 92 (2014) 233-241.
- 18** Ludemann-Homburger O., Nicoud R.M., Bailly M., The “VARICOL” Process: A New Multicolumn Continuous Chromatographic Process, *Separation Science and Technology*, 35 (2000) 1829-1862.
- 19** Krättli M., Müller-Späth T., Morbidelli M., Multifraction separation in countercurrent chromatography (MCSGP), *Biotechnology and Bioengineering*, 110 (2013) 2436-2444.
- 20** Aumann L., Morbidelli M., A continuous multicolumn countercurrent solvent gradient purification (MCSGP) process, *Biotechnology and Bioengineering*, 98 (2007) 1043-1055.
- 21** Janakievski F., Glagovskaia O., De Silva K., Simulated Moving Bed Chromatography in Food Processing, in: K. Knoerzer, P. Juliano, G. Smithers (Eds.) *Innovative Food Processing Technologies*, Woodhead Publishing, 2016, pp. 133-149.
- 22** Costesso D., Rearick G., Kearney M.J.Z., Improved simulated moving bed process for purifying sugar solutions, 125 (2000) 333-335.

- 23** Xie Y., Chin C.Y., Phelps D.S.C., Lee C.-H., Lee K.B., Mun S., Wang N.-H.L., A Five-Zone Simulated Moving Bed for the Isolation of Six Sugars from Biomass Hydrolyzate, *Industrial & Engineering Chemistry Research*, 44 (2005) 9904-9920.
- 24** Freydel E.J., Bulsink Y., van Hateren S., van der Wielen L., Eppink M., Ottens M., Size-exclusion simulated moving bed chromatographic protein refolding, *Chemical Engineering Science*, 65 (2010) 4701-4713.
- 25** Ottens M., Houwing J., Van Hateren S.H., Van Baalen T., Van der Wielen L.A.M., Multi-Component Fractionation in SMB Chromatography for the Purification of Active Fractions from Protein Hydrolysates, *Food and Bioproducts Processing*, 84 (2006) 59-71.
- 26** Nam H.-G., Park C., Jo S.-H., Suh Y.-W., Mun S., Continuous separation of succinic acid and lactic acid by using a three-zone simulated moving bed process packed with Amberchrom-CG300C, *Process Biochemistry*, 47 (2012) 2418-2426.
- 27** Azevedo D.C.S., Rodrigues A.E., Fructose–glucose separation in a SMB pilot unit: Modeling, simulation, design, and operation, *AIChE Journal*, 47 (2001) 2042-2051.
- 28** Hashimoto K., Models for the separation of glucose/fructose mixture using a simulated moving-bed adsorber, *JOURNAL OF CHEMICAL ENGINEERING OF JAPAN*, 16 (1983) 400.
- 29** Hashimoto K., Continuous separation of glucose-salts mixture with nonlinear and linear adsorption isotherms by using a simulated moving-bed adsorber, *JOURNAL OF CHEMICAL ENGINEERING OF JAPAN*, 20 (1987) 405.
- 30** Müller-Späth T., Morbidelli M., Continuous Chromatography in Biomanufacturing\*, in: G. Subramanian (Ed.) *Continuous Biomanufacturing - Innovative Technologies and Methods*, Wiley-VCH, 2017, pp. 393-422.
- 31** Angarita M., Müller-Späth T., Baur D., Lievrouw R., Lissens G., Morbidelli M., Twin-column CaptureSMB: A novel cyclic process for protein A affinity chromatography, *Journal of Chromatography A*, 1389 (2015) 85-95.
- 32** Baur D., Angarita M., Müller-Späth T., Morbidelli M., Optimal model-based design of the twin-column CaptureSMB process improves capacity utilization and productivity in protein A affinity capture, *Biotechnology Journal*, 11 (2016) 135-145.
- 33** Moreno-González M., Girish V., Keulen D., Wijngaard H., Luteslager X., Ferreira G., Ottens M., Recovery of sinapic acid from canola/rapeseed meal extracts by adsorption, *Food and Bioproducts Processing*, 120 (2020) 69-79.
- 34** Bell J.M., Nutrients and Toxicants in Rapeseed Meal: a Review, *Journal of Animal Science*, 58 (1984) 996-1010.
- 35** Nićiforović N., Abramović H., Sinapic Acid and Its Derivatives: Natural Sources and Bioactivity, *Comprehensive Reviews in Food Science and Food Safety*, 13 (2014) 34-51.
- 36** Felinger A., Guiochon G., Comparison of the Kinetic Models of Linear Chromatography, *Chromatographia*, 60 (2004) S175-S180.
- 37** Carta G., Jungbauer A., *Protein chromatography: process development and scale-up*, John Wiley & Sons, 2010.
- 38** Silva M., Castellanos L., Ottens M., Capture and Purification of Polyphenols Using Functionalized Hydrophobic Resins, *Industrial & Engineering Chemistry Research*, 57 (2018) 5359-5369.

- 39** Muller-Spath T.e.a., Chromatographic process for enrichment and isolation, in, ChromaCon AG, United States, 2014.
- 40** Andersson N., Löfgren A., Olofsson M., Sellberg A., Nilsson B., Tiainen P., Design and control of integrated chromatography column sequences, *Biotechnology Progress*, 33 (2017) 923-930.
- 41** Gomis-Fons J., Löfgren A., Andersson N., Nilsson B., Berghard L., Wood S., Integration of a complete downstream process for the automated lab-scale production of a recombinant protein, *Journal of Biotechnology*, 301 (2019) 45-51.
- 42** Gomis-Fons J., Andersson N., Nilsson B., Optimization study on periodic counter-current chromatography integrated in a monoclonal antibody downstream process, *Journal of Chromatography A*, 1621 (2020) 461055.
- 43** McIlvaine T., A buffer solution for colorimetric comparison, *Journal of Biological Chemistry*, 49 (1921) 183-186.

## Appendix 5A. Process set up in chromatography station

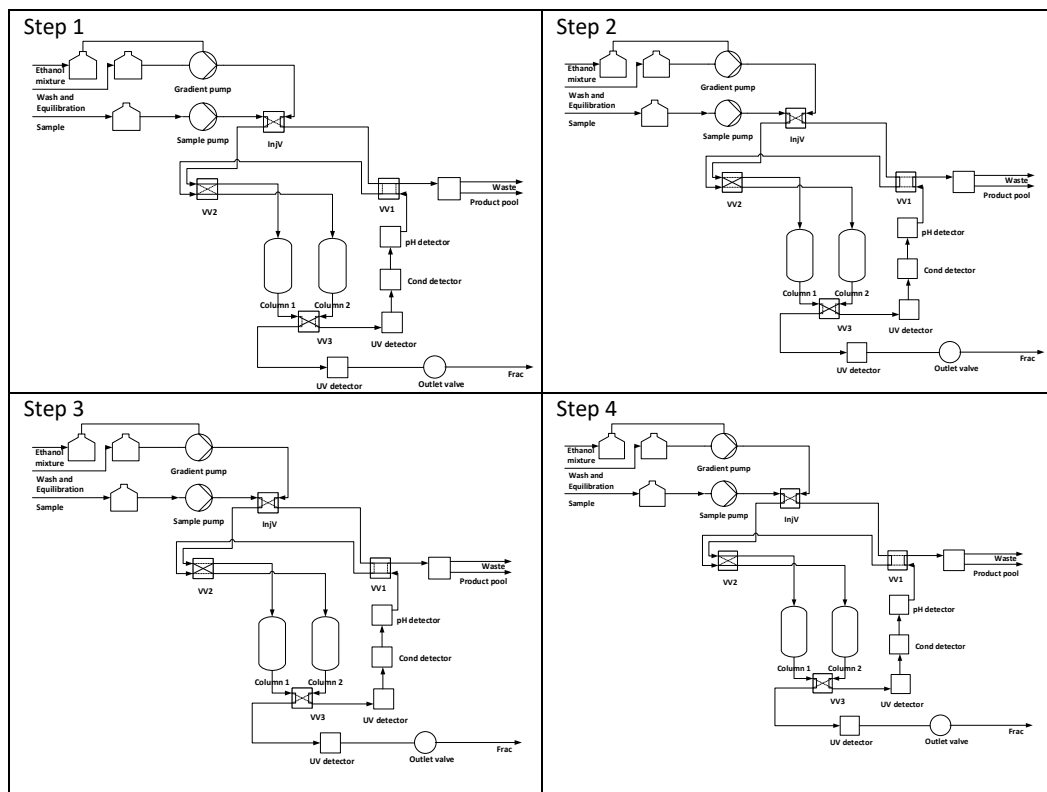
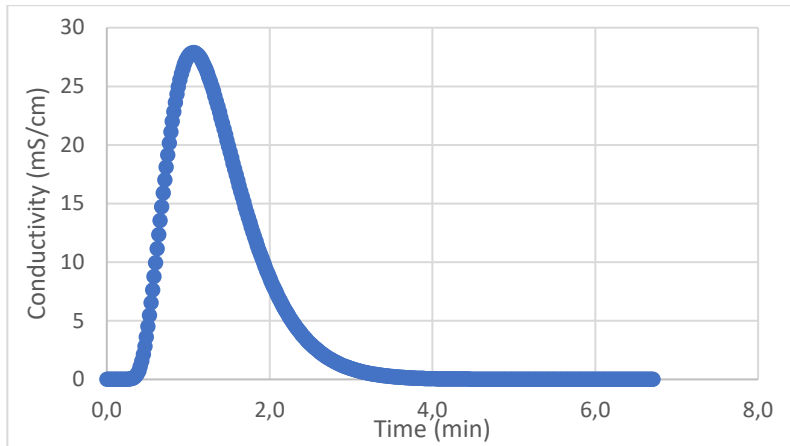


Figure 5.7. Process set-up for the implementation of CaptureSMB in Äkta Avant during process steps 1 to 4

## Appendix 5B. Bed porosity and intraparticle porosity

Extraparticle porosity was estimated with a trace pulse experiment using 50 $\mu$ l of NaCl 2M and accounting the dead volume of the system (0.36 mL). The results of this experiment are shown in Figure 5.8.



**Figure 5.8.** Pulse experiment with 2M NaCl. Column Volume 7.37 mL, at 2mL/min and room temperature.

The pulse was analyzed using the method of moments by calculating the mean residence time (first moment) using the following equation:

$$\tau_T = \frac{\int_{0+}^x C_T(t)tdt}{\int_{0+}^x C_T(t)dt}$$

Where  $C_T(t)$  is the conductivity detected by the presence of NaCl and  $t$  is the time. Here  $x$  is the time when the conductivity reaches the background signal value. The result of the numerical integration corresponds to 1.36 min, also observed in Figure 5.8, as the maximum peak height corresponds to this time. Multiplying the mean residence time by the flow rate results in the volume that the tracer flow through the column, 2.71 mL. This volume is corrected by subtracting the dead volume of the system. The extraparticle porosity can be calculated using the equation below:

$$\varepsilon_b = \frac{\tau_{T,NaCl} * Q_v - V_{dead}}{V_{column}} = \frac{2.71 \text{ mL} - 0.36 \text{ mL}}{7.37 \text{ mL}} = 0.32$$

The intraparticle porosity,  $\varepsilon_p$  was obtained using the difference between the weight of dry resin (after drying for 24 hours at 60 °C) and wet resin. This corresponds to the pore weight, which can be changed to volume using the density of the solvent used to wet the resin (ethanol). The pore volume divided by the amount of wet resin is the pore volume per gram of wet resin (ml/g). The intraparticle porosity in the column was therefore estimated by multiplying the pore volume per gram of resin times the amount of resin packed and dividing by the total column volume.

$$\begin{aligned}\varepsilon_p &= \frac{\text{Total } V_{\text{pore}}}{\text{Total } V_c} = \frac{\text{mL void per gram of resin } \left(\frac{\text{mL}}{\text{g}_R}\right) * \text{total packed resin } * (\text{g})}{\text{Column volume (mL)}} \\ &= \frac{0.82 \left(\frac{\text{mL}}{\text{g}_R}\right) * 5.04 (\text{g}_R)}{7.373 \text{ mL}} = 0.56\end{aligned}$$

Total porosity can be finally estimated using:

$$\varepsilon_t = \varepsilon_b + (1 - \varepsilon_b) * \varepsilon_p = 0.32 + (1 - 0.32) * 0.56 = 0.70$$

## Appendix 5C. CaptureSMB Lab scale simulation results

Concentration profiles of sinapic acid are shown in Figure C1. Note that steady state is accomplished after the first time switch due to the start-up phase. The start-up phase corresponds to the start of the CaptureSMB cycle, when no product is preloaded. The flow rate in this phase is equal to the interconnected flow rate and the time duration of the phase can be calculated as suggested by Angarita, et al.<sup>31</sup> knowing the breakthrough moments at that specific flow rate at a certain column length and when both columns are connected.

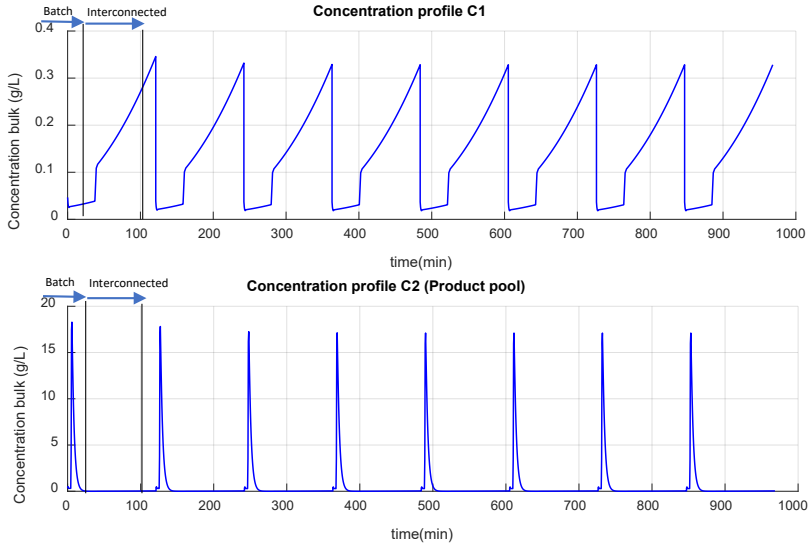


**Figure 5.9.** Sinapic acid concentration profile following the batch and interconnected phase in both columns. Note that columns exchange positions in each switch. Upper figure: breakthrough curve, the breakthrough of the column 1 during the interconnected phase is captured in the next column. Lower figure: product pool in column 2.

Figure 5.10 shows the concentration profile inside the column at the connected and disconnected phases. The upper figures present the concentration profile of the two columns at the end of the batch phase, where the upper-left figure shows a fully regenerated column with no product left, and the upper-right figure shows the pre-load of sinapic acid. The lower figures show the concentration profile at the end of the interconnected phase.

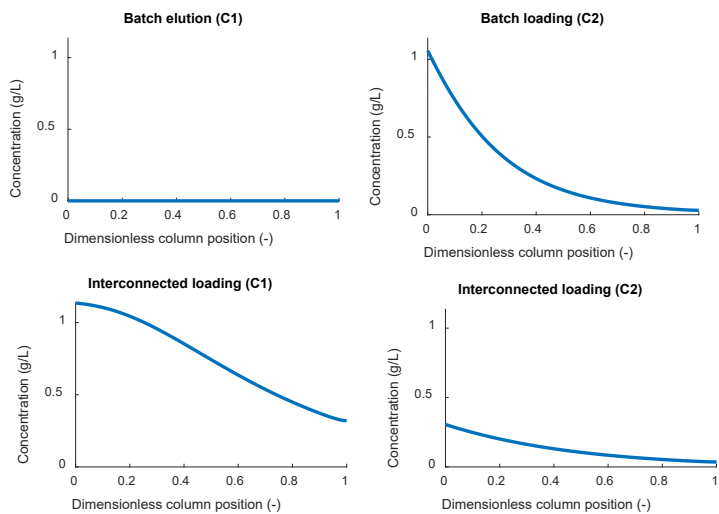


**Figure 5.10.** Concentration profiles of sinapic acid in CaptureSMB system during the disconnected phase (top figures) and connected phase (lower figures). Column dimensions 1cm i.d x 4.5 cm h.

## Appendix 5D. Performance indicators

Productivity is defined as the amount of product that can be produced per unit of time and resin volume.

For the batch process productivity was calculated as

$$\text{Productivity (g/L}_{\text{resin}}/\text{h)} = \frac{M_{\text{product}}}{V_c(1 - \varepsilon_b)t_{\text{batch}}}$$

For the CaptureSMB process productivity was calculated as:

$$\text{Productivity (g/L}_{\text{resin}}/\text{h)} = \frac{M_{\text{product}}}{nV_c(1 - \varepsilon_b)t_{\text{cycle}}}$$

Where  $M_{\text{product}}$  is the mass of product, note that  $M_{\text{product}}$  excludes the product lost in the breakthrough of the column 2 and the product lost during the washing step.  $V_c$  is the volume of the column,  $n$  the number of columns,  $t_{\text{cycle}}$  the total time for obtaining the product including the adsorption, desorption and regeneration time.  $\varepsilon_b$  is the bed porosity. The cycle time is equal to one-time switch, including the interconnected and batch time.

The buffer consumption takes into account the consumed buffer amount for the elution of the product and the regeneration period.

$$\text{Buffer consumption (L/g)} = \frac{V_{\text{buffer}}}{M_{\text{product}}}$$

Where  $V_{\text{buffer}}$  is the amount of buffer used for the elution of the product and the regeneration of the column.

The capacity utilization defines the actual load per cycle divided by the maximum possible load.

$$\text{Capacity utilization(\%)} = \frac{M_{\text{product}}}{V_c(1 - \varepsilon_b)q_{\text{ads}}} * 100$$

Where,  $q_{\text{ads}}$  is equal to the maximum theoretically possible amount that can be loaded per column volume for a certain feed concentration and can be calculated with the isotherm.

Product concentration is calculated

$$\text{Product concentration(g/L)} = \frac{M_{\text{product}}}{V_c CV_{\text{elution}}}$$

Where  $CV_{\text{elution}}$  are the number of column volumes used for elution.

## Appendix 5E. CaptureSMB input parameters

The model requires equilibrium information to perform the simulation. Sinapic acid isotherm on resin FPX66 was determined in previous work,<sup>33</sup> and used as input data for column simulations. A summary of the equilibrium parameter, column dimensions and liquid mobile phase properties is shown in the table below:

**Table 5.5.** Simulation parameters

Adsorption parameters		
<b>H (affinity constant)</b>	L/L <sub>resin</sub>	138.00
<b>q<sub>max</sub></b>	g/mL	105.20
<b>Bed characteristics</b>	Unit	
<b>Diameter</b>	m	0.01 and 1
<b>Height</b>	m	0.045, 3.00, 6.00, 12.00
<b>Total porosity</b>	-	0.70
<b>Extraparticle porosity</b>	-	0.32
<b>Intraparticle porosity</b>	-	0.56
<b>Resin Characteristics (FPX66)</b>		
<b>Particle diameter</b>	m	6.75E-4
<b>Pore size</b>	m	2.50E-8
<b>Pressure limit</b>	kPa/m	226.00
<b>Mobile phase characteristics</b>		
<b>Density</b>	kg/m <sup>3</sup>	1000.00
<b>Viscosity</b>	Pas	8.90E-4

## Appendix 5F. Industrial scale batch and semi-continuous optimization

Figure F1 shows the concentration profile of the CaptureSMB process at different column lengths using the optimum operating parameters. Higher resin utilization can be achieved at a higher column length. Similarly as in Figure C2, upper figures show the profile at the end of the batch phase while lower figures show the concentration profile at the end of the interconnected phase.

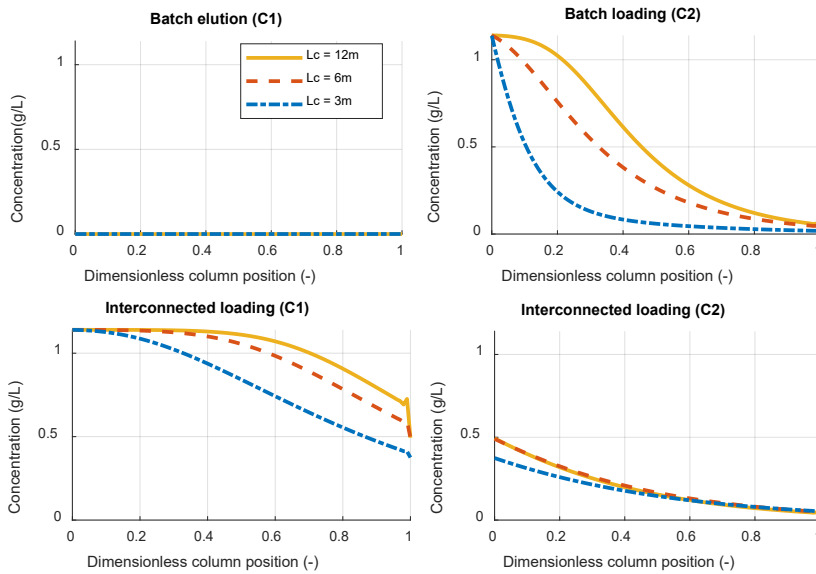


**Figure 5.11.** Column concentration profiles at industrial scale (different column length 3m,6m and 12m) at the end of the batch phase (top figures) and interconnected phase (lower figures).



# Chapter 6

## Upgrading food industry side streams: A techno-economic analysis to remove off-flavors

---

### Abstract

Side streams from food industry are rich sources of dietary fiber, natural antioxidants, biopolymers, and natural food additives. Currently these types of streams are discarded as waste or used as animal feed, which underestimates its potential as sources of valuable products.

This work presents a process design for the upgrading of an agricultural wastewater stream to produce a flavored powder extract. The critical step of the process is the removal of off-flavor components (aldehydes, ketones, furans, carboxylic acids) as they have a significant impact on the quality of the product. Adsorption has proven to be a very effective technology to *capture* valuable components (Chapter 3 and Chapter 4) that can be adapted to continuous operation (Chapter 5). In this work it was evaluated on its technical and economic merits in the *removal* of unwanted components from industrial agri-food side streams, i.e. off flavor removal.

The designed process was simulated using the flow-sheeting program SuperPro Designer, considering a production capacity of 12 kton/year of flavored powder. Required operation units involve, chemical precipitation, centrifugation, evaporation, catalytic conversion, adsorption and drying. The economic analysis indicates that by selling the product at 2.7€/kg, a payback time of around 5 years is obtained at a 20% return of investment (ROI). In addition, the environmental impact was evaluated with a E-factor calculation resulting in a E-factor value of 1.1, which is within the expected range for bulk chemical products. This indicates that a relatively low amount of waste is generated per kg of product and therefore contributes to a decrease of waste generation.

This work demonstrates the potential of using side streams to generate a high-value product.

**Keywords:** Food side stream processing, conceptual process design, process economics, natural ingredients, off-flavor removal.

## 6.1. Introduction

The potential of food side streams to create new opportunities and markets has been underestimated until very recently. However, consumers' consciousness about environmental issues and legislative pressures increases the requirements of new methods for the recovery of food waste, rather than its disposal<sup>1</sup>. Further, these co-streams are inexpensive, affordable, and a valuable starting material for the extraction of value-added products such as dietary fibre, natural antioxidants, biopolymers, and natural food additives<sup>2</sup>. Recent studies<sup>3,4</sup> have demonstrated that production of bulk or fine chemicals from these streams is more profitable and might contribute not only to reduce waste but also to a more circular economy.

Bran, oilseed meal, vegetable and fruit processing wastewater are typical side streams from plant-based products. A major technological challenge presented on the utilization of these side streams, particularly wastewater, is the presence of solids and the removal of low value products such as pigment and off-flavors (defined as unpleasant odors and tastes<sup>5</sup>), therefore effective separation techniques should be applied.

This work presents the technical and economic feasibility of processing an agricultural liquid side stream for the generation of a flavored powder extract. The critical step in this process is to remove off-flavors, as they have a direct impact on the quality of the product. This is a natural product as it originates from wastewater from a plant-based product processing. Typically, off-flavors are generated during food processing by lipid oxidation and as products of the Millard reaction (MR).<sup>6</sup> Amongst the off-flavor compounds presented in the evaluated vegetable stream, the significant Millard reaction products (MRPs) are: carboxylic acids, furans and aldehydes. These MRPs should be removed as they affect the taste of the final food product. The concentration levels at which these off-flavors are present in liquid streams is in micrograms per liter<sup>7</sup> level and many of them are highly hydrophobic (aldehydes, furans medium chain fatty acids). Adsorption, using hydrophobic resins has been proven to be an effective technology to selectively capture organic molecules (Chapter 3<sup>8</sup>) and off-flavors<sup>7,9</sup> and therefore is considered as a promising technique for the removal of these impurities.

The conceptual process design was evaluated following the first three steps of the Stage-Gate<sup>TM</sup> Product-Development Process<sup>10</sup> strategy. The study begins by specifying the different process assumptions and constraints associated with the characteristics of the final powder, followed by selecting the different operation units and the process sequence. Adsorption, using an hydrophobic resin was chosen as a selective technology to remove off-flavors (following the methodology suggested in Chapter 3<sup>8</sup> for resin selection and adsorption equilibrium estimation). A conceptual process design, using the selected unit tasks, was implemented in SuperPro Designer (Intelligen, Inc., USA version 10), to solve the different mass and energy balances.

Adsorption column and catalytic reactor were modelled using thermodynamic models and equilibrium information from literature or experimentally obtained. The identified operating parameters were later implemented in SuperPro Designer to perform process simulations. Finally, economic evaluation was performed to identify process feasibility and environmental impact, which was assessed through an E factor calculation.

## 6.2. Materials and Methods

Process design was evaluated using engineering software such as SuperPro Designer and Matlab R2017b (MathWorks, Inc. USA). Mechanistic models for adsorption and catalytic reactor were coded in Matlab and used for designing the corresponding unit operations (see section 6.2.4 Thermodynamic models ) and equipment sizing.

### 6.2.1. Process Assumptions

Natural food ingredients can be recovered and purified from side streams generated during the manufacturing of food products. The side stream here evaluated is assumed to be a wastewater stream from the processing of pulses. This wastewater contains flavor components (amino acids and nucleotides) to be purified from a number of impurity substances in which stand out off-flavor components (carboxylic acids, aldehydes, ketones). Concentration of this off-flavors is typically on ppm levels.<sup>11</sup> Adsorption is used as a selective technology for the removal of the off-flavor components.

The estimated composition of the side stream is shown in Figure 6.1. It is assumed that the initial stream contains 11% (w/w) solids and an initial water content of 82% (w/w).

The downstream processing will operate in a continuous mode. In order to perform characteristically batch operations like adsorption in continuous mode, multiple columns will be used. The columns will be operated in a synchronized way depending on the adsorption cycle. While one column is loaded and washed, another one is eluted and regenerated.

The final product is intended to be recovered as a solid powder. Among the different technologies to obtain solid products, spray drying is commonly used in milk powders and for encapsulation of food ingredients.<sup>12</sup> For the final extract, the valuable compounds will be microencapsulated in maltodextrin (most applied matrix wall material in spray drying<sup>12</sup>).

### 6.2.2. Process definitions

It is assumed that a year of operation corresponds to 3600 hours as most of the food products are produced depending on growing agricultural seasonality. In addition, the generated liquid side stream will have a mass flow rate of ~ 27.0 MT/h (27 m<sup>3</sup>/h).

For process design, the following constraints were set:

1. Product yield  $\geq$  85%
2. Water and ethanol are the only solvents to be used (food grade solvents)
3. Off-flavor removal based on the specifications presented in Table 6.1.
4. The final dry extract (formulation) is encapsulated in 50% maltodextrin.

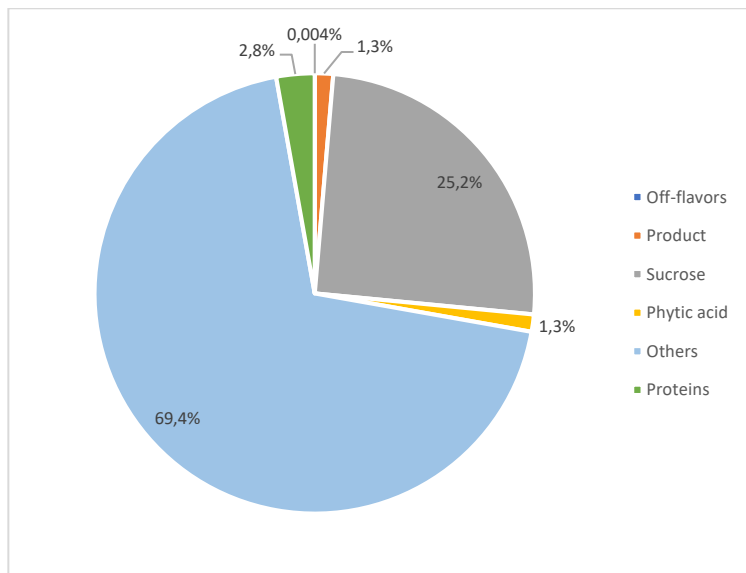


**Figure 6.1.** Stream Composition (dry weight)

**Table 6.1.** Off-flavor concentration of liquid stream after resin treatment.

Compounds	Concentration [ $\mu\text{g/L}$ ]
<b>Hexanal</b>	<1
<b>2-Pentylfuran</b>	<0.5
<b>Acetoin</b>	<12000
<b>Nonanal</b>	<1
<b>Butanoic acid</b>	<1200
<b>Isovaleric acid</b>	<300

### 6.2.3. Design Approach

Conceptual process design was done following the methodology described in Harmsen, et al.<sup>13</sup> which is based on the first three steps of the Stage-Gate™ Product-Development Process<sup>10</sup>. It consists of: 1) a concept-stage, 2) a feasibility-stage and 3) a development-stage.<sup>10</sup>

The concept stage, where the product and the business case are presented, was defined together with the project partners (described in sections 6.2.1 and 6.2.2). In the feasibility stage a flow diagram was defined and different technologies for each unit task were assessed in order to select the most suitable one. This assessment was done by defining a decision table for each unit task. Ranking criteria such as operation efficiency, scalability, operational costs and environmental impact were ranked based on importance. The ranking was defined in collaboration with process design experts and project partners<sup>13</sup> (TU Delft). The different decision matrixes can be found in Appendix 6A. Selection of Unit Operation.

Once the required operation units were selected, the development-stage was evaluated with a conceptual design of the production process, including equipment sizing and profitability analysis. This was done using engineering software, SuperPro Designer and Matlab R2017b.

#### 6.2.4. Thermodynamic models

The required mass and energy balance for the catalytic reactor and the adsorption column were obtained by using mechanistic models. The following section describes both models.

##### 6.2.4.1. Plug-flow modeling

The mass balance of the substrate at steady state ( $dC/dt=0$ ) is expressed in equation (6.1):

$$0 = u_s \frac{dC_s}{dz} - r_s \quad (6.1)$$

Where  $C_s$  is the bulk liquid substrate concentration ( $\text{mol}/\text{m}^3$ ),  $z$  is the axial position (m),  $u_s$  is the superficial velocity (m/s) and  $r_s$  is the reaction rate ( $\text{mol}/\text{m}^3 \text{ s}$ ). Radial dispersion is neglected, as it is assumed that it is much smaller compared to axial dispersion (a  $L/D > 5$  was assumed for sizing). This assumption also holds when small catalyst particles are used. Note that additionally axial dispersion is also assumed to be not significant.

Equation (6.1) is subject to the following initial condition

$$C_s = C_{s0} \text{ at } z = 0$$

The considered reaction rate follows Michaelis-Menten kinetics, as expressed in equation (6.2)

$$r_s = \frac{v_{max} C_{si}}{K_m + C_{si}} \quad (6.2)$$

where  $v_{max}$  is the maximum reaction rate ( $\text{mol}/\text{m}^3 \text{ s}$ ),  $C_{si}$  is the substrate concentration on the surface of the catalyst and  $K_m$  is the Michaelis-Menten constant ( $\text{mol}/\text{m}^3$ ).

The mathematical model suggested by Olafadehan, et al.<sup>14</sup> was adapted to the conversion in this study. The transport of the substrate from the bulk liquid to the catalyst interface compensates its consumption<sup>14</sup>. Assuming no partitioning, the transport equation is expressed next:

$$\begin{aligned} r_s &= k_f a (C_s - C_{si}) \\ a &= 6 * (1 - \varepsilon_b) / d_p \end{aligned} \quad (6.3)$$

where  $k_f$  is the film mass transfer coefficient (m/s) and  $a$  is the surface area of the particle per volume of packed bed.  $\varepsilon_b$  is the bed porosity, and  $d_p$  is the particle diameter (m). The film mass transfer coefficient ( $k_f$ ) was estimated using the Wilson-Geankoplis correlation for packed beds<sup>15</sup>.

$$k_f = D_f Sh / d_p \quad (6.4)$$

where  $D_f$  is the free diffusivity of the substrate ( $\text{m}^2/\text{s}$ ),  $Sh$  is the Sherwood number. The free diffusivity of the substrate was calculated using the Wilke-Chang correlation <sup>16</sup>.

Equation (6.1) was solved using Matlab R2017b and the ode solver *ode15s*.

#### 6.2.4.2. Adsorption column

The equilibrium-transport-dispersive chromatography model in combination with the liquid-film linear driving force approximation is used to describe the dynamic adsorption of one column (equation (6.5)).

$$\frac{\partial C_i}{\partial t} + F \frac{\partial q_i}{\partial t} + v \frac{\partial C_i}{\partial z} = D_L \frac{\partial^2 C_i}{\partial z^2} \quad (6.5)$$

where  $C_i$  represents the bulk liquid concentration ( $\text{g/L}$ ) of component  $i$ ,  $v$  is the interstitial velocity of the mobile phase ( $\text{m/s}$ ) defined as superficial velocity divided by the bed porosity ( $u_s/\epsilon_b$ ),  $q_i$  is the stationary phase concentration of component  $i$  ( $\text{g/L}_R$ ),  $F$  is the phase ratio defined as  $F = (1 - \epsilon_b)/\epsilon_b$ , where  $\epsilon_b$  is the bed porosity, and  $D_L$  is the axial dispersion coefficient ( $\text{m}^2/\text{s}$ ). The solid stationary phase concentration term  $\frac{\partial q}{\partial t}$  is defined according to equation (6.6). The lumped kinetic model was used for column modeling. This model assumes that the mobile phase concentration in the pores and between the particles is the same,<sup>17</sup> therefore a separate mass balance for the pores is not required.

$$\frac{\partial q_i}{\partial t} = k_{ov,i}(C_i - C_{eq,i}^*) \quad (6.6)$$

The model lumps the internal and external mass transfer resistances into an overall mass transfer coefficient  $k_{ov,i}$  ( $1/\text{s}$ ) which is defined as in equation (6.7).

$$\frac{1}{k_{ov,i}} = \frac{d_p}{6k_f} + \frac{d_p^2}{60\epsilon_p D_p} \quad (6.7)$$

where  $d_p$  is the particle diameter ( $\text{m}$ ),  $k_f$  is the film mass transfer coefficient ( $\text{m/s}$ ),  $\epsilon_p$  is the intraparticle porosity and  $D_p$  is the pore diffusivity ( $\text{m}^2/\text{s}$ ).  $D_L$  and other relevant model parameters were calculated using different mass transfer correlations as described in Moreno-González, et al.<sup>8</sup>. The equilibrium concentration  $C_{eq,i}^*$ , is calculated using a linear isotherm (equation (6.8))

$$q_i = H_i C_{eq,i}^* \quad (6.8)$$

where  $q_i$  is the adsorption capacity ( $\text{g/L}_R$ ),  $H_i$  is the isotherm slope. Equilibrium parameters were obtained using batch adsorption experiments (following the methodology described in Chapter 3<sup>8</sup> and Chapter 4, see Appendix 6C. Adsorption) and the vegetable side stream. All the components expressed a linear behavior at feed conditions (pH 6.4 and room temperature), which could indicate that they do not affect each other adsorption<sup>18</sup>, therefore, they could be treated as independent components..

In order to include the isotherm slope dependency on the modifier concentration a power function was used as described elsewhere<sup>8,19</sup> giving  $H_i = \alpha * (C_{mod} + 1)^{-\beta}$ , where  $\alpha$  is the isotherm slope at feed conditions ( $H_i$ ) and  $\beta$  is an empirical parameter. The equilibrium parameters, used for modeling of the adsorption column can be found Appendix 6C. Adsorption.

Equation (6.5) was discretized in space using the method of lines<sup>20</sup> in order to convert this partial differential equation into an ordinary differential equation (ODE) for each component. The corresponding boundary conditions for inlet and outlet are described by the Dankwerts boundary conditions for dispersive systems. It is assumed that the columns are not preloaded (free of components, at  $t=0$   $q_i = 0$ ). The system of ODEs was solved using the ode solver *ode15s* from Matlab R2017b.

### 6.2.5. Equipment sizing

The equipment required in this process was sized using the engineering software SuperPro Designer (Intelligen, Inc., USA version 9.5) with the exception of the plug flow reactor and the adsorption column, modelled in Matlab. SuperPro Designer was used for solving mass and energy balances of the process.

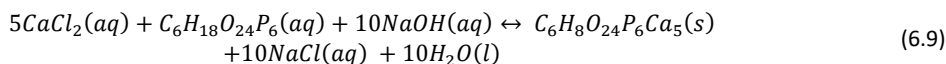
In order to size and design each equipment, additional information is required based on each unit operation. This section describes the information used for each equipment.

#### 6.2.5.1. Continuous Stirred Tank Reactors (CSTR)

##### *Phytic acid removal*

Phytic acid (phytate anion) can bind to different mineral cations and form an insoluble salt (phytate). The choice for this chemical agent lies on several process specific aspects like pH of the medium. In this study, calcium chloride ( $\text{CaCl}_2$ ) is used as precipitating agent.

The precipitation reaction was defined based on literature<sup>21-24</sup> and it is shown in equation (6.9). This equation was used to calculate the required amount of  $\text{CaCl}_2$  and NaOH.



The excess of calcium ions, in relation with phytic acid, will promote the formation of phytate precipitate<sup>21</sup> therefore, a molar ratio of 7 was assumed. The reaction was set to be adiabatic and at room temperature (25 °C). Forty-five (45) mins of reaction time were specified.

In addition, as precipitation depends on pH<sup>21</sup>, the required amount of NaOH needed to reach a value of pH 6.4 was calculated based on the dissociation reaction of NaOH and water and the concentration of hydrogen ions.

Reactor volume was finally estimated assuming 90% equipment occupancy and considering the volumetric inlet flow rate and residence time.

## 6.2.5.2. Disc-stack centrifuge

It was assumed that the cake formed during centrifugation contains 20% moisture. The removal of particulate was set to 100% for insoluble solids, 95% of phytate and 1% of the other components presented in the stream. For this operation an Alfa-Laval VO 30 centrifuge was chosen. In SuperPro Designer, the selected sizing option was based on the throughput, specifying a maximum throughput of 20 m<sup>3</sup>/h (data from supplier).

## 6.2.5.3. Multi-effect Evaporator

In order to design the evaporator in SuperPro Designer, sucrose was selected as the key component, which should be concentrated 3.4 times. The main component evaporated is water. The selected temperature at the exit of the last effect was set to 40 °C. The estimated heat transfer area corresponds to 35.9 m<sup>2</sup>.

## 6.2.5.4. Plug-flow reactor

The catalyst used in the conversion reaction for product formation is a soft media with average particle size of 5.5x10<sup>-3</sup> m. A maximum pressure drop of 2 bar was assumed.

To neglect axial and radial effects in the column, an aspect ratio (L/D) of 10 was defined. Sizing of the column was done for a 99.5% conversion (exit at the plug-flow reactor) and considering the inlet flow rate and pressure drop. A column of 0.4m diameter and 4 m length was designed.

Pressure drop was estimated using the Ergun equation (equation (6.10)) corresponding to 0.11bar.

$$\Delta P = \frac{u_s(1 - \varepsilon_b)}{d_p \varepsilon_b^3} \left[ 150 * \frac{L \mu (1 - \varepsilon_b)}{d_p} + 1.75(\rho_L u_s) \right] \quad (6.10)$$

Where  $\mu$  and  $\rho_L$  are the viscosity and density of the mobile phase respectively. Column dimensions and residence time (calculated based on the superficial velocity) were defined in SuperPro Designer and a reaction temperature of 60 °C was set in order to determine energy requirements.

## 6.2.5.5. Ultrafiltration

Ultrafiltration module was sized in SuperPro Designer. This was done by defining an operation procedure, consisting in washing step with water (15 min) followed by the concentration step (2h) and a cleaning in place using NaOH 1M (15min)

The default value of 80 m<sup>2</sup> of maximum membrane area was kept and a flux of 20 L/m<sup>2</sup>/h was defined. A 90% of the permeate was set to be recovered, this because the valuable compounds and off-flavors are small molecules that can permeate the membrane. To continuously operate this section, 7 ultrafiltration modules are required with a membrane area of 76.5 m<sup>2</sup>.

#### 6.2.5.6. Adsorption column

Operation of the adsorption is performed in flow-through mode, which means that the valuable compounds are not adsorbed to the resin. The product stream is then collected from the loading and washing steps of the adsorption cycle. The adsorption cycle can be found in Appendix 6C. Adsorption.

Resin XAD16N was selected as the most suitable resin for capturing of the off-flavor components (Moreno-González, unpublished data). Performance indicators such as, productivity of valuable compounds ( $\text{g/L}_{\text{resin}}/\text{h}$ ), valuable compound yield (see Appendix 6C. Adsorption), which is intended to be  $> 97\%$  in this unit, were defined for optimization. As different off-flavors are presented in the stream, a design component was selected. This corresponds to the off-flavor component with the weakest interaction with the resin.

Column dimensions were defined considering that there is a specific residence time that maximizes productivity.<sup>25</sup> An additional constraint of meeting off-flavor specifications was set. A maximum pressure drop of 10 bar was specified, as the resin beads are rigid particles.

Column dimensions corresponds to 0.85m diameter and 2m column length.

Pressure drop was estimated using the Ergun equation (equation (6.10)) corresponding to 0.38 bar.

The current process is operated in continuous mode. In order to run the adsorption step continuously, two columns could be used. While one column is loaded with the feed and washed, the other one is eluted, regenerated and re-equilibrated. This is possible because the adsorption step last longer than desorption due to the different superficial velocities applied during loading/ washing and elution/regeneration (see Appendix 6C. Adsorption). To satisfy the demand a third column is needed for operation.

#### 6.2.5.7. Distillation column

Ethanol/water mixture (50 % w/w) is used in the adsorption step to regenerate the column. Ethanol is recovered by distillation. At the required concentration, ethanol/water does not form an azeotrope, therefore only one distillation column is needed. The column was designed in SuperPro Designer by specifying the composition in the distillate and the reflux ratio (1.3).

#### 6.2.5.8. Spray Drying

Spray drying was designed in SuperPro Designer by defining an evaporation rate of  $100 \text{ (kg/h)/m}^3$  and setting a final LOD (loss of drying) of 5%. An aspect ratio (L/D) of 3 was assumed. The spray dryer dimensions correspond to  $85 \text{ m}^3$  volume with a diameter of 3.3 m. The drying capacity is  $8449.3 \text{ kg/h}$ .

#### 6.2.5.9. Holding tanks

Holding tanks are required in order to collect the liquid before and after the units that operate in batch mode such as the adsorption column. Sizing of the holding tanks was done using the methodology applied by Henriques da Silva<sup>26</sup>. Briefly this methodology takes into account the outlet continuous flow rate, which is a function of the incoming flow rate given for a certain period of time and the holding time.

Assuming that 90% of maximum equipment occupancy and a 20% of minimum equipment occupancy, the volume of the holding tanks can be estimated using equation (6.11).

$$V = \frac{Q_{out} \cdot t_{hold}}{0.7} \quad (6.11)$$

Where  $V$  is the volume ( $m^3$ ),  $F_{out}$  is the outlet flow-rate ( $m^3/h$ ) and  $t_{hold}$  in the holding time (h).

#### 6.2.6. Economic evaluation

The economics of the selected process design were estimated using well-known methodologies.<sup>27-29</sup> Purchased equipment cost (PEC) was obtained from equipment cost correlations,<sup>28</sup> cost databases (Matches, [www.matche.com](http://www.matche.com)) and DACE<sup>30</sup>. The price of the adsorption column was calculated using the price correlation suggested in Peskin, et al.<sup>31</sup> (plus the cost of the peripherals assumed to be 25 k€<sup>31</sup>). Equipment cost was corrected to the current year using the chemical engineering plant cost index (CEPCI) and is expressed in euros using a conversion factor of 1.13\$/€.

The capital investment was estimated by determining the direct fixed capital (DFC), working capital and start-up cost. DFC was estimated based on the total equipment cost using different multipliers<sup>29</sup> (see Appendix 6D. Economic evaluation), working capital was considered to be 15% of DFC and start-up & validations cost was assumed to be 20% of DFC<sup>29</sup>. As the goal is to upgrade an agricultural side stream, from a current production facility, it is assumed that the equipment will be installed in the same facility. Therefore, the cost of the land is not considered as part of the capital investment, neither the cost of the agricultural stream as raw material.

Total operating expenditure (OPEX) estimation was done considering raw material, utilities, consumables, labor, laboratory QC/QA, waste disposal and facility overhead. Raw material costs were estimated using data from literature<sup>29</sup>, for common chemicals, icis ([www.icis.com](http://www.icis.com)) and suppliers. Consumables price, namely the price of the adsorbent XAD16N was considered to be 50 \$/Kg, as the price of polymeric resins used for small biomolecules purification is generally under 100 \$/Kg<sup>29</sup>. Membrane cost was assumed to be 50 \$/m<sup>2</sup> as suggested by Harrison, et al.<sup>29</sup>. Utilities, electricity, steam, chilled water and cooled water, were obtained based on the mass and energy balances from the process simulation in SuperPro Designer and the price was assumed to be the one specified by this flow-sheeting program. Labor cost was assumed to be €50/h, as this process operates in continuous mod, 3 operators were assumed to be at all time. 20% of labor cost was considered for laboratory. Wastewater disposal and solid waste were assumed to be 0.5\$/m<sup>3</sup> and 50\$/MT as suggested by Harrison, et al.<sup>29</sup>. Detailed estimation of facility overhead can be found in Appendix 6D. Economic evaluation.

The minimum selling price of the product was estimated for a return of investment (ROI) of 20% (often desired by companies) assuming a venture profit (VP) of zero, as described in Seider, et al.<sup>27</sup>. The project life time is assumed to be 10 years. A discounted cash flow analysis was done considering a MACRS (Modified Accelerated Cost Recovery System) depreciation for a 5-year class life, a 15% nominal interest<sup>27</sup>, and the determined selling price. At the end the investor's rate of return (IRR) was additionally calculated.

### 6.3. Results and discussion

The process flow diagram generated in SuperPro Designer can be found in Figure 6.2. The processing of the side stream starts with the removal of phytic acid. Phytic acid is thought to have a negative impact in human health due to its ability to strongly bind to mineral ions such as magnesium and calcium. This antinutritional component is often found in plant-based products such as oilseed and pulses.<sup>32</sup>

Removal of phytic acid is performed in a continuous reactor with the addition of calcium chloride as a precipitating agent. The precipitate together with the insoluble solids are separated from the liquid stream by centrifugation using a disc stack centrifuge. The collected cake is disposed by incineration (Figure 6.2, stream S-104 Solid waste). The liquid stream is then concentrated in a multi-effect evaporator in order to remove water and additionally decrease the volume of the agricultural side stream for the subsequent operations. This has a positive influence as smaller equipment might be needed for the other unit tasks.

A conversion step is needed, in order to produce one of the products. This conversion is performed in a plug flow reactor (PFR). All calculations regarding this operation can be found in Appendix 6B. Plug-flow catalytic reactor, as these calculations were based on literature<sup>33, 34</sup>, it is important to keep in mind that higher amount of catalyst might be needed. This could be considered in the product cost sensitivity analysis.

The PFR outlet stream is sent to an ultrafiltration unit where the large molecules (namely proteins) are separated. The ultrafiltration set up is operated continuously with multiple units. For this study, the stream S-109-Retentate is discarded as wastewater. However, the recovery and purification of these proteins could be valorized as recommended in Chapter 4.

The critical step in this process is the removal of off-flavors which is done using adsorption with a polymeric resin as previous studies (Moreno-González, unpublished data) suggested that capturing of the unwanted components (typically organic hydrophobic molecules such as ketones, aldehydes and organic acids) is selective. The product is collected during the loading and washing step of the adsorption cycle (Flow-through mode). Collecting the wash dilutes the product stream (1.5fold) but benefits product yield of this unit which is higher than 98%. Elution is performed with 0.5% (w/w) NaOH and regeneration of the column is done with 50% (w/w) ethanol/water. The exit stream containing the elution, regeneration and re-equilibration effluent (S-122 in Figure 6.2) is sent to a distillation column, where ethanol/water 50% is recovered and recycle to the adsorption column. 88% ethanol yield is recovered and recycle in this process, the bottoms stream from the distillation column is a wastewater stream (S-116 in Figure 6.2). The process is performed in continuous mode by having a total of 3 columns. Two columns are synchronized for operation, while one column is loaded as washed the other is eluted, regenerated and re-equilibrated. This is possible due to the different velocities applied during these steps, making the duration of the loading and washing longer than the other steps. In order to satisfy the total mass flow, an additional column is needed. Holding tanks before and after the adsorption columns (vessels V-102 and V-102 in Figure 6.2) allows the flow splitting and collection of the discontinuous product from the adsorption columns.

At last, the stream containing the product is set to the spray dryer where it is combined with maltodextrin, for flavor encapsulation to form the final powder extract. The gas outlet from the spray

dryer is sent to an air filter and released to the atmosphere. Product yield is 87.8%, which is higher than the minimum set in the process constrains. An equipment list is found in Table 6.2.

**Table 6.2.** List of equipment

Equipment	Size			Dimensions	Material
	Diameter(m)	Heigh(m)t	Volume(m <sup>3</sup> )		
<b>Catalyst preparation reactor</b>	0.6	1.63	0.5	NA	304ss
<b>Continuous reactor</b>	2.7	5.3	23.0	NA	304ss
<b>Disk Stack centrifuged<sup>1</sup></b>	NA	NA	NA	20 m <sup>3</sup> /h	304ss
<b>Multi-Effect Evaporator<sup>2</sup></b>	NA	NA	NA	36 m <sup>2</sup>	304ss
<b>Plug flow reactor</b>	0.4	4.0	0.5	NA	304ss
<b>Ultrafiltration module<sup>3</sup></b>	NA	NA	NA	76.1 m <sup>2</sup>	304ss
<b>Adsorption column</b>	0.8	2.0	1.1	NA	304ss
<b>Spray dryer<sup>4</sup></b>	3.3	9.9	85.9	8590 kg/h	304ss
<b>Distillation column</b>	1.8	5.6	14.2		304ss
<b>Heat Exchanger<sup>2</sup></b>	NA	NA	NA	25 m <sup>2</sup>	304ss

NA: Not applicable ss: Stainless steel <sup>1</sup>Based on throughput <sup>2</sup>Based on heat transfer area <sup>3</sup>Based on membrane area

<sup>4</sup>Based on drying capacity

The economic analysis started with the determination of the purchased equipment cost which is presented in Table 6.4. The highest equipment cost is accounted to the spray dryer (28% of PEC), as the product stream coming from the adsorption column possesses around 70% water. Therefore, a high drying capacity is required in order to accomplish the required fine powder. In addition, spray dryer systems consist on several elements (air heater, nozzle or atomizer, drying chamber, cyclones, building)<sup>35</sup> which are considered in this cost. The 3 adsorption columns also represent a significant portion of the equipment cost (22% of PEC) followed by the disc stack centrifuges (12% of PEC), as two units are needed. The Capital Expenditure (CAPEX) breakdown can be found in Table 6.3. The total investment is 44.51 million of euros.

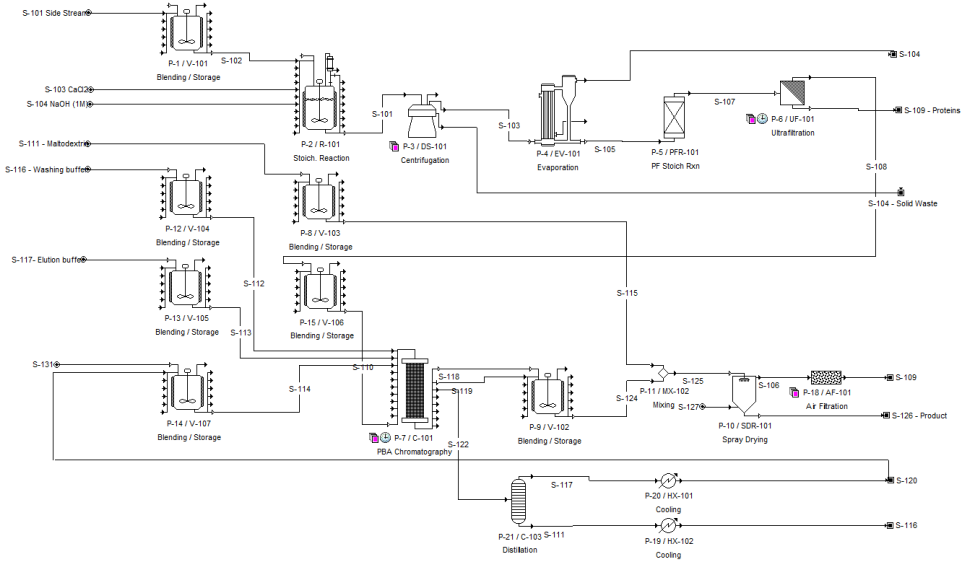


Figure 6.2. Conceptual process design for the removal of off-flavors by adsorption from an agricultural side streams to produce a flavored dry powder

Table 6.3 Capital expenditure breakdown (CAPEX)

Concept	Cost
<b>Purchase Equipment Cost (PEC)</b>	k€ 5,090.80
<b>Installation cost</b>	k€ 2,545.40
<b>Total Plant Direct Cost (TPDC)</b>	k€ 18,225.05
<b>Total Plant Indirect Cost (TPIC)</b>	k€ 10,935.03
<b>Total Plant cost (TPC)</b>	k€ 29,160.08
<b>Direct fixed capital (DFC)</b>	k€ 33,534.09
<b>Working capital</b>	k€ 5,030.11
<b>Startup cost</b>	k€ 6,706.82
<b>R&amp;D</b>	k€ 1,676.70
<b>Total investment</b>	<b>k€ 46,947.72</b>

**Table 6.4.** Purchased equipment cost

Equipment	Cost (k€/unit)	# Units	Total k€	Reference
Catalyst preparation reactor	72.0	1.0	72.0	Towler, et al. <sup>28</sup>
Continuous reactor	413.0	1.0	413.0	Towler, et al. <sup>28</sup> .
Disk Stack centrifuged	304.5	2.0	609.0	Peters, et al. <sup>36</sup>
Multi-Effect Evaporator	230.0	1.0	230.0	Towler, et al. <sup>28</sup>
Plug flow reactor	241.0	1.0	241.0	Peskin, et al. <sup>31</sup>
Ultrafiltration module	18.1	7.0	142.0	Seider, et al. <sup>27</sup>
Adsorption column	353.0	3.0	1,134.0	Peskin, et al. <sup>31</sup>
Holding tanks (5m <sup>3</sup> )	79.0	2.0	159.0	DACE booklet <sup>30</sup>
Holding tanks (3m <sup>3</sup> )	71.0	4.0	286.0	DACE booklet <sup>30</sup>
Holding tanks (1m <sup>3</sup> )	49.0	2.0	99.0	DACE booklet <sup>30</sup>
Spray dryer	1,473.0	1.0	1,473.0	Towler, et al. <sup>28</sup>
Distillation column	125.0	1.0	125.0	Aspen Plus V8.8
Air Filter	52.0	4.0	208.0	SuperPro Designer
Heat Exchanger	69.0	1.0	69.0	DACE booklet <sup>30</sup>
<b>Total PEC (k€)</b>			<b>5,191.0</b>	

Operating cost is composed of raw materials, utilities, consumables, labor, waste disposal, lab QC/QA and facility overhead. The operating cost estimations are presented in Figure 6.3 and Figure 6.4.

Regarding the raw materials, the higher cost is attributed to maltodextrin, which is the encapsulation agent and it accounts 50% of the formulation. Following by ethanol which is used to regenerate the adsorption column. Around 90% of ethanol is recovered and recycled to the adsorption, which significantly reduces the contribution of this component to the raw material cost. Sodium hydroxide is the third raw material that significantly contributes to the raw material cost (11%). This chemical is used in several operation units (precipitation, ultrafiltration and adsorption). The raw materials accounted for the catalysis preparation do not contribute significantly to the cost, due to the reusability of the catalyst.

The cost of the adsorption resin is the highest consumable cost (accounting 98% of this cost). The cost per year is comparable to the purchased cost of the three columns needed. In terms of utilities steam is the main contributor. This is expected as three thermal units are used in this process, multi-effect evaporator, distillation column and the spray dryer. Forty percent (40%) of the total steam is used in the distillation column, 37% in the spray dryer and 22% in the evaporator.

Solid waste obtained from the centrifugation, which includes phytate salt and insoluble solids (mainly plant based fibers) are incinerated which accounts 95% of waste disposal. The generated wastewater comes from the ultrafiltration (retentate), the distillation (bottoms) and the catalyst preparation (total wastewater 71,050 m<sup>3</sup>/year).

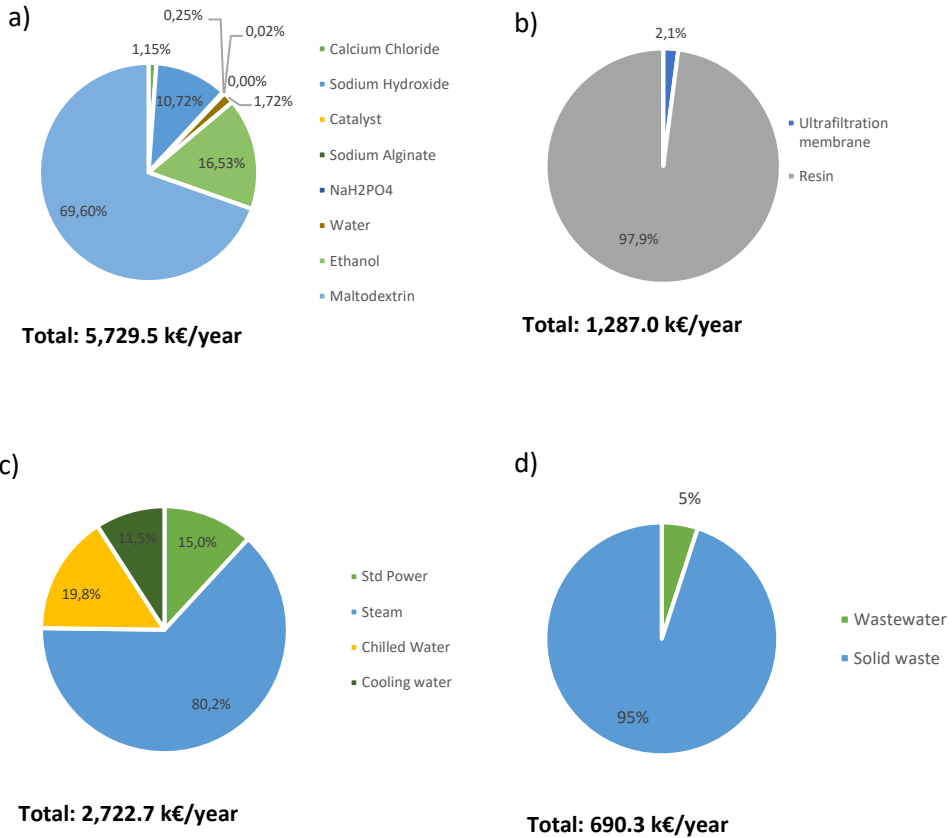
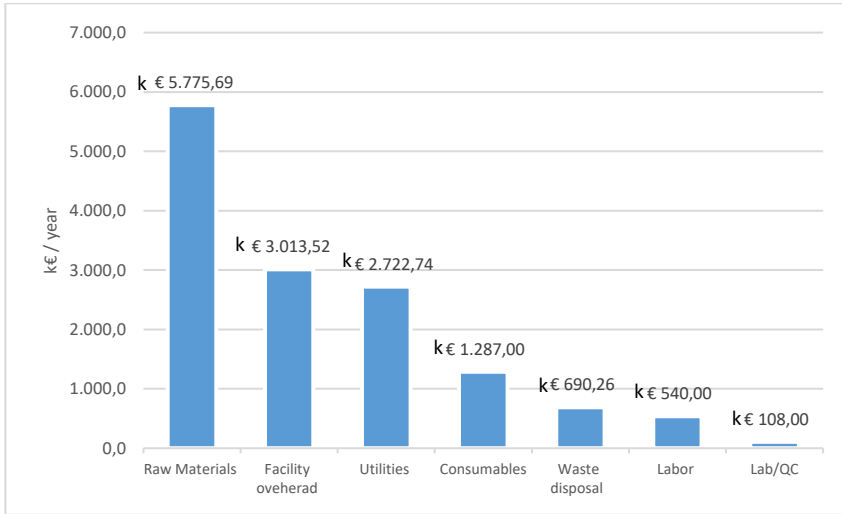


Figure 6.3. Operating cost a) Raw Materials, b) Consumables, c) utilities and d) waste disposal

Operating expenditure breakdown is shown in Figure 6.4, and corresponds to €14.13 million per year.

The minimum selling price of the product for profitability is 2.5 €/kg, estimated assuming a 20% ROI. A discounted cash flow analysis assuming a 15% nominal interest, MACRS depreciation for a 5-year period was evaluated. With this analysis, the observed payback time is ~6 years with a net present value (NPV) of € 16.42 million. Increasing the product price to 2.7 €/kg reduces the payback time to less than 5 years and increases the NPV to € 21.93 million. This minimum increment in the product price is justified, as flavor product prices are expected to range up to 30€/kg. Figure 6.5 shows the graphical representation of the discounted cash flow analysis. Lastly, IRR (investors' rate of return) which is the interest that gives a NPV of zero was calculated, in other words is the maximum nominal interest rate that the project could pay to break even at the end of the project lifetime. The calculated IRR is 28% for a selling price of 2.7€/kg.



**Figure 6.4.** Operating Expenditure (OPEX). Total: 14,137.2 k€/year

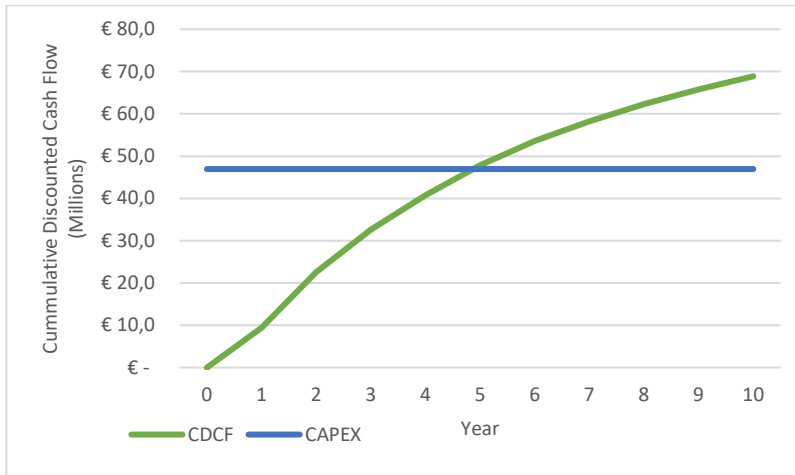


**Figure 6.5.** Cumulative Discounted Cash flows (CDCF) at a nominal interest rate of 15%. Product price 2.7€/kg

Comparing this process to the one suggested by Souza Filho, et al.<sup>37</sup> where heat treated potato liquor (HTPL, the byproduct from potato starch production) is evaluated, it is clear that recovery of added-value products (such as flavor products or proteins) will lead to a positive economic balance. Potato liquor is rich in proteins which have similar characteristics than proteins from egg.<sup>38</sup> Current protein recovery strategies are only based on heating processes that affect their functionality and therefore are only used for cattle feed and not for human consumption. The authors<sup>37</sup> suggested the treatment of this potato side stream for production of biogas or protein rich biomass. A techno-economic analysis of a treatment plant processing ~48 m<sup>3</sup>/h of liquid stream is presented. Their economic analysis showed

a negative NPV after a 15-year period, which is mainly due to the low selling price of biogas and biomass (33 €/MW·h and ~ 0.929 €/kg). Even though capital investment and operating cost are around 3.2 times lower than in the present study, the produced flavor powder is a clear example of how the process is more profitable than its conversion into animal feed or energy (biofuels).<sup>3</sup>

A quick environmental assessment could be done by determining the E factor (total mass of waste divided by the total amount of product). An E-factor value of 7 is calculated. This value is obtained considering also water as part of the waste which is usually neglected. Neglecting water as waste, the E-value decreases to 1.1. The obtained value ranges between the typical values for bulk chemicals and fine chemicals in the chemical industry.<sup>39</sup> As this is a food product, one could conclude that the E-factor is in an acceptable range.

Considering that the highest operating cost are maltodextrin and the adsorbent a simplified sensitivity analysis was done varying the amount of these components. In addition, the catalyst, and the raw materials needed for its preparation were also increased, as all the calculations for the PFR were considering literature data. From the sensitivity analysis the product price will range between 2.5 – 5.0€/kg.

## 6.4. Conclusions

This work presents the technical and economic feasibility for the production of a flavored powder extract from an agricultural side stream. The evaluation indicates that the obtained product could be competitive with current flavor products available in the market. In addition, the economic assessment showed the potential of using agricultural side streams for the generation of natural ingredients.

In the presented work, it was observed that one of the biggest costs is the encapsulation matrix (maltodextrin) used in the spray drying and the adsorbent. Steam is the highest utility cost, as three operation units of this design requires the use of it, mainly the evaporator and the distillation column.

Profitability might be increased by valorizing the generated waste streams. Particularly the solid waste, composed of calcium phytate which could be used as a phosphorus source.<sup>40</sup> Additionally, the proteins from the retentate stream in the ultrafiltration could be purified (as suggested in Chapter 4) and sell as plant-based proteins.

This work shows the potential of upgrading side stream from the food sector to contribute to reduce waste generation, obtaining natural ingredients and to a more circular economy.

## 6.5. Acknowledgments

This work is supported by the ISPT (Institute for Sustainable Process Technology) under the project code CM-20-07 Adsorption of non-volatiles from food products. Thank you to the industrial partners for their valuable contribution. In addition, thank you to Luis Perreira (PDEng Trainee) from Delft University of technology for its valuable contribution on the selection of the different operation units and the research on catalyst preparation.

## 6.6. List of symbols

Symbol	Description	Units
$a$	Surface area of particles per unit of volume	$m^{-1}$
$C_i$	Liquid concentration of components $i$ (adsorption)	$g/m^3$
$C_{eq,t}^*$	Liquid equilibrium concentration of component $i$ (adsorption)	$g/m^3$
$C_{s0}$	Initial substrate concentration (catalytic reactor)	$mol/m^3$
$C_{si}$	Substrate concentration on catalyst surface	$mol/m^3$
$C_s$	Substrate concentration (catalytic reactor)	$mol/m^3$
$D_f$	Free diffusivity	$m^2/s$
$D_L$	Axial dispersion coefficient	$m^2/s$
$d_p$	Particle diameter	$m$
$D_p$	Pore diffusivity	$m^2/s$
$F$	Phase ratio	-
$H_i$	Adsorption isotherm slope of component $i$	$m^3/m^3_r$
$K_i$	Adsorption equilibrium constant	$m^3/g$
$k_{f,i}$	Film mass transfer coefficient	$m^2/g$
$K_m$	Michaelis-Menten constant	$mol/m^3$
$k_{ov,t}$	Overall mass transfer coefficient	$s^{-1}$
$L$	Column length	$m$
$q_i$	Stationary phase concentration of component $i$	$g/m^3$
$q_{max,i}$		
$Q$	Volumetric flow rate	$m^3/h$
$Sh$	Sherwood number	-
$t$	Time	$s$
$u_s$	Superficial velocity	$m/s$
$v$	Interstitial velocity	$m/s$
$v_{max}$	Maximum reaction rate	$mol/m^3s$
$z$	Axial position	$m$
<b>Greek</b>		
$\epsilon_b$	Bed porosity	-
$\epsilon_p$	Intraparticle porosity	-
$\mu$	Viscosity of liquid	$Pa.s$
$\rho_L$	Density of the liquid	$Kg/m^3$
$\rho_b$	Catalyst beads density	$Kg/m^3$

## 6.7. Abbreviations

Abbreviation	Description
<b>CAPEX</b>	Capital Expenditure
<b>CEPCI</b>	Chemical Engineering Plan Cost Index
<b>CSTR</b>	Continuous Stirred Tank Reactor
<b>CV</b>	Column volume
<b>DFC</b>	Direct Fixed Capital
<b>MACRS</b>	Modified Accelerated Cost Recovery System
<b>MR</b>	Millard reaction
<b>OPEX</b>	Operating expenditure
<b>NPV</b>	Net Present Value
<b>PEC</b>	Purchased equipment cost
<b>PFR</b>	Plug flow reactor
<b>ROI</b>	Return of investment

## 6.8. References

- 1 Galanakis C.M., Food Waste Recovery - Processing Technologies and Industrial Techniques, Elsevier, USA, 2015.
- 2 Virtanen S., Chowreddy R.R., Irmak S., Honkapää K., Isom L., Food Industry Co-streams: Potential Raw Materials for Biodegradable Mulch Film Applications, Journal of Polymers and the Environment, (2016) 1-21.
- 3 Tuck C.O., Pérez E., Horváth I.T., Sheldon R.A., Poliakoff M., Valorization of Biomass: Deriving More Value from Waste, Science, 337 (2012) 695-699.
- 4 Pfaltzgraff L.A., De bruyn M., Cooper E.C., Budarin V., Clark J.H., Food waste biomass: a resource for high-value chemicals, Green Chemistry, 15 (2013) 307-314.
- 5 Baigrie B., Taints and off-flavours in food, Woodhead Publishing Limited, Cambridge, England 2003.
- 6 Arnoldi A., The Maillard reaction as a source of off-flavours, in: B. Baigrie (Ed.) Taints and off-flavours in food, Woodhead Publishing Limited, Cambridge, England 2003, pp. 162-175.
- 7 Gernat D.C., Brouwer E., Ottens M., Aldehydes as Wort Off-Flavours in Alcohol-Free Beers—Origin and Control, Food and Bioprocess Technology, 13 (2020) 195-216.
- 8 Moreno-González M., Girish V., Keulen D., Wijngaard H., Luteslager X., Ferreira G., Ottens M., Recovery of sinapic acid from canola/rapeseed meal extracts by adsorption, Food and Bioproducts Processing, 120 (2020) 69-79.
- 9 Weil J.R., Dien B., Bothast R., Hendrickson R., Mosier N.S., Ladisch M.R., Removal of Fermentation Inhibitors Formed during Pretreatment of Biomass by Polymeric Adsorbents, Industrial & Engineering Chemistry Research, 41 (2002) 6132-6138.
- 10 Seider W.D., Seader J.D., Lewin D.R., Widagdo S., Steps in product-development in: Product and process design principles : synthesis, analysis, and evaluation, John Wiley & Sons, Hoboken, NJ, 2010, pp. 32-54.

- 11** Saffarionpour S., Ottens M., Recent Advances in Techniques for Flavor Recovery in Liquid Food Processing, *Food Engineering Reviews*, 10 (2018) 81-94.
- 12** Desai K.G.H., Jin Park H., Recent Developments in Microencapsulation of Food Ingredients, *Drying Technology*, 23 (2005) 1361-1394.
- 13** Harmsen J., Haan A.B.d., Swinkels P.L.J., Grievink J., Pat-El I., Reisen J.v., *Product and Process Design*, De Gruyter, 2018.
- 14** Olafadehan O.A., Aribike D.S., Adeyemo A.M., Mathematical modeling and simulation of steady state plug flow for lactose-lactase hydrolysis in fixed bed, *Theor. Found. Chem. Eng.*, 43 (2009) 58-69.
- 15** Wilson E.J., Geankoplis C.J., Liquid Mass Transfer at Very Low Reynolds Numbers in Packed Beds, *Industrial and Engineering Chemistry Fundamentals*, 5 (1966) 9-14.
- 16** Wilke C.R., Chang P., Correlation of diffusion coefficients in dilute solutions, *AIChE Journal*, 1 (1955) 264-270.
- 17** Felinger A., Guiochon G., Comparison of the Kinetic Models of Linear Chromatography, *Chromatographia*, 60 (2004) S175-S180.
- 18** Gernat D.C., Penning M.M., Swinkels F.M., Brouwer E.R., Ottens M., Selective off-flavor reduction by adsorption: A case study in alcohol-free beer, *Food and Bioproducts Processing*, 121 (2020) 91-104.
- 19** Silva M., Castellanos L., Ottens M., Capture and Purification of Polyphenols Using Functionalized Hydrophobic Resins, *Industrial & Engineering Chemistry Research*, 57 (2018) 5359-5369.
- 20** Schiesser W.E., *The numerical method of lines : integration of partial differential equations*, Academic Press, San Diego, 1991.
- 21** Grynspan F., Cheryan M., Calcium phytate: effect of pH and molar ratio on in vitro solubility, *Journal of the American Oil Chemists' Society*, 60 (1983) 1761-1764.
- 22** Hoff-Jørgensen E., *Investigations on the Solubility of Calcium Phytate*, by E. Hoff-Jørgensen, E. Munksgaard, 1944.
- 23** Evans W., Pierce A., Calcium-phytate complex formation studies, *Journal of the American Oil Chemists' Society*, 58 (1981) 850-851.
- 24** Crea F., De Stefano C., Milea D., Sammartano S., Formation and stability of phytate complexes in solution, *Coordination Chemistry Reviews*, 252 (2008) 1108-1120.
- 25** Carta G., Jungbauer A., *Protein chromatography: process development and scale-up*, John Wiley & Sons, 2010.
- 26** Henriques da Silva M.D., *Downstream Process Development for Bio-based Production of Phenolics*, in: *Bioprocess Engineering Delft University of Technology Delft, The Netherlands* 2019.
- 27** Seider W.D., Seader J.D., Lewin D.R., Widagdo S., *Product and process design principles : synthesis, analysis, and evaluation*, Third ed., John Wiley & Sons, Hoboken, NJ, 2010.
- 28** Towler G.P., Sinnott R.K., *Chemical engineering design : principles, practice, and economics of plant and process design*, in, Butterworth-Heinemann, Oxford ;, 2013.
- 29** Harrison R.G., Todd P.W., Rudge S.R., Petrides D.P., *Bioseparations Science and Engineering 2nd Edition ed.*, Oxford University Press, New York, USA, 2015.

- 30** Management T.D.N.a.C.C.f.C.E.a.V., DACE Price Booklet 33 Edition ed., Johan Schot, The Hague 2018.
- 31** Peskin A.P., Rudge S.R., Optimization of large-scale chromatography for biotechnological applications, *Applied Biochemistry and Biotechnology*, 34 (1992) 49-59.
- 32** Schlemmer U., Frølich W., Prieto R.M., Grases F., Phytate in foods and significance for humans: food sources, intake, processing, bioavailability, protective role and analysis, *Molecular nutrition & food research*, 53 (2009) S330-S375.
- 33** Masataka Y., Keiko M., Effect of temperature on the kinetics of the yeast AMP deaminase, *International Journal of Biochemistry*, 18 (1986) 235-239.
- 34** Noguchi S., Shimura G., Kimura K., Samejima H., Production of 5'-mononucleotides using immobilized 5'-phosphodiesterase and 5'-AMP deaminase, *Journal of Solid-Phase Biochemistry*, 1 (1976) 105-118.
- 35** Berk Z., Dehydration, in: *Food Process Engineering and Technology*, Elsevier Science & Technology, San Diego, USA, 2013.
- 36** Peters M.S., Timmerhaus K.D., West R.E., *Plant Design and Economics for Chemical Engineers*, McGraw-Hill Education, 2003.
- 37** Souza Filho P.F., Brancoli P., Bolton K., Zamani A., Taherzadeh M.J., Techno-Economic and Life Cycle Assessment of Wastewater Management from Potato Starch Production: Present Status and Alternative Biotreatments, *Fermentation*, 3 (2017) 56.
- 38** Ralet M.-C., Guéguen J., Fractionation of Potato Proteins: Solubility, Thermal Coagulation and Emulsifying Properties, *LWT - Food Science and Technology*, 33 (2000) 380-387.
- 39** Phan T.V.T., Gallardo C., Mane J., GREEN MOTION: a new and easy to use green chemistry metric from laboratories to industry, *Green Chemistry*, 17 (2015) 2846-2852.
- 40** Thiel A., Muffler K., Tippkötter N., Suck K., Sohling U., Hruschka S.M., Ulber R., A novel integrated downstream processing approach to recover sinapic acid, phytic acid and proteins from rapeseed meal, *Journal of Chemical Technology and Biotechnology*, 90 (2015) 1999-2006.
- 41** Straathof A.J.J., Ottens M., van Gulik W.M., Zomerdijk M., LB2791-P Integrated Practical Biotechnology, Delft, The Netherlands, 2016.
- 42** Sevillano D.M., van der Wielen L.A.M., Hooshyar N., Ottens M., Resin selection for the separation of caffeine from green tea catechins, *Food and Bioproducts Processing*, 92 (2014) 192-198.

## Appendix 6A. Selection of Unit Operation

## Phytic acid removal

Two methods are analyzed and compared for the phytic acid removal unit operation: enzymatic treatment and chemical precipitation. The selection matrix is presented in Table 6.5.

**Table 6.5.** Selection matrix for the phytic acid removal unit operation options.

Criteria	Optional Importance Weighting	Enzymatic Treatment	Chemical Precipitation
<b>Operation Efficiency</b>	8	+	+
<b>Removal/Final Product</b>	7	-	+
<b>Scalability</b>	6	+	+
<b>Operational Costs</b>	5	-	+
<b>Operation Time</b>	4	-	+
<b>Environmental Impact</b>	3	+	-
<b>Storage Stability</b>	2	-	+
<b>Selectivity</b>	1	0	0
<b>Total Score</b>	-	<b>-1</b>	<b>29</b>

## Solid/Liquid Separation

The objective of this step is to separate insoluble solids. Two types of solids are presented in this stream: solids from the agricultural material and phytic acid precipitate with two different sizes. Phytic acid precipitate with a particle size of ~2 microns were considered as a critical particle size for this separation. The selection matrix is shown in Table 6.6.

**Table 6.6.** Selection matrix for the solid-liquid separation unit operation options.

Criteria	Optional Importance Weighting	Decanter Centrifuge	Disc Stack Centrifuge	Basket Centrifuge	Rotary Vacuum Filter
<b>Particle Size</b>	8	+	+	+	-
<b>Concentration Range</b>	7	+	+	+	-
<b>Operation Efficiency</b>	6	-	+	-	+
<b>Scalability</b>	5	+	+	+	+
<b>Operational Costs</b>	4	-	-	+	+
<b>Continuous/Batch Flexibility</b>	3	+	+	-	+
<b>Clogging Issues</b>	2	+	+	-	-
<b>Maintenance Complexity</b>	1	-	-	+	+
<b>Total Score</b>	-	<b>14</b>	<b>18</b>	<b>14</b>	<b>2</b>

Based on the previous matrix a disc stack centrifuge was selected.

### Stream concentration

A concentration step is usually performed at the first stages of the purification process in order to reduce the volume of the stream to be treated in the following units.

The selection matrix to determine this unit operation is shown next (Table 6.7)

**Table 6.7.** Selection matrix for the water removal unit operation options.

Criteria	Optional Importance Weighting	Reverse Osmosis	Evaporation
<b>Operation Efficiency</b>	5	-	+
<b>Scalability</b>	4	+	+
<b>Operational Costs</b>	3	-	+
<b>Operation Time</b>	2	+	-
<b>Environmental Impact</b>	1	+	-
<b>Total Score</b>	-	<b>-1</b>	<b>9</b>

Evaporation was selected as the most suitable unit for this step.

### Conversion (Product formation)

A conversion step is required in order to produce one of the valuable compounds. This conversion step is performed with a catalyst can be executed in a conventional stirred vessel or in a plug flow reactor. The selection matrix used to select this step is presented in Table 6.8.

**Table 6.8.** Selection matrix for the conversion.

Criteria	Optional Importance Weighting	Stirred tank	Plug flow reactor
<b>Operation Efficiency</b>	8	+	+
<b>Scalability</b>	7	+	+
<b>Operational Costs</b>	6	0	0
<b>Operation Time</b>	5	0	0
<b>Catalyst Stability over Time</b>	4	-	+
<b>Catalyst thermal Stability</b>	3	-	+
<b>Catalyst pH Stability</b>	2	-	+
<b>Environmental Impact</b>	1	+	+
<b>Total Score</b>	-	<b>7</b>	<b>25</b>

A plug flow reactor was designed for this unit task.

### Small molecule separation

Agricultural streams contain other molecules that could be recovered. Among these molecules, proteins which significantly differ in size from other like sugars or flavor components, could be separated using precipitation or ultrafiltration. Separation of these molecules is recommended as they could interfere on the following step which is the most critical, the removal of off-flavors. The selection matrix in can be found in Table 6.9.

Ultrafiltration was selected to separate small molecules from large molecules.

## Off-flavor removal

Off-flavor separation is considered the critical step in this process. This step is challenging due to the type of molecules to be separated which as with the valuable compounds are organic molecules. The main difference between them is their hydrophobicity. Three separation techniques were assessed for this unit task selection and the decision matrix can be found in Table 6.10. Adsorption using an hydrophobic resin was selected for this objective.

**Table 6.9.** Selection matrix for small molecule separation.

Criteria	Optional Importance Weighting	Ultrafiltration	Protein Precipitation
Operation Efficiency	5	+	-
Scalability	4	+	+
Operational Costs	3	-	+
Operation Time	2	-	+
Environmental Impact	1	+	-
<b>Total Score</b>	-	<b>5</b>	<b>3</b>

**Table 6.10.** Selection matrix for off-flavor removal.

Criteria	Optional Importance Weighting	Activated Carbon Adsorption	Selective Resin Adsorption	Supercrit. CO <sub>2</sub> Extraction
Operation Efficiency	6	+	+	+
Scalability	5	+	+	-
Selectivity	4	-	+	+
Operational Costs	3	-	+	-
Operation Time	2	-	-	+
Environmental Impact	1	+	-	+
<b>Total Score</b>	-	<b>3</b>	<b>15</b>	<b>5</b>

## Drying (product encapsulation)

Few drying methodologies can be applied with liquid streams. The selection matrix for this unit task is shown in Table 6.11.

**Table 6.11.** Selection matrix for drying/formulation.

Criteria	Optional Importance Weighting	Spray Drying	Freeze Drying	Drum Drying
Operation Efficiency	8	+	+	+
Scalability	7	+	+	+
Operational Costs	6	-	-	+
Operation Time	5	+	-	+
Mild operation conditions	4	+	+	-
Production Capacity	3	+	+	-
Ease of Operation/Control	2	+	-	-
Environmental Impact	1	-	-	+
<b>Total Score</b>	-	<b>22</b>	<b>8</b>	<b>18</b>

Spray drying technique will be used to formulate the final dry powder in this process.

Appendix 6B. Plug-flow catalytic reactor

**Table 6.12.** Plug flow reactor kinetic parameters

Parameter	Value	Remarks	Reference
$V_{max}$	3.78 mol/m <sup>3</sup> s	Maximum reaction rate Was calculated taking into account the carrier density.	Masataka, et al. <sup>33</sup>
$K_m$	2.30 mol/m <sup>3</sup>	Michaelis-Menten constant	Masataka, et al. <sup>33</sup>
$\rho_b$	875.50 kg/m <sup>3</sup>	Calcium alginate beads	
$d_p$	5.5E-3 m	Particle diameter	

The concentration profiles of substrate and product, in the column, are shown in Figure 6.6.

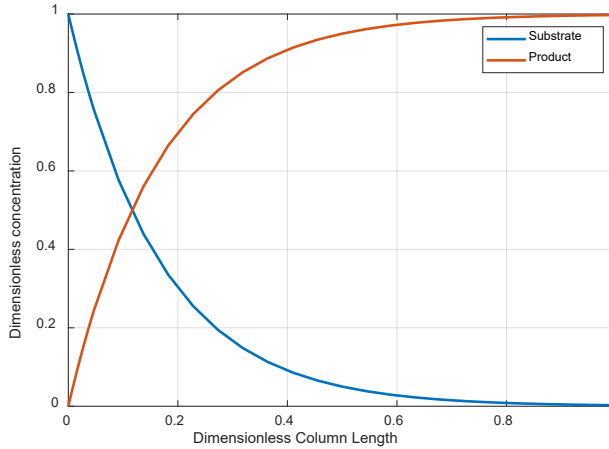


**Figure 6.6.** Dimensionless concentration profile over the length of the catalytic plug flow reactor. Flow rate 8.03 m/h, column dimensions 0.4m id x 4m h.

The above parameters are assumed to be of the catalyst beads will be prepared in the production facility. For this, a preparation procedure using sodium alginate (22g/L) as solid carrier is used. The catalyst concentration is 19.8<sup>34</sup> g /L prepared in buffer of sodium phosphate and sodium alginate (gel forming component). Sodium alginate forms a gel in the presence of calcium chloride. The catalyst solution is pushed through a nozzle and a membrane to form droplets which are instantaneously solidified when the contact the calcium chloride solution<sup>41</sup>.

Using the density catalyst and the volume of the beads required in the column the amount of catalyst can be calculated as follows:

$$V_c * (1 - 0.3) = 0.5 \text{ m}^3 * (0.7) = 0.351 \text{ m}^3 \text{ beads}$$

$$V_b * \rho_b = 0.351 \text{ m}^3 * 875.50 \frac{\text{kg}}{\text{m}^3} = 308.05 \text{ Kg beads}$$

The density of the catalyst solutions corresponds to  $998.2 \text{ Kg/m}^3$ , the volume of catalyst solution could be estimated, and given the concentration of catalyst in the solution, the amount of catalyst can be calculated. This corresponds to 8.2 kg of catalyst. Assuming that the catalyst needs to be replaced every 15 days, the amount of catalyst required per year is 82.0 kg/year.

## Appendix 6C. Adsorption

### Resin selection and Adsorption equilibrium isotherms

#### Materials and Methods

Ten different food grade hydrophobic resins were selected for off-flavor removal. The resins are: from Amberlite series FPX66 and FPX68, Amberlite XAD series: XAD16N, XAD7, XAD4, XAD1180N, and XAD761, from Diaion, resin HP20 and Sephabead resins SP70 and SP710. All were obtained from Sigma-Aldrich, The Netherlands. Off-flavors (listed in Table 6.15) were purchased, food grade from Sigma-Aldrich.

#### Adsorption/Desorption equilibrium

The methodology suggested in Chapter 3<sup>8</sup> and Chapter 4, for resin selection and determination of adsorption equilibrium was followed with some modification. Briefly, resins were contacted with the stream (around 5g of stream) under agitation until equilibrium is reached (3 hours). Once equilibrium is reached, the supernatant was collected to measure off-flavor and product concentrations. A control experiment (stream without resin) was evaluated in order to obtain the initial concentration and perform mass balance and capacity calculations. The stream was spiked with the off-flavors in order to increase their concentration in it at different ratios, this allowed to obtain adsorption data a different equilibrium concentration.

Adsorption capacity of all the components was calculated based on the mass balance (equation (6.12))

$$q_i = \frac{(C_{0,i} - C_{e,i}) * M}{m_{resin}} \quad (6.12)$$

Were  $q_i$  is the capacity of component  $i$ ,  $C_{0,i}$  is the initial concentration of component  $i$   $C_{e,i}$  is the equilibrium concentration,  $M$  is the mass of the stream and  $m_{resin}$  is the mass of resin used in the experiment.

After adsorption resins were contacted with NaOH (0.5 M) for 2 hours under agitation in order to evaluate desorption. The resins were centrifuged and the supernatant was collected to measure off-flavors concentration. Off-flavor recovery (yield) was calculation using the following equation:

$$Yield = \frac{C_{i,NaOH} * V_{NaOH}}{q_i * m_{resin}} \quad (6.13)$$

Where  $C_{i,NaOH}$  is the concentration of component  $i$  in the supernatant after desorption,  $V_{NaOH}$  is the volume of NaOH used in the experiment.

#### Resin selection

The aim of this case study is to selectively remove the off-flavors. The defined criteria defined was based on **selectivity, number of adsorbed off-flavors, capacity and desorption**. The selection criteria was established based on the strategy proposed by Sevillano, et al.<sup>42</sup>.

### Selectivity

A weight of 0.5 was given to this criterion. The selectivity of the off-flavors over the valuable product was calculated using equations (6.14) and (6.15). First the selectivity of the different function groups (ketones, alcohols, aldehydes, carboxylic acids and aromatic ring) over the valuable compounds was determined with the following equation:

$$S_{FG,Valuable} = \frac{\prod_{FG} n \sqrt[m_i]}{\sqrt[m_{Product1}] \cdot \sqrt[m_{Product2}]} \quad (6.14)$$

Where S is the selectivity,  $m_i$  the slope of the isotherm and n is defined as the number of the off-flavors presented in that specific functional group.  $\prod$  represent the product mathematical operator and the subscript FG refers to the functional group.

In order to compare all the resins and since five functional groups were evaluated, the selectivity values of each functional group (FG) were normalized (equation (6.16))

$$S_{FG,Valuable}^{Ri} = \frac{\text{value of criterion of resin } i}{\text{maximum value of criterion of all resins}} \quad (6.15)$$

Finally, the total selectivity score per resin was accounted using

$$S_{off-flavors,Valuable}^{Ri} = \sum S_{FG,Valuable}^{Ri} \quad (6.16)$$

### Number of off-flavors adsorbed

A weight of 0.2 was given to this criterion. The total of measured off-flavors presented in the stream is 11. However, some of the experimental results showed very poor or no adsorption for some components, especially the carboxylic acids. This was taken into account by counting the number of compounds adsorbed per resin.

### Adsorption Capacity

The weight given for this criterion was 0.1. That weight was selected because, the main objective is to select a resin able to capture the off-flavors and not the valuable compounds, if additionally, the resin can capture a high amount of the off-flavors, this will contribute to the selection.

Around 11 off-flavors are presented in the stream. The capacity of each component, at the stream conditions, is calculated using the determined isotherms parameters. The capacity of the off-flavors was calculated as the average capacity of all the components equation (6.17).

$$q_{off-flavors}^{Ri} = \frac{\sum q_i}{N_{off-flavors}} \quad (6.17)$$

Where  $q$  is the capacity of component  $i$  and  $N$  is the number of off-flavors adsorbed. The superscript  $R_i$  refers to resin  $i$ .

### Desorption

A weight of 0.2 was given to this criterion. Similarly to the capacity criterion, total recovery yield was the sum of all off-flavor per resin.

Final resin score was calculated by normalizing the different criteria, as suggested in Sevillano, et al.<sup>42</sup>

$$\text{Resin score} = \sum \text{weight} \cdot \frac{\text{criterion}}{\text{maximum value of criterion}}$$

### Off-flavors quantification

Off-flavor concentrations were analyzed using a SPME-HS-GC (headspace gas chromatography) coupled with an autosampler and a Mass Spectrophotometer (MS). The GC column is J&W 121-7023DB-WAX column (20 m x 180  $\mu\text{m}$  x 0.3  $\mu\text{m}$ ) and the SPME fiber is PDMS 100 $\mu\text{m}$ . The selected carrier gas was Helium. To favor the transition of the components to the gas phase NaCl was added to each sample in addition sample pH was decreased to 2. Different internal standards (see Table 6.13) were used to account the changes in the matrix.

**Table 6.13.** SPME-HS-GC/MS internal standards

Compound	Functional group	Internal Standard
Acetoin	Ketones	2,3 Pentanedione
Pentanol	Alcohols	Hexanol
Hexanal and Nonanal	Aldehydes	Heptanal
2 pentyl furan	Ring	2 butylfuran
Carboxylic acids	Carboxylic acids	Heptanoic acid
pCresol	Ring	Phenol

## Results

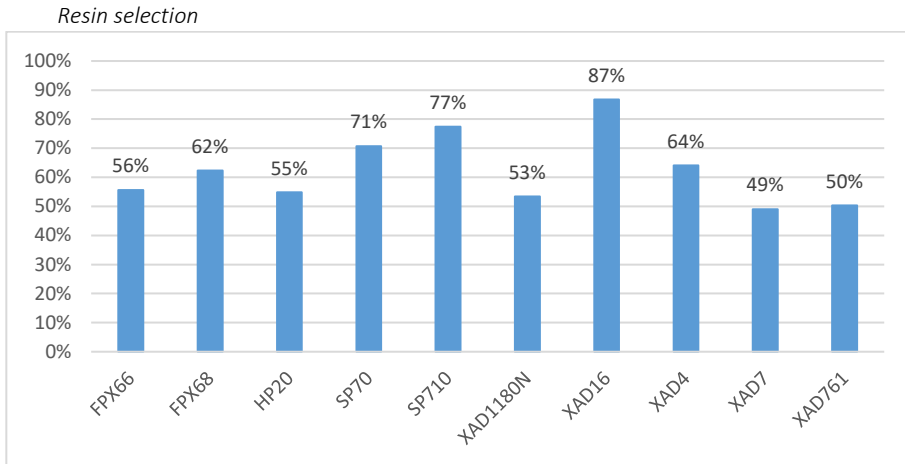


**Figure 6.7.** Resin scores

Results of the different normalized criteria: selectivity, number of off-flavors adsorbed, capacity and desorption are shown next:

**Table 6.14.** Normalized resin selection criteria

	Selectivity	Off Adsorbed	Desorption	Capacity
<b>Weight</b>	<b>0.5</b>	<b>0.2</b>	<b>0.2</b>	<b>0.1</b>
<b>FPX66</b>	0.39	0.85	0.67	0.72
<b>FPX68</b>	0.53	0.92	0.67	0.67
<b>HP20</b>	0.46	0.77	0.69	0.51
<b>SP70</b>	0.71	0.77	0.57	0.81
<b>SP710</b>	0.88	0.85	0.54	0.70
<b>XAD1180N</b>	0.50	0.77	0.58	0.46
<b>XAD16</b>	1.00	0.92	0.74	0.63
<b>XAD4</b>	0.50	0.92	0.49	1.00
<b>XAD7</b>	0.27	1.00	0.79	0.48
<b>XAD761</b>	0.34	0.62	1.00	0.36

Adsorption equilibrium

The data was treated as independent components in order to identify if the behavior was linear.

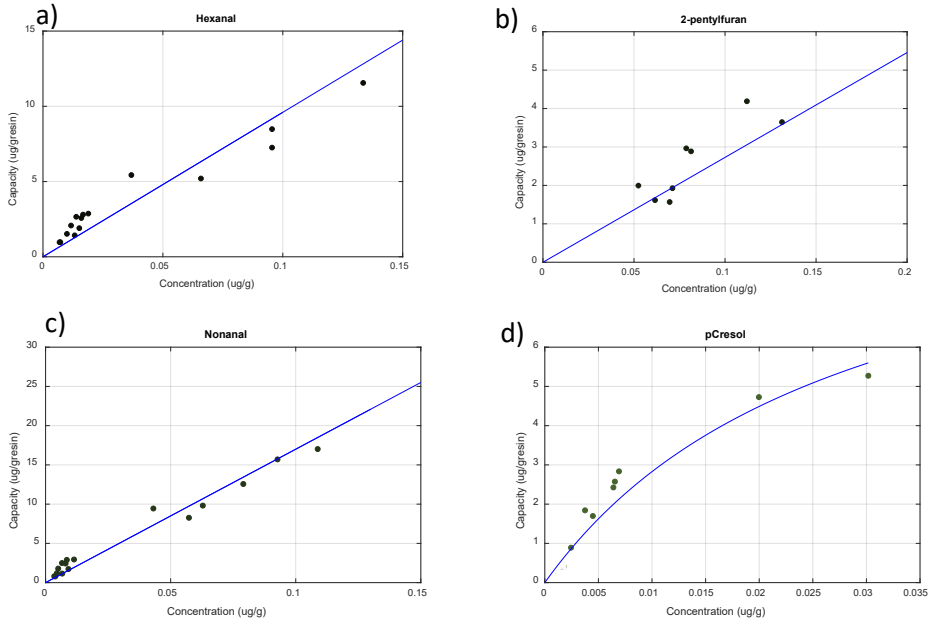


**Figure 6.8.** Off-flavor adsorption isotherms a) hexanal, b) 2-pentylfuran, c) nonanal and d) pCresol in Resin XAD16N at room temperature and pH 6.4. Lines are used to guide the eye

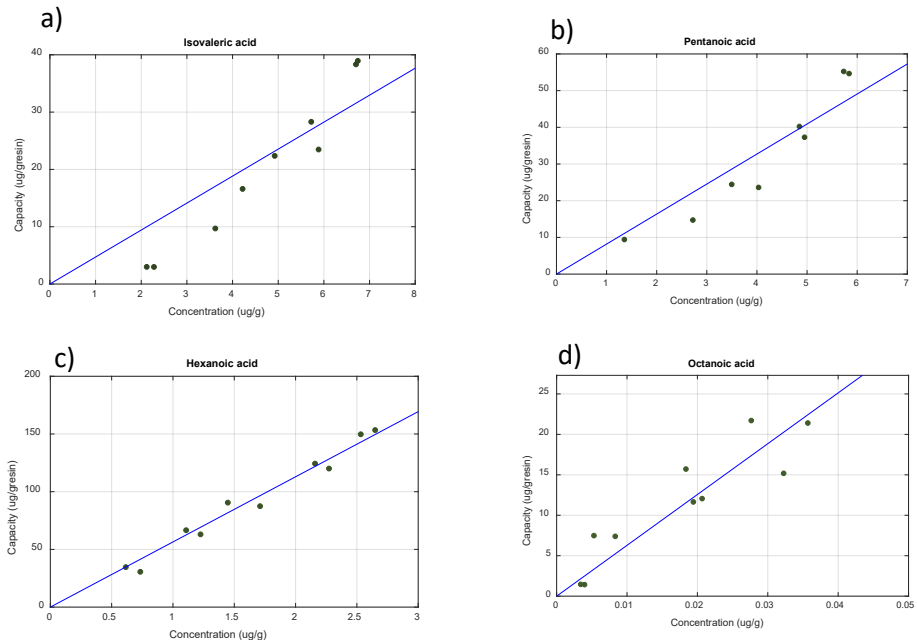


**Figure 6.9.** Carboxylic acids adsorption isotherms a) isovaleric, b) pentanoic, c) hexanoic and d) octanoic in Resin XAD16N at room temperature and pH 6.4

As can be seen in the above figures, most of the components present linear behavior, as expected due to the low concentration at which they are presented in the agricultural stream. Only the last two points of pCresol seems to not follow the linear trend, however, at feed conditions, is in the linear range.

The data of isovaleric acid shows an exponential behavior, this shape is characteristic of unfavorable isotherms. For butanoic acid and acetoin, the change in concentration in the liquid phase was very low. This difference is very close to the detection limit of these two compounds, and no tendency could be observed with the data. This is a strong indication of the poor interaction between these components and the resin. As at these concentration levels linear behavior is expected the isotherm slope was calculated from the average value of the ratio between the solid concentration ( $q_i$ ) and the equilibrium concentration ( $C_e$ ).

Finally, column experiments were performed, in order to validate the model described in Chapter 3<sup>8</sup> but applying the equilibrium data presented in Table 6.15.

Results are presented in Figure 6.10, indicating that the model can describe the adsorption behavior of the different off-flavor components presented in the agricultural side stream as the simulations are in good agreement with experimental results.

**Table 6.15.** Adsorption equilibrium parameter between components and resin XAD16N

Compounds	H (L/L <sub>resin</sub> )	$\beta$ (-)	Remarks
<b>Product</b>	1.4	5.70	Valuable product
<b>Acetoin</b>	5.76	5.70	Ketone
<b>Hexanal</b>	96.76	3.40	Aldehyde
<b>Nonanal</b>	255.40	1.70	
<b>Pentanol</b>	169.25	1.70	Alcohol
<b>Pentylfuran</b>	51.53	1.70	Aromatic ring
<b>Butanoic Acid</b>	4.45	5.70	Carboxylic acids
<b>Isovaleric Acid</b>	10.01	5.70	
<b>Pentanoic Acid</b>	15.00	5.70	
<b>Hexanoic Acid</b>	45.00	5.70	
<b>Octanoic Acid</b>	593.37	5.70	
<b>pCresol</b>	142.10	1.70	Aromatic ring

It can be seen in Figure 6.10 that butanoic, isovaleric and pentanoic acids have a weaker interaction with the resin than the aldehydes, hexanoic and octanoic acids, as suggested by the lower value obtained of the isotherm slope.

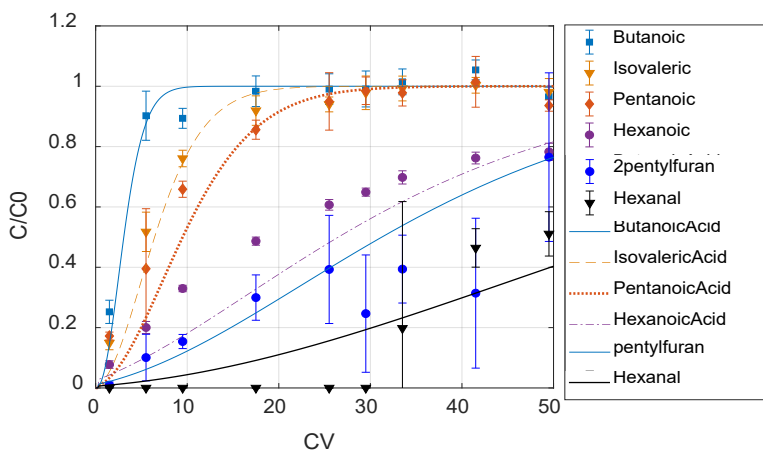


**Figure 6.10.** Critical off-flavors breakthrough curves in XAD16N at room temperature (6mL column). Markers are experimental results; lines represent simulation results. Error bars correspond to the standard deviation of duplicate experiments.

The product showed very poor interaction with the resin and reached saturation ( $C=C_0$ ) soon after one column volume (CV) of passed liquid<sup>25</sup> (data not shown).

## Performance indicators

Productivity is defined as the amount of product that can be produced per unit of time and resin volume. Productivity can be estimated using the following equation:

$$Prod_{valuable} = \frac{M_{product}}{(1 - \varepsilon_b) * V_c * t_{cycle}} = \frac{M_{p,Load} + M_{p,wash}}{(1 - \varepsilon_b) * V_c * t_{cycle}} \quad (6.18)$$

Where  $M_{product}$  is the mass of product, which is calculated with the sum of the mass of product during loading and mass of product during washing (g),  $V_c$  is the column volume (L) and  $t_{cycle}$  is the cycle time defined as  $t_{cycle} = t_{equilibration} + t_{loading} + t_{washing} + t_{elution} + t_{regeneration}$

The yield of the valuable products was estimated as:

$$Yield = \frac{M_{product}}{M_{feed}} = \frac{M_{product}}{Q_{load} * C_{feed}} \quad (6.19)$$

$M_{feed}$  is the mass of product applied in the column (g),  $Q_{load}$  is the volumetric flow rate during loading ( $m^3/h$ ) and  $C_{feed}$  is the product concentration at the feed.

## Adsorption optimization

The maximum productivity that satisfies all off-flavors specifications corresponds to 1.56 g/L<sub>resin</sub>/h, operating the column at 12.5. m/h with a residence time of ~10 mins.

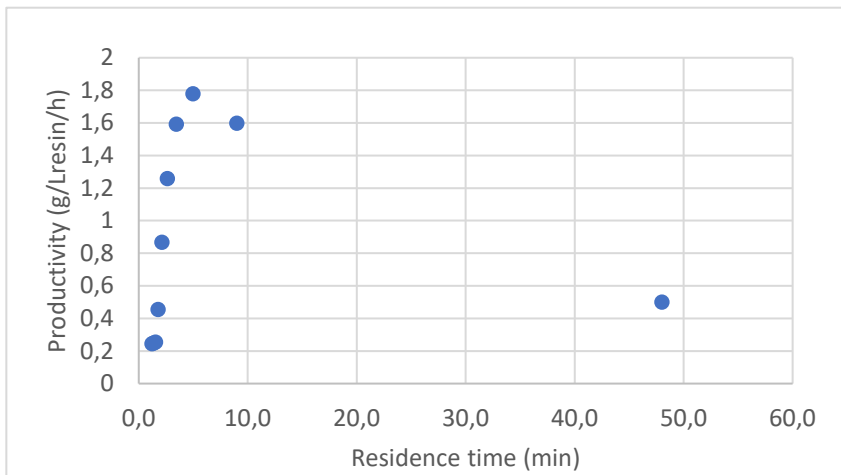


**Figure 6.11.** Productivity vs residence time

Given than the flow rate of the feed and knowing the required superficial velocity to operate the adsorption column, column diameter can be estimated using equation (6.20).

$$D_c = \sqrt{\frac{4 * Q_v}{\pi * u_s}} \quad (6.20)$$

Finally, column height should be selected based on the established pressure drop.

### Column operation

Column operating parameters are summarized in Table 6.16. Loading and washing are operated at a superficial velocity of 12.5 m/h while elution, regeneration and re-equilibration at 50 m/h.

The selected column size for off-flavor removal is 0.85 m diameter and 2 m height, corresponding to a volume of 1.13 m<sup>3</sup>. Using these dimensions and simulating the adsorption cycle, the following results are obtained.

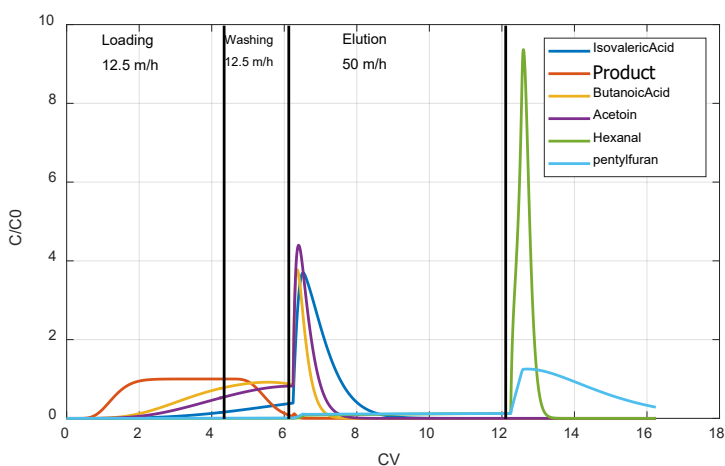


**Figure 6.12.** Normalized concentration profile of critical off-flavors and product during the adsorption cycle. From 12CV on, column is assumed to be washed with 50% Ethanol.

The final concentration of the different off-flavor presented in the stream accomplished all the specifications.

Given that each column is loaded every 86 min, this means that each column can perform 2525 cycles per year, and recovers a total of 10.2 product tons/year, 0.26 tons lower than the amount of product that is aimed to be produced. Therefore, an additional column operating in parallel is needed to satisfy the demand. Operation of the 3 columns could be done by having two holding tanks, one before the adsorption column and another after the adsorption column. This in order to split the flow to be sent to columns.

Packing of the resin should be replaced. Assuming that the packing is replaced every 200 cycles, for the two-column operating system (5050 cycles) the packing of each column should be replaced 13 times per year. To satisfy the demand of product the third column need to be operated 131 cycles and therefore no packing replacement is needed. The corresponding amount of resin needed per year is 22.31 tons/year.

**Table 6.16.** Adsorption operating parameters

Adsorption/Desorption	Value	Unit	Remarks
<b>Equilibration</b>	5.0	CV	Water
<b>Loading</b>	4.2	CV	Ultrafiltrate stream
<b>Washing</b>	2.0	CV	Water
<b>Elution</b>	6.0	CV	0.5% NaOH
<b>CIP</b>	4.0	CV	50% Ethanol
<b>Column Volume</b>	1134.9	L	$V_c$
<b>Volume resin</b>	794.4	$L_R$	$V_c \cdot (1 - \epsilon_b)$
<b>Ac</b>	0.6	$m^2$	Superficial area
<b><math>v_{ads}</math></b>	12.5	m/h	Adsorption superficial velocity
<b><math>v_{des}</math></b>	50.0	m/h	Desorption superficial velocity
<b>Cycle time</b>	98.0	min	43 min adsorption 19 min washing 36 min desorption, regeneration and re-equilibration

## Appendix 6D. Economic evaluation

### CAPEX

Lange Factors used to estimate Direct Fixed Capital<sup>29</sup> and capital expenditure.

Total Plant Direct Cost (TPDC)			
S.No	Cost Parameter	Cost factor	Value (€)
1	Purchased equipment cost (PEC)		5,090,795.44
2	Installation Cost	(0.50 * PEC)	2,545,397.72
3	Process Piping	(0.35 * PEC)	1,781,778.40
4	Instrumentation	(0.30 * PEC)	1,527,238.63
5	Insulation	(0.03 * PEC)	152,723.86
6	Electrical	(0.15 * PEC)	763,619.32
7	Building	(1.00 * PEC)	5,090,795.44
8	Yard Improvement	(0.15 * PEC)	763,619.32
9	Auxiliary Facilities	(0.10 * PEC)	509,079.54
<b>Total Plant Direct Cost (TPDC)</b>			<b>18,225,047.66</b>
Total Plan Indirect Cost			
10	Engineering	(0.25 * TPDC)	4,556,261.92
11	Construction	(0.35 * TPDC)	6,378,766.68
<b>Total Plant Indirect Cost</b>			<b>10,935,028.60</b>
Total Plan cost			
<b>Total Plant Cost (TPC)</b>		<b>(TPDC+TPIC)</b>	<b>29,160,076.26</b>
12	Contractor's fee	(0.05 * TPC)	1,458,003.81
13	Contingency	(0.10 * TPC)	2,916,007.63
14	<b>Direct Fixed Capital (DFC)</b>	<b>(TPC + 12 + 13)</b>	<b>33,534,087.70</b>
Capital Expenditure (CAPEX)			
15	Direct fixed capital		33,534,087.70
16	Working Capital	(0.15 * 15)	5,030,113.16
17	Startup Cost	(0.20 * 15)	6,706,817.54
18	Up-front R and D	(0.05 * 15)	1,676,704.39
<b>Total Investment</b>		<b>15+16+17+18</b>	<b>46,947,722.78</b>

## OPEX

Facility overhead was estimated using the following multipliers<sup>29</sup>:

Concept	Remarks
<b>Maintenance</b>	3% of DFC
<b>Equipment depreciation</b>	10% Equipment cost
<b>Building depreciation</b>	5% Building cost
<b>Insurance</b>	0.7% of DFC
<b>Taxes</b>	3% of DFC
<b>Factory expenses</b>	1% of DFC

## Discounted Cash Flow analysis

**Table 6.14.** Calculation of Cash flows (Millions of Euros)

Year	Investment	Depreciation	$C_{Excl Dep}$	Revenues	Net Earnings	Annual cash flow	Discounted Cash flow (PV)	Cum PV
0	(46.95)	-	-	-	-	(46.95)	(46.95)	(46.95)
1	-	9.39	21.11	32.65	1.44	10.83	9.42	(37.53)
2	-	15.02	14.14	32.65	2.34	17.36	13.13	(24.40)
3	-	9.01	14.14	32.65	6.37	15.38	10.11	(14.29)
4	-	5.41	14.14	32.65	8.78	14.19	8.11	(6.18)
5	-	5.41	14.14	32.65	8.78	14.19	7.05	0.88
6	-	2.70	14.14	32.65	10.59	13.30	5.75	6.63
7	-	-	14.14	32.65	12.40	12.40	4.66	11.29
8	-	-	14.14	32.65	12.40	12.40	4.06	15.34
9	-	-	14.14	32.65	12.40	12.40	3.53	18.87
10	-	-	14.14	32.65	12.40	12.40	3.07	21.94

$$Net\ Earnings = (Revenues - C_{Excl\ Dep} - Depreciation) * (1.0 - income\ tax)$$

Income tax was assumed to be 33%

$$Annual\ Cash\ flow = Net\ earnings + Depreciation$$

# Chapter 7

## Conclusions and Outlook

---

This thesis focused on the valorization and recovery of valuable products from food side streams. As proven in previous studies, adsorption is a promising technique and this work demonstrates that its application in the food sector can be expanded.

The work here performed consisted of the following:

- Identification of the valuable compounds present in food side streams (plant-based exclusively), specifically in rapeseed meal extract and fruit and vegetable wastewater.
- Evaluation of adsorption for capturing of valuable compounds or removal of impurities by:
  1. Identified suitable adsorbents for capturing target compounds
  2. Experimental evaluation of adsorption equilibrium and application of isotherm adsorption models for its description
  3. In-silico assessment of adsorption column dynamics and experimental validation
  4. Column optimization (in-silico)
- Industrial process design for upgrading a side stream.

From the literature study performed in Chapter 2, one could conclude that multiple valuable products can be recovered from one single side stream. However, this will be dependent on the source origin (strong matrix, soft matrix or wastewater) and the components to be recovered. This work also discussed that if the recovered products are intended to be applied in fields that require high purity adsorption is a suitable technique to be applied for purification.

Currently food adsorptive processes are limited to citrus debitterness, desugarization of molasses or fructose glucose separation, mainly because it is considered an expensive technology. However, it has been proved to be very promising and effective for capturing and separating different components. This work studied the side product from plant-based oil, rapeseed meal, with the objective to recover: sinapic acid (polyphenol), napin and cruciferin. It was proven (Chapter 3 and Chapter 4) that the used of high throughput experimentation (HTE) allows fast and proper resin choice. In addition, reliable equilibrium information under different conditions is obtained.

It was shown (Chapter 3) that food grade hydrophobic resins selectively capture sinapic acid, and the other components present in the liquid extract (glucosinolates, sugars and phytic acid) poorly interact with the selected resin. As this is a product that can be used in the food sector, ethanol and water are the only food grade solvents that can be applied. With the strong selectivity, mixtures of ethanol water resulted in efficient desorption.

The study presented in Chapter 4, proposed a technically feasible process for the recovery of sinapic acid and proteins for rapeseed meal extract. Protein purification is performed using ion exchange adsorption where napin protein is selectively captured with cruciferin in the flow through (as it poorly interacts with the resin). Like Chapter 3, adsorption/desorption equilibrium is accurately determined and used as input in an adsorption column model. The model is in good agreement with the experimental results, which corroborates the benefits of using HTE. In Chapter 4, design of an industrial scale chromatography column is accomplished with the validated column model.

Chapter 5 demonstrates the efficient application of continuous chromatography in the food sector for capturing sinapic acid. This study opens the possibility of using relatively new continuous chromatography systems, specifically, the CaptureSMB process, to efficiently operates the adsorption step. The CaptureSMB process performed best compared to packed bed in terms of maximizing productivity, higher resin utilization and lower buffer consumption. This chapters indicates the potential of using other continuous chromatography systems, and not only SMB, for processing side streams. As the CaptureSMB process only uses two identical columns for operation, this consequently might reduce the investment needed for its application in the food sector compared to SMB. The study performed in Chapter 5, is a clear example of how systems developed for biopharmaceutical purposes can be adapted to food processes.

The last scientific chapter of this thesis (Chapter 6) presented all the concepts applied in this work for the upgrading of a food side stream. Chapter 6 evaluated a different case study, where the objective is to capture, by means of adsorption, the *impurities* rather than the *products*. This chapter presented the use of a food grade hydrophobic resin for the capture of different off-flavors compounds. Here selectivity towards several off-flavor is accomplished as well as continuous operation. The use of specialized software (SuperPro Designer and Matlab) for process design and simulation permits process evaluation. This work proved the technical and economic feasibility of generating a high-value product from a food side stream. Although, in this chapter, recovering of multiple valuable compounds was not evaluated, it is clearly shown as a possibility.

This thesis shows that adsorption can be efficiently implemented in the food sector for processing and upgrading of food side streams. The utilization of modeling techniques and a proper understanding of the interactions between the adsorbed molecules and the adsorbents is a powerful tool for process optimization. This, additionally, allows the minimization of experimental trials and a better definition of experimental plans, which can be performed by HTE.

Future research should focus on: better understanding of the influence of the inherent multicomponent nature of the feed on process robustness, fouling and operability. Pilot studies should be performed to assess these aspects in an industrial setting. Additionally, other modes of adsorption should be investigated, like batch and continuous suspension adsorption and expanded bed adsorption. The latter promising mode, issues on operational stability needs to be solved for a successful implementation in industry. Further minimization of the still generated waste, by e.g. process

integration, to fulfill the concept of circular economy by closing material loops and enhance resource utilization (Bioeconomy) should be investigated.

The work presented in this thesis shows the applicability of adsorption as a techno-economically efficient technique for processing and recovering products in the food sector, specifically, side streams. This may lay the foundation of its application in other food processes.



# Appendix

## Acknowledgments, List of publications & Curriculum Vitae

---

### Acknowledgments

Obtaining a PhD degree has been one of the most gratifying and challenging experiences in my life. A decision that not only formed me as a scientist but also made me growth as a person. I am very satisfied with the results of this work. This amazing achievement could not be possible without all the people that collaborated with me and helped me to achieve this milestone in my life, and now it is time to thanks them.

This journey started with my promotor Marcel Ottens, thank you very much for giving me the opportunity to work with you and for all your guidance and trust. I really appreciate all our meetings where we discuss the progress of my project and for always keeping me on track. Thank you for letting me lead the project and for considering all my ideas. For all the opportunities to learn in all the conferences that I could attend and for all your support. I really enjoyed working with you and I hope we can work together again in the near future.

Many thanks to my other promotor Luuk van der Wielen, for all your input and for the challenging discussions, you always gave me “food for thought”.

I would like to acknowledge the mild fractionation ISPT cluster and their members for not only giving me the opportunity to evaluate this project but also for letting me collaborate closely to industry. Peter de Jong, thank you for all your kind words during the cluster meetings and for always encourage me to continue with my work. I want to thank the people from Unilever, collaborating with you was a super nice experience. Hilde, thank you for always be critical and for all the great suggestions on resin screening. Xavier, Alphons, Max and Hans thanks for all the technical support and for always make me feel part of the flavor team.

Let’s move on to the people that make all these chapters possible, my students. Roos, my first student, you joined my project for your bachelor’s thesis and you surprised me. You executed experiments in the Tecan precisely and also applied some of my models showing good understanding. Your work served as a based not only to all my next students but also to other members in the BPE group. Vasu, thanks for joining this project, your engineering mind and enthusiasm made us achieve excellent results and a

nice publication. Pattra, with your amazing set of lab skills, always precise we managed to get lost of data. Thanks for all that perseverance, after quite some work, we manage to developed an appropriate analytical method for protein quantification. Daphne thanks for joining this project, thanks for your challenging questions, your modelling skills, set the ground of many (published) chapters of this thesis. Thanks for always being more a colleague than a student. Alexandra, thanks for your resilience, your project changed scope a couple of times, but you continue with it showing enthusiasm, I still believe that EBA could be implemented for our case. Sara thanks for all your questions and your critical way of working, I really enjoyed all our discussions, we found out that model solutions not always describe the “real” stream, however, your thesis allows us to understand more the phenomena. Each of you has taught me so much, thanks for letting me guide you during your projects.

Thank you to all the BPE members, the former PhDs, Carlos, for guiding me during my MSc thesis, for introducing me the fascinating world of adsorption and for inspiring me to do a PhD. Susana, Joana, and Shima thanks for always made the BPE atmosphere so nice. Marcello thanks for all your patience and for always be willing to discuss with me and my students, particularly at the beginning of my project, you taught us so much. Silvia thanks for all the nice adsorption and modelling discussions. Debby thanks for always discuss with me, your insight and working in a similar topic really helped me on how to conduct this research. Thanks for all our excellent scientific discussions and for being such a nice friend, I still want to do the brewing contest. Vic, you were the first one that welcomed me in our office in the new TNW building, thanks for always support me and for all the nice beers after work. Bianca my beautiful friend, definitely doing a PhD together with you was amazing, I love all your positive attitude, your willingness to discuss, your curiosity, all our conference travels, and every nice chat about everything. To all the “new” BPE PhD candidates, Roxana, Tiago, Mariana, Marijn and Oriol, thanks for letting me be part of your discussions, teaching me about new topics and supporting my students in their mock defenses. I wish you success in your projects.

To the BPE staff members, Kawieta, thanks for always helping me when I struggle with administrative work, for being always supportive and for sharing with us your amazing cooking skills (in pictures). Stef and Max thanks for helping me and my students in the lab. Song, you are an amazing person, thank your for always be there for me, willing to help me with my experiments, we learned so much together about the Tecan and the Aktas. Thanks to Adrie, Ludo and Maria, I always enjoyed our conversations and the nice coffee breaks.

To my master friends, almost 7 years in this beautiful country together. Vidhvath, thanks for all your advice and also to make time for me and discuss my ideas, for helping me with my English writing skills and for your friendship. Marina, thanks for your happiness and enthusiasm, super nice that you joined the BPE group so we can see each other more often and talk about science, thanks for letting stay occasionally on your place and enjoy the afternoon in Delft without the need to travel to Utrecht.

Thanks to all the PDEngs that I meet during this journey, Sara for always discussing with me about adsorption, we learned a lot together about how to troubleshoot with the Tecan. Paco, thanks for always discussing with me about engineering, EBA, packing columns and process design etc... we have so much fun in the lab. Your input was very valuable for my process design chapter.

Now it's time to thanks my paranymphs, Daphne and Gustavo. Daphne, thanks again for always be there for me, without your work I think this thesis would have been very different. Thanks for accepting

being my paranymp and of course for being a very nice friend, I look forward to celebrating with you this milestone.

Gustavo, mi mejor amigo, nos conocemos desde hace tanto tiempo, cuando estudiábamos en la Facultad de Química de la UNAM. Tantas cosas que hemos vivido juntos y tanto que me has enseñado. Gracias por siempre estar presente y disponible para discutir conmigo ciencia. Tu mente brillante no deja de sorprenderme, sé que siempre puedo contar contigo, gracias por tantos años de amistad.

Es momento de agradecer a mi hermosa familia, a los cuales dedico esta tesis. A mi papa, Ramon Moreno, por siempre ser esa fuente de inspiración, el otro científico en nuestra familia. A mi madre Martha, por siempre apoyarme en mis decisiones y ser esa persona que siempre me motiva a ser mejor. A mis hermanas, mis cómplices en la vida y mis compañeras de juegos, Adi por siempre ser mi segunda madre, Ceci mi hermana divertida, nunca olvidare el verano que pasaste con nosotros (Stefan's roomie), tenerte aquí hizo mis días mas felices. Y Marce, la artista de la familia, por hacer la maravillosa portada de este libro. Todos me han inspirado de diferente manera para terminar este trabajo.

I want to thank to my Dutch family, Gerda, Cornel, Marloes, Koen and Mark for their unconditional support. I am very happy to share with you this amazing achievement.

Finally, I want to thank to one of the most important people in my life, Stefan. You are partner in life, that person that is always there for me. Thanks for all your support and encourage, I want to dedicate this work to you. Thanks for always listening to me and for letting me share with you my PhD adventures. To encourage me to be the best version of myself. Thanks for always make me feel like home by bringing a bit of Mexico into our life. I look forward to sharing with you more accomplishments in this journey call Life.

Monica Moreno Gonzalez

## List of Publications

### Journal Publications

Moreno-González, M., Chuekitkumchorn, P., Silva, M., Groenewoud, R., & Ottens, M. (2021). High throughput process development for the purification of rapeseed proteins napin and cruciferin by ion exchange chromatography. *Food and Bioproducts Processing*, 125, 228-241

Moreno-González, M., Keulen, D., Gomis-Fons, J., Lopez-Gomez, M. G., Nilsson, B., & Ottens, M. (2021). Continuous adsorption in food industry: The recovery of sinapic acid from rapeseed meal extract. *Separation and Purification Technology*, 254, 117403

Moreno-González, M., Girish, V., Keulen, D., Wijngaard, H., Lanteslager, X., Ferreira, G., & Ottens, M. (2020). Recovery of sinapic acid from canola/rapeseed meal extracts by adsorption. *Food and Bioproducts Processing*, 120, 69-79.

Cabrera-Rodríguez, C. I., Moreno-González, M., de Weerd, F. A., Viswanathan, V., van der Wielen, L. A. M., & Straathof, A. J. J. (2017). Esters production via carboxylates from anaerobic paper mill wastewater treatment. *Bioresource technology*, 237, 186-192.

### Conference contributions

Moreno-González, M., Keulen, D., Ferreira, G., & Ottens, M. (2019). Continuous adsorption of sinapic acid from rapeseed meal extract. Biopartitioning and Purification Conference, Guarujá, SP, Brazil (oral presentation)

Moreno-González, M., Keulen, D., Wijngaard, H., Ferreira, G., & Ottens, M. (2019). Continuous adsorption of sinapic acid from rapeseed meal extract. 16<sup>th</sup> Netherlands Process Technology Symposium, Eindhoven, The Netherlands (oral presentation)

Moreno-González, M., Keulen, D., Wijngaard, H., Ferreira, G., & Ottens, M. (2019). Recovery of valuable compounds from food industry side streams. American Chemical Society (ACS) Spring Meeting, Orlando FL, United States (poster presentation)

Moreno-González, M., Lopez-Gomez, M.G., Madsen, S., (2019). Production of a human mesenchymal stem cell therapy product. American Chemical Society (ACS) Spring Meeting, Orlando FL, United States (oral presentation)

Moreno-González, M., Hylkema, N., Wijngaard, H., Ferreira, G., & Ottens, M. (2018). Recovery of valuable compounds from side streams of food industry. NBV-PZ Mini-symposium on biorefineries, Amersfoort, The Netherlands (oral presentation)

Moreno-González, M., Wijngaard, H., Ferreira, G., & Ottens, M. (2018). Recovery of valuable compounds from side streams of food industry. 12<sup>th</sup> European Symposium on Biochemical Engineering Sciences, Lisbon Portugal (oral presentation)

Moreno-González, M., Girish, V., Chuekitkumchorn, P., Wijngaard, H., Ferreira, G., & Ottens, M. (2018). High throughput resin selection for the recovery of valuable compounds from food products. American Chemical Society (ACS) Spring Meeting, New Orleans, United States (poster presentation)

Moreno-González, M., Hylkema, N., Wijngaard, H., Ferreira, G., & Ottens, M. (2017) Adsorption of non-volatiles from food products. Biopartitioning and Purification Conference, Copenhagen, Denmark (poster presentation)



*'Everybody is a genius. But if you judge a fish by its ability to climb a tree, it will live its whole life believing that it is stupid' – Albert Einstein*



## Curriculum Vitae

Mónica Moreno González was born in Mexico City on the 4<sup>th</sup> May 1987. After completing her High school education in 2006, she started her Bachelor education (Licenciatura) in Chemical Engineering at the National Autonomous University of Mexico (UNAM) in Mexico City. During her Bachelor, she worked in the Biotechnology group. Her bachelor thesis investigated different pretreatment processes of agave bagasse (residue from Tequila industry) to recover reducing sugars for the production of bioethanol. After obtaining her bachelor's degree, she started her professional career in the pharmaceutical company Bristol Myers Squibb, where she worked as a manufacturing technology chemist.



In 2014 she received a full scholarship to pursue her MSc studies in Life Science and Technology, specialization in Bioprocess Engineering at Delft University of Technology (TU Delft). She evaluated her MSc thesis in the Bioprocess Engineering group with a project focused on the recovery of carboxylates from acidified wastewater. In her MSc thesis she used anion exchange chromatography (IEX) to separate carboxylates from inorganic anions. During this period, she discovered her passion for downstream processing (DSP) and particularly chromatography.

In September 2016 she continued in the Bioprocess Engineering group (TU Delft) as a PhD candidate under the supervision of Dr.ir Marcel Ottens and Prof.dr.ir Luuk van der Wielen. During her PhD research she valorized food industry side streams to recover valuable products, such as natural ingredients. She used adsorption technology (ion exchange and hydrophobic interaction) for separation and purification of natural products (flavor ingredients and proteins) in batch and semi-continuous operation.

From September 2020, she joined the Process Development CMC team of uniQure as a Scientist.

Cover design by Marcela Moreno Gonzalez

Printed by GVO drukkers & vormgevers B.V.

Edition: 80 copies

Monica Moreno Gonzalez, 2021